# Liquid crystal thermography in neuropathic assessment of the diabetic foot

**Manish Bharara**

**A thesis submitted in partial fulfilment of the requirements of Bournemouth University for the degree of Doctor of Philosophy.**

**May 2007**

**Bournemouth University**

# Abstract


## Liquid crystal thermography in neuropathic assessment of the diabetic foot

### Manish Bharara

Primary aetiologic factors of diabetic foot disease include peripheral neuropathy and peripheral vascular disease. Assessment of circulation, neuropathy, and foot pressure is employed routinely to determine the risk of foot ulceration in the patient with diabetes mellitus. Routine neuropathic evaluation includes assessment of sensory loss in the plantar skin of the foot using both the Semmes Weinstein monofilament and the biothesiometer. Progressive degeneration of sensory nerve pathways is thought to affect thermoreceptors and mechanoreceptors. However, thermological measurements of the foot to assess responses to thermal stimuli and cutaneous thermal discrimination threshold are relatively uncommon. Recent improvements in liquid crystal technology (LCT) including insensitivity to pressure, faster response times, lower cost and fast image acquisition offer potential for routine thermographic assessment of the diabetic foot. The present study was designed to evaluate if an association exists between abnormal plantar thermal images and sensory loss under conditions of normal loading. The system comprises a robust measurement platform, thermochromic liquid crystal polyester sheet (TLC), instrumentation and analysis software. In vitro calibration was performed to characterise three physical forms of TLC on the basis of linearity, hysteresis, pressure sensitivity and response time. An in vivo pilot evaluation study of the system was performed using three sub-groups (i) neuropathic diabetic (n=30), (ii) non neuropathic diabetic (n=30) and (iii) a healthy control group (n=30). The principal results of this study indicate raised plantar temperatures for the diabetic groups at baseline and post stress relative to the control group. Furthermore, poor recovery response to thermal stimulus in the neuropathic diabetic group suggests degeneration of thermoreceptors. Thus by assessing the thermal parameters at the same sites as that of sensory testing, the new LCT based approach appears capable of providing an alternative confirmation of clinical neuropathy and offers potential as an improved method compared to existing techniques.

# List of contents

# List of supporting publications

## Journal Papers

1. Grewal, G.S., Bharara. M, Cobb, J.E., Dubey, V.N., Claremont, D.J.(2006) A Novel Approach to Thermochromic Liquid Crystal Calibration Using Neural Networks, Measurement Science & Technology 17 1918-1924.

2. Bharara. M, Cobb, J.E., Claremont, D.J.(2006) Thermography and Thermometry in the Neuropathic Assessment of the Diabetic Foot: A Case for Furthering the Role of Thermal techniques, International Journal of Lower Extremity Wounds, 5 (4) 250-260.

3. Bharara. M, Cobb, J.E., Claremont, D.J., Anderson, A.M. (2006) Characterisation and Calibration of Three Physical Forms of Thermochromic Liquid Crystals Imaging Science, Journal (In Press).

## Abstracts in Journals

1. Bharara M., Vishwanathan V., Cobb JE., Ramachnadran, A., Claremont DJ., Hadley G., Seena, R., (2006) Thermal Imaging Initiative for better clinical management of diabetic foot disease, Diabetic Medicine 23(S4):488-489.

2. Bharara M., Cobb JE., Claremont DJ., Hadley G., Grewal GS., Vishwanathan V., Anderson AM., Ramachandran, A. (2006) Association of plantar foot temperatures and sensory loss in diabetic foot disease, Thermology International, 16(3):101-102.

3. Bharara M., Cobb JE., Claremont DJ., Hadley G., Grewal GS., Vishwanathan V., Anderson AM., Ramachandran, A. (2006) Association of plantar foot temperatures and sensory loss in diabetic foot disease, Acta Bio-Optica et Informatica Medica, 12(2):9-10.

4. Bharara. M, Cobb ,J.E., Claremont, D.J., Anderson, A.M.(2005) Thermochromic Liquid Crystal Thermography: Application in neuropathic assessment of Diabetic foot, Thermology International 15(4) 154-155.

## Conference Presentations

1. Bharara M., Vishwanathan V., Cobb JE., Ramachnadran, A., Claremont DJ., Hadley G., Seena, R., (2006) Thermal Imaging Initiative for better clinical management of diabetic foot disease, **World Congress on Diabetes, International Diabetes Federation**, Cape Town (South Africa).

2. Bharara M., Cobb JE., Claremont DJ., Hadley G., Grewal GS., Vishwanathan V., Anderson AM., Ramachandran, A. (2006) Association of plantar foot temperatures and sensory loss in diabetic foot disease, **European Congress on Medical Thermology**, Zakopane (Poland).

3. Bharara M, Cobb J.E., Claremont, D.J., Anderson, A.M.(2005) Thermochromic Liquid Crystal Thermography: Application in neuropathic assessment of Diabetic foot, **Medical Thermography and Thermometry**, National Physical Laboratory, London (UK).

4. Bharara, M., Cobb, J.E and Claremont, D.J. (2005) Thermographic measurement in plantar foot using TLC for early detection of risk of ulceration. **LSI Conference**, University of Southampton(2005),UK

5. Bharara, M. and Cobb, J. (2005). Liquid crystal thermography in biomechanical assessment of diabetic foot, **5th Academic Biomedical Engineering Research Group (ABERG) Workshop**, 2005, Bournemouth, UK, Bournemouth University.

6. Bharara, M. and Cobb, J. (2004). Liquid crystal thermography in biomechanical assessment of diabetic foot, UK, **Britain's Younger Engineers Special reception at House of Commons**; Poster Competition.

# List of illustrations and tables

**Figures** **Pages**

**Photographs** **Pages**



**Tables** **Pages**

# List of accompanying material

# Acknowledgements

I take this opportunity to convey my sincere thanks and gratitude to everyone who made it possible for me to successfully complete the study presented in this thesis. I would like to give special thanks to:

**Supervisors & Collaborators:**

- Dr. Jon Cobb for supervision, constant support, encouragement and advice. My friendship with Jon throughout my research training has made this experience wonderful and instilled strong work ethics in me.
- Prof. Denzil Claremont for support and cooperation.
- Prof. Ann Anderson for her kind support, guidance and access to liquid crystal thermography laboratory at Union College, New York.
- Dr. Vijay Viswanathan, (Consultant Diabetologist and Joint Director of MV Hospital for Diabetes, Chennai, India) for encouragement and providing patients for the study.

**Family:**

- My grandparents for their blessings and encouragement. I would like to dedicate this thesis to my grandmother Mrs. Krishna Bharara, who passed away in 2005.
- My wife Dr. Ekta Marwah for her constant support, affection and sacrifice.
- My parents and siblings for their continuous love, unconditional support and faith.

**Colleagues:**

- Dr. Gurtej Singh Grewal for his tireless assistance and advice.
- Dr. Glyn Hadley for general help and assistance with calibration.
- Dr. Tom Teng for general help and reviewing the manuscripts.
- Mr. Gary Toms and Mr. Kevin Smith for help with the mechanical design.
- Mr. Balamurugan Karunamurthy and Dr. Bright Twumasi for general help.

## Declaration

This thesis contains the original work of the author except where otherwise indicated.

# Abbreviations

Abbreviations used throughout the thesis are defined at first usage and listed below, where possible in their standard form.

| | |
|---|---|
| °C | Temperature Degree Celsius |
| KPa | Kilo ($10^3$) Pascal |
| ABPI | Ankle Brachial Perfusion Index |
| AV | Arteriovenous |
| CCD | Charge Coupled Device |
| CIR | Cold Immersion Recovery |
| DAT | Dynamic area telethermometry |
| FSR | Force Sensing Resistor |
| HSI | Hue, Saturation and Intensity |
| HSV | Hue, Saturation and Value |
| IDDM | Insulin Dependent Diabetes Mellitus |
| IR | Infrared |
| LCT | Liquid Crystal Thermography |
| LDF | Laser Doppler Flowmetry |
| LED | Light Emitting Diode |
| MRI | Magnetic Resonance Imaging |
| NHS | National Health Services |
| NICE | National Institutes for Clinical Excellence |
| NIDDM | Non Insulin Dependent Diabetes Mellitus |
| NIH | National Institutes of Health |
| NIR | Near Infrared |
| PCA | Principal Component Analysis |
| PVD | Peripheral Vascular Disease |
| RGB | Red, Green and Blue |
| RMSE | Root Mean Square Error |
| ROI | Region of Interest |

| | |
|---|---|
| SD | Standard Deviation |
| SSE | Sum Squared Error |
| $TcPO_2$ | Transcutaneous Oxygen Tension |
| TLC | Thermochromic Liquid Crystals |
| VPT | Vibration Perception Threshold |
| WHO | World Health Organization |

# Chapter 1 Introduction

## 1.0 Introduction

This thesis documents a research project to develop a liquid crystal thermography (LCT) system capable of dynamically monitoring microvascular response to thermal stimulus and to provide quantitative measurements of response thresholds, at the plantar surface of the human foot.

## 1.1 Rationale

Foot ulcers are the main cause of lower extremity amputation in patients with diabetes. Currently, there are 1.8 million people suffering from diabetes in the UK (World Health Organization 2004). Fifty percent of diabetic patients have some degree of neuropathy, resulting in at least one foot ulcer during a patient's lifetime (Palubo and Melton 1985). Recent clinical guidelines suggest foot ulcers occur in five percent of diabetic patients in the UK (Hutchinson, McIntosh et al. 2000). Despite technological advances in the prevention and treatment of diabetic foot complications, the incidence remains unacceptably high. Prevention of foot ulcers by identifying individuals at high risk represents the most effective way of reducing the incidence of lower limb amputation in diabetic patients (Reiber 1992; Boulton, Connor et al. 1998; Bharara, Cobb et al. 2006).

Primary etiologic factors of diabetic foot disease include diabetic peripheral neuropathy and peripheral vascular disease. Progressive degeneration of sensory nerve pathways is thought to affect thermoreceptors and mechanoreceptors (Ziegler, Mayer et al. 1988; Viswanathan, Snehalatha et al. 2002). Neuropathy in diabetic patients is the most common reason for hospital admissions in developed countries and accounts for 50-75% of all amputations (Tanenberg, Schumer et al. 2001; World Health Organization 2004). This leads to a socio-economic burden for the national healthcare services and a poor quality of life for the patients. The neuropathic foot is characterised by heightened colouration and increased foot temperature (Stess RM, Sisney PC et al. 1986; Benbow,

Chan et al. 1994). The reactive hyperaemia following a period of loading is impaired in the neuropathic foot (Flynn, Edmonds et al. 1988; Cobb 2000). There is little evidence of thermally stimulated reactive hyperaemia in the neuropathic foot from other studies (Rayman, Hassan et al. 1986a; Rayman, Williams et al. 1986b). In comparison, there is better understanding of hyperaemia in Raynaud's phenomenon, which commonly affects the hands (Ring 1988; O'Reilly, Taylor et al. 1992; Ring, Aarts et al. 1998; Clark, Dunn et al. 2003). Assessment of thermal patterns and hyperaemic response in patients with Raynaud's disease has provided a suitable outcome measure for clinical evaluation (Boignard, Salvat-Melis et al. 2005; Foerster, Wittstock et al. 2006; Foerster, Kuerth et al. 2007). On the contrary, foot temperature and response of thermoreceptors is not routinely assessed in the diabetic foot clinic. Foot temperature is often assessed manually i.e. warm to the touch is often quoted.

To the author's knowledge, quantitative clinical evaluation of thermal response is not routinely assessed in the diabetic foot clinic. This may be due to unavailability of low cost thermal measurement technique and lack of research focus on thermal patterns under the plantar foot. A simple thermometer is obviously such a technique; it is the problem of relating temperature to the clinical condition that is the problem. Development of a suitable full field thermal measurement technique for objective analysis could enable clinicians/biomedical scientists to further understanding of plantar foot ulceration and offers potential in the routine clinical assessment of the diabetic foot. This research project investigates the design and evaluation of such a system.

## 1.2 Diabetes mellitus

### 1.2.1 Introduction

The World Health Organization (WHO) defines Diabetes Mellitus as 'a metabolic disorder of multiple aetiology characterised by chronic hyperglycaemia with disturbances of carbohydrate, fat and protein metabolism resulting from defects in insulin secretion, insulin action or both' (World Health Organization 1999).

According to the current WHO characterisation, the two major sub-classes of diabetes mellitus classification are defined as: (World Health Organization 1999)

a) Type 1 or Insulin Dependent Diabetes Mellitus (IDDM)

b) Type 2 or Non Insulin Dependent Diabetes Mellitus (NIDDM)

Table 1-1 compares the two primary features of type 1 and type 2 diabetes mellitus.

| Parameters | Type 1 | Type 2 |
|---|---|---|
| **Aetiology** | Genetically inherited; Exposure to viral infections or environmental toxins. | Multifactorial; Obesity; Genetically inherited. |
| **Description** | Beta cell destruction by autoimmune process; Absolute insulin deficiency; Abnormal variations of sugar levels and starving of body cells due to non absorption of glucose. | Insulin resistance in peripheral tissue and insulin secretion effect of peripheral tissue; Reduced beta cell function. |
| **Incidence** | 10% of diabetics | 90% of diabetics |
| **Age groups** | Mostly before 25 years of age; Peak onset age 10-13 years. | Middle old age; Incidence increases with growing age. |
| **Treatment** | Regular injections of insulin for efficient glycaemic control. | Diet; anti-hyperglycaemic drugs and physical exercise. |
| **Principle complications** | Retinopathy, nephropathy, hypoglycaemia, diabetic ketoacidosis, atherosclerosis, neuropathy, diabetic foot disease | Atherosclerosis, neuropathy, diabetic foot disease, retinopathy, nephropathy |

**Table 1-1: Primary features of type 1 and type 2 diabetes mellitus.**

Diabetic foot complications are typical of type 2 diabetes mellitus imposing a huge socio-economic (accounting for 5% of the total National Health Services resources in the UK) burden on the patient and healthcare services (Boulton 1998; Currie, Poole et al. 2007).

### 1.2.2 Epidemiology and outlook

There were 171 million diabetics worldwide in the year 2000 (World Health Organization 2004), an increase of nearly 150 million during the last 15 years. This dramatic rise has been widely attributed to sedentary lifestyle, lack of awareness/education, high population density and obesity (Gill 1998; Ha and Lean 1998). It is predicted that by the year 2030, the total number of diabetics worldwide will reach approximately 366 million, with a 150% increase in diabetics in developing countries (World Health Organization 2004).

In the developed countries, the number of diabetics is typically estimated to be 2-6% of the population. However, the prevalence is relatively higher i.e. 10-20% of the population, for those over the age of 65 (Campbell and Lebovitz 1996). In 2003, the countries with the highest number of diabetic population were India (35.5 million), China (23.8 million), USA (16 million), Russia (9.7 million) and Japan (6.7 million) (International Diabetes Federation 2003). Currently, there are 1.8 million people suffering from diabetes in the UK (World Health Organization 2004). Recent statistics published by the American Diabetic Association suggest that prevalence of diabetes in the United States is 16 million and onset of type 2 diabetes mellitus preceded its diagnosis by 7 years on average (O'Brien, Patrick et al. 2003).

The use of insulin and anti-hyperglycaemic drugs has greatly improved the life expectancy of those affected by diabetes. Impaired glycaemic control leads to similar acute and chronic complications in both types of diabetes mellitus. In type 2 diabetes mellitus, abnormal blood sugar levels even at early stages can cause damage to nerves, blood vessels, heart, eyes leading to neuropathy, peripheral vascular disease, diabetic foot

disease and retinopathy (Herman and Crofford 1998; Pendsey 2003). Diabetic complications lead to a reduced quality of life for the patient and impose high costs on the health care service (World Health Organization 2004). The costs associated with the treatment and management of diabetic foot disease include treatment of foot ulcers, clinical diagnosis of underlying complications and limb amputations. A total annual cost of £252 million has been estimated towards the management of foot complications alone for the National Health Services in the UK (Gordois, Scuffham et al. 2003).

### 1.2.3 Aetiology

Diabetes is an incurable and chronic disease; yet it is treatable and long term complications can be prevented by glycaemic control. Insulin is primarily manufactured, stored and released by the pancreas through Beta cells in the Islets of Langerhans. Insulin is crucial for regulation of blood sugar by transporting it to various body cells. Thus, it is an anabolic hormone. It instructs the liver and muscles to manufacture and store glycogen, which is useful in the event of low blood sugar. The conversion of stored glycogen into glucose is facilitated by release of glucagon hormone by Alpha cells in the pancreas. Failure to regulate blood sugar appropriately can lead to hypoglycaemia or hyperglycaemia.

Type 2 diabetes is a heterogeneous collection of conditions resulting from various degrees of insulin resistance and beta cell failure (Tooke 1996). Obesity is the major cause for insulin resistance in type 2 diabetes mellitus and affects the ability of the body to utilize the glucose transporting effects of insulin. The overweight tend to be insulin resistant as a group. This hereditary condition is directly related to the ratio of visceral and total body fat to lean body mass (Bernstein 2003).This increases the body's need for insulin and therefore, puts pressure on the pancreas. This also leads indirectly to high blood pressure (hypertension), a prevalent complication of diabetes.

## 1.2.4 Complications of diabetes mellitus

Diabetes mellitus leads to both acute and chronic complications, particularly affecting the microvascular and macrovascular systems (Boulton, Connor et al. 1998; Herman and Crofford 1998). Microvascular dysfunction is associated with the prevalent complications of retinopathy, nephropathy and neuropathy. Macrovascular disease is associated with cardiovascular, cerebrovascular and peripheral vascular complications. Macroangiopathy is common to both diabetic and non-diabetic populations and is marked by plaque deposition and endothelial wall damage (atherosclerosis). However, there is a higher incidence and rate of development of macroangiopathy in the diabetic. The adhesion molecules that facilitate binding of monocytes, leukocytes and platelets to the endothelium are elevated in diabetes (Shaw and Boulton 1997). These macrovascular complications have a reduced rate of occurrence in the non diabetic groups and are less likely to co-exist (Levin 2001). The most commonly occurring diabetic complications that specifically affect the lower extremities are peripheral vascular disease and neuropathy.

Peripheral vascular disease (PVD) is characterised by atherosclerosis in patients with long standing diabetes mellitus. Peripheral vascular disease is up to twenty times more prevalent in diabetic than in the non diabetic population (Currie, Morgan et al. 1998). Peripheral vascular disease leads to rheological changes in the blood and can impair the nutritional supply to the lower extremities, making the foot more susceptible to ulceration in the presence of a triggering factor such as minor trauma.

Neuropathy refers to metabolic changes and poor blood supply in nerve cells as a result of altered blood glucose in diabetes. Diabetic neuropathy is the most common complication of diabetes, a major cause of foot ulceration and a considerable clinical burden (Elkeles and Wolfe 1991). The true prevalence of diabetic neuropathy is difficult to quantify because of variations in diagnostic criteria (Tooke 1996). Neuropathy is divided into sensory neuropathy, motor neuropathy and autonomic neuropathy. Sensory neuropathy affects the bodies ability to sense pain, thermal or vibratory stimuli (Shaw and Boulton 1997). Motor neuropathy affects muscle control (imbalance of flexor and

extensor muscles) and involuntary bodily functions (Ward and Tesfaye 1998). Autonomic neuropathy is characterised by sympathetic dysfunction in which blood flow in most of the microcirculation increases (Watkins and Edmonds 1998).

Good glycaemic control is the best preventive measure against microangiopathic or neuropathic complications. This is especially important for people with insulin dependent diabetes in order to retard the development of retinopathy, nephropathy and neural disease. This was confirmed by the Diabetes Control & Complication Trial (1993), in which a long term prospective study to gauge the effects of improved glycaemic control in diabetics found: a 75% reduction in progression of early neuropathy; 50% reduction in the risk of kidney disease; a 60% reduction of risk for nerve damage; and, a 35% reduction in the risk of cardiovascular disease (The Diabetes Control & Complication Trial Research Group 1993). It is not known if the benefits of good glycaemic control could be extrapolated to the larger (type 2) non insulin dependent diabetic group (Tooke 1996). Lack of awareness or motivation, presence of sensory neuropathy and failure to adopt simple preventive measures leads to limb threatening complications and lengthy hospital stay (Brand 1990; Knowles and Boulton 1996; Viswanathan, Madhavan et al. 2005). This shows the need of alternative preventive strategies, especially to identify pre-ulcerous symptoms in order to reduce the clinical burden and improve patient lives. Unfortunately, glycaemic control alone cannot substitute the benefits of preventive strategies like patient education (St. Vincent's Declaration, Appendix A) and special care of patients with past history of ulceration. Studies have shown that many diabetics do not have adequate glycaemic control, due primarily to sedentary lifestyle, inappropriate administration of hypoglycaemic drugs and delayed insulin treatment (Groop 1998). However, the relatively recent availability and use of visual modalities for home monitoring and clinical assessment may improve current management of the diabetic foot disease (Lavery, Higgins et al. 2004; Bharara, Cobb et al. 2006).

## *1.3 Diabetic foot*

### 1.3.1 Introduction

Complications, risk factors and symptoms of the diabetic foot are summarised. Diabetic neuropathy and its effect on the diabetic foot are discussed in detail.

### 1.3.2 Complications, risk factors and symptoms

Diabetic foot is the most commonly occurring complication of type 2 diabetes mellitus. It is associated with foot ulceration, which has traumatic consequences for the patient, often leading to amputation of the lower limb. Two precursors of ulceration in diabetic patients are peripheral vascular disease and neuropathy which may occur independently or coexist. Peripheral vascular disease is also referred to as ischaemic foot disease.

Although, neuropathy and ischaemia are regarded as primary risk factors in the diabetic foot, a clear understanding of the pathophysiology of foot ulceration needs to be established. Other pathologic states or secondary risk factors that contribute to ulceration are structural changes in the foot (or foot deformities), callus, previous history of ulceration/lower limb amputation, chronic renal failure, impaired vision, low education status, non-compliant patient, inappropriate footwear, abnormal biomechanics and infection (Grunfield 1992). It is believed that the occurrence of ulcers is due to a combination of two or more risk factors. The risk of foot ulceration is higher in people with a previous history of ulceration, poor circulation in the feet, smokers and those who have anatomical deformities in feet (Boulton, Connor et al. 1998).

Ulcers invariably occur as a consequence of interaction between environmental hazards and specific changes in the lower limbs of certain patients (Boulton, Connor et al. 1998; Perkins and Bril 2002). Intrinsic or extrinsic trauma triggers foot ulceration. Consequently, the foot becomes prone to ulceration especially at sites of abnormal pressure such as the prominent metatarsal heads. There is no compelling evidence to

suggest that infection is a cause of foot ulcers. Infection occurs as a complication of an existing neuropathic or ischaemic ulcer or alternatively, results from breaks in the skin due to dryness or fungal infection (Grunfield 1992). With improved diabetic foot management and early detection of high risk patients, the rate of foot infections can be significantly controlled (Boulton, Connor et al. 1998).

Foot ulcers can be classified as neuropathic, neuroischaemic and ischaemic. It is suggested that an average rate of occurrence for neuropathic ulcers is 60-70%, whereas the rate of occurrence for ischaemic ulcers is just 15-20% (Grunfield 1992; Boulton, Connor et al. 1998). One of the longer studies in UK, involving 6336 diabetics showed a 58% and 16% rate of occurrence for neuropathic and ischaemic ulcers in type 2 diabetic patients (Nabarro 1991). The study population was limited to tertiary referrals. It is important to discriminate between the neuropathic and neuroischaemic foot; the clinical presentation of these conditions is different, so are subsequent therapeutic strategies (Tanenberg, Schumer et al. 2001). Photographs 1-1 and 1-2 show examples of a neuropathic ulcer and a neuroischaemic ulcer respectively in the plantar foot (Pendsey 2003).

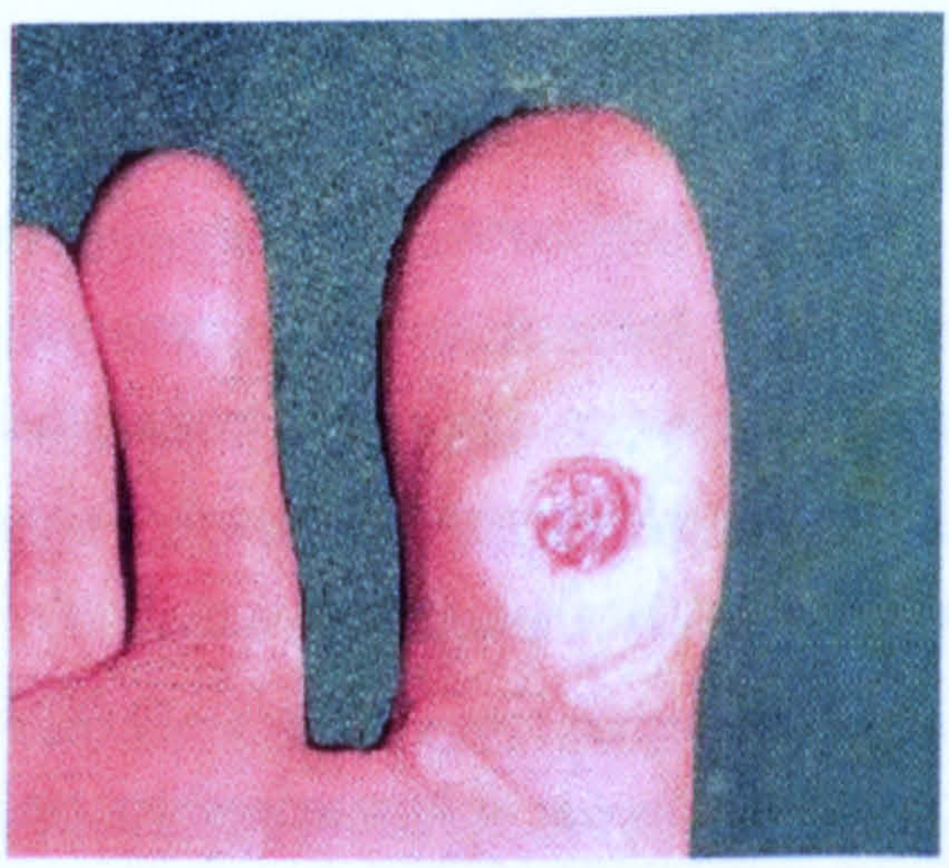

**Photograph 1-1: Neuropathic ulcer on the great toe. Forty percent of plantar ulcers are situated either on the ball of the great toe or the head of first metatarsal. A neuropathic foot is typically warm, painless and has palpable foot pulses. (With Permission- Pendsey 2003)**

**Photograph 1-2: Neuroischaemic ulcer on the periphery of little toe. Typically, this ulcer results from ill-fitting shoes leading to high frictional forces at the margins of the toe. A neuroischaemic foot is typically cold, painful and has feeble or non palpable foot pulses. (With Permission - Pendsey 2003)**

Three parameters that may be used for identification of neuropathy or neuroischaemia in the diabetic foot are skin temperature, pain and the Ankle Brachial Pressure Index (ABPI) (Pendsey 2003). Of these, both temperature and ABPI are objective measurements, the latter being widely available. It is important to point out that ABPI in the diabetic foot may be subject to errors (falsely high) on account of stiffening of the intimal layer of the arteries that is known to occur as a result of arterial calcification (Palubo and Melton 1985; Hurley, Jung et al. 2001). Methods of assessment and treatment of the diabetic foot are considered in more detail in the following sections.

### 1.3.3 Assessment techniques for complications of the diabetic foot

Various screening and monitoring techniques are routinely employed in hospitals as well as speciality diabetic clinics. Presently, clinicians routinely assess circulatory function, neuropathic complications and pressure distribution under the foot to identify the risk of foot ulceration (NHS 2004). This combined approach is accepted in diabetic clinics and research centres as a means of preventing the onset of foot ulceration. National Institute of Clinical Excellence (NICE) guidelines suggest considering the risk category of patients, relative influence of all contributory factors and incorporating the respective

management strategies for the treatment of diabetic foot disease during initial examination and subsequent treatment.

During a routine inspection, detailed physical examination of the whole foot is performed and important clinical symptoms such as swelling/oedema, increased temperature, ischaemia, scar tissue, callus, reduced sensitivity, deformities, dry fissured skin, injury by a sharp object, limited joint mobility, thermal trauma and any other sign of deterioration of the foot are recorded (Millington and Ellenzweig 2003; Pendsey 2003). Most diabetic clinics use patient case sheets to monitor the foot along with other complications. Detailed physical examination of the foot must be followed by inspection of the patient footwear for signs of excessive wear, any embedded objects and adequacy of fit. These signs may act as a triggering factor for the insensitive foot leading to ulceration.

Clinical criterion for diagnosing diabetic foot complications have been defined by various groups. It is common in clinical practice to assess the presence and extent of peripheral neuropathy to identify the risk of foot ulceration. Diabetic neuropathy accounts for almost 60-70% of foot ulcers (Grunfield 1992; Morbach, Lutale et al. 2004; Viswanathan, Madhavan et al. 2005; Viswanathan, Madhavan et al. 2006) especially on the plantar surface of the foot at areas subjected to high pressure during walking. Traditionally the Semmes-Weinstein monofilament (SW) is used though biothesiometry may also be used for the assessment of neuropathy (Viswanathan, Snehalatha et al. 2002; Miranda-Palma, Sosenko et al. 2005). The presence and extent of peripheral vascular disease can be assessed using Doppler ultrasound (Hill 1987; Williams , Picton et al. 1993), plethysmography (Felder, Russ et al. 1954; Hurley, Jung et al. 2001) or laser Doppler flowmetry (Cobb 2000), to determine systolic pressure/perfusion status at the ankle or great toe respectively.

### 1.3.4 Management of foot in diabetes

Management of the 'at risk' diabetic foot is essential to prevent the serious consequences of ulceration. Current focus is on a nutritious diet, patient education, collaborative

research and early diagnosis of the high risk patients to control disease complications (St. Vincent Declaration, Appendix A). The International consensus on the Diabetic Foot proposes that good management, patient & staff education, evidence based medicine and multidisciplinary treatment for foot ulcers can reduce amputation rates by 49-85% (IWGDF 1999). This will reduce the high rate of morbidity/mortality associated with the disease and high treatment costs. The overall burden of diabetes mellitus and its complications includes financial cost, pain, anxiety, immobility, inconvenience and reduced quality of life (World Health Organization 2004).

Modern medical imaging techniques such as magnetic resonance imaging (MRI), scintigraphy, radiography (Fisher, Gilula et al. 2001) and ultrasonography (Hill 1987), can be used to test the bone and vascular supply to the foot. However, this is usually not cost effective for routine evaluation. Thermography and scintigraphy (to detect infection in the bone) are also used, particularly to test for the Charcot's foot i.e. a destructive arthropathy in a single or multiple joints (Pendsey 2003). Both techniques are used independent of each other, the former shows better sensitivity for foot infections (Harding, Banerjee et al. 1999) and the latter benefits from high specificity (Poirier, Garin et al. 2002).

MRI is capable of resolving between the skin, soft tissues, blood vessels and bone and has proved useful in identifying areas of oedema and infection (Brash, Foster et al. 1999; Kao, Davis et al. 1999). MRI has proved to be a useful research tool to design suitable orthotic interventions, reducing rates of re-ulceration, identifying soft tissue damage, PVD, muscle atrophy and toe deformities (Foster, Damion et al. 1994; Bus, Yang et al. 2002; Cavanagh, Lipsky et al. 2005). Further, the availability of small bore MRI scanners customised for lower extremity scanning (ONI Medical Systems, USA) has facilitated the above initiatives. It is the high cost of clinical scanning and limited availability in developing economies that discount its use in routine investigations. Although imaging is used for a broad range of clinical conditions, its application to the diabetic foot is recent (Brash, Foster et al. 1999; Fisher, Gilula et al. 2001; Aspres, Egerton et al. 2003; Armstrong, Sangalang et al. 2005; Minamishima, Kuwaki et al. 2005). Traditionally,

clinicians use visual inspection of the superficial skin surface followed by histopathology of biopsy samples (Boulton, Connor et al. 1998). Interest in using imaging techniques such as photography of the skin (Aspres, Egerton et al. 2003), surface microscopy (Lamah, Mortimer et al. 1999), ultrasonography (Williams , Picton et al. 1993) and laser Doppler (Cobb 2000) to image underlying tissue characteristics and blood vessels (for perfusion and haemodynamics) has grown over the past few years.

## *1.4 Summary*

Diabetes mellitus is a disease with multi-system complications and it involves breakdown or partial breakdown of one or more of the important self regulating mechanisms in the body. Diabetic foot is the most commonly occurring complication of diabetes mellitus. The most important socio-economic consequences of the diabetic foot are the risk of foot amputation to the patient and economic burden on the health care services. In the UK, the total annual cost of treating diabetic neuropathy and its complications was £252 million (Gordois, Scuffham et al. 2003). Early detection of risk factors is important in preventing the development of ulceration. Current methods for determination of the risk of foot ulceration are the assessment of circulation, neuropathy and foot pressure. These methods are widely used clinically as well as in the research domain. Routine neuropathic evaluation includes assessment of sensory loss in the plantar skin of the foot using both the Semmes Weinstein monofilament and vibratory perception using the Biothesiometer. These methods use point based measurements and are subjective in nature, relying on verbal feedback from the subject.

Although, there is extensive evidence in the literature suggesting degeneration of thermoreceptors in the plantar foot due to underlying neuropathic complications, thermological measurements of the foot to assess responses to thermal stimuli and cutaneous thermal discrimination threshold are relatively uncommon (Armstrong, Lavery et al. 2003; Bharara, Cobb et al. 2006). Applications of thermography and thermometry in lower extremity wounds, vascular complications and neuropathic complications have progressed as result of improved imaging software and transducer technology. However,

the uncertainty associated with the independent thermal testing modalities, the costs, and processing times make currently available techniques unsuitable for routine clinical assessment. Furthermore, assessment of plantar foot temperature in the diabetic foot is complicated by the problem of obtaining data during normal conditions of loading i.e. standing and walking. This is important as ulceration is strongly related to tissue loading and does not occur in patients with pressure relief. Armstrong et al. (2003) suggest that one time thermal screening of the plantar foot is not useful and emphasise the importance of home monitoring of temperatures under the feet to record trends and inflammatory responses. Ideally, the thermal technique and associated measurement protocol used should be economical, simple and safe. Risks associated with the measurements such as thermal injury to the foot, any physical trauma during measurement (such as fall from the platform, caused by potential instability due to sensory impairment) and cross infection must be minimised.

The objective of this research is to overcome the preceding difficulties and thus enable reliable temperature measurements of the plantar foot to be made in order to establish if abnormal thermological measures are associated with sensory neuropathy. It is envisaged that this may be used as a full-field quantitative screening technique to identify diabetics at high risk of foot ulceration and allow improved intervention (i.e. pressure relief orthotics) to reduce the risk of ulceration.

## 1.5 Aims

Two main aims of this research are:

- To develop a liquid crystal thermography system capable of dynamically monitoring microvascular response to thermal stimulus at the plantar surface of human foot.
- To develop a robust method for obtaining an independent measure of plantar sensory neuropathy.

Thermal measurement techniques can be employed to study pathophysiology of the vascular system and neuronal control in the diabetic foot disease (Bharara, Cobb et al. 2006). LCT offers the potential to improve current diagnostic potential of diabetes and foot related disorders. However, the use of this technology and engineering techniques complementing the development of such a clinical system must be justified and validated using existing knowledge of the diabetic foot disease. A supporting clinical study is required to provide reasonable evidence in furthering the role of thermal measurements in clinical measurement of diabetic foot disease. The system under consideration and its measurement protocol must be independent of the LCT studies in the past (Stess RM, Sisney PC et al. 1986; Benbow, Chan et al. 1994). The limitations of the past studies and justification for the LCT system are discussed in the literature review. The system must be capable of both static and dynamic assessment of the diabetic foot. In order to supplement the existing measures of clinical neuropathy, an independent measure of sensory neuropathy is required, the proposal being to use a LCT system to assess the response of thermoreceptors under the plantar foot to thermal stimulus.

## *1.6 Overview of the thesis*

In Chapter 2 'Theoretical background', important anatomical and physiological aspects of the plantar foot relevant to the diabetic foot disease are discussed. Temperature regulation in the plantar foot and underlying factors are presented.

In Chapter 3 'Literature review', prior work in the field of clinical thermography, various thermological techniques and their application to the diabetic foot are reviewed, including practical details about the technology. Fundamentals of LCT and justification for its use in the assessment of the diabetic foot are described.

Chapters 4 'Development of a liquid crystal thermography system' and 5 'Results' focus on the specific issues of system development, and analysis of results from preliminary in vitro and clinical data. Chapter 4 covers the methodology adopted, various designs of the measurement system, characterisation of different forms of TLC and clinical study

protocol. Chapter 5 'In vitro characterisation and clinical results' describes the handling of results and presents both in vitro evaluation and in vivo evaluation of the LCT system.

Chapter 6 'Discussion' considers the clinical implications of the study and presents discussion of the preceding results related to the physiological issues and current knowledge of the diabetic foot. Chapter 7 'Conclusions' is a critical review of the study and provides recommendations for future work emphasising the wider clinical perspective.

# Chapter 2 Theoretical Background

## *2.0 Introduction*

The aim of this section is to review the anatomy and physiology of the foot with emphasis on those aspects of particular relevance to the diabetic foot. Foot skin structure and properties, microcirculatory mechanisms and temperature regulation are considered in detail. Additionally, the biomechanics of the plantar foot are considered with emphasis on their status in normal healthy human beings and pathophysiological changes in the diseased state. In the second half of the chapter, diabetic neuropathy and relevant assessment techniques are discussed.

## *2.1 The plantar foot*

### 2.1.1 Anatomy & physiology of the plantar foot

The foot comprises 26 bones and 11 muscles along with various ligaments and tendons. Both tendons and ligaments are support structures made up of collagen fibres. The skeletal structure of foot includes posterior tarsus (hind foot), central metatarsus (mid foot) and interior phalanges (forefoot). Two bones of the hind foot provide a structural link between the foot and bones of the lower leg. A large number of ligaments form a strong connection between the calcaneous and the bones of the mid foot as well as forefoot. The calcaneous is connected to the Achilles tendon and plantar fascia, both of which provide support allowing the foot to arch during gait.

Under the calcaneous a thick layer of adipose tissue provides a protective cushioning that accommodates high pressure during gait. The internal structure of the bone is also adapted for weight bearing. The midfoot comprises of cuboid, navicular bones and three anterior cuneiform bones. The anterior surface articulates with the cuboid bone of the midfoot. The talus is angled slightly forward and medially to couple the force between the tibia and the calcaneous. The anterior aspect of the talus connects to the navicular

bone of the midfoot. The five tarsal bones (connected to the metatarsal bones) work together as a group and help during gait by conforming to the underlying contact surface. The first, second and third metatarsals are articulated by anterior medial, intermediate and lateral cuneiforms respectively. There are five metatarsal bones in the forefoot and a similar number of phalanges that form corresponding toes. The joints between the metatarsal bones and phalanges are the metatarsophalangeal (MTP) joints. Figure 2-1 illustrates skeletal structure of the foot.

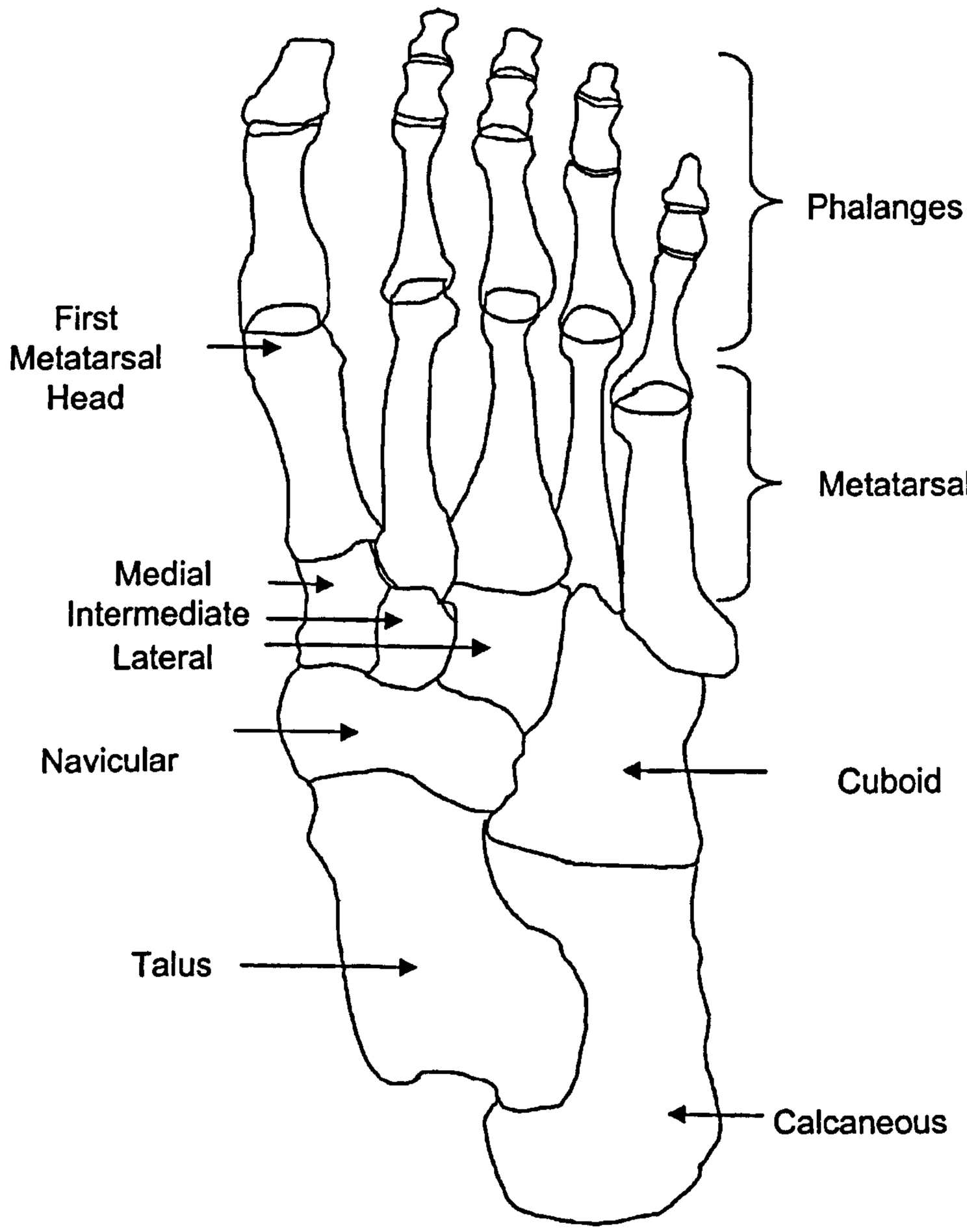


**Figure 2-1: Skeletal structure of the foot**

Two important arteries of the plantar foot are the posterior tibial artery and anterior tibial artery. These main arteries branch into further segments, supplying the midfoot and the forefoot. The lateral and medial plantar arteries supply the Planta pedis - a rich network of blood vessels in the plantar foot. The venous network in the dermal tissue converges into the dorsal venous network. The plantar veins do not have valves and therefore, the direction of blood blow is determined by the dorsal veins (McMillan 2001).

### 2.1.2 Skin structure of the plantar foot

The skin is the largest organ of the human body, accounting for 7-10% of body weight. The three main layers of the skin are the epidermis, dermis and subcutaneous fat tissue. Figure 2-2 illustrates the structure of the skin and microvasculature.

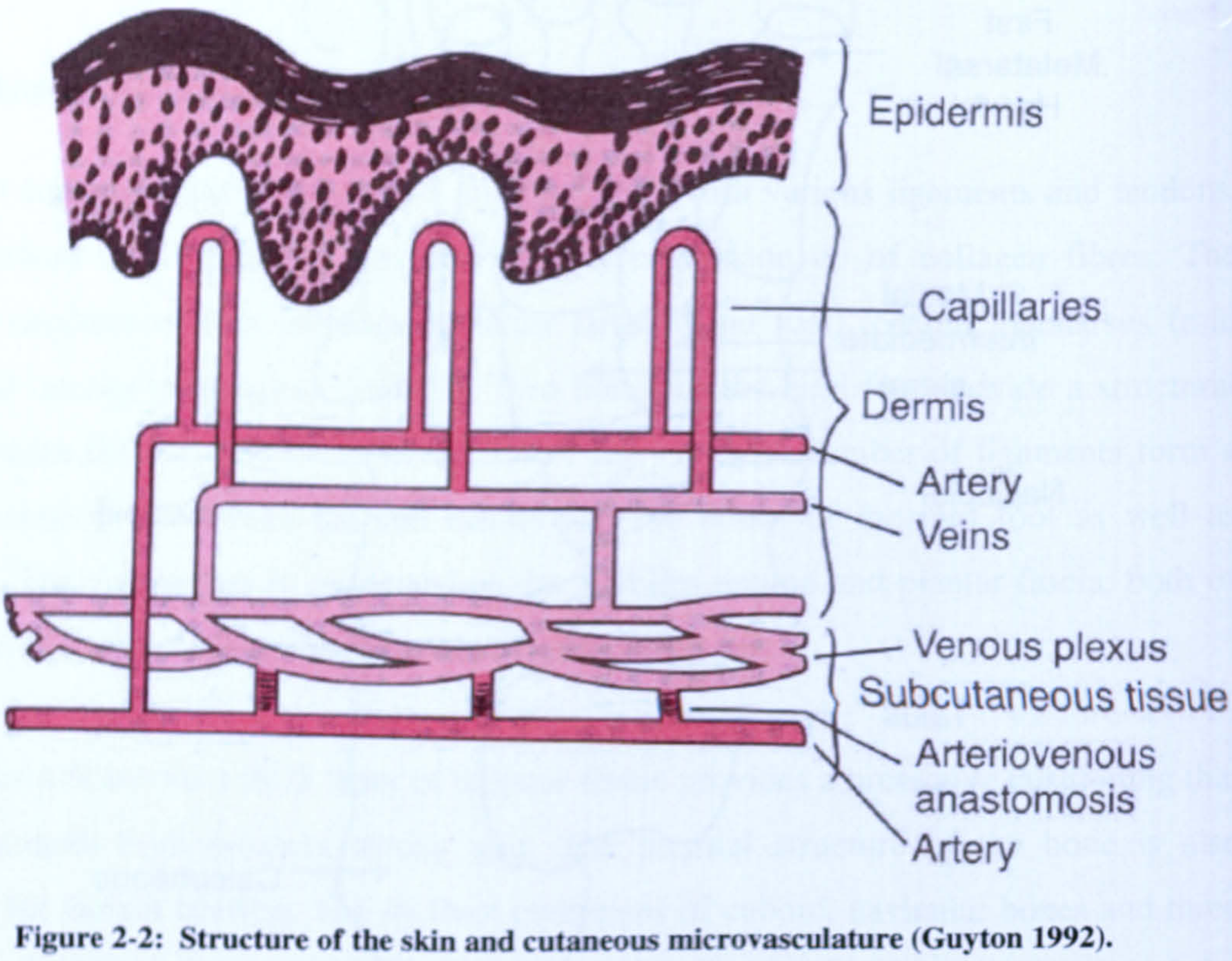


**Figure 2-2: Structure of the skin and cutaneous microvasculature (Guyton 1992).**

The top layer of the epidermal tissue, the stratum corneum, acts as a physical barrier between the skin and the environment. It prevents ingress of harmful chemicals and

micro organisms. It is produced by keratinocytes in the lower epidermal tissue (also termed stratum basale or basal layer). The epidermal tissue is typically 0.007-0.12mm thick (Van De Graff and Fox 1992).

The dermal layer (also termed as corium) lies beneath the epidermis, containing circulatory network, lymphatic vessels, sweat glands and neural fibres/tissues. This layer is typically 1-2 mm thick (Van De Graff and Fox 1992). It supports localised metabolic requirements and plays an important role in regulating body temperature and blood pressure.

The subcutaneous tissue (also referred to as hypodermis) contains adipose tissue and bridges the skin to the underlying tissues. This is typically a thick layer extending several millimetres. The adipose tissue provides thermal insulation for the body and protection against physical shock. In the context of the present study this protective mechanism is of particular importance at those plantar locations subject to repetitive wear. Consequently, skin thickness on the sole of the foot can increase to about 6mm in normal subjects (Palastanga, Field et al. 1994).

### 2.1.3 Plantar sensory system

The dermis is extensively innervated with effectors and sensory receptors. Sensory receptors are specialised tissues that detect stimuli and are represented by tactile, pressure, thermal or pain sensitive nerve cells. The concentration of sensory receptors is relatively high in the sole of the foot (Kennedy and Inglis 2002). The receptors and pathways of cutaneous sensation are categorised as somatosensory systems.

Thermoreceptors are structurally simple and are located near the surface of the skin (extereoceptors). Mechanoreceptors have a more complicated structure and are differentiated according to their response characteristics: The slowly adapting type is sensitive to the intensity of pressure; The rapidly adapting and very rapidly adapting

types respond to dynamic changes in plantar pressure (Guyton 1992). Skin temperature changes activate both, specific thermoreceptors and tactile receptors.

Sensory receptors have a punctate distribution over the skin surface i.e. specific points are sensitive to different stimuli. Cold receptors are located at a depth of 0.16 mm at the endings of thin myelinated Aδ fibres and increase their firing rate with a decreasing temperature (Van Someren, Raymann et al. 2002). Figure 2-3, gives a schematic overview of specific temperature ranges that affect thermoreceptors (Guyton 1992).

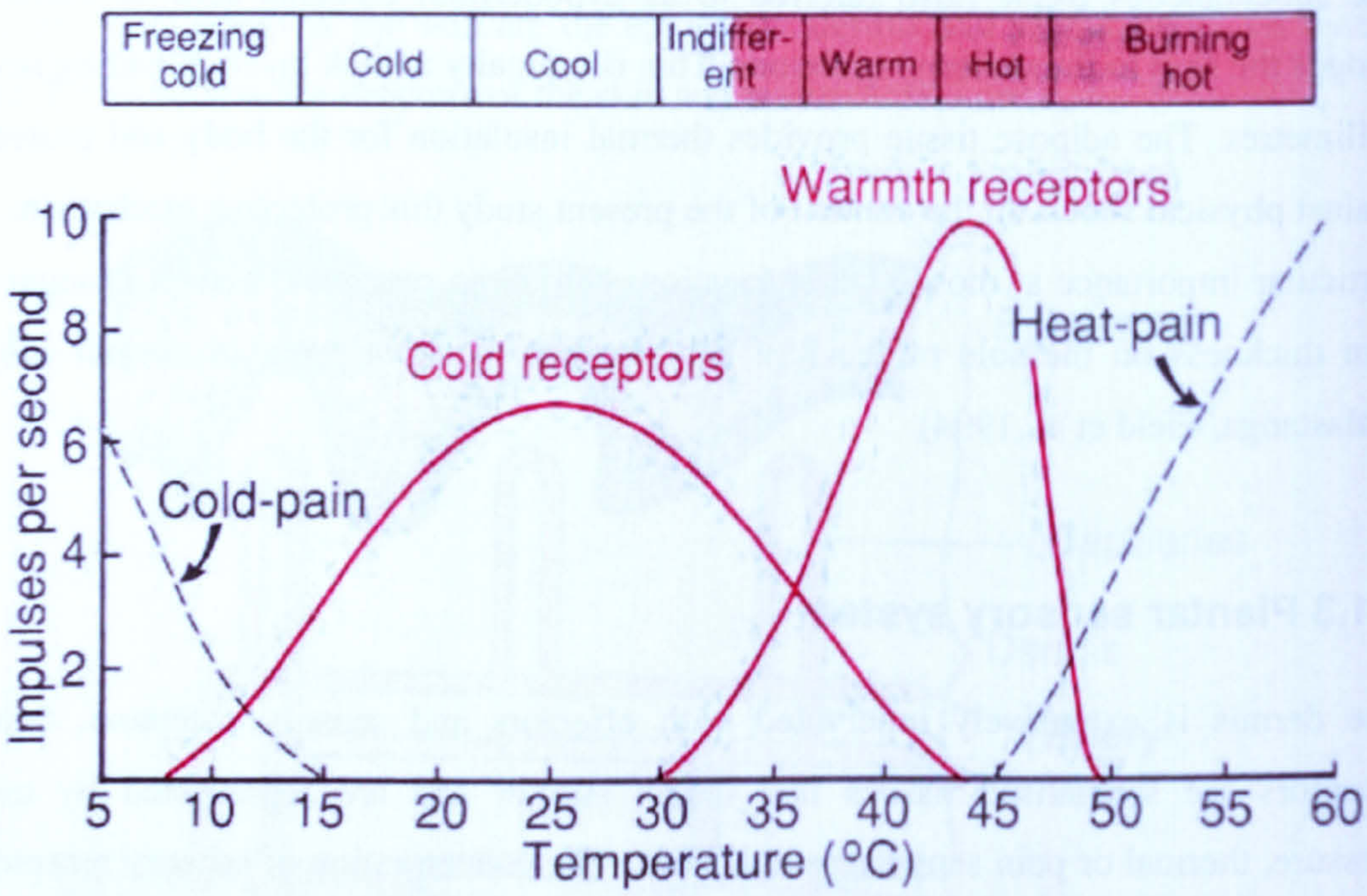


**Figure 2-3: Overview of the temperature range that affects thermoreceptors (Guyton 1992)**

Warm receptors are located typically at a depth of 0.45 mm at the endings of slower unmyelinated C fibres and increase their firing rate with increasing temperature (Van Someren, Raymann et al. 2002). Cold receptors outnumber warm receptors by a factor of 3-10 in most areas of the body, this may be linked to evolution and is independent of the habitat (Guyton 1992). Both types of thermal receptors communicate with the central nervous system to adapt to the environmental/ambient conditions, vascular changes,

skeletal changes, infection or a combination of these factors, mainly by the use of thermoregulatory capillaries.

### 2.1.4 Structure of cutaneous microcirculation

The arterioles terminate in meta-arterioles (link between arteriole and venule) and capillaries that together form the microcirculatory network. Capillaries are thin walled micro-vessels (less than 100μm diameter) that extend orthogonal to the meta-arterioles to perfuse the tissue. The anatomy of the microcirculatory components vary considerably at different body sites and between individuals (Ryan 1985). At some body sites especially fingers, toes, palms and face arteriovenous (AV) anastomoses or AV-shunts are observed. The AV-shunts are larger diameter vessels and are the primary heat exchange mechanism and play no role in tissue nutrition (Little and Little 1989). AV-shunts do not exhibit autoregulatory behaviour in response to physical or metabolic triggering factors.

Cutaneous microvascular blood flow in diabetic patients is frequently abnormal and has been linked to microangiopathy and impaired blood flow regulation as a consequence of autonomic neuropathy (Rayman, Williams et al. 1986b; Flynn, Edmonds et al. 1988; Flynn and Tooke 1995).

Clinically, the consequences of diabetic microangiopathy are most significant in relation to complications of the retina and kidney. However the process is systemic progressively involving the majority of capillary beds. Relatively high blood flow rates lead to pressure gradients in the lower extremities which are responsible for the increased incidence of cutaneous microangiopathy (Rendell and Bamisedun 1992). This accounts for the relatively low incidence observed in the upper extremities.

### 2.1.5 Regulation of microvascular blood flow

There are 2 main types of capillaries involved in skin perfusion: thermoregulatory and nutritive. Thermoregulatory capillaries facilitate the primary heat exchange mechanism

required to maintain body temperature. Blood flow in these vessels is controlled by the hypothalamus in response to thermoreceptor signals. Heightened metabolic activity produces vasoactive substances, which triggers a vasodilatory response in skin (Guyton 1992). This is an autoregulatory mechanism which results in a hyperaemic response (elevated blood flow) following short term occlusion of blood vessels, biomechanical trauma or thermal stress. From the physiological standpoint, hyperaemia is a transient phase triggered by mechanical trauma to the muscular walls of arterioles or following release of a vasoactive substance, such as histamine, leading to full arteriole vasodilation (Michel and Gilliot 1990; Guyton 1992) .

Below 25°C skin surface temperatures, centralised control of microcirculation, plays a dominant role to stabilise changes in core body temperature (Guyton 1992). At skin surface temperatures above 30°C, thermoreceptors initiate sweating to radiate heat away from the body. At rest, nutritional perfusion is greatly reduced in comparison to the thermoregulatory component (Fagrell 1984).

### 2.1.6 Biomechanics of the foot

Poor glycaemic control in diabetes results in plantar sensory neuropathy, which coupled with biomechanical abnormalities, such as, high stresses, deformity, limited joint mobility and injury leads to high rates of morbidity in diabetic patients (Pendsey 2003; Viswanathan, Snehalatha et al. 2003; Edmonds, Foster et al. 2004). It is therefore, relevant to discuss biomechanical aetiology and its role in plantar ulceration/wound healing, especially in patients with loss of protective sensation (Cavanagh, Ulbrecht et al. 2001). Such patients are at an even greater risk of plantar ulceration because of elevated mechanical stress on the plantar surface (Cavanagh and Ulbrecht 1995; Cavanagh, Ulbrecht et al. 2001). Although plantar sensory neuropathy is a precursor of ulceration, a triggering factor, which may often be unperceived tissue trauma and/or a biomechanical abnormality, initiates the individual ulcerative process.

The underlying mechanisms initiated by biomechanical abnormalities are well established (Bauman, Girling et al. 1963; Brand 1981; Cavanagh, Ulbrecht et al. 2001). In the current biomechanical framework, foot pressure (both in shoe and barefoot) and gait analysis are the two main type of assessment used to understand and measure the affects of abnormal biomechanics. Prescription footwear is followed as an intervention therapy to redistribute stresses under the foot. However, foot temperature under load could also be a useful assessment in order to further current understanding of causative factors leading to foot ulceration. Artificial provocation tests for repetitive stress measurements, such as a treadmill or normal walking can be used to determine temperature gradients before and after the stress in both normal subjects and diabetic neuropaths. This is discussed in detail in the next chapter. Presently, it is beneficial to review the effects of pressure on the plantar foot and techniques to quantify such pressures. This identifies some of the key issues in assessing the diabetic foot which are also pertinent for thermal assessment modalities.

### 2.1.7 Plantar pressure and measurement techniques

Mechanical stresses on the plantar surface comprise two components i.e. normal and orthogonal components. Alternatively, these stresses are termed vertical and shear respectively. The term 'plantar pressure' used consistently in the literature is actually the force measured over a small defined area, especially plantar prominences and the heel. Plantar measurement technologies are summarised here, the reader is referred to several review papers for a more detailed consideration of the techniques (Lord, Reynolds et al. 1986; Cobb and Claremont 1995).

A number of commercially available plantar pressure measurement systems capable of assessing load and shear are finding increasing clinical adoption in diabetic care centres throughout the world (Lord and Hosein 2000; Raspovic, Newcombe et al. 2000; Viswanathan, Madhavan et al. 2004; Viswanathan, Sivagami et al. 2004) . Critical reviews by Lord M et al. (1986), Cobb and Claremont (1995) discuss transducers for foot pressure measurement and their respective clinical findings.

Although the use of plantar pressure measurement is widely accepted from an investigational and clinical standpoint in the diabetic foot assessment, there is variability between different instruments due to inconsistent calibration and measurement protocols (i.e. variations in gait characteristics such as speed, stride length) and a lack of agreement regarding the threshold pressure for ulceration (Hayes and Seitz 1997; Middleton, Sinclair et al. 1999; Urry 1999; Chesnin, Selby et al. 2000; Randolph, Nelson et al. 2000; Taylor, Menz et al. 2004).

The majority of the plantar pressure systems enable barefoot measurements via arrays of: force sensing resistors (FSR) (Nicolopoulos, Solomonidis et al. 1995), piezoelectric sensors, optical waveguides (Wolinski, Nasilowski et al. 1998) and photoelastic materials (Arcan and Brull 1976; Rhodes, Sherk et al. 1988). Discrete sensors such as capacitive, piezoelectric, optical and magneto resistive sensors have also been used for insole pressure measurement devices (Akhlagi and Pepper 1996; Lord and Hosein 2000; Barnett, Cunningham et al. 2001). Insole pressure transducers provide localised information across multiple gait cycles. The popular Tekscan matrix insole technique uses FSR transducers embedded in a thin flexible sole. Such an arrangement overcomes the problems of targeting and barefoot walking as transducers can be located at appropriate sites of interest (Lord M, Hosein R et al. 1992).

Forceplate type systems capture one step from a walk. For such systems, synchronised measurement of specific periods of the gait cycle (for example: heel strike) is difficult (Hurkmans, Bussmann et al. 2003). The centre of pressure pattern (COPP), quantified by its absolute integral has been used to describe abnormal foot movement and to asses foot orthoses (Middleton, Sinclair et al. 1999; Chesnin, Selby et al. 2000). For data collection purposes, EMED-SF & EMED PEDAR pressure platforms were used for data at the shoe-floor interface and to obtain in shoe data, respectively.

The use of the preceding types of system in a large number of clinical studies over the last two decades has provided definitive evidence that diabetic neuropathic ulcers are

associated with elevated plantar pressures. The effects of such pressures on foot physiology are considered in the following section.

## 2.1.8 Effects of plantar pressure on the microcirculation

An immediate effect of applying pressure to skin tissue is reduction in perfusion, evidenced by blanching. If sustained pressures are higher than the normal capillary pressure of 30-32 mmHg, collapse of blood vessels occurs (Kabagambe, Swain et al. 1994). Whilst recovery is usually possible within a typical period of 12 hours following unloading, longer periods or repetition result in tissue necrosis as a consequence of inadequate nutrition (Tsay 1991; Huether 1998). The same process results from the elevated pressures prevalent under the plantar surface of the neuropathic foot (Meinders, Lange et al. 1996; Boulton, Connor et al. 1998). Furthermore, this problem is compounded by the simultaneous shear forces (due to anatomical abnormalities) and thin subcutaneous fat layer in patients with long standing type 2 diabetes mellitus (Cavanagh, Ulbrecht et al. 2001). Thinning of the subcutaneous fat layer compromises the ability of the tissue to distribute forces efficiently (Cobb 2000). It must be emphasised that both compressive and shear forces are considered to contribute to plantar foot ulceration (Cobb 2000; Perry, Hall et al. 2002).

The main interventional techniques to identify plantar tissue at risk of ulceration in the neuropathic foot include: plantar pressure assessment, objective assessment of the hyperaemic response to pressure induced ischemia and histological examination of the tissue to assess structural damage to capillaries. Rapid assessment following symptoms is essential since under perfused tissue is at a significantly increased risk of infection, which frequently spreads to affect deeper tissues, such as, muscle and bones (Sandeman and Shearman 1999). In some cases this process can occur in as little as two weeks and this sub-classification of the diabetic foot, - the Charcot's foot is in itself of great clinical importance although not considered further in the present work.

It is straightforward to demonstrate that temperature changes occur in superficial plantar foot tissue subject to dynamic loading. The significance of this in the aetiology of diabetic foot ulceration arises from the metabolic demands of skin tissue which are known to vary considerably with temperature in normal skin (Scott 1986). However, to the author's knowledge there has only been limited consideration of the significance of this association by the diabetic research community (Brand 1981; Bharara, Cobb et al. 2006). Such a temperature dependence may have direct implications for the duration over which elevated pressures can be sustained before tissue hypoxia (Cobb 2000). This is more important at high temperatures, where the tissue becomes hypoxic at a faster rate under the effect of compressive forces. At low temperatures, the hyperaemic response compensates for the thermal vasoconstriction. Neuropathic diabetic patients are therefore, more susceptible to limb threatening complications, considering the effect of sensory neuropathy, high plantar pressures (Boulton, Hardisty et al. 1983) and failure of hyperaemic response (Rayman, Hassan et al. 1986a).

## *2.2 Temperature regulation in plantar foot*

### 2.2.1 Introduction

In this section the role of thermal physiology, sensory receptors and thermal properties of the tissue are considered.

### 2.2.2 Physiology of human temperature regulation

Human beings belong to homeothermic species i.e. they have a constant state of internal environment, maintained in a very narrow range despite differences in surroundings & any physical activity. This phenomenon of temperature regulation along with psycho-physiological functions to keep body variables within normal range is termed homeostasis. Although there is a biological variation (i.e. 36°C - 37.2°C) in core temperatures for normal human beings, the average normal core body temperature is generally considered to be 37°C. Assuming a naked body and dry air, core temperature in

the body is regulated within 0.6°C, when ambient temperature is approximately between 13° C - 60° C (Guyton 1992).

A change in blood flow to skin is an important process in temperature regulation. Up to 30% of cardiac output flows through the skin. Though heat is continuously transferred from blood vessels to skin surface, blood vessel dilation increases heat transfer and makes skin red and hot. The main physiologic mechanisms that regulate heat production and heat loss to maintain a stable core body temperature are (Bahill 1981):

- **Metabolic Thermogenesis** - Large number of metabolic pathways in the body are accompanied by heat liberation, with the greatest metabolic source being skeletal muscle. Metabolic rate is regulated by several hormonal and neuro-regulatory mechanisms. Secretion of norepinephrine, epinephrine and thyroxin triggers metabolic activities.

- **Contractile Thermogenesis** - This incorporates muscle contractile activity i.e. conversion of chemical energy to mechanical energy followed by liberation of frictional heat. A large amount of heat is produced during any useful muscle activity and a neurologically regulated heat source is activated when reflex 'shivering' is produced by drop in core body temperature below the optimum.

- **Lipolysis** - This is basic fat decomposition mechanism in the body and is a significant factor in keeping the body warm during cold climates such as extreme environmental conditions. This process is triggered by sympathetic nervous system.

The human body takes a very active role in thermoregulation & incorporates neural feedback mechanisms, sensors, a control centre and effectors. These sensors are found throughout the body, especially skin, body core and brain. Additionally, there are receptors found in the spinal cord, medulla, abdominal viscera, muscles and respiratory tract. The hypothalamus in the brain acts as control centre and has a mechanism similar to a thermostat. About 90% of body heat is lost through the skin, under control of these

mechanisms. Heat production of body remains almost constant under such a condition whereas, if the skin temperature drops below the core body temperature a large number of responses are initiated to conserve body heat and increase heat production such as vasoconstriction, cessation of sweating, shivering, increased metabolic rate and erection of body hair to increase insulation. In the following section consideration is given to the thermal properties specific to skin on the sole of the foot.

### 2.2.3 Thermal properties of the skin

Human skin structure and thermal receptors have been discussed in previous sections. The skin surface is an essential element in the thermoregulatory processes in humans, facilitating heat exchange with local tissues and ambient environment via conduction, convection and radiation (Jung and Zuber 1998).

Skin temperature is affected by the internal tissues of the human body and its environment, controlled by the effectiveness of the circulatory system, anatomical position and ambient conditions respectively. Moreover, localised factors such as anatomical changes, thickness of muscular and adipose tissue (both act as heat insulators) also affect the skin temperature. These factors are particularly important when assessing thermal parameters in a diabetic neuropathic foot, where Charcot's foot, muscle atrophy and thinning of the adipose tissue at the heel are indicated. The conductivity of skin is dynamically modulated by the underlying perfusion, resulting from the effector reactions of the thermal regulation system, leading to restoration of thermal equilibrium (Jung and Zuber 1998). For a neuropathic foot, degeneration of thermoreceptors and arteriovenous shunting due to autonomic neuropathy may affect this normal response. Assessment of thermal patterns under the plantar foot and measuring response to thermal stimulus can be helpful to identify patients at high risk of ulceration (Bharara, Cobb et al. 2006).

### 2.2.4 Thermoregulatory vasodilation

Cutaneous vasodilatation is one means by which body temperature can be reduced. Increased blood flow results in more heat transfer from body core to periphery of skin. Increased blood per unit time through the skin is proportional to greater heat loss per unit time from its surface. Vasodilation is produced by two influences, both acting to reduce precapillary vascular resistance:

- diminished neural signals from the hypothalamus descending via sympathetic efferent fibres
- local factors e.g. heat, humidity and hypoxia acting on smooth muscle

Thus, blood flow is shunted from deep to more superficial plexuses within the skin. The autonomic nervous system may also decrease volume of blood passing through alternative vascular beds to skin e.g. the gut. Finally, a greater volume of blood per unit time through the skin also reduces the efficiency of counter-current exchange mechanisms between arterioles and venules. This results in less heat conservation. In patients with severe diabetic neuropathy, this mechanism may be affected due to degenerated thermoreceptors. Thermographic assessment of the plantar foot may therefore, further improve our current understanding about the causal pathways for degeneration of thermoreceptors. This may also also provide useful information about association between plantar ulceration and sensory loss in type 2 diabetes mellitus.

### 2.2.5 Posture related blood flow and temperature regulation

Integrity of venoarteriolar reflex, which results in raised precapillary resistance is deteriorated in patients with type 2 diabetes mellitus, especially in those having peripheral sensory neuropathy (Rayman, Hassan et al. 1986a). Under normal circumstances, for a healthy individual this increase in precapillary resistance leads to vasoconstriction and limits the rise in capillary pressure resulting from vertical column of blood between heart and foot (Flynn and Tooke 1995). Rayman G et al. (1986a) suggests two important reasons for investigating the venoarteriolar reflex.

(a) Patients with diabetic neuropathy are prone to oedema which may represent failure to limit rise in capillary pressure during dependency.

(b) Due to raised capillary pressure in diabetic neuropaths, thickening of basement membrane is promoted.

The venoarteriolar reflex is particularly important during standing as hydrostatic pressure in capillaries of lower extremities is higher upon dependency. Hydrostatic pressure in capillaries helps in movement of fluid to interstitial spaces. It is dependent on arterial pressure, venous pressure, precapillary resistance and post capillary resistance. Mathematically, it can be represented as following:

$$P_c = [(R_v / R_a)P_a + P_v]/[1 + (R_v / R_a)] \qquad \textbf{Equation 2-1}$$

Where:

$P_c$ = Capillary hydrostatic pressure

$P_a$ = Arterial Pressure

$P_v$ = Venous Pressure

$R_a$ = Precapillary resistance

$R_v$ = Postcapillary resistance

Its impairment is associated with autonomic neuropathy in type 2 diabetic patients. Figure 2-4, shows the precapillary and postcapillary resistances for calculation of capillary hydrostatic pressure (Berne and Levy 1986).

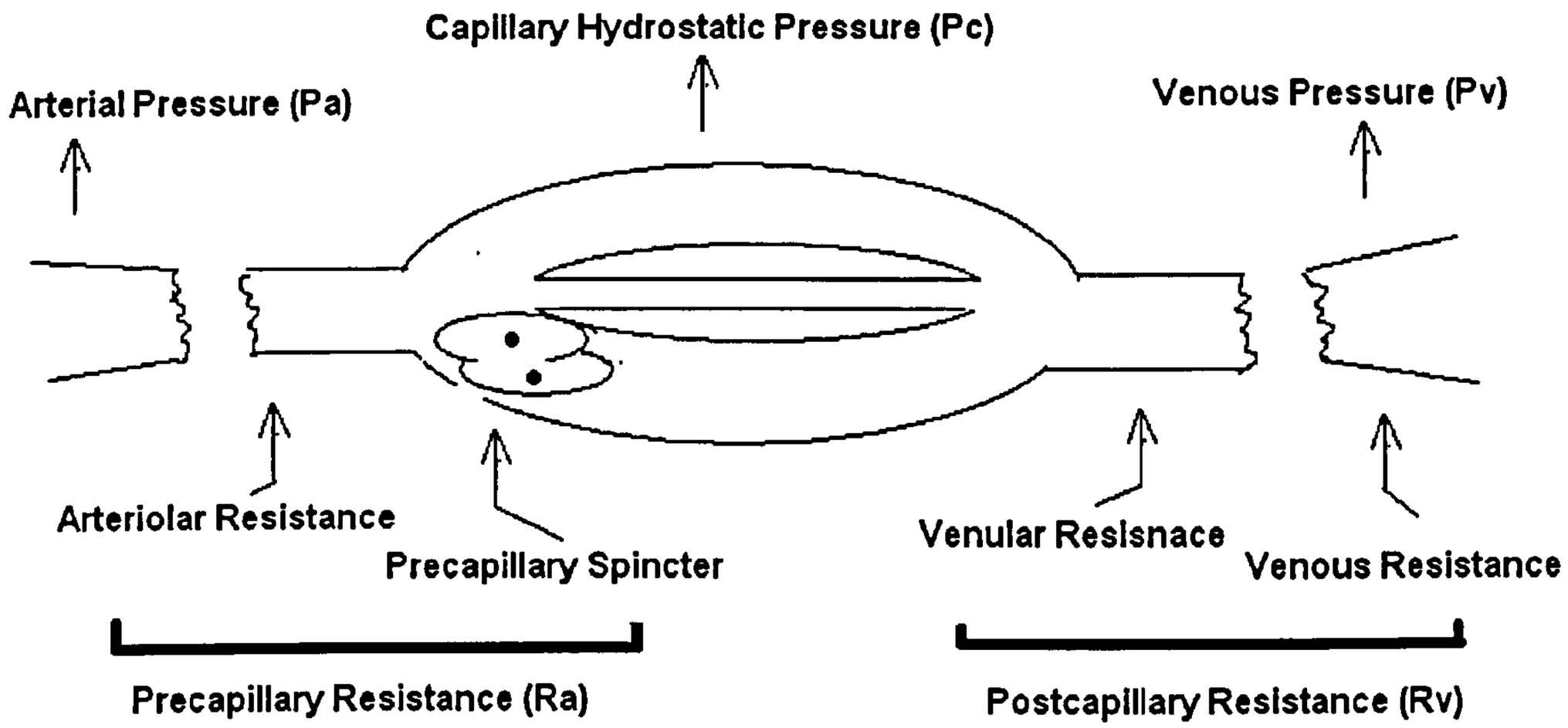


**Figure 2-4: Precapillary and postcapillary resistance for capillary hydrostatic pressure (Berne and Levy 1986)**

Rayman G et al. (1986a) examined vasoconstriction (reflex rise in precapillary resistance) using laser Doppler flowmeter in diabetic patients with & without neuropathy and compared their results with those from age & sex matched healthy controls. Observations were recorded in two sets, one with the patient supine (foot at the heart level) and other with the leg lowered (foot below the heart level). Skin temperature on lower extremity was also recorded for all patient groups. Foot skin temperature was raised indirectly by pressing a heat blanket to the abdominal wall in order to release central sympathetic drive and raise temperature of peripheral skin.

Skin temperature was highest for diabetic patients with neuropathy along with highest resting blood flow and highest blood flow during dependency. During dependency blood flow fell to 18.9 (SD 11.9) %, 28.9 (18.6) % and 53.5 (23.7) % of the original resting flow for normal healthy subjects, diabetics without neuropathy and diabetics with neuropathy respectively (Figure 2-5).

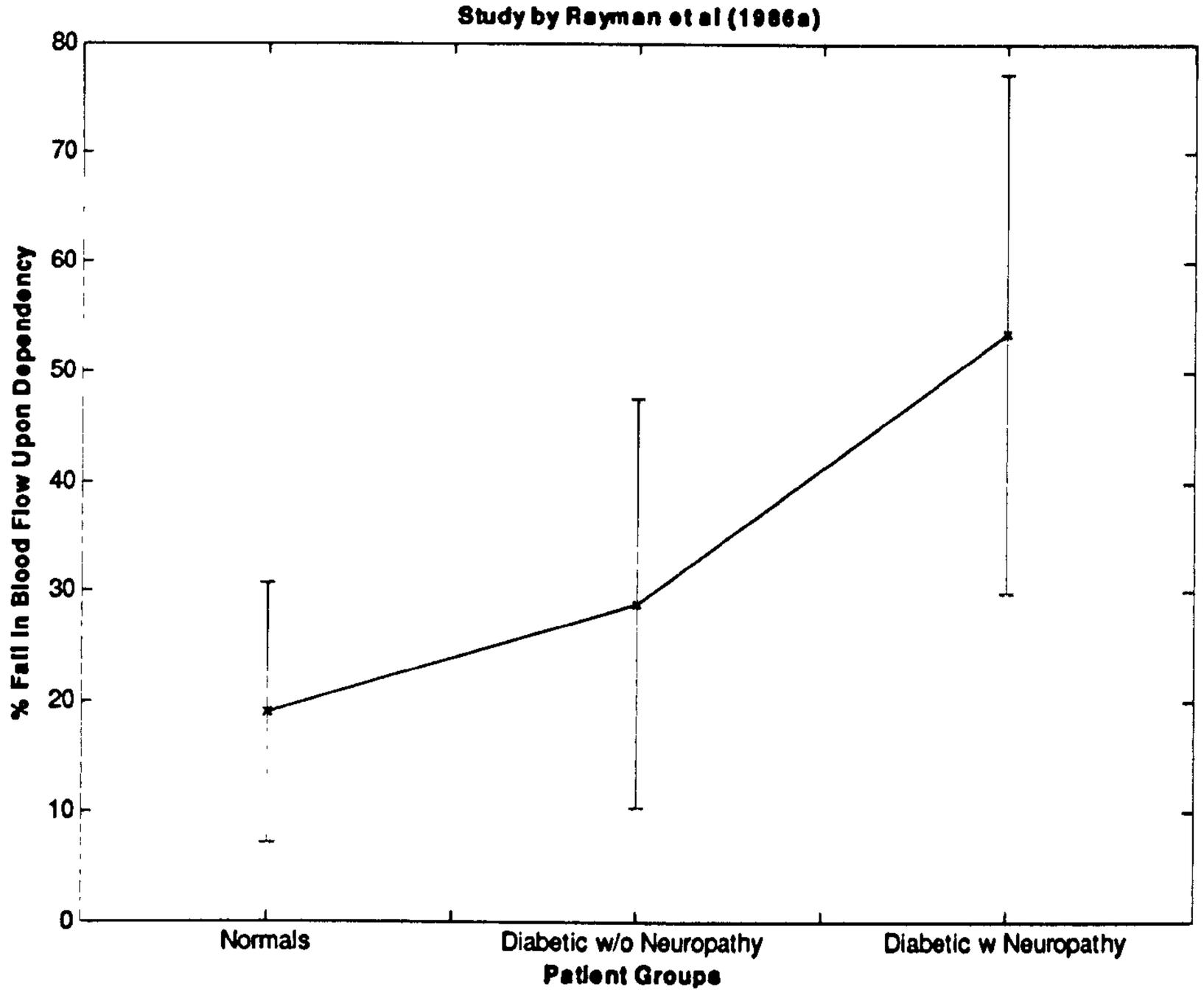


**Figure 2-5: Graph showing percentage fall in blood upon dependency in the study by Rayman et al. (1986a). Data was collected from three study groups that included healthy controls, diabetics without neuropathy and diabetics with neuropathy.**

Both skin temperature and vascular response to dependency in normal subjects after indirect heating closely resembled the measurements of diabetics with neuropathy. This exaggerated blood flow in diabetics with neuropathy indicates the failure of venoarteriolar reflex. These findings are in agreement with the work carried by Belcaro G et al. (1989) to evaluate skin blood flow in diabetics and patients with peripheral vascular disease during resting and dependency. The venoarteriolar reflex was also reduced in patients with claudication and was absent in patients with rest pain and impending gangrene (Belcaro G, Vasdekis S et al. 1989).

Arteriovenous shunting allows blood to be transferred from the arterial side to venous side of circulation, thereby, bypassing capillary circulation. If this happens for a long period of time it can result in arterial calcification and susceptibility of the foot tissue to injury. This is supported by the animal study conducted by Manley & Darby (1980)

wherein it was found that denervated rat pads subjected to repeated stresses were found to ulcerate at a faster rate than non denervated controls (Manley and Darby 1980).

## *2.3 Introduction to the diabetic foot*

The term 'diabetic foot' refers to complications of the foot specific to the diabetic, distinctive underlying factors of which include peripheral neuropathy and peripheral

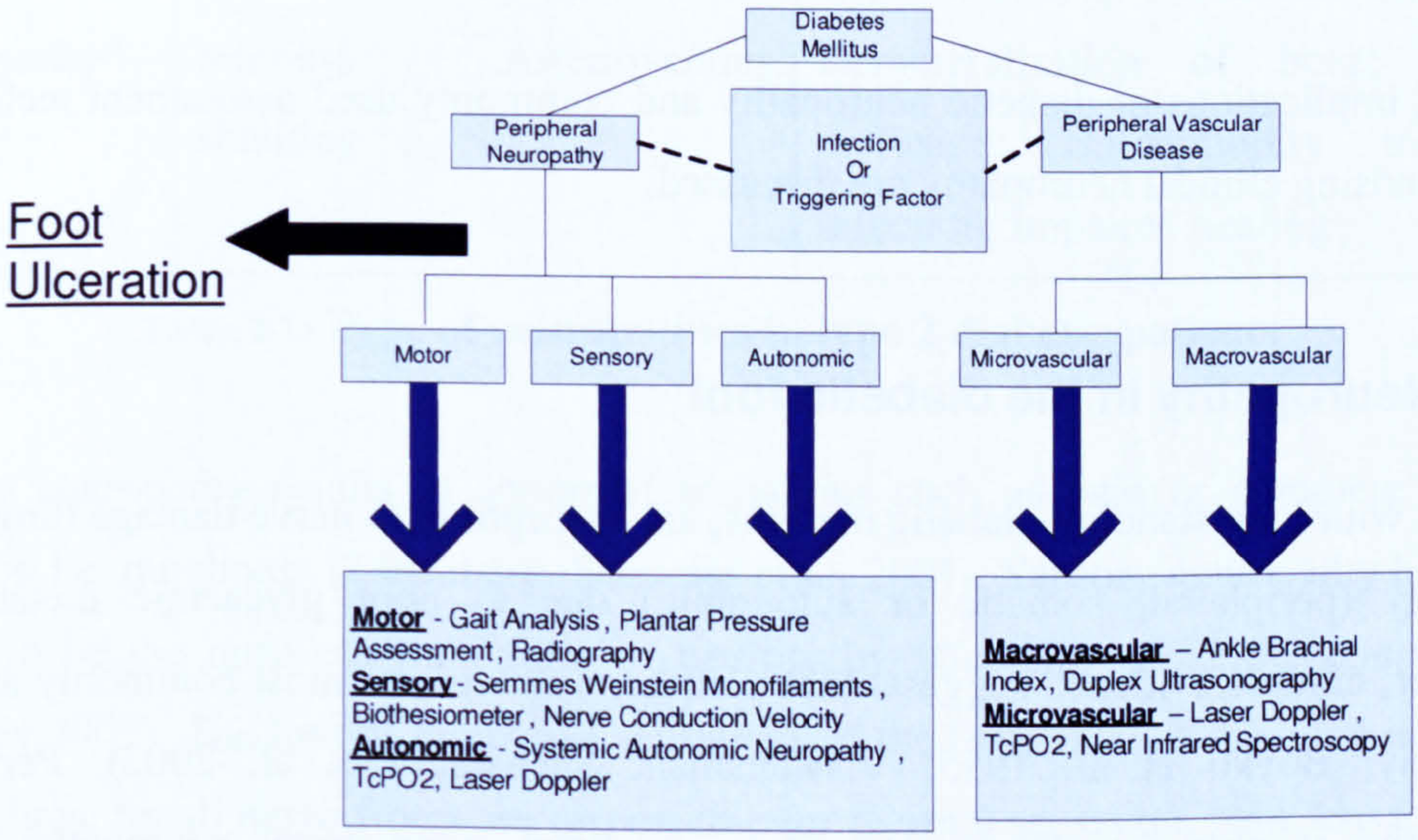


**Figure 2-6: The underlying pathophysiological factors leading to foot ulceration in the diabetic foot. Various treatment regimes for independent assessment of neuropathy and peripheral vascular disease are illustrated.**

vascular disease. Figure 2-6, illustrates the underlying pathophysiological factors leading to diabetic foot ulceration. It must be emphasised that infection is not a causative factor for foot ulceration; it may result from underlying neuropathic condition, which leads to cracks, physical trauma due to sensory neuropathy. Epidemiological findings suggest that neuropathic ulceration is the most prevalent form observed in the diabetic foot (Grunfield 1992; Boulton, Connor et al. 1998). The most important feature of a neuropathic foot is the absence of ability to sense pain due to sensory neuropathy. The combined role of microangiopathy and loss of sympathetic control in the pathophysiology of diabetic foot disease is poorly understood. Clinical studies suggest that patients with long standing

neuropathy may have poor regulatory mechanisms and hence altered blood flow (Rayman, Williams et al. 1986b; Flynn and Tooke 1995). Evidence linking neuropathy and microvascular disease as underlying factors for diabetic foot ulceration is reviewed in the following sections.

## *2.4 Insensitive foot and undetected trauma in neuropathy*

### 2.4.1 Introduction

Clinical implications of diabetic neuropathy and commonly used assessment techniques for diagnosing clinical neuropathy are discussed.

### 2.4.2 Neuropathy in the diabetic foot

Patients with long standing diabetic mellitus, are susceptible to nerve damage throughout the body (peripheral, somatic or autonomic) due to poor glycaemic metabolism. However, clinical evidence suggests that peripheral nerves are most commonly affected (McNeely, Boyko et al. 1995; Viswanathan, Snehalatha et al. 2002). Peripheral neuropathy is also sometimes referred to as distal symmetrical neuropathy in the literature (National Institutes of Health). Table 2-1, summarises types of neuropathies occurring in type 2 diabetics along with their symptoms and consequences.

| Type of Neuropathy | Symptoms | Consequences |
|---|---|---|
| **Sensory Neuropathy** | Loss of pain perception; Loss of temperature sensation | Repeated burn injuries; Abrasions; Repeated mechanical stresses |
| **Motor Neuropathy** | Weakening of muscles (muscle atrophy); Weakening of extrinsic peroneal nerve muscle | Foot deformities; claw toe; Equinovarous deformities; Abnormal weight bearing; Charcot Foot |
| **Autonomic Neuropathy** | Loss of sweating; Dilated arteries; Arteriovenous shunting | Dry skin; Relative distal ischaemia; oedema; Demineralisation of bone; Raised foot perfusion; Susceptibility to injury & infection; Impaired healing |

**Table 2-1: Type of neuropathies in type 2 diabetic patients**

Sensory neuropathy results in abnormal sensations such as pain or complete loss of sensation i.e. numbness (Tanenberg, Schumer et al. 2001). Sensory neuropathy has been shown to be the most common form of neuropathy affecting type 2 diabetic patients (Pendsey 2003). The loss of protective sensations of the feet affects both small and large nerve fibres. Small nerve fibres are responsible for thermal sensation, pain sensation and sweating, whereas, large nerve fibres affect vibration perception, touch sensation, position sense and deep tendon reflexes (Guyton 1992).

For the insensitive foot, thermal trauma may lead to blisters, bullae, excoriation of skin or even full thickness burns (Pendsey 2003). Foot lesions commonly occur in the great toe and this may be related to the nerve length (Guy, Clark et al. 1985; Nasseri, Strijers et al. 1998; Pendsey 2003). The heel is the toughest part of the foot and bears most of the body weight during heel-strike, despite this ulcers are more prevalent at the forefoot this can be explained by:

a) Presence of thick subcutaneous tissue on the heel pad

b) Neuropathy is thought to be length related; longest nerve fibres are preferentially affected in the forefoot leading to greater loss of protective sensitivity (Nasseri, Strijers et al. 1998; Pendsey 2003).

Motor neuropathy results in imbalances between the muscles of the foot which can lead to poor load distribution and over time can lead to bone deformities in the foot. The risk of bone deformity can also be accentuated by sensory neuropathy. Such deformities can significantly increase the risk of foot ulceration by producing large increases in internal biomechanical stresses acting upon tissue. They occur frequently in the great toe, and ankle. Deformity is considered a surrogate marker for elevated plantar pressure (Pendsey 2003). It significantly reduces the total weight bearing area of the foot, increasing plantar pressure. For a neuropathic foot, it leads to hyperkeratosis (thickening of the outer layer of the skin) and callus formation with eventual ulceration. The elevated blood supply due to autonomic neuropathy supports callus formation (Tanenberg, Schumer et al. 2001).

Autonomic neuropathy leads to abnormal blood flow in the lower extremities and decreased sudomotor (pertaining to nerves that stimulate sweating due to activity) function (Tanenberg, Schumer et al. 2001). Figure 2-7, illustrates established pathways leading to neuropathic foot ulcers. The independent role of each type of neuropathy implicated in a diabetic foot is summarised in table 2-1. It must be emphasised that sensory neuropathy is most frequently associated with a neuropathic ulcer. The anatomic and physiological changes induced by motor as well as autonomic neuropathy lead to chronic tissue damage due to abnormal weight bearing. Intuitively, autonomic neuropathy plays a significant role in peripheral circulatory changes and results in arteriovenous shunting. The AV- shunts support callus formation which, further increases plantar pressure. Therefore, it is important to perform diagnosis based on the type of neuropathy by using appropriate measurement technique and well designed clinical protocols.

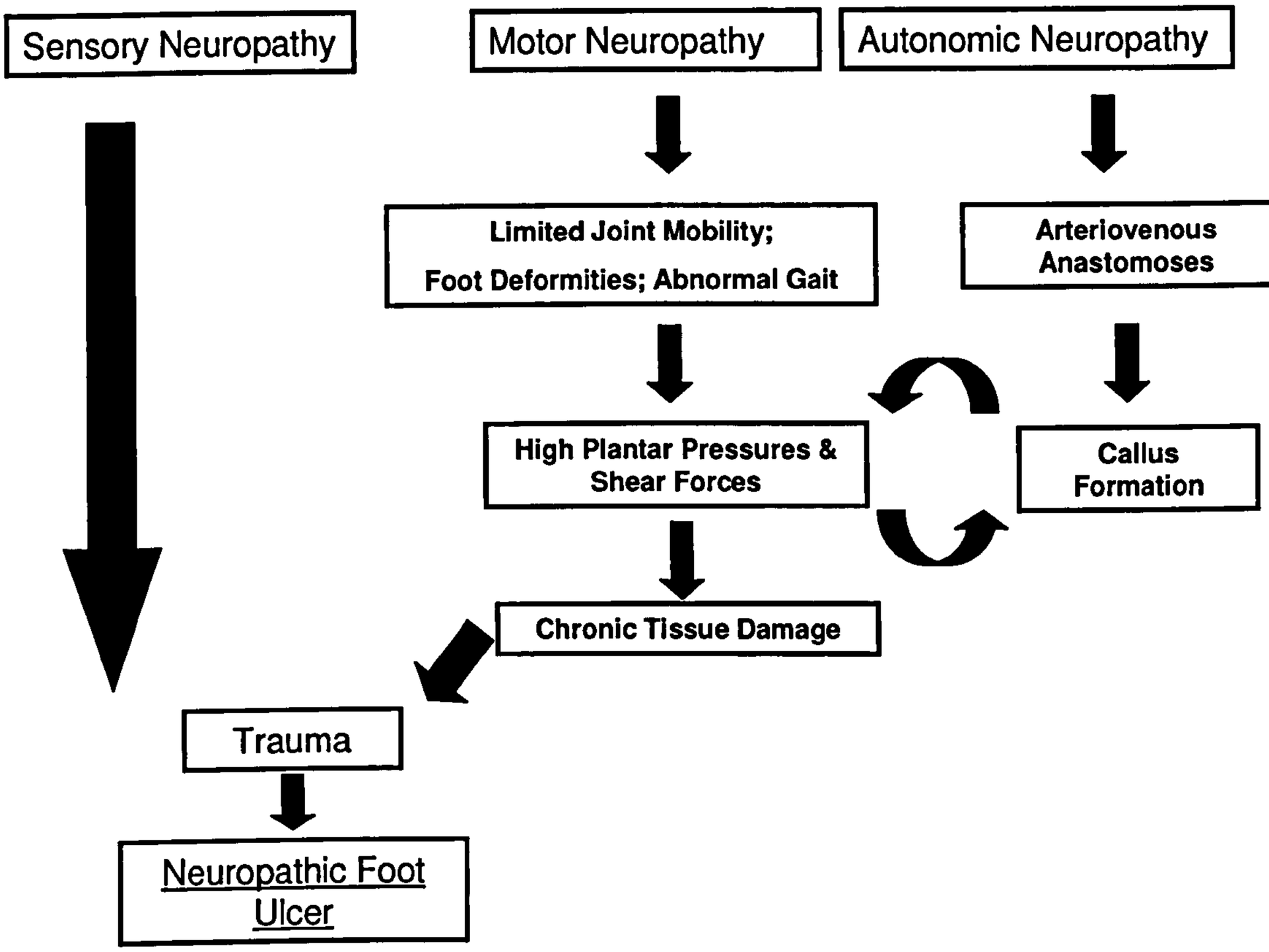


**Figure 2-7: Pathways leading to neuropathic foot ulcers are illustrated. Sensory neuropathy is an important permissive factor for foot ulcers. The mechanisms leading to high plantar pressures and subsequent tissue damage are illustrated, which predispose a neuropathic foot to ulcers. Growth of callus further increases foot pressures.**

Causative factors for neuropathic ulcers can be intrinsic or extrinsic. Two or more factors must be present to result in a neuropathic ulcer (Pendsey 2003). The extrinsic factors (damaging stimuli or trauma) trigger foot ulceration under the presence of intrinsic factors which include limited joint mobility, bony prominences, foot deformities, plantar callus, scar tissue, fissures and neuro-arthropathy. Commonly cited extrinsic factors include ill fitting footwear, barefoot walking, thermal trauma, injury by sharp objects and falls/accidents.

It is important to distinguish between the neuropathic and neuroischaemic foot; their complications are entirely different and so are the respective therapeutic strategies (Grunfield 1992). In the neuroischaemic foot increased pressure leads to direct tissue

damage and ulceration. Three important parameters used to distinguish neuropathic or neuroischaemic foot are skin temperature, pain, Ankle Brachial Pressure Index (ABPI) i.e. ratio between the highest systolic pressure at the ankle and the systolic brachial pressure.

The neuropathic status of foot is confirmed by clinical symptoms and abnormal neurologic examination. The diagnostic criteria for diabetic neuropathy varies across clinical centres. This variability combined with subclinical (symptomatic with absent clinical or neurophysiological signs) neuropathy in certain diabetic patient groups adds to the problem of identifying patients with increased risk of foot ulceration. The techniques used for neuropathic assessment of the foot are discussed.

### 2.4.3 Techniques for sensory neuropathy assessment

The clinical diagnostic criterion for diabetic foot complications is well established. From the clinical standpoint, it is common to assess the presence and extent of peripheral neuropathy to identify risk of foot ulceration. Diabetic neuropathy accounts for almost 60-80% of foot ulcers (Grunfield 1992; Morbach, Lutale et al. 2004; Viswanathan, Madhavan et al. 2005; Viswanathan, Madhavan et al. 2006) especially on the plantar surface of the foot at areas subjected to high pressure during gait and routine activities. Traditionally, Semmes-Weinstein monofilaments and biothesiometry are used for the assessment of neuropathy (Armstrong, Lavery et al. 1998; Viswanathan, Snehalatha et al. 2002; Miranda-Palma, Sosenko et al. 2005). Photographs 2-1 and 2-2, illustrate clinical monofilament and biothesiometer measurements respectively (Katsilambros, Tentolouris et al. 2003). Both methods relate to neuropathy affecting mechanoreceptors in the plantar foot and hence, provide evaluation of sensory neuropathy.

According to the National Institute of Health and Clinical Excellence (NICE) guidelines, neuropathy is detected by using a 10g nylon monofilament that buckles at a reproducible stress and measures cutaneous pressure perception threshold.

**Photograph 2-1: Semmes-Weinstein monofilament measurement (Katsilambros, Tentolouris et al. 2003)**

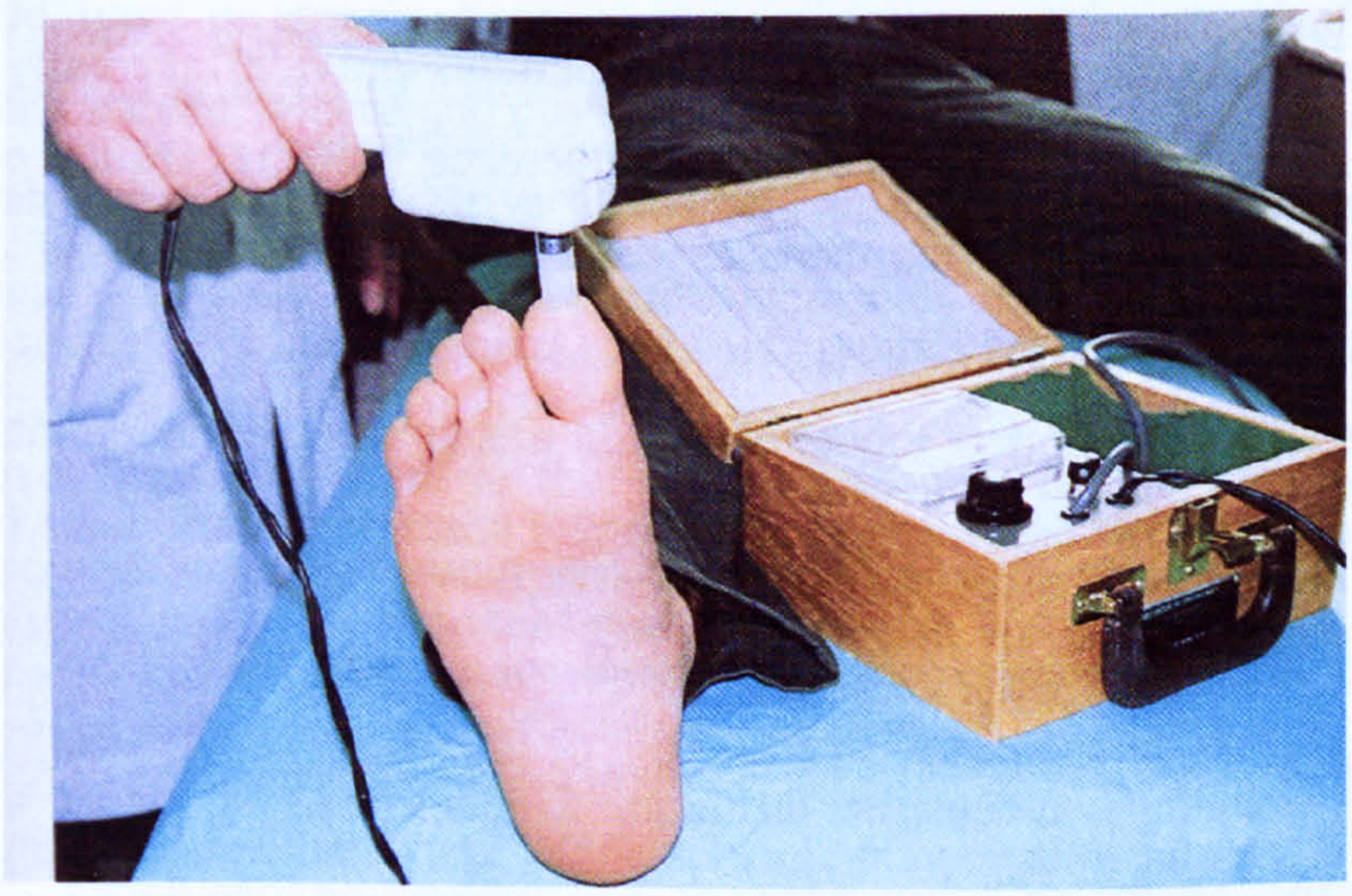

**Photograph 2-2: VPT (Biothesiometer) measurement (Katsilambros, Tentolouris et al. 2003)**

Additionally, a vibration perception threshold (VPT) of greater than 25 Volts is also considered indicative of sensory neuropathy. However, these methods are subjective and objective data in support of specific sites to be tested and minimum number of insensate sites required for prediction of foot ulceration have not been published in the literature (Miranda-Palma, Sosenko et al. 2005).

### 2.4.4 Optical Imaging of blood vessels

Optical imaging is a recent technique that gives clinical investigators the ability to obtain real time in-vivo information such as neural activity and concentration of biochemicals such as haemoglobin and cytochrome, using appropriate lasers and optical fibre bundles. Some of the commonly used techniques that fall under the scientific discipline of optical imaging include small vessel imaging, spatially resolved diffused reflectance (Fridolin and Lindberg 2000) , NIR spectroscopy (Delpy, Cope et al. 1988; Yong, Cobb et al. 2005), laser Doppler perfusion imaging, confocal microscopy and surface microscopy (Aspres, Egerton et al. 2003).

Optical imaging techniques are broadly classified into direct and indirect approach. The direct approach assumes that least scattered photons provide inherently better spatial resolution and contrast, also termed optical coherence imaging. On the other hand, the indirect approach assumes that there exists a unique distribution of scatterers and absorbers for every acquired dataset (Hebden, Arridge et al. 1997) . Such an approach usually requires an appropriate model of photon transport to be incorporated and solving the inverse problem i.e. extracting absorption and scattering coefficients from measured data.

Small vessel imaging is a sensitive technique to identify physiological and anatomical changes in the microcirculatory network i.e. underlying capillaries. The important considerations for this technique include image resolution, video mode, data storage, source detector arrangement, light propagation model and vessel identification. The imaging system may include NIR spectroscopic model (Fridolin and Lindberg 2000), surface microscope (Aspres, Egerton et al. 2003) or capillariscopy.

Spatially resolved diffuse reflectance, based on the NIR spectroscopic model holds good potential for its use as an optical imaging technique for blood vessels. Fridolin and Lindberg (2000) have discussed prerequisites for vessel imaging (i.e. colour-coded vessel map to represent spatial information for veins) based on diffuse reflectance measurements. This technique can be extended to image the capillary loops in the plantar

foot surface by incorporating appropriate photon transport models using Monte Carlo simulations (Delpy, Cope et al. 1988; Meglinski and Matcher 2003) . Both scatter and absorption play a crucial role in forward propagation of light in the tissue. However, both have varying contributions at different wavelengths. The attenuation coefficient '$\mu$' is a function of both scatter coefficient '$\mu_s$' and absorption coefficient '$\mu_a$'.

NIR spectroscopy uses the optical window between 700nm to 1000nm to assess the properties of chromophores. It has potential to provide quantitative information regarding haemoglobin (oxidised and de-oxidised) and cytochrome oxidase concentration in tissue (Yong, Cobb et al. 2005). For the success of any spectroscopic measurements of skin tissue, the spatial distribution of the blood, index of blood oxygen saturation, water content in tissue, types of chromophores, data acquisition/need for tomography, type of detector, temperature dependence and physiological parameters must be considered. NIR spectroscopy may provide an objective assessment of toe perfusion using transmission approach; clinically important as toe tips are prevalent sites of foot ulceration.

For clinical investigation of diabetic foot disease, imaging capillary loops under the plantar surface a high imaging resolution is required due to the small size of capillaries, typically 4-12 μm. As the source to detector distance increases, light photons are collected from deep spatial locations of the subject (Meglinski and Matcher 2003). Ability to measure dynamic behaviour of the arteriole may be clinically useful to identify arteriovenous shunting in diabetic patients. Due to large scatter in skin tissue and complex photon transportation, a direct approach such as spatial filtering, polarisation discrimination and coherent gating cannot be used for diabetic foot assessment. These techniques are suitable for thin or non-scattering human tissue and maximum tissue thickness of a few millimetres. Skin acts as a complex inhomogeneous multi-layered highly scattering and absorbing medium.

foot surface by incorporating appropriate photon transport models using Monte Carlo simulations (Delpy, Cope et al. 1988; Meglinski and Matcher 2003) . Both scatter and absorption play a crucial role in forward propagation of light in the tissue. However, both have varying contributions at different wavelengths. The attenuation coefficient '$\mu$' is a function of both scatter coefficient '$\mu_s$' and absorption coefficient '$\mu_a$'.

NIR spectroscopy uses the optical window between 700nm to 1000nm to assess the properties of chromophores. It has potential to provide quantitative information regarding haemoglobin (oxidised and de-oxidised) and cytochrome oxidase concentration in tissue (Yong, Cobb et al. 2005). For the success of any spectroscopic measurements of skin tissue, the spatial distribution of the blood, index of blood oxygen saturation, water content in tissue, types of chromophores, data acquisition/need for tomography, type of detector, temperature dependence and physiological parameters must be considered. NIR spectroscopy may provide an objective assessment of toe perfusion using transmission approach; clinically important as toe tips are prevalent sites of foot ulceration.

For clinical investigation of diabetic foot disease, imaging capillary loops under the plantar surface a high imaging resolution is required due to the small size of capillaries, typically 4-12 µm. As the source to detector distance increases, light photons are collected from deep spatial locations of the subject (Meglinski and Matcher 2003). Ability to measure dynamic behaviour of the arteriole may be clinically useful to identify arteriovenous shunting in diabetic patients. Due to large scatter in skin tissue and complex photon transportation, a direct approach such as spatial filtering, polarisation discrimination and coherent gating cannot be used for diabetic foot assessment. These techniques are suitable for thin or non-scattering human tissue and maximum tissue thickness of a few millimetres. Skin acts as a complex inhomogeneous multi-layered highly scattering and absorbing medium.

### 2.4.5 Superficial imaging of the vascular bed under plantar foot

There is significant difference between the appearance of the plantar surface of diabetic patients and healthy controls due to altered perfusion. Clinicians at present use visual inspection of the foot surface to identify normal, neuropathic and neuroischaemic feet. Measurement of capillary blood flow as an indication of foot pressure was first proposed by Seitz (Seitz 1901). In his experiments, he observed colour changes resulting from tissue ischaemia due to acting pressure by using a simple glass and mirror arrangement. It must be emphasised that it is important to assess the diabetic foot under loaded condition, replicating the stresses that the foot is subjected to during normal gait. Complex imaging techniques such as MRI (Brash, Foster et al. 1999) and computed tomography (Smith, Commean et al. 2001; Commean, Mueller et al. 2002) have also been applied to diabetic foot research. Although useful research tools, there application is limited by high cost.

Digital photography, polarised photography and ultraviolet light photography are the most commonly used surface imaging techniques (Aspres, Egerton et al. 2003). The latter two provide selective representation of the imaged tissue i.e. areas of hyper pigmentation, collagen fluorescence, surface/sub-surface features of the tissue. High-resolution dynamic images provide useful information on the perfusion distribution, capillary density and hyperaemic response. Static digital images acquired represent the vascular state of the foot and can be a useful tool to assess wound healing (Rajbhandari, Harris et al. 1999). This is a simple technique but the results can be quantified and statistical significance proven.

In assessing the diabetic foot, digital images supplemented with plantar pressures and loading durations can be a useful tool to predict possible sites of ulceration. At present, both imaging and pressure datasets are evaluated independently since a simultaneous combined measurement is not possible. Digital photography is used for a wide range of dermatological pathologies; however, for diabetic foot assessment visual inspection is preferred over digital photography due to cost issues (Boulton, Connor et al. 1998).

## 2.4.6 $TcPO_2$ measurements

Transcutaneous oxygen saturation ($TcPO_2$) is a sensitive measure of dermal perfusion. It is a non invasive technique, gives functional information about cutaneous blood flow used to quantify skin oxygenation and determine ischaemic sites (Romanelli and Falanga 1999; Wilmer, Voroshilova et al. 2001). A platinum electrode provides current proportional to the $PO_2$ (oxygen tension) at the measured site. The skin oxygen tension is measured in 'mmHg' units as illustrated in Figure 2-8. At normal skin temperate $PO_2$ at the skin surface is close to zero mmHg. Typically, values greater than 60mmHg are considered to be normal (Pendsey 2003). Therefore, a vasodilatory stimuli such as warming the skin surface in the range of 37- 44°C is used to measure the $PO_2$ (Iiuch, Franzeck et al. 1983; Gaylarde, Fonseca et al. 1988). This metabolic consumption of oxygen can be used to define a figure of merit for perfusion profile of larger vessels as well as capillary loops and provide supporting evidence to clinicians for revascularisation surgery, amputation level and suitable drug treatment (Got 1998)..

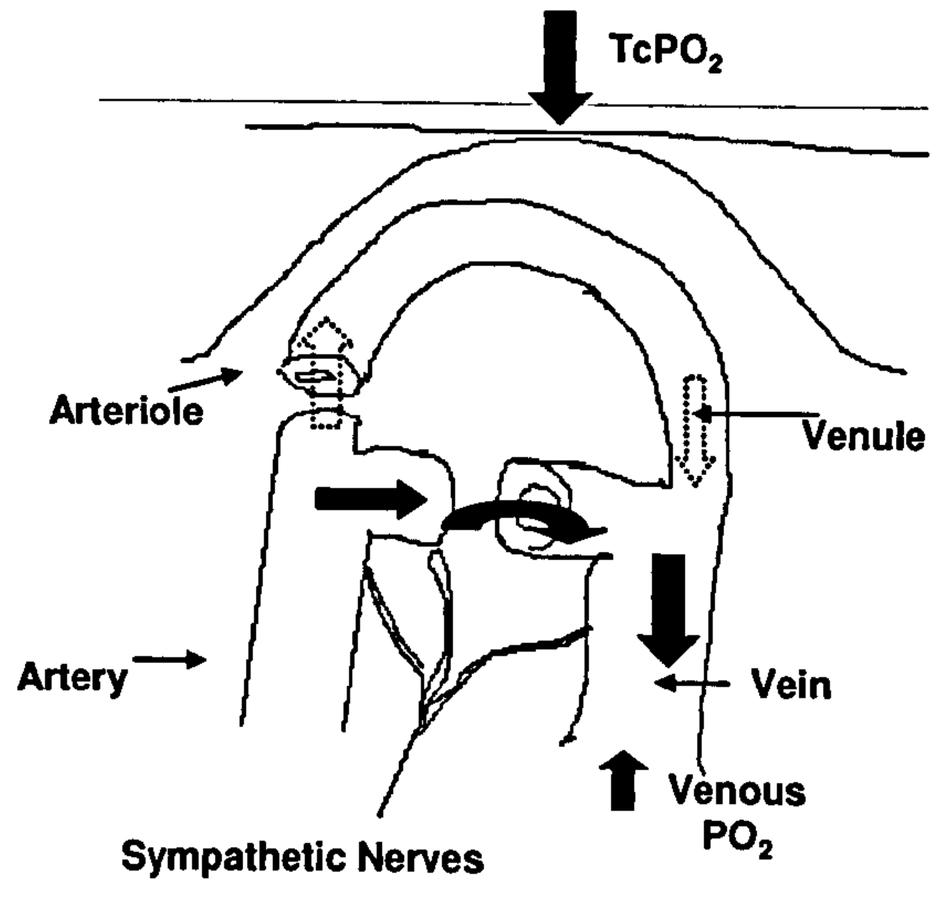


**Figure 2-8: Typical TcPO2 measurement in assessment of diabetic neuropathy. Autonomic neuropathy results in decreased sympathetic innervations of the AV shunts resulting in dilation of the AV shunts (Arteriovenous Shunting). This produces a decrease in the nutritive capillary blood flow and a decrease in TcPO2**

Transcutaneous oxygen tension in legs and feet has been used to characterise the diabetic foot (Boulton, Scarpello et al. 1982; Kalani, Brismar et al. 1999). Peripheral vascular disease results in reduced $PO_2$ in type 2 diabetes mellitus.(Gaylarde, Fonseca et al. 1988).

However, when compared with control subjects having equivalent degree of vascular disease, $TcPO_2$ values are still lower, implicating possible involvement of autonomic neuropathy (Uccioli, Monticone et al. 1994). Boulton et al. (1982) have demonstrated the presence of increased venous oxygenation implicating arteriovenous shunting in the diabetic neuropathic foot. Gaylarde et al. (1988) report inability to increase $TcPO_2$ with increase in temperature in diabetic subjects with neuropathy, consistent with the laser Doppler flowmetry study by Rayman et al. (1986).

Diabetic neuropathy results in thick epidermal layer. This may affect the stabilisation time of the $TcPO_2$ measurement. Furthermore, $TcPO_2$ measurements provide localised assessment of the perfusion status; discounting its clinical use in the routine assessment of the diabetic foot disease. However, $TcPO_2$ measurements correlate well with the rate of healing (Pecoraro, Ahroni et al. 1991) and therefore, can be used to assess benefits revascularisation surgery or drug treatment.

## *2.5 Summary*

The foot is well adapted to load bearing with a robust anatomical structure that helps in distribution of compressive forces during loading. The integrity of weight bearing tissues is essential to protect deeper tissues. Use of plantar pressure measurement is common in the assessment of the diabetic foot. Advances in the plantar pressure measurement technology, have contributed significantly in the current understanding of foot ulceration. However, the results from one plantar pressure study cannot be extrapolated to the other, leading to difficulty in determination of threshold values for elevated plantar pressures in diabetic foot patients.

In diabetic neuropathy, there is an increased likelihood of impaired mechanics of the lower extremities, the effects of which including pressure and temperature can be measured in static and ambulatory tests. Local tissue temperature may be a permissive factor for tissue necrosis and eventual ulceration. Therefore, from the clinical standpoint, it may be useful to further the current understanding about combined effect of local tissue

pressure and temperature changes at the load bearing tissue. There is a substantial amount of published information on the independent effects of elevated plantar pressure. However there exists much less data regarding the thermal physiology of the diabetic foot.

Human core body temperature is maintained constant over a wide range of environmental conditions with the help of coexistence between physical and physiological conditions. Skin is the largest organ in human beings. Its temperature depends upon the intensity of underlying metabolic processes and perfusion (Arcan and Brull 1976). Thermal measurements of the plantar surface of the foot offer possibilities of monitoring the neurologic modulation of the circulation, essentially involving thermoreceptors and underlying capillary network.

# Chapter 3 Literature Review

## *3.0 Introduction*

In diabetic neuropathy, both mechanoreceptors and thermoreceptors are thought to be affected. The responses of thermoreceptors in the neuropathic diabetic foot to thermal changes at the plantar surface are of central importance in this project. In the first half of the literature review, liquid crystal thermography (LCT) and its application specific to the diabetic foot are discussed. The second half of this chapter focuses on developing the basic justification for using this technique as a modality for routine clinical assessment of the diabetic foot.

## *3.1 Liquid crystal thermography*

Thermochromic liquid crystals (TLC) respond to temperature by selectively reflecting incident light. This is the basis for the technique of liquid crystal thermography which provides a colour response proportional to the temperature of a heated surface in contact with the crystals. Thermographic image represents a two-dimensional field in which temperature varies both spatially and temporally (Hay and Hollingsworth 1998).

From a clinical standpoint, LCT is an economical, non-invasive and nonionising diagnostic tool used to produce temperature distribution and identify local hot spots (pathology). It can be used as an adjunct to other diagnostic modalities such as radiography, ultrasound, nuclear medicine and neurophysiological tests; or in some cases as a primary diagnostic tool where other modalities are contraindicated.

## *3.2 Determination of surface temperature using liquid crystal thermography*

### 3.2.1 Introduction

Details related to the LCT technique, its development as a diagnostic tool, practical consideration and recent advances are discussed.

### 3.2.2 Physics of liquid crystal thermography

Liquid crystals are organic substances exhibiting mesomorphic (liquid crystalline) states within which elements occupy spatially fixed positions with respect to one another. However, the relative position itself is not fixed (Flesch 1985). Liquid crystals can be obtained either thermotropically or lyotropically. Those obtained by the former process are conventionally divided into three types i.e. the smectic, the nematic and the cholesteric (Portnoy 1970; Hallcrest 1991). This classification is primarily based on the molecular arrangement and optical properties of the liquid crystals. Liquid crystals show optical properties of crystals but exhibit mechanical behaviour of liquids. They reflect polarised light in a narrow region of wavelengths.

Cholesteric liquid crystals are clinically most significant as they exhibit dichroism i.e. a phenomenon involving differential absorption of right hand and left hand circularly polarised light due to molecular asymmetry and are the most optically active substances known. Unpolarised incident illumination contains approximately equal amounts of right hand and left hand polarised light. Within the reflected wavelengths about 50% is reflected and 50% is transmitted (Flesch 1985). They are birefringent and optically negative; i.e. light in the crystal travels more rapidly perpendicular to the layers than parallel to them. These crystals are characterised by the presence of layers with all molecules in a single layer oriented in same direction. These layers trace a helical path whose single turn is 550nm (Flesch 1985).

*Unpolarised white light falling* on a cholesteric crystal is resolved into two circularly polarised components rotating in opposite directions (Azar, Benson et al. 1991). One component is absorbed, while the other is reflected. This reflected component upon scattering produces colour depending upon the crystal type. For a fixed angle between source of light and observer, colour is a function of temperature, chemical environment and electric field. Wavelength of reflected light is dependent on spacing between layers of the helical structure. The temperature represented is inversely proportional to both layer spacing and wavelength (Meyers, Cros et al. 1989).

Figure 3-1, shows the principle of measurement of skin surface temperature with liquid crystals. The black absorbing layer acts as a barrier between skin and liquid crystals; it prevents reflection by skin surface.

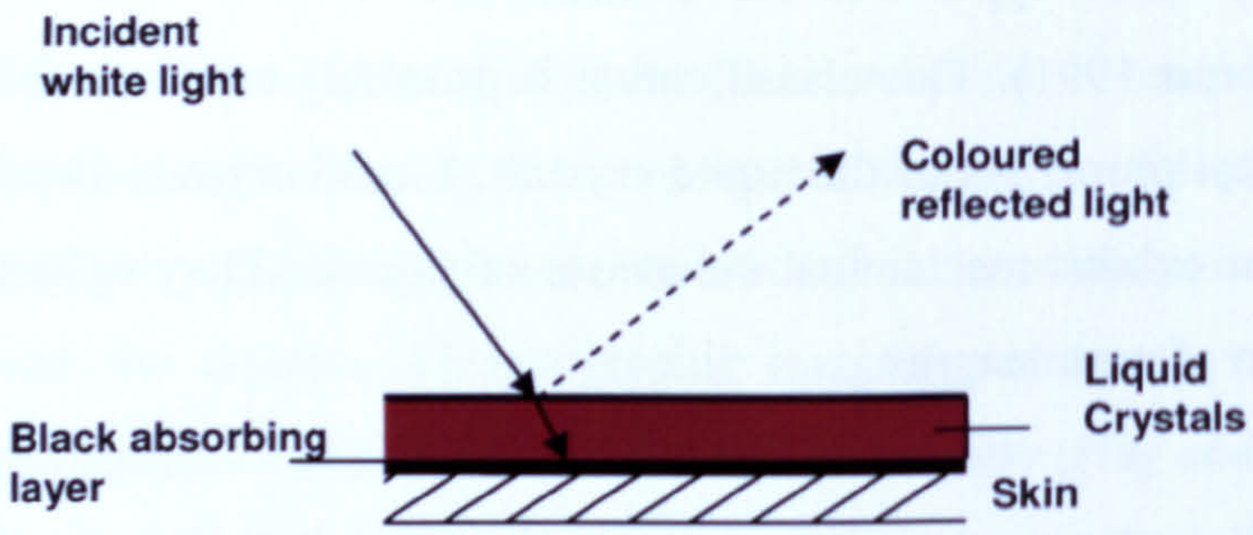


**Figure 3-1: Principle of the measurement of skin surface temperature with liquid crystals**

The temperature range over which the TLC material actively reflects visible light and can be distinguished by the imaging equipment is termed the colour bandwidth or colour play interval (Anderson 1999; Bakrania and Anderson 2002). The operating range of TLC's varies from -30°C to 150°C. Liquid crystals with colour bandwidth less than 5°C are narrow band and those with greater than 5°C are wide band liquid crystals.

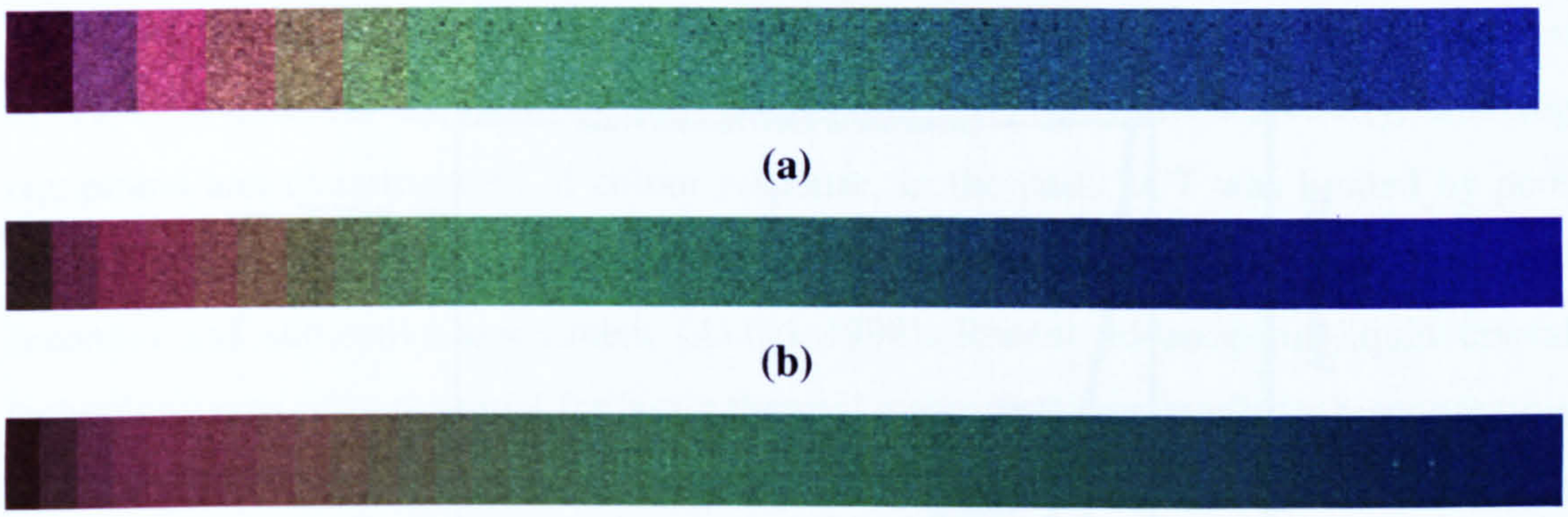

**(a)**

**(b)**

**(c)**

**Figure 3-2: Typical sequence of colours for thermochromic liquid crystal sheets. Figure illustrates R25C5W (a), R25C10W (b) and R25C15W (c) TLC sheets from Hallcrest. The nomenclature adopted is typically, used in the literature to represent the colour bandwidth of the TLC material. R'T'C'X'W where T denotes the event temperature and X denotes the clearing point temperature.**

The sequence of colours most commonly observed is red followed by yellow, green, blue and finally violet (Hallcrest 1991). However, some liquid crystals only produce selective transitions i.e. red-green-red, or green to red during warming. Figure 3-2 illustrates typical sequence of colours in the commercially available TLC materials. The chemical formulation of liquid crystal material determines its colour versus temperature characteristics at manufacturing stage (Hallcrest 1991). Details related to the physics and characteristics of thermochromic liquid crystals (TLC) are widely published (Behle, Schulz et al. 1996; Hay and Hollingsworth 1996; Hay and Hollingsworth 1998; Anderson 1999; Bakrania and Anderson 2002).

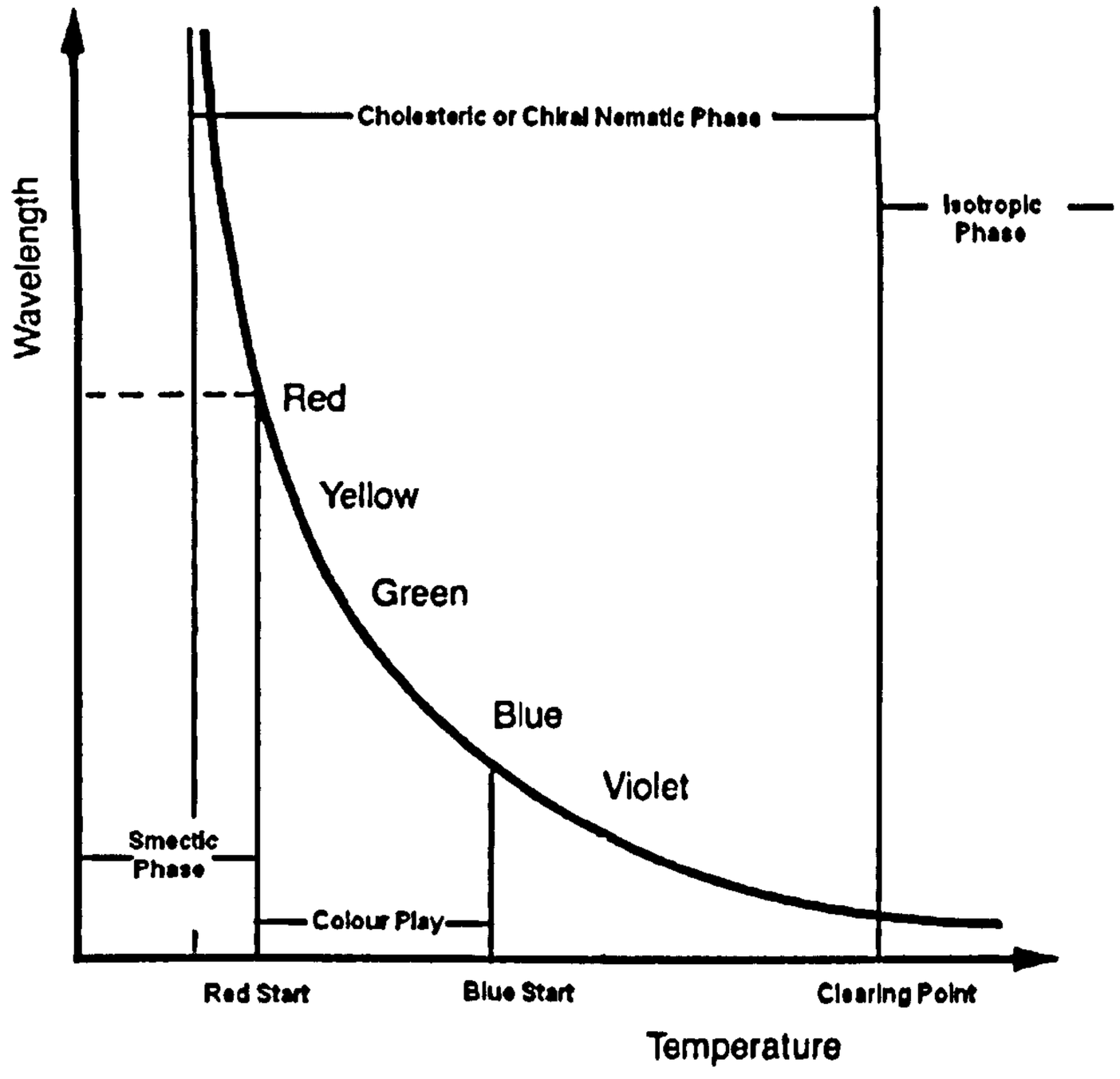


**Figure 3-3: Typical reflected wavelength Vs temperature response of a temperature sensitive thermochromic liquid crystal mixture.**

Figure 3-3, illustrates the reflected wavelength versus temperature response of a temperature sensitive thermochromic liquid crystal mixture. The clearing point is the temperature at which the TLC becomes transparent as a consequence of the crystals achieving a non reflecting isotropic state. When TLC is cooled, the change back to the anisotropic semi-crystalline state is principally dependent on the rate of cooling which leads to a shift in the hue versus temperature profile. This change is reversible provided that the TLC is allowed to cool to a formulation dependent temperature termed the event temperature.

### 3.2.3 Development of thermochromic liquid crystals

Contact liquid crystal thermography exploits the fact that all objects with a temperature above absolute zero emit infrared radiation. The magnitude of emitted radiation is high in human skin, especially in diseased state (Dribbon 1983). The earliest applications of

liquid crystals were qualitative due to lack of robust imaging equipment. Wider adoption of LCT in medical applications has been limited by pressure sensitivity, imaging equipment and quantification of colour response. In the past, LCT was limited by poor thermal resolution (±0.5°C), poor spatial resolution (±5mm), slow response time (>60 seconds) and subjective assessment (Anbar 1998). Recent advances in liquid crystal technology now offer potential for better thermal mapping, accuracy, faster response time (Hallcrest 1991) and temperature resolution using digital image processing (Anderson 1999; Bakrania and Anderson 2002; Roth and Anderson 2005; Grewal, Bharara et al. 2006).

LCT is primarily used in thermal mapping, industrial heat transfer (Camci, Kim et al. 1992; Jambunathan, Hartle et al. 1996; Ireland, Neely et al. 1999), non destructive testing (NDT), fluid flow visualisation (Brown and Saluja 1978; Ashforth and Rudel 2003), civil engineering to assess thermo isolation properties of building elements (Pospisil and Pospisilov 1990), aerospace engineering (Hallcrest 1991) and in studies of electronic cooling and boiling heat transfer (Hay and Hollingsworth 1996; Ireland, Neely et al. 1999; Stasiek and Kowalewski 2002).

Pure TLC material is difficult to work with due to its oily form, risk of chemical contamination and exposure to ultra violet (UV) light. Liquid crystals can be altered by catalytic action of surrounding substances. Cholesteric liquid crystals are oily substances and when they combine with fat present within skin surface, they produce a mixture with different properties (Flesch 1985). These difficulties can be avoided through polymer micro-encapsulation of the TLC (Hallcrest 1991; Massi 2004).

Liquid crystals are enclosed in capsules typically, 10-15 microns in size. Smaller capsule sizes result in scattering of incident light i.e. milky colour of the film (Klosowicz, Jung et al. 2001). The capsule wall acts as a barrier and provides insulation from neighbouring liquid crystal capsules. This improves thermal mapping capability (Armstrong 2004) and solves the problem of stress dependency of liquid crystals (Wozniak, Wozniak et al. 1996; Armstrong 2004) and prevents physical or chemical deterioration (Zharkova,

Khachaturyan et al. 1980; Stasiek and Kowalewski 2002). Encapsulation improves the accuracy of temperature measurements and ensures long term stability (Quagliardi 2005).

Various production techniques are used to enable TLC to be offered in the form of an emulsion, polymer sheet or latex support. Table 3-1 provides the most common properties of three physical forms of thermochromic liquid crystals i.e. polyester sheet, water based emulsion and latex sheet.

| Property | TLC Polyester Sheet | TLC Emulsion | TLC Latex Sheet |
|---|---|---|---|
| **Description** | Silk screen printing onto acetate carrier | Water based liquid crystal emulsion applied to target using airbrush | Liquid crystals embedded on latex carrier |
| **Typical Size** | Rectangular outline. Typical size - 0.45m by 0.3m | Depends on the target surface area. | Rectangular window with pneumatic control system. Typical size- 0.25m by 0.25m |
| **Protection** | Encapsulation and transparent acetate sheet through which colour response is seen. | Only encapsulation | Encapsulation and transparent acrylic plate through which colour response is seen. |
| **Application** | Industrial heat transfer (flat surfaces) and research domain | Flexible approach; Aerospace research, flow visualisation in fluids and particle velocitimetry. | Sports injury assessment, breast thermography and back pain assessment. |

**Table 3-1: Properties of three physical forms of thermochromic liquid crystals. All details provided refer to the most common applications.**

Customised sizes and geometries of TLC sheets can also be procured for specific applications. The acetate carrier sheet is usually black to enhance image contrast. TLC sheets are in general, restricted to measurement on flat surfaces/interfaces.

A more flexible measurement approach is afforded through the use of water based liquid crystal emulsions which are typically sprayed onto the target surface using an airbrush. This approach does not allow additional protection beyond that afforded by the polymer encapsulation, therefore external physical influences must be avoided. A compromise between the sheet and spray forms is provided through embedding TLC in a thin compliant latex carrier which allows conformance to the underlying geometry of the target surface whilst providing a high degree of protection to the crystals. Latex LCT technology is used commercially in sports injury assessments, breast thermographic studies and back pain assessment (Ng, Chen et al. 2001; Leinidou 2003). In practise, flexing of the latex sheet can lead to birefringence which introduces noise into the colour image. This can be compensated for in critical applications through use of a pneumatic control system employed to equilibrate pressure over the contact surface.

In the past, emulsion based liquid crystals were used, applied directly onto anatomical site over a black absorbing layer during investigation (Benjamin 1973). Microcapsules of different liquid crystal formulations could be mixed together to produce emulsions with multiple distinct active ranges (Hay and Hollingsworth 1996). When mixtures of several liquid crystals are applied to skin; differences in skin temperature cause crystallisation to occur at some places and not at others, which affects the original mixture and hence, the calibration (Flesch 1985).

### 3.2.4 Liquid crystal thermography in medicine

LCT helps to determine underlying physiology (local metabolic and vascular conditions), with lower skin temperatures indicating vasoconstriction and higher temperature indicating a state of inflammation or raised blood flow due to higher metabolic activity.

Biomedical applications and quantitative thermal imaging using TLC have been reviewed (Portnoy 1970; Ashforth 1996).

There are numerous applications in medicine namely andrology (Goblyos and Szule 1987), rheumatology, sports medicine, dermatology, dolorology, vasculopathies (Leinidou 2003), diagnostic podiatric medicine (Dribbon 1983), pulmonological diagnostics (Klosowicz, Jung et al. 2001) and consumer thermometry (Hallcrest 1960). LCT was used in evaluation low back pain for patients with degenerative discogenic lesions, acquired lesions, congenital and developmental lesions and back pain resulting from unknown causes (Rubal, Traycoff et al. 1982). Shlens et al. (1975) used thermochromic liquid crystals to evaluate inflammatory conditions and identifying underlying pathology (Shlens, Stoltz et al. 1975). Latex based LCT plates were used in detecting deep vein thrombosis with reported sensitivity of 97% and specificity of 62% (Sandler and Martin 1985; Free and Faerber 1989; Kalodiki, Marston et al. 1992). Latex based liquid crystal plates were also used in determination of baseline data for thermal patterns in the face of healthy individuals, with the intent of objective assessment for nerve injuries and monitoring recovery (Ariyaratnam and Rood 1990).

A positive relationship exists between temperature changes and nerve injuries in lower and upper limbs (Nakano 1984; Uematsu 1985). Steele et al. (1994) used LCT to assess peripheral thermal changes in the hands of patients with chronic liver disease and established significant differences in the response to cold water immersion tests which were independent of changes mediated by the autonomic neuropathy (Steele, Dillon et al. 1994). Dribbon (1983) suggested use of liquid crystal thermography in assessing neurovascular complications by studying characteristic patterns of hypoemissivity, taking contralateral foot as control. Normal thermographic patterns in humans are characterized by remarkable symmetry of temperature in homologous body parts as confirmed in their study of controls (Meyers, Cros et al. 1989). This fact is useful in bilateral studies of various pathologies, where thermographic patterns in the contralateral part are compared to the affected part. Diabetic neuropathy is generally symmetric i.e. both feet should represent similar thermal patterns.

### 3.2.5 Liquid crystal thermography in assessment of diabetic foot

Baer et al. (1988) reviewed the use of liquid crystal thermography in podiatric medicine with emphasis on vascular, neurologic and musculoskeletal complications. Bergholdt proposed that results from thermal assessment of the insensitive foot can be used as objective evidence of potential damage to the patient (Bergtholdt 1979). Goller et al. (1971) reported the significance of pressure acting on the foot and associated thermal changes, proposing thermography as a useful tool in selecting suitable orthotic devices (Goller, Lewis et al. 1971).

Boyko et al. (2001) re-examined the association of skin temperature in diabetic neuropathic foot in their study of diabetic subjects. The results show that diabetics with sensory or autonomic neuropathy do not have higher foot skin temperature. These results are contradictory to those obtained by other studies; which report that diabetic neuropathy results in elevated microcirculation in the foot and hence, raised foot temperature (Stess RM, Sisney PC et al. 1986; Benbow, Chan et al. 1994). Firstly, the two studies used different thermal modalities and hence, there is no direct correlation between the results. Secondly, there were no measurements on the healthy controls to assess the degree of variation in foot temperatures. There remains uncertainty with the protocol as to location of the patient feet (exposed to air or on thermally conductive sheet) and lack of baseline temperature measurements prior to walking.

In cases of tissue trauma, liquid crystals can be used to differentiate between regions of normal and impaired vascularity (Portnoy 1970). Stess RM et al. (1986) and Benbow et al. (1994) have used LCT for diabetic foot assessment. Two major problems with these studies were low quality imaging equipment and pressure sensitivity of thermochromic liquid crystals. Both the studies under consideration had supine measurements for feet, which do not replicate normal loading conditions to which the feet are subjected for most of the time. Both studies used latex based TLC to evaluate plantar thermal emission patterns. A TLC characterisation study by the author found TLC on latex support to be pressure sensitive (Bharara, Cobb et al. 2005). Due to its manufacturing procedures and

material properties, it suffers from non-homogeneities resulting in high uncertainties in measured hue values, which further leads to limited temperature resolution. Chemical formulation and sealed/unsealed states of the TLC determine the pressure sensitivity of the liquid crystal (Wozniak, Wozniak et al. 1996; Armstrong 2004).

Tables 3-2 and 3-3 list the results from the two LCT studies for their respective patient groups. Both the tables present, readings as temperature in °C± Standard Deviation (SD) for the study groups used. Stess RM et al. (1986) have reported significantly increased plantar foot temperature and mottled thermographic patterns for patients with active foot ulceration. Three patient study groups were used, diabetics with history of foot ulcerations, diabetics with active foot ulceration and non diabetic healthy controls.

| Stess RM et al. | | |
|---|---|---|
| Group 1 (Non Diabetic Controls) | Group 2 (Diabetic without ulcers) | Group 3 (Diabetic with active ulcer) |
| **27±0.3** | **26±0.3** | **28±0.3** |

**Table 3-2: Research study by Stess RM et al. (1986). MFT (Temperature in °C±SD) for three study groups as determined by liquid crystal thermography.**

| Benbow et al. | | |
|---|---|---|
| Group 1 (Non Diabetic Controls) | Group 2 (Diabetic with Neuropathy, without PVD ulcers) | Group 3 (Diabetic with Neuropathy, with PVD ulcers) |
| **25.7±2.1** | **28.2±2.9** | **25.6±1.9** |

**Table 3-3: Research study by Benbow et al. (1994). MFT (Temperature in °C±SD) for three study groups as determined by liquid crystal thermography.**

Elevated temperatures at weight bearing sites i.e. metatarsal heads and heel may indicate pressure trauma or increased arteriovenous shunting (Chan, MacFarlane et al. 1991). The study by Benbow et al. (1994) found increased mean foot temperature (MFT) temperature in diabetic neuropathic patients leading to foot ulceration measured using

temperature sensitive liquid crystals. The study comprised of three study groups i.e. neuropathic with PVD, neuropathic without PVD and non diabetic healthy controls. Benbow et al. (1994) proposed that a normal or low MFT in the neuropathic foot is a marker of PVD, which confers an increased risk of ischaemic foot disease.

### 3.2.6 Practical considerations for liquid crystal thermography

During the clinical thermographic assessment, both static and dynamic studies are performed. Typically for static assessment, subjects are allowed 15-20 minutes for thermal adaptation prior to the test. Exchange of heat within the surroundings is uniform and takes account of both physiological and pathological hyperthermia/hypothermia. Dynamic assessment is important in diagnosis of thermal gradients on the measured site. Dynamic measurements can be accomplished by using appropriate thermal or mechanical stimulation of the measured tissue. Considering thermal stimulation, it may be beneficial to perform forced cooling and warming independently in order to distinguish any local phenomenon from a systemic phenomenon.

There are four important factors which must be evaluated to judge performance of liquid crystal thermography. These include temperature resolution, spatial resolution, temporal resolution and insensitivity to pressure (Armstrong 2004; Bharara, Cobb et al. 2006). External factors such as ambient radiation, heat exchange between skin surface and surroundings and presence of fat, moisture and air between skin surface and liquid crystal film can affect the measured temperature (Behle, Schulz et al. 1996).

Temperature resolution depends on temperature range within which the colour spectrum is observed (colour play), this further depends on the mixture and purity of the liquid crystals (Hallcrest 1991; Massi 2004). It also depends on the amount of overlap of reflected colour band and those of adjacent temperatures (Farina, Hacker et al. 1994; Grewal, Bharara et al. 2006). Encapsulated liquid crystals are limited by varying colour-temperature characteristics for different capsules (Armstrong 2004).

Spatial resolution of the thermochromic liquid crystals is limited by the size of individual crystal i.e. 10-15 microns and resolving capability of the optical system (Hallcrest 1991). In a study by the author the spatial averaging of colour images is investigated by image analysis at the pixel level and microscope studies which revealed a non-homogeneous distribution of thermo liquid crystals at the microscopic level (Bharara, Cobb et al. 2005).

Temporal resolution is directly related to the response time of the liquid crystal detector. It is the time required for the detector output to reach 1/e of its final value following a step change in the input. In the early applications of LCT, reponse times of the order of 60 seconds were clinically acceptable for static assessment (Portnoy 1970; Anbar 1998). However, improvements in the LCT technology coupled with better imaging systems provide flexibility towards dynamic assessment (Farina 1995; Bharara, Cobb et al. 2006). The importance of dynamic assessment using LCT for the present study has been discussed. Details of response times of TLC are not readily available although a study by Ireland and Jones (1987) indicated relatively fast response times on the order of a few milliseconds for unsealed TLC (Ireland and Jones 1987). However, the response time is affected by the heat capacity of the film which is dependent on the construction and precise formulation. Wozniak et al. (1996) have suggested the response times on the order of 50 ms for microencapsulated TLC.

Sensitivity to incident load and shear forces can affect TLC calibration and can be a limiting factor in application of the technology (Bharara, Cobb et al. 2006). This is critical in the context of the proposed study since thermal measurements are to be obtained at the plantar surface under normal loading conditions. This constraint is important since ulceration does not normally occur in an unloaded condition (Boulton, Connor et al. 1998). However, it is currently not possible to obtain simultaneous thermal and pressure measurements at the sole. This implies that pressure compensation for TLC will not be possible in the proposed study and a TLC formulation that is insensitive to pressure within the expected range is essential. Some formulations and encapsulation techniques appear to exhibit good insensitivity to pressure although to the author's knowledge objective data in support of such observations has not been published in the

literature. For this reason an extensive and detailed evaluation of pressure sensitivity was conducted for TLC sheets supplied by the manufacturer.

In order to attain good repeatability and comparability of pathological thermal patterns, conditions in which thermographic assessment is performed must be standardised. A brief outline of optimum conditions is given below (Armstrong 2004).

- Constant ambient temperature (20-24 °C)
- No direct exposure to heat sources in immediate vicinity
- Controlled humidity
- Minimum basal temperature of body to avoid affect of internal and external factors on body temperature. (Basal metabolism refers to energy used to maintain constant body temperature).
- All examinations must be performed at the same time of day to avoid any errors due to circadian rhythm variations (Klosowicz, Jung et al. 2001).
- Liquid crystal sheets can be destroyed by exposure to water, solvents or ultra violet light. Therefore, care should be taken to prevent such exposure.

### 3.2.7 LCT - Recent work and current status

Preliminary thermographic results show good correlation between liquid crystal thermography and conventional infrared thermography (Baer, Hetherington et al. 1988). However, there were no further research initiatives to develop the liquid crystal technology. The current work is consistent with the requirement of developing liquid crystal thermography as a useful tool to study thermal patterns at the lower extremities in diabetics.

Thermological measurements provide data related to influence of total blood flow (i.e. both thermoregulatory and nutritional) in the tissue. Results from infrared thermographic studies show that rate of warming, maximum recovery temperature, degree of temperature variation at the anatomical site and lag time (time interval between onset of

thermal stress to onset of cooling/warming) are useful when assessing response to thermal cycling (Merla, Di Donato et al. 2002). Careful interpretation of results is necessary with respect to their physiological meaning.

One of the key points that justifies current work as a progression of past research initiatives is the pressure insensitivity of thermochromic liquid crystals used. Better chemical formulations and manufacturing processes have led to availability of pressure insensitive TLC's (Armstrong 2004). For flow visualisation studies on solid surfaces, temperature insensitive and shear sensitive formulations with unsealed TLC are available (Armstrong 2004). Microencapsulation of the raw TLC eliminates the shear-stress dependencies of the liquid crystals (Wozniak, Wozniak et al. 1996).

Using microscopic optics, non-invasive temperature mapping to 0.1 C with micron-level spatial resolution can be obtained using the ThermView[1] system. However, cost of such a system is a prohibitive factor for use in the current study.

## *3.3 Calibration procedure*

### 3.3.1 Introduction

Typical calibration procedure, alternative approaches, calibration parameters and determination of optimum parameters are discussed.

### 3.3.2 Calibration of thermochromic liquid crystals

In early applications of LCT, manual interpretation of single colour isotherms was used. The colours selected were yellow or green as human sight is most sensitive to these wavelengths. However, this interpretation was subjective, inaccurate and had poor thermal resolution. These methods were time consuming when a large dataset had to be analysed with detailed distribution of surface temperature. Digital image processing has

[1] ThermView by Advanced Thermal Solutions, Inc., MA (USA)

greatly reduced time to process thermographic data and provides good spatial and thermal resolution. Both chromatic and monochromatic techniques are used to assess temperature distribution.

Colour detection either involves human observation, intensity based image processing (either by using monochromatic filters or monochromatic illumination) or colour based image processing (camera transforms the incoming light into RGB intensities). Colour detection using human observation has high uncertainty and inaccuracy (Behle, Schulz et al. 1996). Thermal resolutions better than 0.02°C have been reported using hue based calibration technique (Ashforth 1996).

Temperature measurement using thermochromic liquid crystals requires calibration of the reflected wavelength using either a steady state or a transient technique. Calibration of thermochromic liquid crystals involves illumination by a source with well defined characteristics and measurement of the reflected wavelength at a given calibration temperature. The steady state approach (Camci, Kim et al. 1992; Hay and Hollingsworth 1996; Hay and Hollingsworth 1998; Grewal, Bharara et al. 2006) provides accurate measurements that are independent of variations in response time that occur within the colour bandwidth (the change in hue is not a linear function of temperature). However, the time required for stabilisation of the reference temperature results in a lengthy calibration procedure.

A faster calibration cycle is afforded by the transient technique in which the thermal reference is ramped over the colour bandwidth (Bakrania and Anderson 2002). However care must be taken to ensure that the rate of change of the temperature is slower than the response time of the LCT sheet, which in some formulations can be as high as 60s (Anbar 1998). The complexity or duration of the calibration is further complicated by the need to obtain measurements that are spatially averaged over the sensing area. This requirement arises from variations in the homogeneity of the liquid crystals due to manufacturing tolerances.

Modern approaches to LCT calibration employ RGB image sensors which provide measures of the reflected intensities of the three primary colours i.e. red, green and blue intensities. These are then encoded using a suitable colour model to produce a single hue value which has a one to one mapping with temperature (Behle, Schulz et al. 1996; Hay and Hollingsworth 1996; Jambunathan, Hartle et al. 1996; Hay and Hollingsworth 1998; Chan, Ashforth-Frost et al. 2001; Anderson and Baughn 2004).

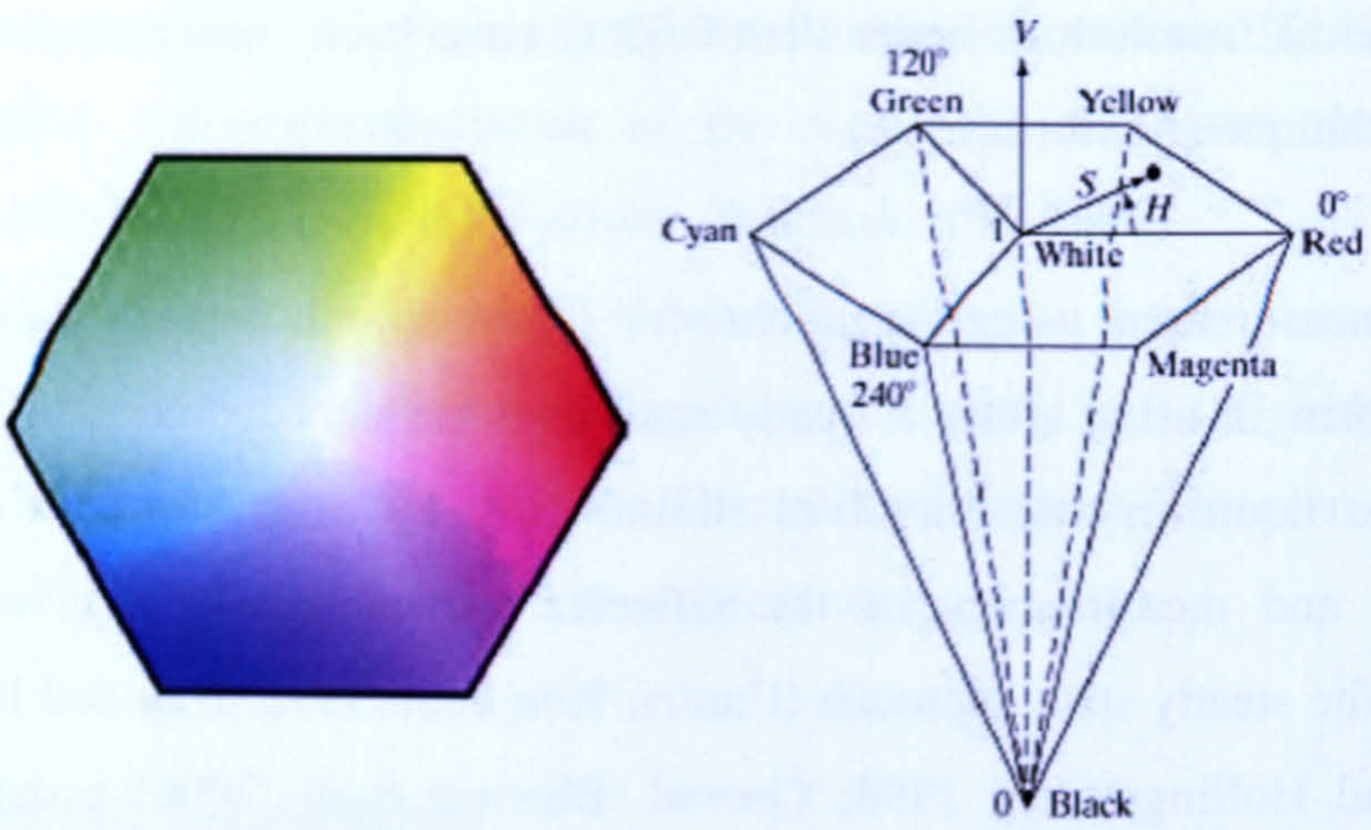


**Figure 3-4: The HSI colour model. Angle from the red axis gives hue and length of the vector gives saturation. Intensity is given by position of the plane on vertical axis. (Gonzalez et al. 2004)**

Typically, hue intensity from HSV colour space is used in TLC calibration to describe surface temperature. Hue based measurements are also known as HSI chromatic interpretation technique. HSI colour system is considerably closer than the RGB colour system to the way in which humans experience and describe colour sensations (Gonzalez, Woods et al. 2004). Figure 3-4, illustrates the hue-saturation-intensity (HSI) colour model. The remaining two variables are saturation and value, representing the purity of the colour and maximum RGB intensities respectively. The hue represents the dominant wavelength of colour and is derived from the RGB triplet value.

$$H = \begin{cases} \theta & if \ B \le G \\ 360 - \theta & if \ B > G \end{cases}$$ **Equation 3-1**

$$\theta = \cos^{-1}\left\{ \frac{1/2[(R-G)+(R-B)]}{[(R-G)^2+(R-B)(G-B)]^{1/2}} \right\}$$ **Equation 3-2**

$$S = 1 - \frac{3}{(R+G+B)}[\min(R,G,B)]$$ **Equation 3-3**

$$I = 1/3(R+G+B)$$ **Equation 3-4**

RGB colour intensities can be transformed into HSI colour space by using equations 3-1 to 3-4 (Gonzalez, Woods et al. 2004). Here, 'R', 'G', 'B' denote the red, green, blue intensities; 'H','S', 'I' denote hue, saturation and intensity. '$\theta$' is the measure of hue.

The hue is not affected by light intensity and therefore, theoretically, does not change as a function of distance to the light source (Anderson 1999). Changes in light intensity only affect the saturation and intensity in the image. Another important characteristic of the hue is that it increases monotonically with the temperature. Thus, it is the single most robust variable offering a one to one mapping between colour and temperature. For each image acquired by the steady state technique, the mean and standard deviation in the hue is calculated for the region of interest. In order to minimise the measured hue uncertainty, saturation and intensity should be maximised by improving the TLC coverage factor (the ratio of TLC reflection to the background reflection) and proper choice of illumination source respectively (Anderson 1999).

Hue temperature calibration is the most common technique used for almost all applications of LCT (Behle, Schulz et al. 1996; Hay and Hollingsworth 1996; Jambunathan, Hartle et al. 1996; Hay and Hollingsworth 1998; Chan, Ashforth-Frost et al. 2001; Anderson and Baughn 2004). However, other colour maps such as RGB

(Matsuda, Ikeda et al. 2000) and artificial intelligence techniques such as neural networks (Kimura, Uchide et al. 1992) have also been used. Matsuda et al. (Matsuda, Ikeda et al. 2000) used normalized RGB values to develop a smooth calibration curve in three dimensions by interpolating the missing values. The advantage of this technique is that the entire colour bandwidth can be used unlike the hue temperature calibration. However, Matsuda et al. (Matsuda, Ikeda et al. 2000) have not considered the high standard deviation in RGB values leading to higher uncertainty in the measured temperature. Small variations in light intensity will further affect the RGB values raising uncertainty in the measured temperature. Kimura et al. (Kimura, Uchide et al. 1992) used neural networks to improve the hue based calibration technique, but did not consider other image parameters and the effect of lighting which may affect the temperature accuracy. Using the proposed approach, a calibration map for the entire colour bandwidth of the TLC can be constructed based on training from all datasets i.e. datasets from repeated calibration runs. Neural network based calibration technique for TLC is helpful to minimise dependence of measured temperature on variations in background illumination (Grewal, Bharara et al. 2006).

### 3.3.3 Calibration parameters

Since hue is dependent only on wavelength, TLC calibration data is independent of the intensity of the illuminating source (Anderson 1999). However the image data can be corrupted by artefacts that depend on the optical path (distance and angle) between the illumination source and imaged object as well as illumination from external sources. Bakrania and Anderson (Bakrania and Anderson 2002) have shown that sensitivity to illumination artefacts is reduced by polymer encapsulation of the liquid crystals. Farina et al. (1994) demonstrated that such artefacts could be minimised through use of on axis illumination and a cross polariser in the optical path to the imager.

Additionally, achieving a reliable calibration requires that the characteristics of the illumination source, hysteresis and pressure sensitivity of the TLC must be considered. Hysteresis effects can significantly affect TLC calibration. Several investigators have

reported that liquid crystals exhibit hysteresis when heated above the clearing point temperature (Anderson 1999; Bakrania and Anderson 2002). The clearing point is the temperature at which the TLC becomes transparent as a consequence of the crystals achieving a non reflecting isotropic state. When TLC is cooled, the change back to the anisotropic semi-crystalline state is principally dependent on the rate of cooling which leads to a shift in the hue versus temperature profile. This change is reversible provided that the TLC is allowed to cool to a formulation dependent temperature termed the event temperature. The event temperature also signifies the lowest temperature at which a change in hue can be detected.

The final complicating factor in the calibration of TLC is a discontinuity of the hue versus temperature response over part of the operating bandwidth close to the red-green transition (Anderson 1999). If compare the normalised hue value for red (~0.9), green (~0.2 - 0.3) and blue (~0.6), there is a discontinuity in hue in the red to green transition. Consequently, it is difficult to apply a least squares polynomial fit to the calibration data. Traditionally, this problem requires manual intervention to complete the calibration which further lengthens the procedure. The discontinuity in the hue must be eliminated before a polynomial fit can be successful. This reduces the usable colour bandwidth of the TLC. Recently, a novel solution based on a neural network that allows a calibration curve to be obtained over the full operating bandwidth without manual intervention has been developed (Grewal, Bharara et al. 2006). Specific details of this neural network based calibration approach are discussed in the next chapter.

### 3.3.4 Determination of optimum characteristics

Different physical forms of thermochromic liquid crystals, their specific applications and typical calibration procedures have been discussed in the preceding sections. The purpose of this section is to converge above facts leading to specific characteristics of a clinical LCT system. It must be emphasised that choice of TLC material, calibration approach, image analysis and reporting of results is task specific. The important factors to be considered include colour bandwidth of the TLC, hysteresis assessment, pressure

sensitivity and choice of calibration. A robust calibration determines the accuracy and thermal resolution of the measurement system. Independent assessment for the spatial resolution and temporal resolution must be performed, in accordance with the desired parameters such as measurement surface, its geometry and response times.

The focus of current work is to use LCT for static and dynamic measurements of the plantar foot. In order to characterise the measurement system, a consistent protocol must be developed and followed to achieve useful results. Keeping in mind the benefits and ease of calibration, hue temperature calibration will be most appropriate for the current work.

In order to develop LCT as a tool for neuropathic assessment of the diabetic foot, the issues related to independent thermal measurements must be resolved. Considering this, various thermal measurement modalities such as electrical contact thermometry, infrared thermography and cutaneous temperature discrimination thresholds were considered. Each technique is independently discussed with a brief background, data processing requirements, medical applications, and suitability for diabetic foot assessment in the following section.

## *3.4 LCT versus other thermological methods*

### 3.4.1 Introduction

Different methods used clinically to assess small fibre function are discussed.

### 3.4.2 Electrical contact thermometry

Electrical contact thermometry in general means use of appropriate transducers (individual or arrays) to measure surface temperature of the body in contact. Thermistors or semiconductor resistors are used for accurate local measurements. Thermocouples are

application of Seeback effect, where two different metals under a temperature differential produce a contact voltage or thermal electromotive force (depends upon contact site).

Kelechi et al. (2006) propose a limit of agreement of ± 1.5°C between infrared and thermistor thermometers (Kelechi, Michel et al. 2006). However, these are only suitable for localised skin temperatures for symptomatic sites and do not have whole field capability (Baer, Hetherington et al. 1988). Foot sized arrays or smaller local arrays could be built to measure foot temperature under the plantar surface (Anderson 2001). Giansanti et al. (2006) have simulated and developed a thermal odoscope for the wearable dynamic thermography (Giansanti, Maccioni et al. 2006; Giansanti and Maccioni 2007). This is a device based on thermocouples for contact thermography with typical applications in breast thermography, viability studies, dermatological studies and rheumatic disorders. A similar electronic thermometer for ambulatory measurements in the diabetic foot with neuropathy has been reported (Kang, Hoffman et al. 2003).

Fundamental considerations associated with electrical contact thermometry are response time, calibration, temperature dependence of measured variable and effects on object being measured. Response time depends on measurement conditions, sensor (or probe) size and heat capacity. Calibration for skin surface measurements is difficult (unlike for fluid calibration). Special thermal phantoms can be made for comparative measurements with calibrated electrical surface thermometers. Excessive pressure from the sensor (or probe) could alter the blood supply and hence, surface temperature.

However, there were issues relating to patient isolation, variable response times for different thermocouple units, compensation electrical circuits for thermocouple units and real time data logging instrumentation.

### 3.4.3 Infrared thermography

Infrared (IR) thermography is real time temperature measurement technique used to produce a coloured visualisation of thermal energy emitted by the measured site at a

temperature above absolute zero. Jones and Plassmann (2002) have provided an excellent review on IR technology along with related image processing considerations. Traditionally, a 2-D image representing 3-D thermal distribution is acquired using standard image acquisition hardware. Each pixel in the image depicts the radiance falling on the focal plane array/microbolometer type detector used in IR camera.

Technological advances in IR cameras in terms of speed and spatial resolution now make it possible to quantitatively assess thermal patterns. It is recommended that IR imaging equipment must be regularly calibrated and characteristic parameters must be determined using simple tests like spatial resolution, stability of temperature measurement and linearity of field. The imaging protocol and quantitative techniques in medical thermography have been well described (Ring and Ammer 2000). Jones et al. (2005) identified a common need to establish a reference database of normal thermograms from which the abnormal findings can be reliably assessed (Jones, Ring et al. 2005). The reference database is a multi-centre effort to standardise infrared imaging for reproducible and clinically relevant thermal measurements.

IR thermography finds numerous applications in medicine which include breast thermography, vascular complications (Wang, Wade et al. 2004), skin thermal properties (Otsuka, Okada et al. 2002), inflammatory response (Rajapakse, Greennan et al. 1981; Ring, Dieppe et al. 1981; Ring 1987; Armstrong, Lipsky et al. 2006), Raynaud's phenomenon (Howell, Kennedy et al. 1997; Merla, Di Donato et al. 2002; Foerster, Wittstock et al. 2006), sleep research (Heuvel, Ferguson et al. 2003) and pain related thermal dysfunction. IR thermography is non invasive and high resolution technique used to measure physiological changes complementing standard radiographic investigations (Jones and Plassmann 2002). Wang et al. (2004) used IR thermography in a small patient group with vascular or neurological complications and emphasised the need for establishing normal variation of skin temperature, before establishing abnormal criterion. The technique has been used to assess both anatomical and functional changes.

Langer et al. (1972), Reardon et al. (1982), Armstrong and Lavery (1997), Armstrong et al. (1997) and Harding et al. (1998) have used IR thermography to study vascular complication and foot ulceration in diabetes mellitus (Langer, Fagerberg et al. 1972; Reardon, Curwen et al. 1982; Armstrong and Lavery 1997; Armstrong, Lavery et al. 1997; Harding, Wertheim et al. 1998). Ideally, it will be beneficial to employ thermographic measurements to prevent foot ulceration by studying and documenting thermal findings in lower extremities in well designed clinical studies (Armstrong, Lavery et al. 2003; Lavery, Higgins et al. 2004).

Other physiological techniques like capillary microscopy, laser Doppler flowmetry and plethysmography do not have the whole field measurement capability like IR thermography. Blood vessels close to skin surface can be easily traced by the IR images (Jones and Plassmann 2002). Merla et al. (2002) used IR thermography to assess vasoconstrictive response to cold stress for patients with Raynaud's phenomenon in a pilot study. One of the significant findings of the study was the ability to follow up pharmacological treatment effects.

High sensitivity IR cameras are available but at an increased cost. Besides, IR thermography has poor specificity, for example, thermographic images cannot identify the cause heightened perfusion which could be inflammation, trauma, angiogenesis, systemic or local degeneration. It must be emphasised that the measurements can complement existing results from other modalities. Dynamic area telethermometry (DAT) is an useful biomedical technique based on IR imaging and can be used to assess diabetes mellitus (Anbar and Milescu 1998). It employs assessment of haemodynamic and neurogenic variations in the tissue and offers an objective and quantitative diagnostic figure of merit.

### 3.4.4 Cutaneous temperature discrimination thresholds

Temperature discrimination threshold is a measure of small fibre function and is clinically relevant as temperature sensation is affected early in diabetic patients

(Bertelsmann, JJ. et al. 1985; Guy, Clark et al. 1985; Ziegler, Mayer et al. 1988). Loss of small fibre function due to diabetic neuropathy is a major cause of morbidity in diabetic patients (Liniger, Albeanu et al. 1991). Viswanathan et al. (2002) investigated cutaneous temperature discrimination using TipTherm[2] device (based on different conductivity of materials) for diagnosis of distal symmetrical polyneuropathy. It is a pen like device with two flat sides (one made of metallic material and the other from synthetic material) independent of external power sources, easy to handle and light weight. Its effectiveness was evaluated against standard methods of assessing neuropathy and it showed 97.3% sensitivity and 100% specificity when compared with biothesiometry. Comparison with monofilament produced a comparable sensitivity (98.3%) and reduced specificity at 92.1%.

Bertelsmann et al. (1985) used two- alternative forced choice procedure method that employed thermostimulator (based on Peltier principle) to assess cutaneous thermal perception at foot dorsum and hand dorsum. Both warmth and cold receptors were tested using the thermal stimulator. Two most important findings of this research were the age related differences in thermal discrimination and length dependent nature of diabetic neuropathy. 36 normal subjects and 20 diabetic subjects with neuropathy were selected for this study. It can be argued that these subjects were not age and sex matched. Secondly, to understand the age related differences a larger number of both elderly and younger patient groups are required. The operator bias, intra subject variability and overall subjective nature of the technique discount its use as a routine assessment tool for thermal measurements in diabetic patients. The size of the Peltier stimulator (3cm by 4cm) used means only a local measurement can be performed at a time. This technique is based on subjective assessment and considers response of either cold receptors or warmth receptors due to two reasons (a) specific points are sensitive to either warmth/cold stimuli and (b) cold receptors outnumber warmth receptors by a factor of 3-10 in most areas of the body (Guyton 1992).

---

[2] TipTherm by Axon GmBh Dusseldorf, Germany

Liniger C et al. (1991) assessed thermal sensitivity in diabetic neuropaths using specially developed Thermocross tool (based on thermoresistances). They reported that the deficit in thermal sensation detected by Thermocross paralleled the decline of nerve conduction.

## *3.5 Justification for using LCT in the present study*

Presently, clinicians assess circulatory function, neuropathic complications and pressure distribution in the lower extremities to identify risk of foot ulceration (NHS 2004). This combined approach is well accepted throughout the diabetic clinics and research centres to prevent the onset of foot ulceration. NICE guidelines suggest considering the risk category of patients, relative contribution of all contributory factors and incorporating the respective management strategies for the treatment of diabetic foot disease.

Pathways leading to ulceration and underlying pathophysiology have not been fully identified. Although it is widely accepted that risk of traumatic consequences of foot ulceration can be reduced by clinical intervention following a reliable diagnosis based on clinical presentation and appropriate tests (Armstrong, Lavery et al. 1998; Viswanathan, Madhavan et al. 2005). It is highly unlikely, that a severely neuropathic foot will respond to any form of intervention, thus accentuating the need for early diagnosis of the neuropathic condition (Perkins and Bril 2002).

The clinical diagnostic criterion for the diabetic foot is well documented in literature (NHS 2004). However, the research efforts in refining the diagnostic algorithm for diabetic foot disease have been limited. Armstrong et al. (1998) report on the marriage of simple sensory testing modalities to screen for risk of diabetic neuropathic ulceration with emphasis on the technique characterisation. They recommend selecting a quick, inexpensive and accurate instrument (high sensitivity and specificity) for clinical use followed by appropriate intervention modalities. It may also be beneficial to evaluate alternative relevant modalities for the same purpose.

Thermal changes under the plantar foot may be compounded by vascular insufficiency, diabetic neuropathy, skeletal changes, infection or a combination of these factors. Reactive hyperaemia following a period of loading is impaired in the neuropathic foot (Flynn, Edmonds et al. 1988; Cobb 2000). There is however, very little evidence suggesting the status of a similar response to thermal cycling specific to diabetic foot assessment. Systemic thermal stimulation increases skin blood flux through reduced sympathetic neural action on AV shunts, whereas local heating affects capillary perfusion irrespective of sympathetic neural activity (Hales, Iriki et al. 1978; Hales 1983; Hales, Jessen et al. 1985). A laser Doppler study (Rayman, Williams et al. 1986b) demonstrated impaired hyperaemic response to thermal stimulus in type 1 diabetic patients.

Diabetic neuropathy results in increased microcirculation and dissipates heat due to increased metabolic rate (Archer, Roberts et al. 1984; Stess RM, Sisney PC et al. 1986; Clark, Goff et al. 1988; Benbow, Chan et al. 1994). Dynamic measurements may be sensitive for detection of perfusion abnormalities owing to neuropathy in diabetic subjects. The change in temperature when warming or cooling the foot are described by the change in environment, heat exchange between surrounding tissue by conduction, heat exchange owing to perfusion and heat production by metabolism. Figure 3-5, illustrates the measurement parameter when using LCT for a clinical assessment. It is therefore appropriate to consider the affect of neuropathy on regulation of blood flow, in the foot. Ring et al. (1984) recommended the use of thermography for information on the normal and abnormal functioning of the sensory and sympathetic nervous systems, vascular dysfunctions and local inflammatory processes (Ring and Phillips 1984).

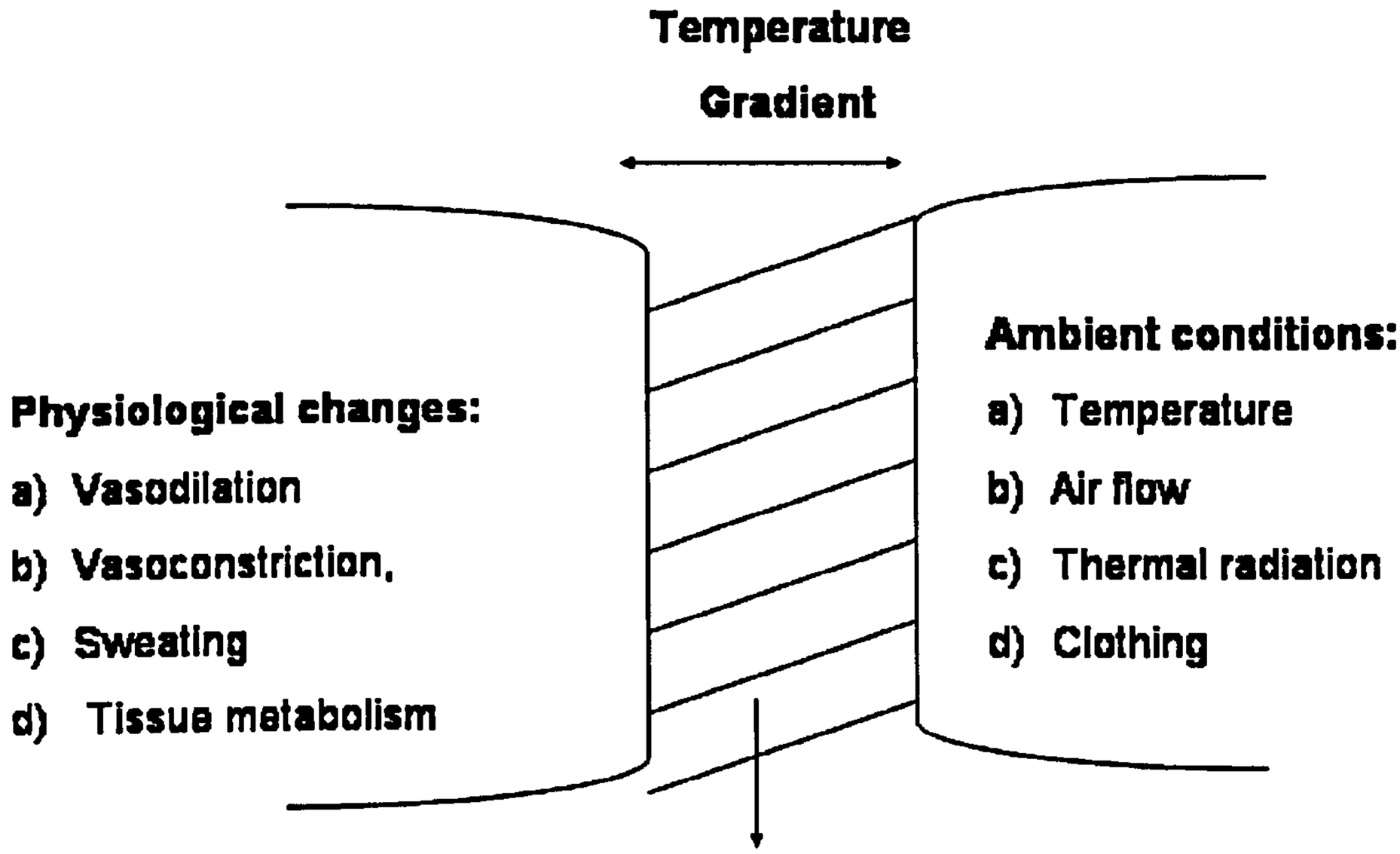


**Figure 3-5: Schematic diagram showing the measured parameter when using LCT. Contact thermography disturbs thermal conditions at the measurement site. Ideally, thermal patterns must be recorded before ambient conditions significantly induce physiological changes.**

Neurogenic modulations result from neuroregulatory processes which involve feedback from peripheral and visceral thermosensors (Anbar and Milescu 1998). It is suggested that diabetes disturbs unmyelinated nerve fibre function prior to and more severely than large fibre function (Guy, Clark et al. 1985; Ziegler, Mayer et al. 1988). The neuropathic foot exhibits increased skin temperature and heightened colouration under rest, indicative of increased blood flow (Cobb and Claremont 2002). There is supporting evidence from other studies (Stess RM, Sisney PC et al. 1986; Benbow, Chan et al. 1994) which confirm these findings.

The above findings are also well supported by the developed hypothesis of 'capillary steal' theory which incorporates arteriovenous shunting (Uccioli, Mancini et al. 1992). There are two main types of capillaries involved in skin perfusion, nutritive and thermoregulatory. According to the 'capillary steal theory', microcirculatory blood bypasses nutritional capillaries through the dermal thermoregulatory capillaries leading to

tissue hypoxia due to maldistribution of skin microvascular blood flow (Uccioli, Mancini et al. 1992). Mork et al. (2000) provided a hypothesis similar to the popular 'capillary steal' theory for arteriovenous shunting as the pathogenetic factor in erythromelalgia (Condition of red, warm and burning painful extremities). Mork et al. (2000) suggest disease etiology may be of neural or local vasoactive origin. Erythromelalgia is a rare disorder of unknown etiology (Mork, Asker et al. 2000) producing similar symptoms (AV shunting and denervated sympathetic pathways) as in diabetic neuropathy (Vendrell, Nubioda et al. 1988; Staub, Munger et al. 1992). An alternative proposal the 'haemodynamic hypothesis' (Netten, Wollersheim et al. 1996) links microangiopathy and rheological changes in blood vessels with the observed impaired hyperaemic response.

Despite evidence from the preceding studies suggesting local changes in the response to thermal variations may be significant in ulceration, there is no conclusive link and evaluation of thermal sensitivity remains a research topic that has seen little progress towards adoption as a routine clinical measure. A key development has been the relatively recent availability of pressure independent temperature measurements using liquid crystal films. The development and application of this technology in assessing the diabetic foot is primary goal of the present study.

## *3.6 Summary*

In order to provide a reliable diagnosis for peripheral neuropathy and compensate for the frequently mild, subclinical or moderate nature of the disease, it is essential to supplement the standard array of neurophysiological tests. It has been discussed that assessment of small fibre function can further clinician's understanding about the extent of neuropathic damage. Quantitative assessment of small fibre degeneration offers possibility of monitoring effects of drugs and metabolic status in lower extremities due to altered glycaemic levels in diabetes.

The focus of current work is to determine association between thermal changes in plantar foot and sensory loss in diabetic foot disease using an appropriate thermal imaging

technique. The development of appropriate technique must be able to emerge from the complex research protocol into a simple clinical tool, supporting evidence management of the diabetic foot.

Measurement of plantar pressure and determination of extent of sensory neuropathy cannot be used to establish the mechanisms that lead to tissue damage and initiate ulceration. Thermological techniques can be used to supplement above measurements by providing both qualitative and quantitative data. Skin temperature is a product of influences arising from both internal structures and external conditions. In early stages, the affected areas appear as hot spots but later on appear cold due to significant vascular impairment. A low cost imaging technique with high sensitivity, high specificity and a well defined measurement protocol can significantly contribute to evaluation and treatment of diabetic foot.

LCT allows the clinician to localise symptomatic areas and employ appropriate intervention and monitor its effects. The determination of a normal or abnormal thermal pattern must be by the thermal uniformity of temperature and by comparisons of symptomatic and asymptomatic areas.

# Chapter 4 Development of a liquid crystal thermography system

## *4.0 Introduction*

The purpose of the work presented in this chapter is to evaluate three physical forms of liquid crystals based on their characteristic parameters, including calibration, spatial density, pressure sensitivity, hysteresis and response time. The following sections discuss the development of the prototype system, characterisation of commercially available thermochromic liquid crystals, a new calibration algorithm using neural networks and implementation of a novel clinical LCT system. Analysis was accomplished through detailed hue-temperature calibration data for both narrow band and wide band TLC. The experiments described below were performed with the intent of developing a low cost clinical thermography system for assessing the diabetic neuropathic foot. The principal need for such a system is to further understanding of the pathogenic mechanisms of plantar ulceration in diabetic patients.

## *4.1 Pre development work*

### 4.1.1 Design of initial prototype system

The commercial contact thermography system (Contflex System[3]) was considered for the intended application. It consists of a measurement plate with an air inlet valve to enable the sensing surface of the sensor to adapt to the contours of the anatomical part. This system is intended for use in rheumatology, orthopaedics, dermatology, sports medicine, angiology and for detection of breast tumours (Leinidou 2003). This device is typically useful in breast thermography to assess the curved surface. Although, a similar system has been used for diabetic foot assessment (Stess, Sisney et al. 1986). Pneumatic control is not an essential permissive factor in the design of a typical LCT system. The measurement plate consists of thermochromic liquid crystals on latex support which is

[3]By I .P.S. s.r.l. - International Products & Services, Milan (Italy)

imaged by a Polaroid camera illuminated using a diffused flash light. However, this system was found to be unsuitable for assessment of the diabetic foot with neuropathy for the following reasons:

a) The cost of the system[4] (circa £2000.00) was discussed with diabetic consultants and is generally considered prohibitive for routine assessment. This is a central justification for the current study which aims to provide a lower cost solution employing thermochromic liquid crystals (a maximum target cost of £1000.00 has been specified following discussion with consultants).

b) The Contflex System was not capable of recording thermal patterns under the foot in the presence of underlying pressures as there was a danger of physical damage to TLC plates. Moreover, the thermochromic crystals employed in this system are not tested for pressure sensitivity (Quagliardi 2005). Conversely, TLC sheets (available from Hallcrest, UK) specifically employ a pressure insensitive chemical formulation (Armstrong 2004).

c) Temperature measurements using TLC plates in the Contflex system were limited by the manufacturer's calibration. This system is typically, used for qualitative analysis and it is difficult to calibrate latex based TLC using conventional approaches (Bharara, Cobb et al. 2005).

d) The conformal properties of latex provide a cushioning effect such that the thermal measurements are not representative of actual loading conditions of the foot during standing and gait.

To evaluate the feasibility of producing a low cost LCT system for assessing plantar temperatures under normal loading a simple measurement platform was constructed (Appendix B). A thermochromic liquid crystal polyester sheet (450mm x300 mm) was fixed onto an optical grade polycarbonate glass[5] of 6mm thickness using single sided

---

**[4] Cost includes prices for Contflex AGT8 system and TLC plates**
**[5] By Edmund Optics, York, UK**

adhesive tape. This assembly was then located in a recess such that it was flush with the surface of reinforced wooden box. Four fluorescent bulbs[6] (20 watts each), colour temperature 6500K were located within the platform to uniformly illuminate the TLC sheet through the polycarbonate window. Photograph 4-1 illustrates this prototype measurement platform.

To ensure stable illumination, matched fluorescent bulbs were used and driven from a filtered mains supply of 240V. A variable mains control was used which allowed the illumination to be switched and the illumination level accurately adjusted. These controls were mounted at the base of the platform in accordance with standard electrical safety procedures.

The inside of the measurement platform was painted matt white to ensure diffuse scattering of light from the source. This was necessary to eliminate bulb artefact from the acquired images. Image capture was achieved using a three chip CCD (charge coupled device) video camera (Panasonic NV-MX 500, RGB) with integral digital (SD) memory card. The camera did not allow automatic image acquisition.

The prototype measurement system was carefully assessed for safety under static loading using a 200 litre water butt filled with water to simulate loads up to 120 Kg. The system was then used to obtain test images from four healthy volunteers in accordance with University ethical regulations.

Prior to image acquisition, all subjects were made comfortable and seated on a chair with feet flat on ground. The subjects were barefoot, with feet resting on their footwear. After 15 minutes of temperature acclimatisation with the ambient temperature, they were instructed to place their right foot on the platform. A set of eight images were acquired for each subject in the seated position with a two second sampling rate. There was no stimulus (either thermal or physical), therefore only static data was acquired. The images were taken manually (whilst the camera rested on a tripod) and the sampling rate of two

---

**[6] By Light Bulbs Direct Ltd., Bucks, UK**

seconds was chosen for ease of operation. Photograph 4-2 illustrates individual images of the plantar surface of right foot for the four healthy test subjects. Image resolution was 640x480 and all images stored on the SD memory card had to be manually transferred to the hard disk for analysis.

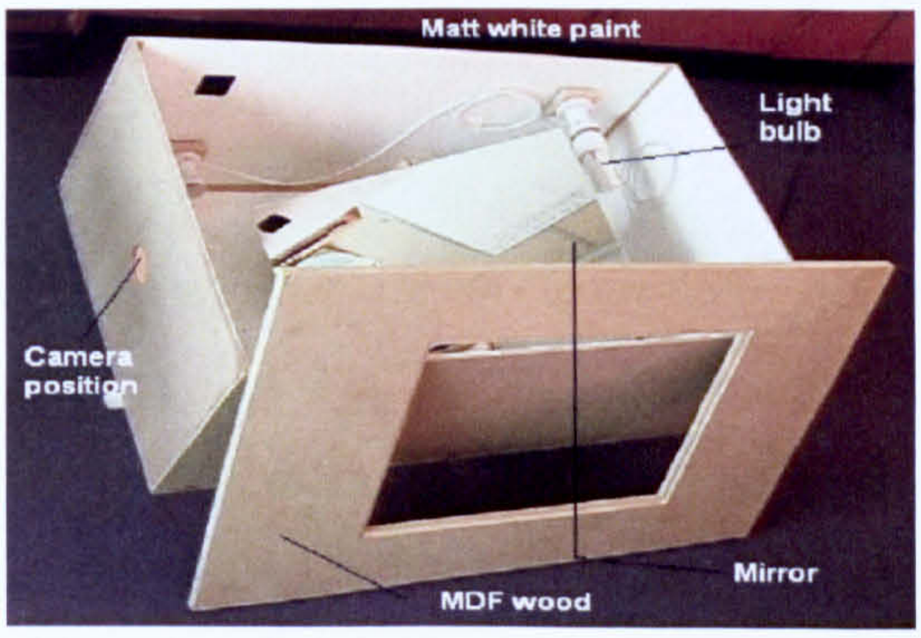


**Photograph 4-1: Photograph of the first prototype measurement platform.**

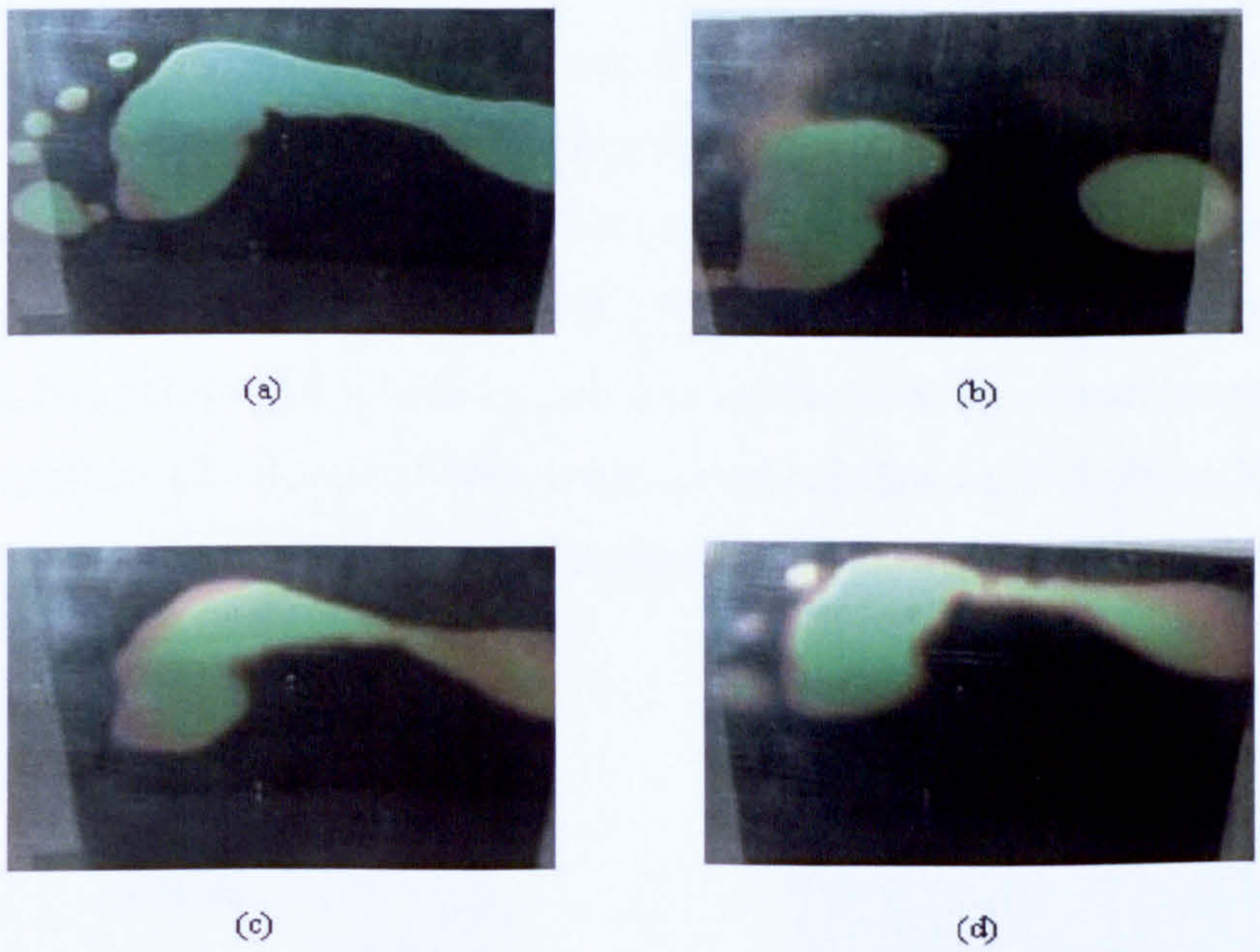


**Photograph 4-2: Typical images of plantar surface of the feet from four subjects acquired with TLC sheet.**

It can be seen that the anatomical shape of the foot, especially the foot arches has a considerable affect on overall image. Furthermore, small differences of temperature affect image content, for example compare toe area between images (a) and (c).

### 4.1.2 Evaluation of initial prototype system

When testing the effectiveness of the LCT prototype system, several drawbacks were identified. There was optical distortion in the image due to flexing of the polycarbonate under load. Heat from the light source was found to induce thermal noise in the TLC sheet. Furthermore, the imaging approach employed in the original system resulted in a large physical size which was cumbersome to manoeuvre.

To address this issue, imaging path length was reduced by employing two small mirrors which allowed for a smaller system with improved modular construction, greater portability and robustness. It was found that adequate image illumination was achievable using two rather than four sources. This fact coupled with the revised construction allowed the illumination sources to be effectively thermally isolated from the TLC sheet eliminating thermal noise. The revised position of the bulbs also solved the original problem of source artefacts in the image. Consequently it was no longer necessary to whiten the interior of the platform and a black matt paint was used instead to optimise image contrast. A further significant improvement provided by the final design was the ability to image both feet. This can further aid in evaluating bilateral symmetry in the diabetic neuropathic foot, by comparing the thermal patterns of contralateral foot with those from the symptomatic foot. However, due to design limitations and the need for expensive optics, both feet could not be assessed simultaneously. By shifting the camera module over the slider as illustrated in photograph 4-3, each foot can be assessed.

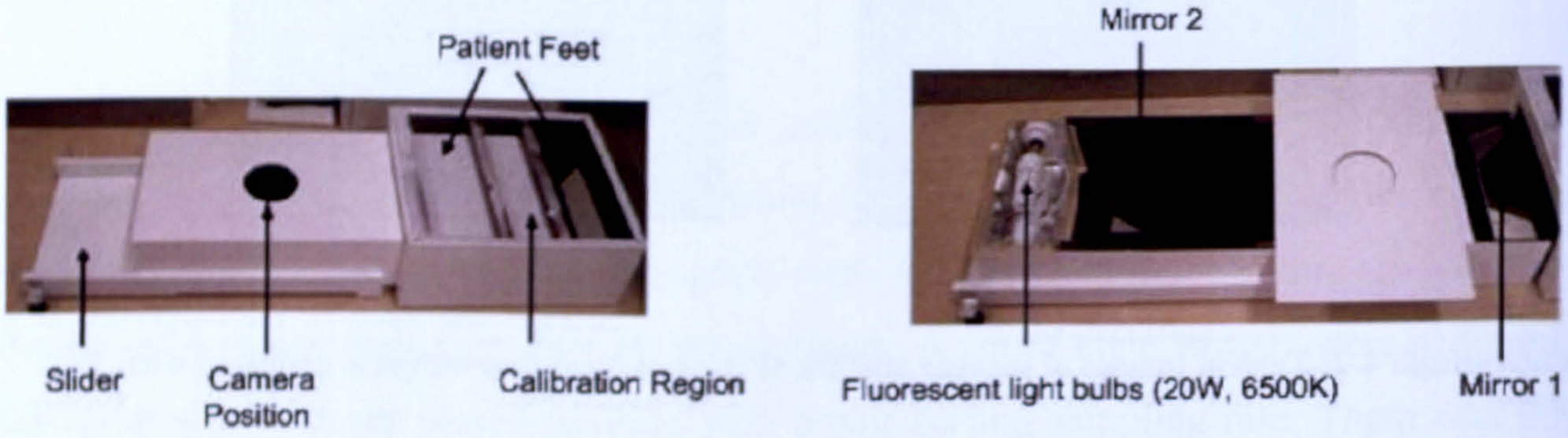


**Photograph 4-3: Second measurement platform with modular design and ability to image both feet.**

### 4.1.3 Final prototype of the measurement platform

To improve the mechanical strength, image quality and portability of the of the measurement platform, a third prototype was designed. This eliminated the need for the modular design of the second prototype and the system was converted into a single smaller unit. The final prototype includes improved light sources (LED strip lights[7]), a high reflectivity mirror[5] and a firewire™ (Apple Inc.'s trade name for IEEE 1394 high speed serial bus) CCD imaging device[8]. This design compromised on the ability to assess both feet simultaneously, however it significantly improved the image quality.

The third (final) prototype was fabricated from reinforced wood in accordance with the design drawing given in Appendix B. Optical grade polycarbonate of 15mm thickness was used as the support for the TLC polyester sheet. This provided good optical access and low thermal conductivity. Three minutes was found to be suitable for the polycarbonate sheet to return to ambient temperature, after removing the calibration plate. This avoids any residual artefacts in the subsequent TLC images. In the final design, a small and portable imaging device based on the Institute of Electrical and Electronics Engineers (IEEE) firewire™ interface was included. This camera (DFK 4102[8]) is a progressive scan, single CCD device offering a maximum resolution of 1280x960 pixels. Detailed specification and camera dimensions are provided in Appendix C. The camera uses DCAM protocol (standardised by Instrumentation & Industrial Digital Camera), approved for scientific and medical applications for transfer of image data and transfer of parameters to control the camera such as brightness, exposure and white balance.

The light emitting diode (LED) strip lights are special solid state devices running on low power (12V DC) and producing high intensity light. Each LED produces cool white light with colour temperature 8000K and has a viewing angle of 85°. The LED strips are self adhesive and are mounted on steel brackets. The LED's replace the fluorescent bulbs in second prototype and offer flexibility, low cost, energy efficiency, shock/vibration

---

**[7] By Ledtronics, Torrence, California, USA**
**[8] By The Imaging Source Europe GmbH**

resistance, no RF interference, noise free operation, and high life. The most important advantage is however, that LED's produce no heat and do not effect the clinical measurement of plantar foot temperatures. Technical details and optical spectrum are discussed in Appendix C.

In order to improve the image quality, it is important to maximise reflection from the mirror into the camera. One of the most important benefits of the third prototype design over its predecessor was that, it discounted use of two mirrors. In the latest design, a high reflectivity (>90%) was used in a rectangular shape (254x313mm; 6mm thickness). These are special mirrors coated with enhanced aluminium for high reflectivity. A rectangular shape provides additional benefit for the intended application i.e. mirror at 45° for a 90° bend in the path of light.

Photographs 4-4 and 4-5, illustrate the top view and side view for the improved measurement platform. This approach reduced the construction time, cost of the material, portability, mechanical strength and made the unit easily serviceable. The need to prevent cross infection when designing a clinical system was also considered. However, the study protocol excludes patients with any active foot ulcers or infections.

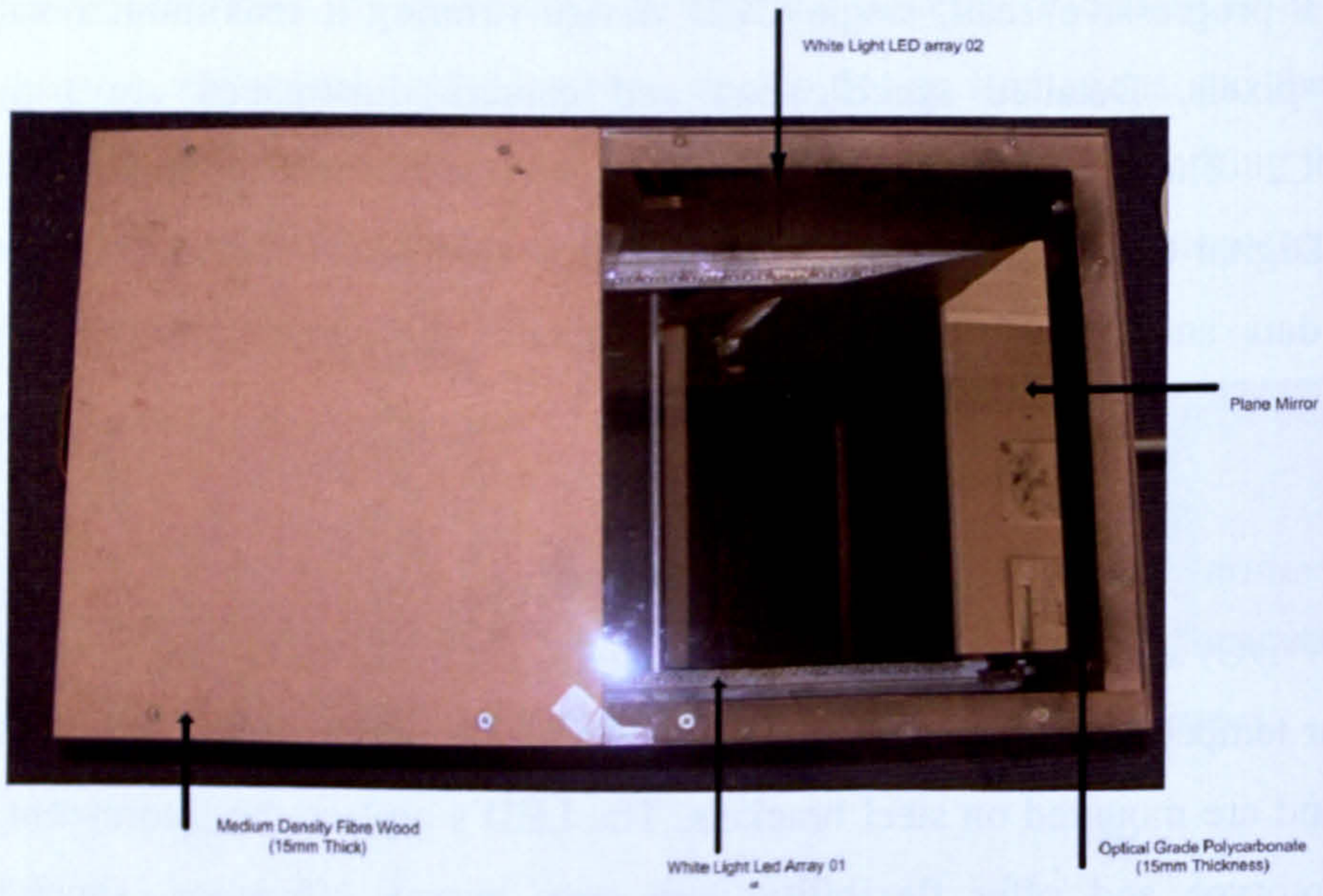


**Photograph 4-4: Photograph of the LCT measurement platform illustrating top view.**

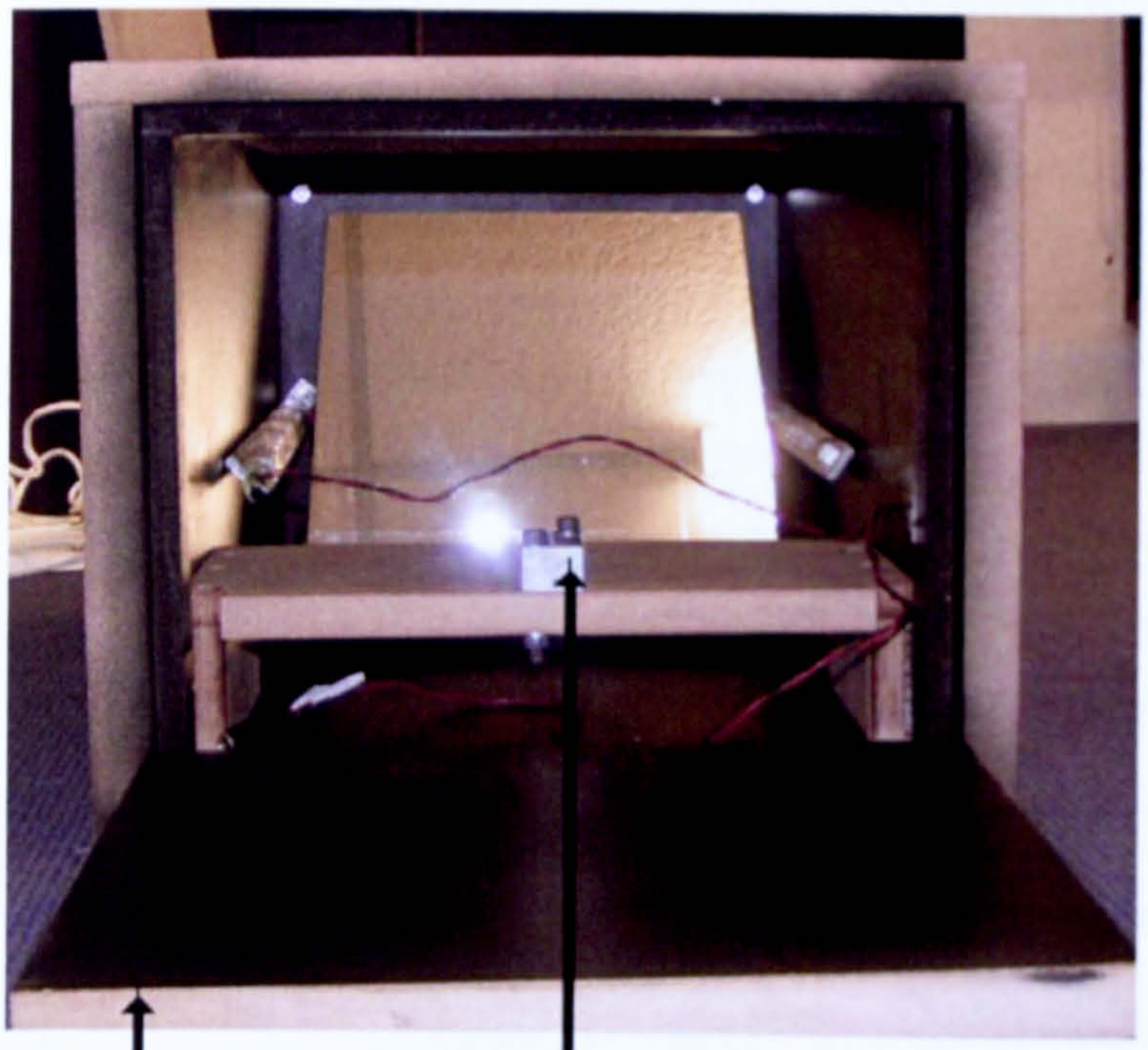


**Photograph 4-5: Photograph of the LCT measurement platform illustrating side view and camera position.**

Having established the design of the measurement system, it was important to identify the most suitable TLC material for use as temperature sensor. Unfortunately, it became apparent that TLC manufacturers were only able or willing to provide very limited characterisation data. Therefore it was considered necessary to conduct an extensive analysis of various TLC materials to assess the following performance characteristics: thermal and spatial resolution, repeatability, sensitivity, hysteresis, pressure sensitivity and response time. The experimental procedures of this investigation are described in the following sections.

## *4.2 Evaluation of thermochromic liquid crystals*

### 4.2.1 Introduction

This section focuses on the methodology adopted to choose the most suitable TLC formulation for use in the LCT system under consideration. This was accomplished by the independent, in vitro characterisation of three physical forms of TLC using a commercial liquid crystal thermography system, TempView[9]. Two different calibration approaches were implemented for the analysis of acquired data. The following sections discuss the experimental setup and procedures used.

### 4.2.2 In vitro characterisation of three physical forms of TLC

#### *4.2.2.1 Experimental setup*

The experimental set up comprised an image acquisition system and a calibration plate as shown in figure 4-2. Three TLC polyester sheet[10] materials with different colour bandwidths were used: R25C5W, R25C10W and R25C15W. A standard TLC emulsion formulation[10] R25C10W was used. A sample of latex based TLC composite material was obtained from IPS[3] (Milan, Italy) and was specified by the manufacturer as a 5°C colour bandwidth and event temperature of 26°C.

Samples of each TLC sheet and latex material were prepared by cutting them into 25mm x 25mm squares using a scalpel. Due to practical difficulties, the edges cannot be resealed, however the TLC material is encapsulated and bonded to the sheet so cutting has no effect on the colour response of the sheets (Armstrong 2004). Any direct contact with water can destroy the sheet, therefore this was avoided. These samples were mounted using a thermal epoxy on the aluminium carrier of a

---

**[9] By ImageTherm Engineering, Waltham, MA, USA**
**[10] By Hallcrest Ltd., West Meadows Industrial Estate, Derby, UK**

hotplate. For the emulsion specimens, TLC's were mounted onto aluminium hotplate carriers which had previously been painted matt black.

The image acquisition system comprised a personal computer, a Sony XC-003 CCD colour video RGB camera, a 20W halogen light source[11], a PC based National Instruments IMAQ PCI-1408 image processing board and a temperature controller[9] (Watlow Series 96 Temp Controller). RGB images were captured and saved in TIFF format with a resolution of 320x240 pixels. The calibration plate was a thermoelectric unit[9] interfaced to the computer via LABVIEW to collect and store data.

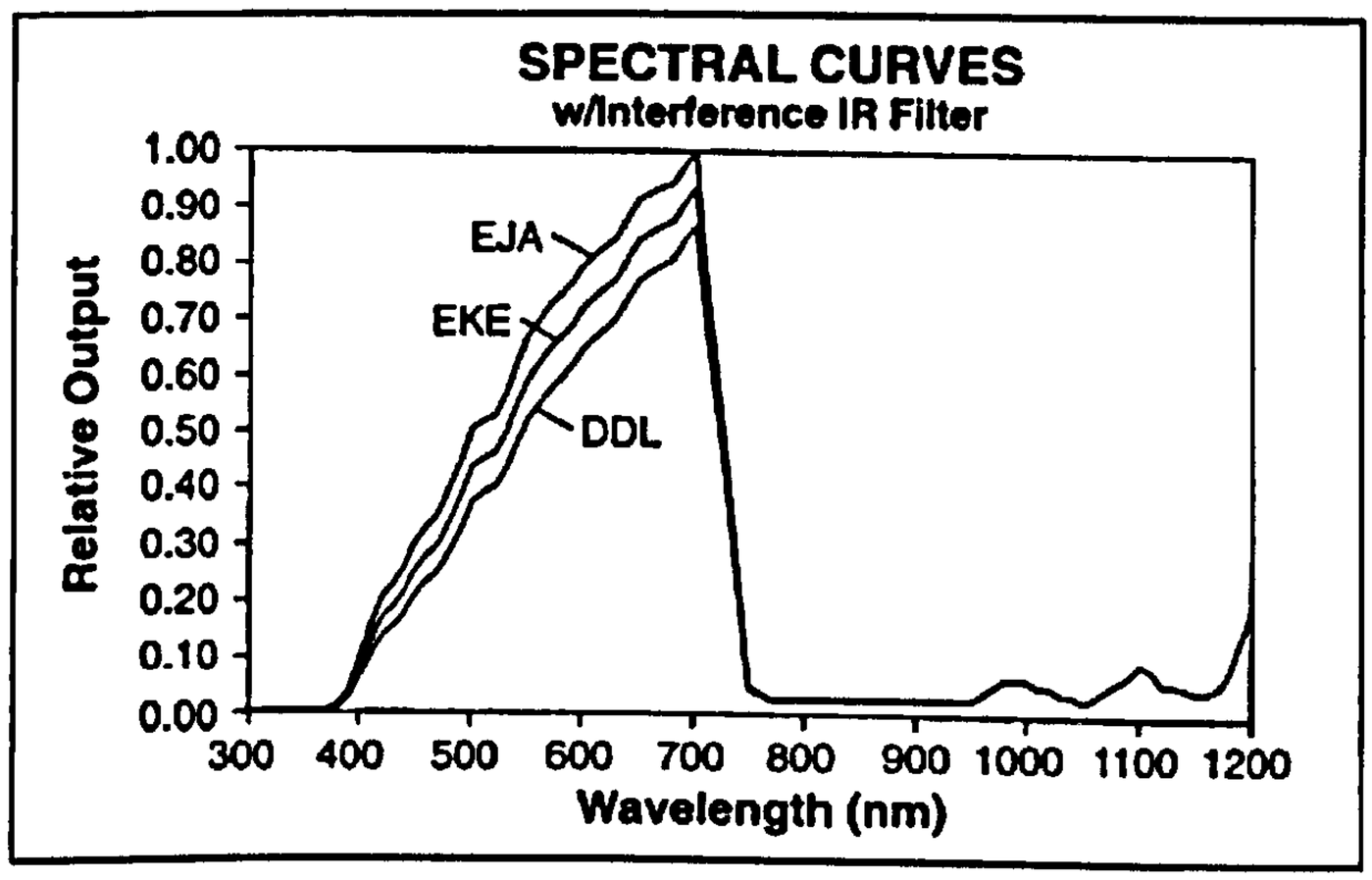


**Figure 4-1: The optical spectrum curve for the A20800 EKE halogen bulb. The graph shows relative output versus wavelength curves for the three variants of the bulb. The experimental setup used 'EKE' bulb for the work under consideration. It is a fairly linear spectrum with low intensity at the blue end (400 nm) and high intensity at the red end (700 nm) (Schott 2005).**

Figure 4-1, illustrates the optical spectrum for the illumination source (colour temperature, 3200K). This illumination source represents commonly used sources for TLC work, with a relatively flattest possible spectrum (Anderson 1999). The unit comes with an IR interference filter for cool illumination (Schott 2005). The power level of the light source could be manually controlled. The system lighting level was adjusted to avoid colour saturation. The camera and light source were placed above the calibration

---

[11] **By Schott North America Inc., NY, USA**

surface with an optimum separation of 25cm. This value was determined empirically in order to maximise image clarity whilst minimising thermal coupling from the source to the TLC specimen. Room temperature regulation and forced cooling of the source were in accordance with manufacturers instructions. Additionally a silicon photodiode was used to monitor any fluctuations in light intensity and it was found necessary to allow a 10 minute stabilisation period following changes in output power. Instabilities occurring during the measurement period were monitored using the silicon photodiode coupled to an 8-bit analogue to digital converter which provided intensity measurements in arbitrary units. Mean illumination intensity was calculated from 10 measurements obtained prior to the duration of each calibration cycle. This basic set up was held constant for all tests.

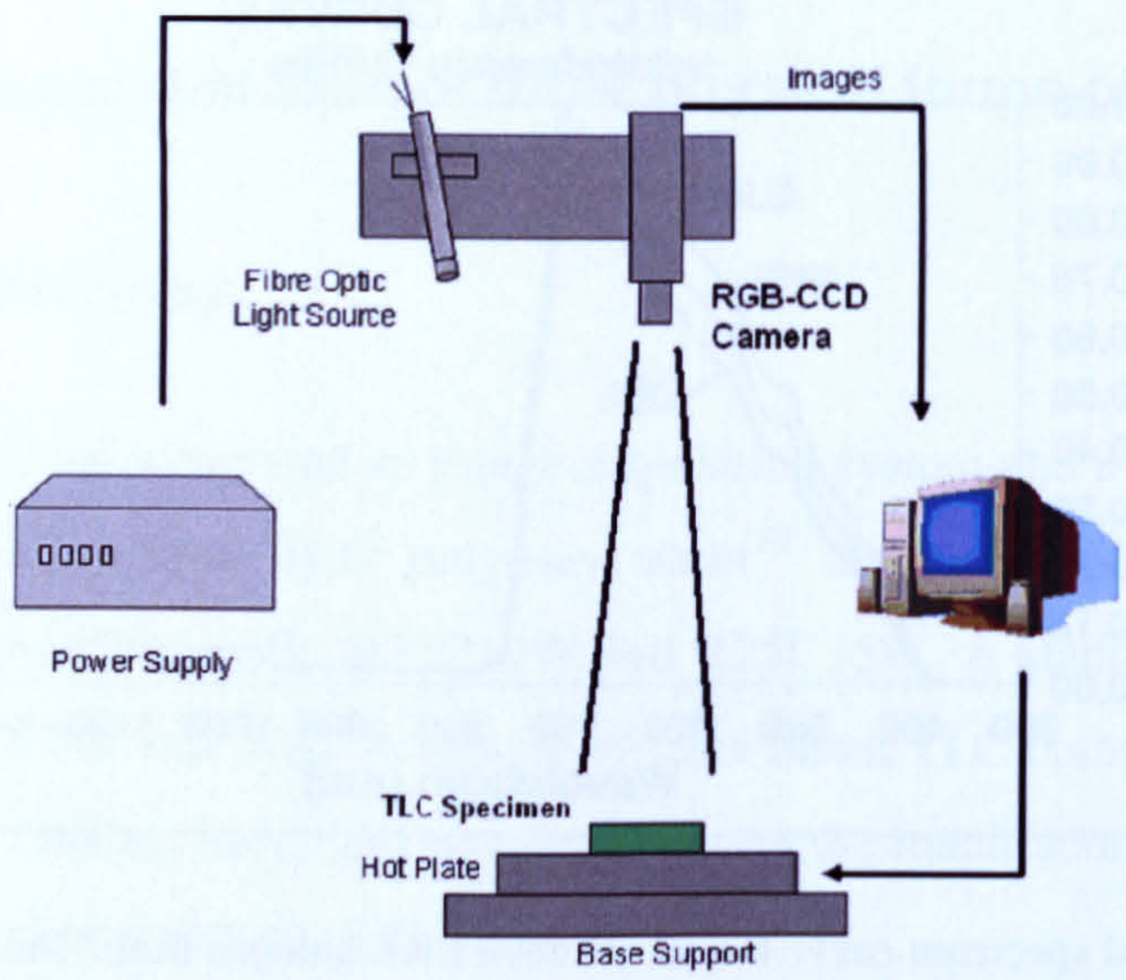


**Figure 4-2: Basic experimental setup showing the image acquisition and temperature measurement system used for calibration of the TLC specimens.**

### *4.2.2.2 Hue versus temperature calibration*

Using the conventional calibration approach described in the previous chapter, data was acquired using the above setup. Table 4-1 defines the useful operating range for the various TLC materials considered in the calibration experiments.

| Material | Event Temperature Deg C | Clearing Point Temperature Deg C | Colour Bandwidth Deg C | Useful Calibration Range Deg C |
|---|---|---|---|---|
| R25C5W S | 25 | 46 ±0.1 | 25-30 | 28-36 |
| R25C10W S | 25 | 50±0.1 | 25-35 | 29-41 |
| R25C15W S | 25 | 52±0.1 | 25-40 | 29-46 |
| R25C10W P | 25 | 50.5±0.1 | 25-35 | 29-41 |
| R27C5W L | 26.3 | 42±0.1 | 26.3-31.3 | *n/a* |
| *S- TLC Sheet; P- TLC Paint and L- TLC on Latex Support* | | | | |

**Table 4-1: Useful operating ranges for several TLC materials. The event temperature and colour bandwidth were supplied by the manufacturer. Clearing point temperature and usable calibration bandwidth were measured using the thermoelectric unit (Accuracy ±0.1 Deg C).**

Images were acquired at each set point temperature (0.5°C apart) within the calibration range for all TLC materials. Detailed procedure and time taken for each calibration is discussed in Appendix D.

MATLAB software was used to analyse the captured images and generate hue versus temperature calibration curves for each TLC sample. RGB values for all pixels were converted to hue in MATLAB using the 'rgb2hsv' function. This algorithm is equivalent to the most common hue definition (Hay and Hollingsworth 1996), but it is numerically more efficient. The algorithm can be approximated by equation [1] (Bakrania and Anderson 2002).

$$Hue = \frac{90 - \arctan(F/\sqrt{3}) + \begin{cases} G > B \rightarrow 0 \\ G < B \rightarrow 180 \end{cases}}{360} \qquad \textbf{Equation 4-1}$$

$$\textbf{Where, } F = \frac{2R - G - B}{G - B} \qquad \textbf{Equation 4-2}$$

Detailed results using the above experimental setup and procedure are presented in the next chapter. Measurement repeatability was evaluated to assess ageing and environmental behaviour these are considered in the following section.

### *4.2.2.3 Measurement repeatability*

To assess measurement repeatability per sample, 30 data sets were collected for the R25C5W TLC sheet. Considering the time taken for each calibration run i.e. 45 minutes, the complete data set was collected over five days. Figures 4-7 and 4-8 illustrate hue versus temperature calibration curve and hue data points for the R25C5WTLC sheet respectively. Mean normalised (8 bit hue scale converted to 0-1 scale by dividing all values by 255) hue is based on n=30 samples i.e. the calibration procedure was consistently repeated for 30 times consecutively on the same sample of R25C5W TLC sheet.

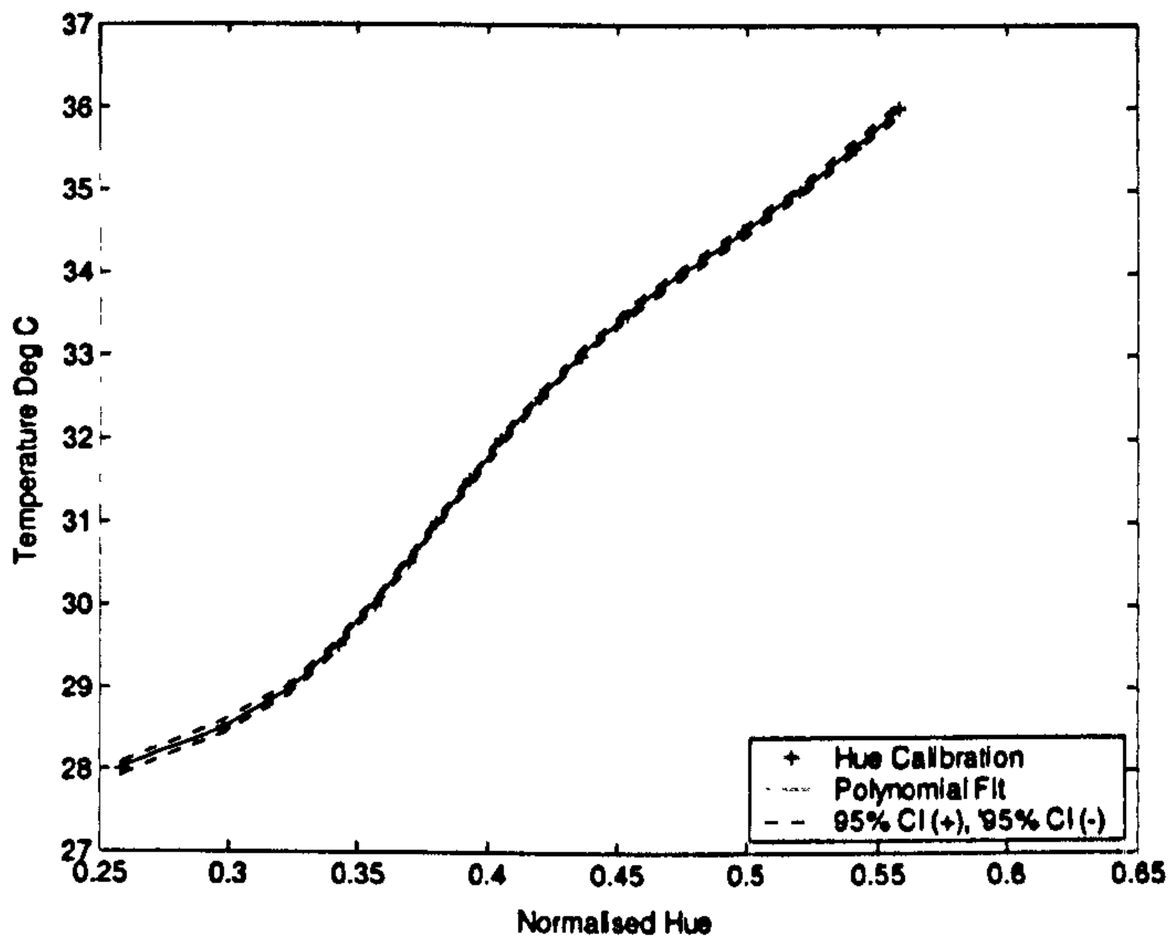


**Figure 4-3: Hue versus temperature calibration curve for a TLC sheet material, in this case R25C5W. Only the useful hue range is displayed with temperatures from 28°C – 36°C. Mean normalised hue is based on n=30 samples.**

The temperature range shown in figures 4-3 and 4-4 is 28°C – 36°C corresponding to the temperature set points for the useful hue calibration range. The discontinuity in hue was removed before fitting the polynomial. This process of fitting a polynomial through the calibration data provides a continuous function describing the relationship between hue and temperature. The technique has been validated for LCT work (Camci, Kim et al. 1992; Hay and Hollingsworth 1996; Bakrania and Anderson 2002). The order of the fit was decided by assessing the accuracy of the fit parameters such as SSE (sum squared

error), R-Squared error, Adjusted R-Squared error, and RMSE (Root mean square error). These parameters are further discussed in Appendix D.

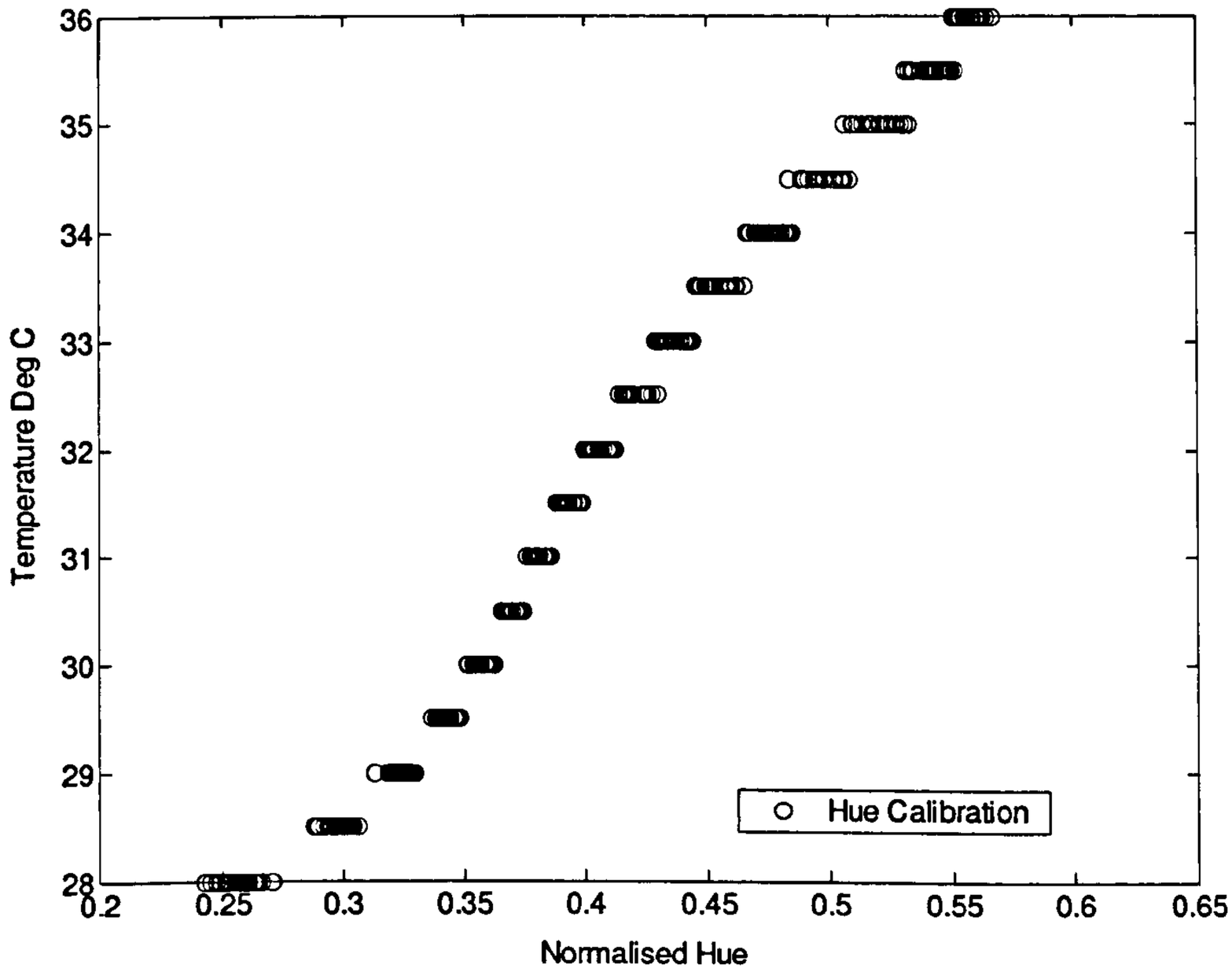


**Figure 4-4: Hue versus temperature data points for a TLC sheet material R25C5W. Only the useful hue range is displayed with temperatures from 28°C – 36°C. Normalised hue for n=30 samples is shown within the useful hue range at each temperature set point. Mean normalized hue and standard deviation for 30 samples is used to fit the appropriate polynomial and calculate the 95% confidence interval for the data, as shown in figure 4-7.**

Following data acquisition, additional hue versus temperature data can be added through interpolation by satisfying the requirements of the fitted curve. An example of interpolation is shown in figure 4-5. This implies that individual calibration for each TLC sheet must be performed for better results.

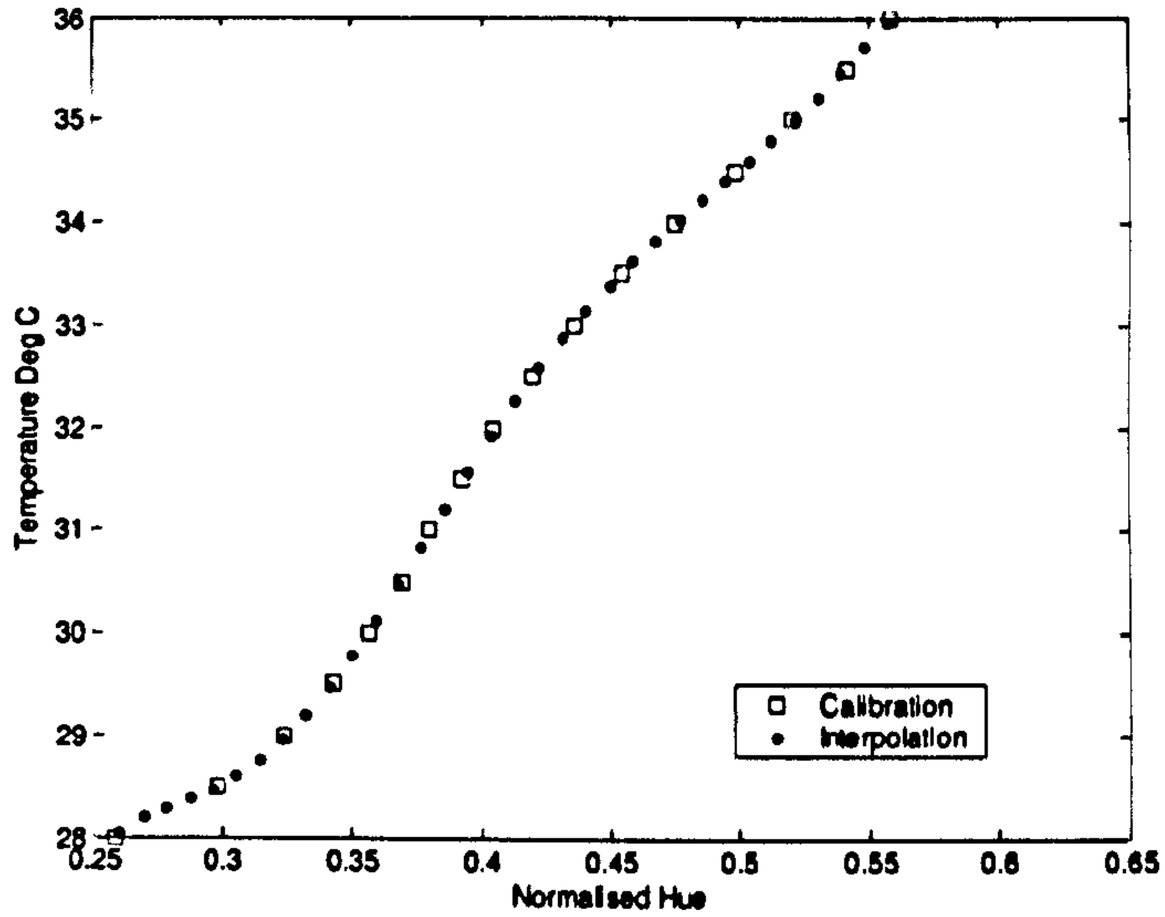


**Figure 4-5: Illustration of interpolation for hue values using the polynomial fit for the calibration. By substituting the mean hue vales from a region of interest or hue values at individual pixels, the corresponding temperatures can be calculated.**

Figure 4-6 illustrates hue versus temperature calibration data points with error bars for n=30 samples. The upper and lower limits on the error bars indicate the standard deviation associated with the mean normalised hue at each temperature set point.

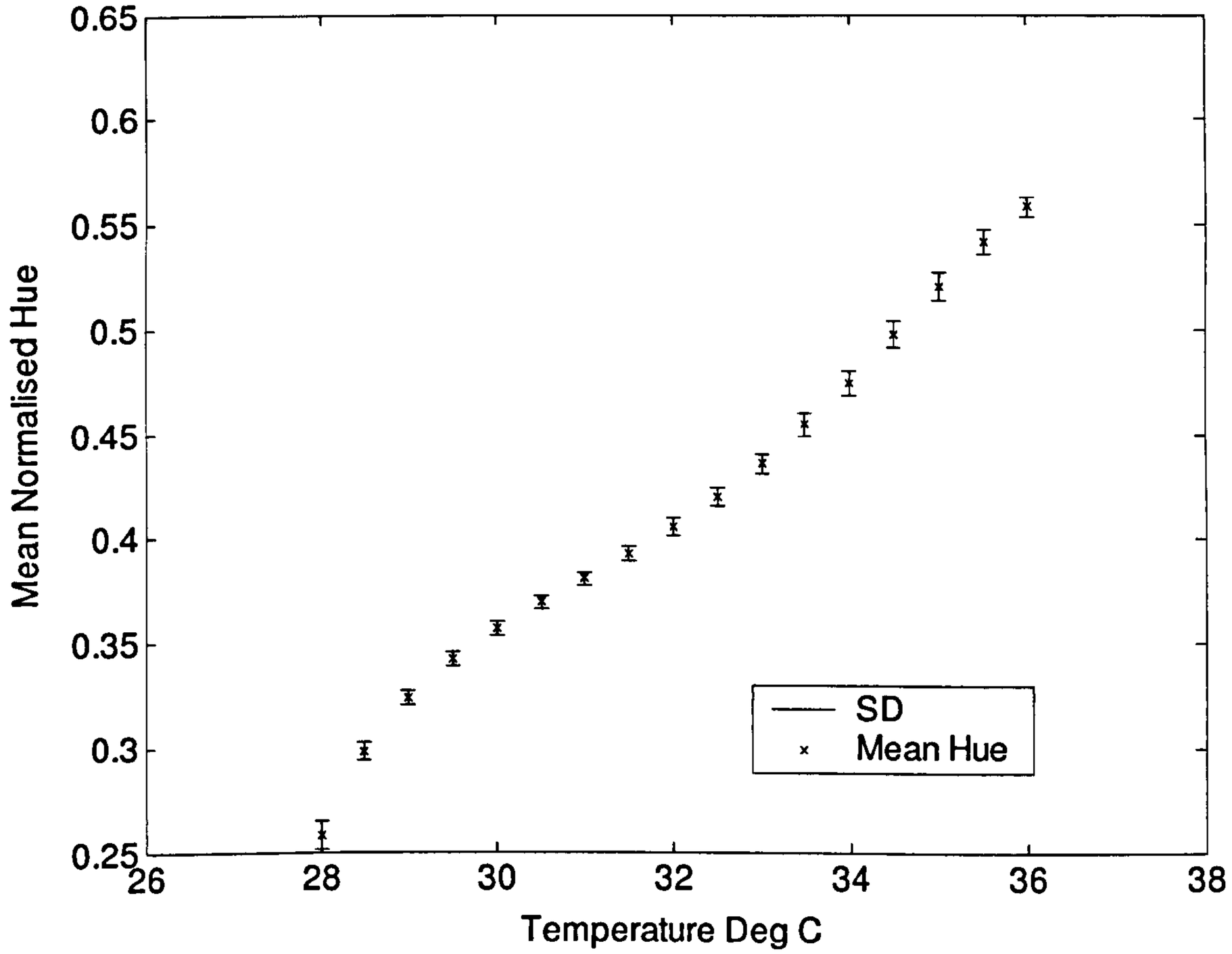


**Figure 4-6: Hue versus temperature data points for a TLC sheet material R25C5W. Error bars shown indicate the standard deviation in hue for n=30 samples within the useful hue range at each temperature set point.**

The results of the preceding study indicated that the R25C5W TLC formulation has measurement repeatability within 5% under carefully controlled conditions. Table 4-2 lists the correlation coefficients for mean hue data (n=30 samples) and mean hue data (n=5 samples) for each day. The results suggest good repeatability of the hue temperature relationship. The most important factors affecting this result were stability of the ambient light source and stability of the ambient room temperature.

| | Set 01-05 | Set 06-10 | Set 11-15 | Set 16-20 | Set 21-25 | Set 26-30 |
|---|---|---|---|---|---|---|
| Correlation Coefficient | 0.999 | 0.999 | 1.000 | 0.983 | 0.978 | 0.998 |

**Table 4-2: Correlation coefficients for mean hue data points from n=30 samples and mean hue data points from n=5 samples. These values suggest good repeatability of the TLC calibration using a consistent experimental setup.**

Figure 4-7 illustrates hue versus temperature calibration data points with error bars for n=5 samples. The upper and lower limits on the error bars indicate the standard deviation associated with the mean normalised hue at each data point. The datasets illustrated are sets 01-05 and sets 21-25 from the calibration data collected. These sets were selected randomly, to consider delayed repeatability (over different days) of the calibration run by comparing datasets from first day and fourth day.

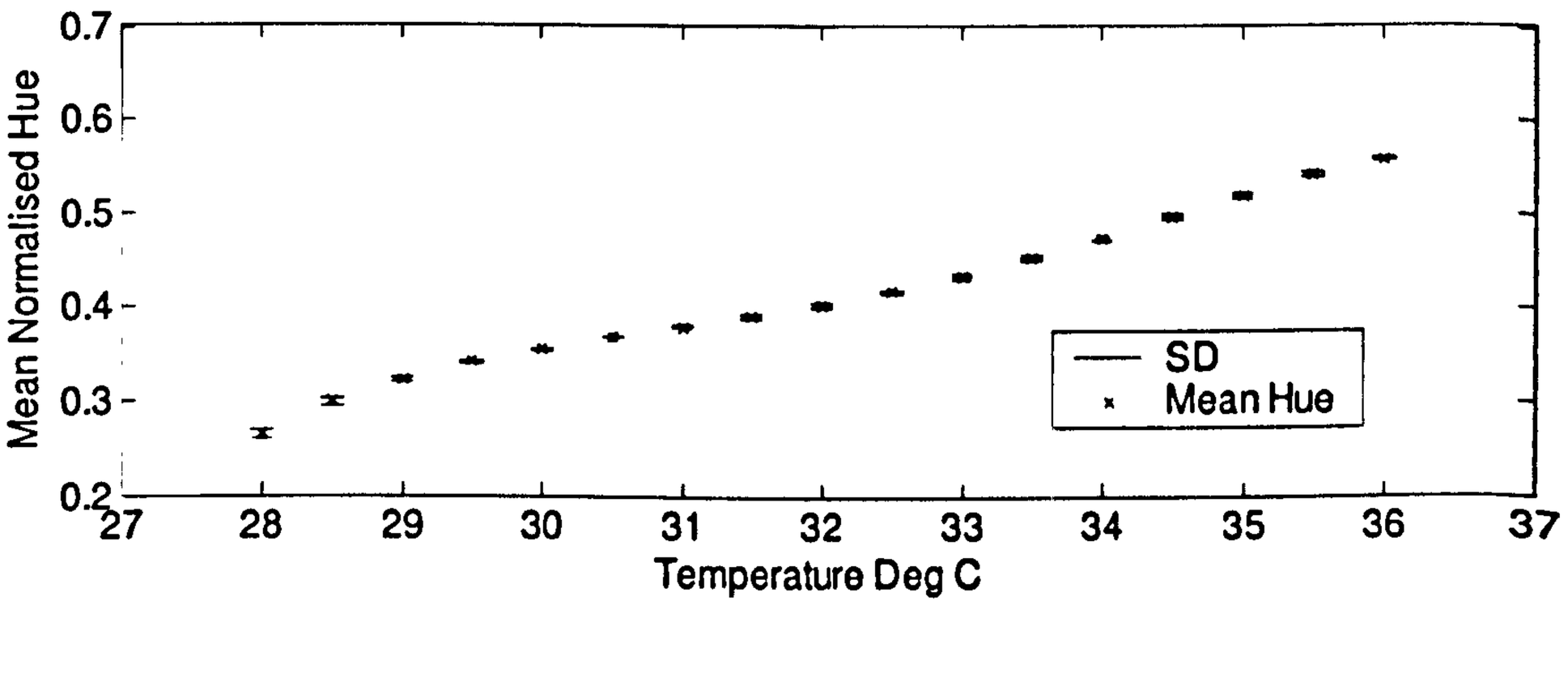


(a)

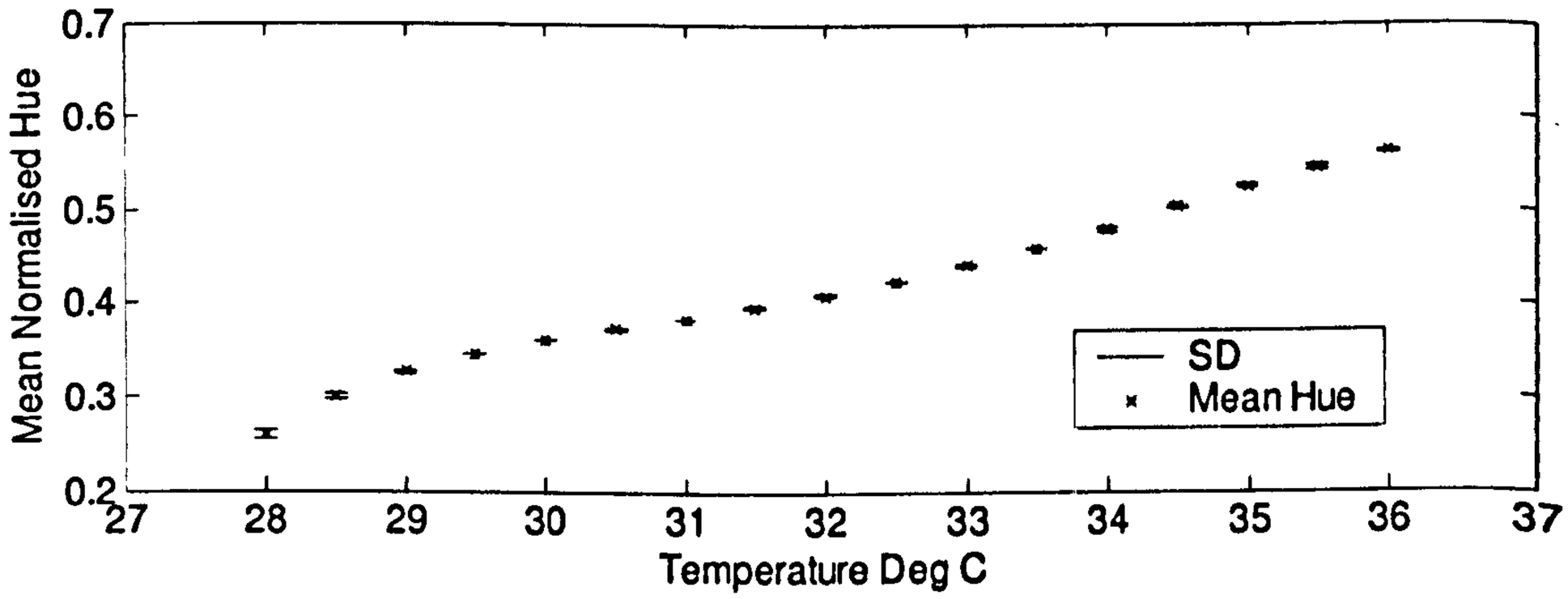


(b)

**Figure 4-7: Hue versus temperature data points for a TLC sheet material R25C5W. Error bars shown indicate the standard deviation in hue for n=5 samples within the useful hue range at each temperature set point. The graph on top illustrates the results for sets 01-05 and the graph on bottom illustrates the results for sets 21-25. 'SD' is the standard deviation, represented as error bars.**

Figure 4-8 illustrates the standard deviation in the mean hue calculated from all 30 datasets and sets 01-05 (n=5) as well as sets 21-25 (n=5). The pattern of the standard deviation distribution is similar for all the above sets considered in figure 4-8. Correlation coefficients for standard deviation from n=30 samples (sets 01-30) and standard deviation from n=5 samples (sets 01-05 & sets 21-25) are 0.942 and 0.998 respectively. The mean distribution of standard deviation also suggests that temperature resolution is not uniform across the useful temperature range for the TLC. However, prior knowledge of the calibration and TLC performance can be used to compensate for this non linearity and report accurate temperatures. However, this is a task specific procedure and accuracy can thus be determined based on the intended application. This issue has been further addressed in section 4.2.6, where the effect of colour bandwidth of the TLC is also considered when determining the accuracy.

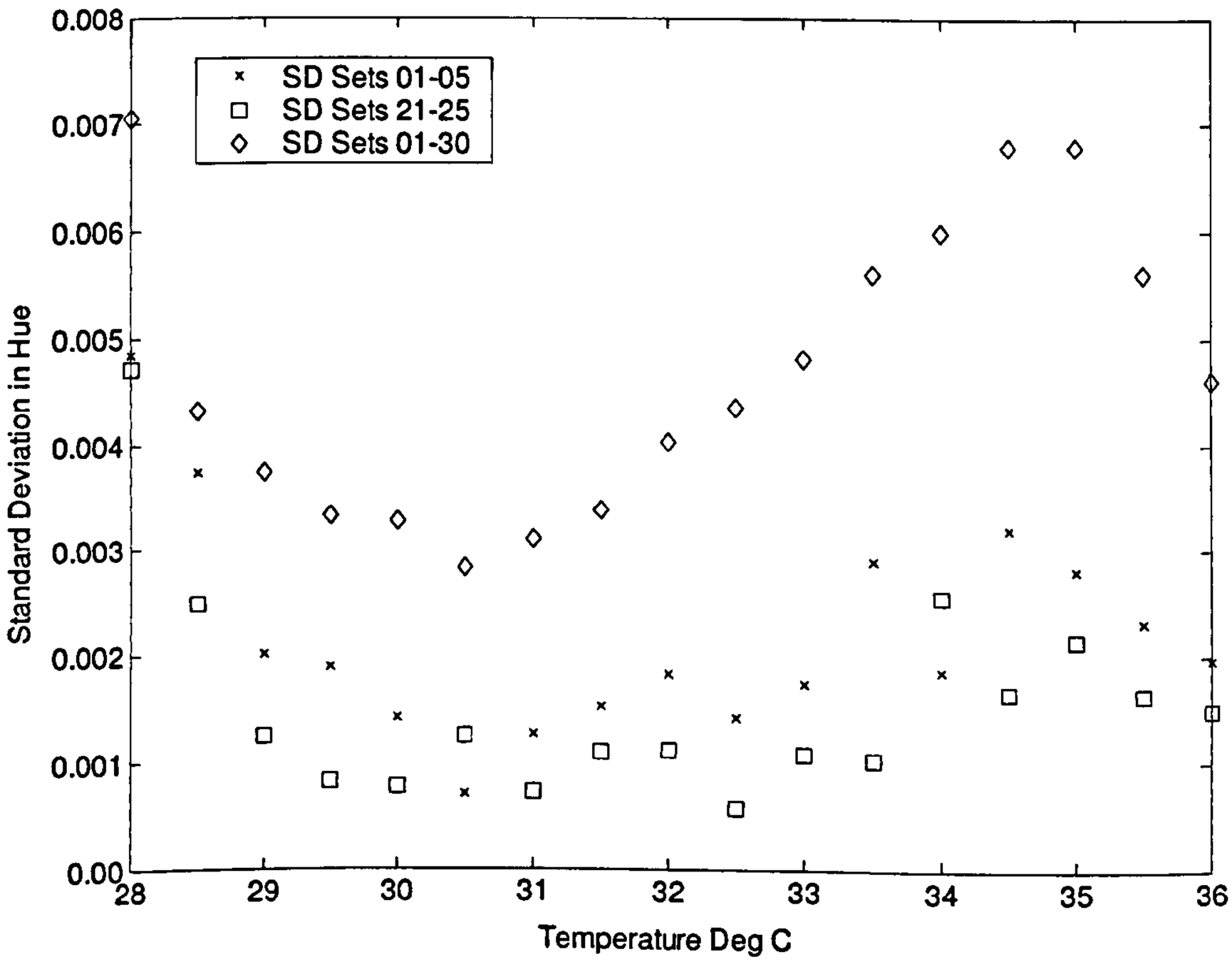


**Figure 4-8: Distribution of standard deviation within the useful temperature range for the R25C5W TLC sheet. Standard deviations are plotted for sets 01-05, sets 21-25 and sets 01-30 and have the units of 8-bit hue intensity measured from the calibration data.**

Consider figure 4-9, the standard deviation distribution from sets 16-20 leads to the overall higher standard deviation from sets 01-30. The reason for this is unknown. However, this standard deviation does not affect the accuracy of the calibration, as seen from the correlation coefficients in table 4-1. Furthermore, these results justify employing only five sample calibrations for further analysis.

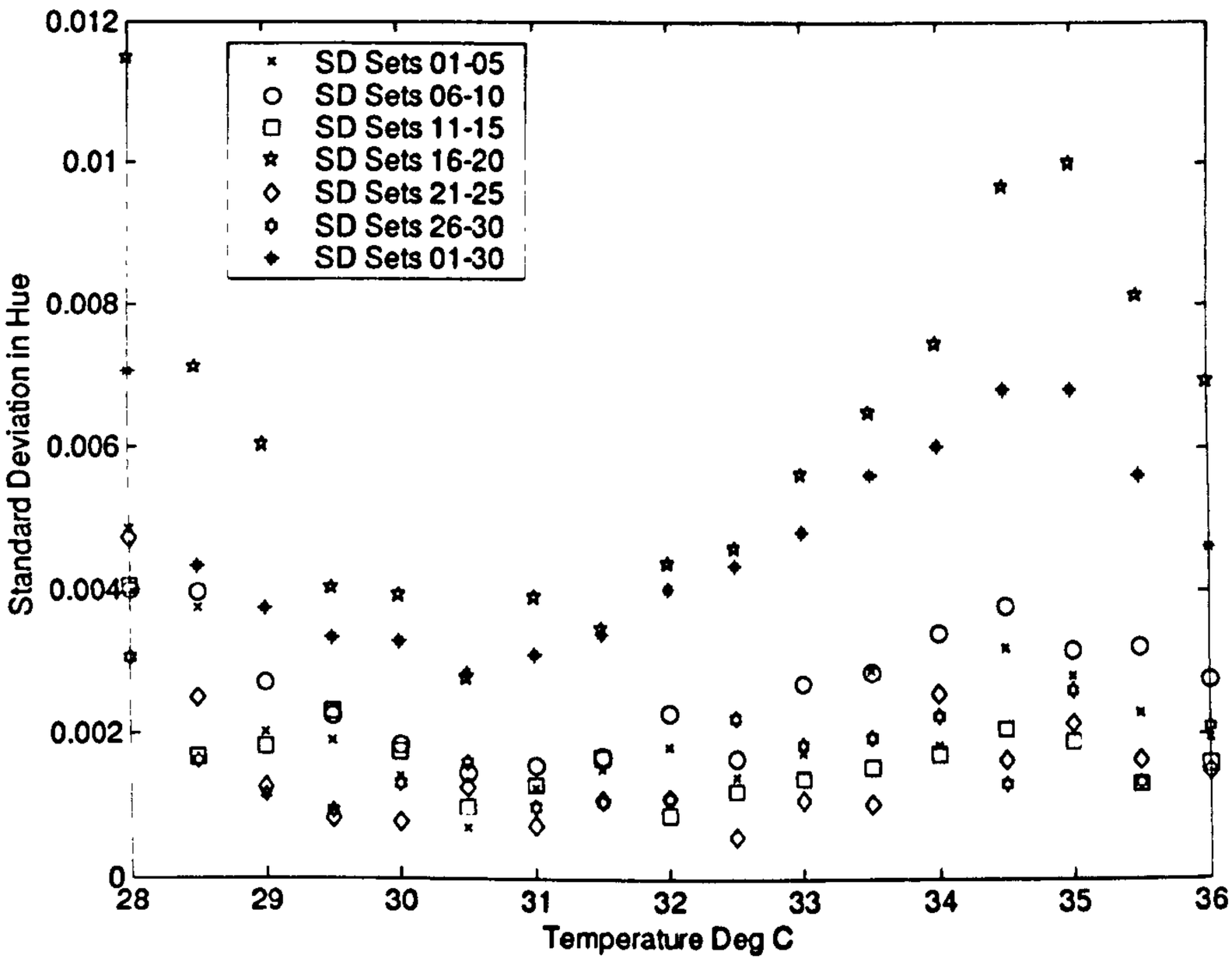


**Figure 4-9: Distribution of standard deviation within the useful temperature range for the R25C5W TLC sheet. Standard deviations are plotted for sets 01-30 and a group of five sets to view the consistency in hue measurement. Standard deviation has units of 8-bit hue intensity measured from the calibration data.**

This graph shows that at some temperatures, the variation about the mean hue is much greater that at other temperatures (especially, at the colour transition temperatures). This implies that the error is systematic. This may have a considerable impact on the LCT application, typically where high accuracy and temperature resolution is intended. It must be emphasised here that in the context of current application, this issue can be discounted as thermal patterns under the plantar foot are desired instead of highly accurate temperature measurement. The following section considers microscopic analysis of the TLC materials.

### *4.2.2.4 Microscopic analysis of TLC materials*

Sample to sample repeatability for TLC samples was assessed by obtaining 10 spatially averaged hue values from a region of interest, which was centred on the specimen to eliminate the possibility of edge effects. The importance of spatial averaging is evidenced by detailed image analysis at the pixel level and microscope studies which reveal non-homogenous distribution of thermo liquid crystals at the microscopic level.

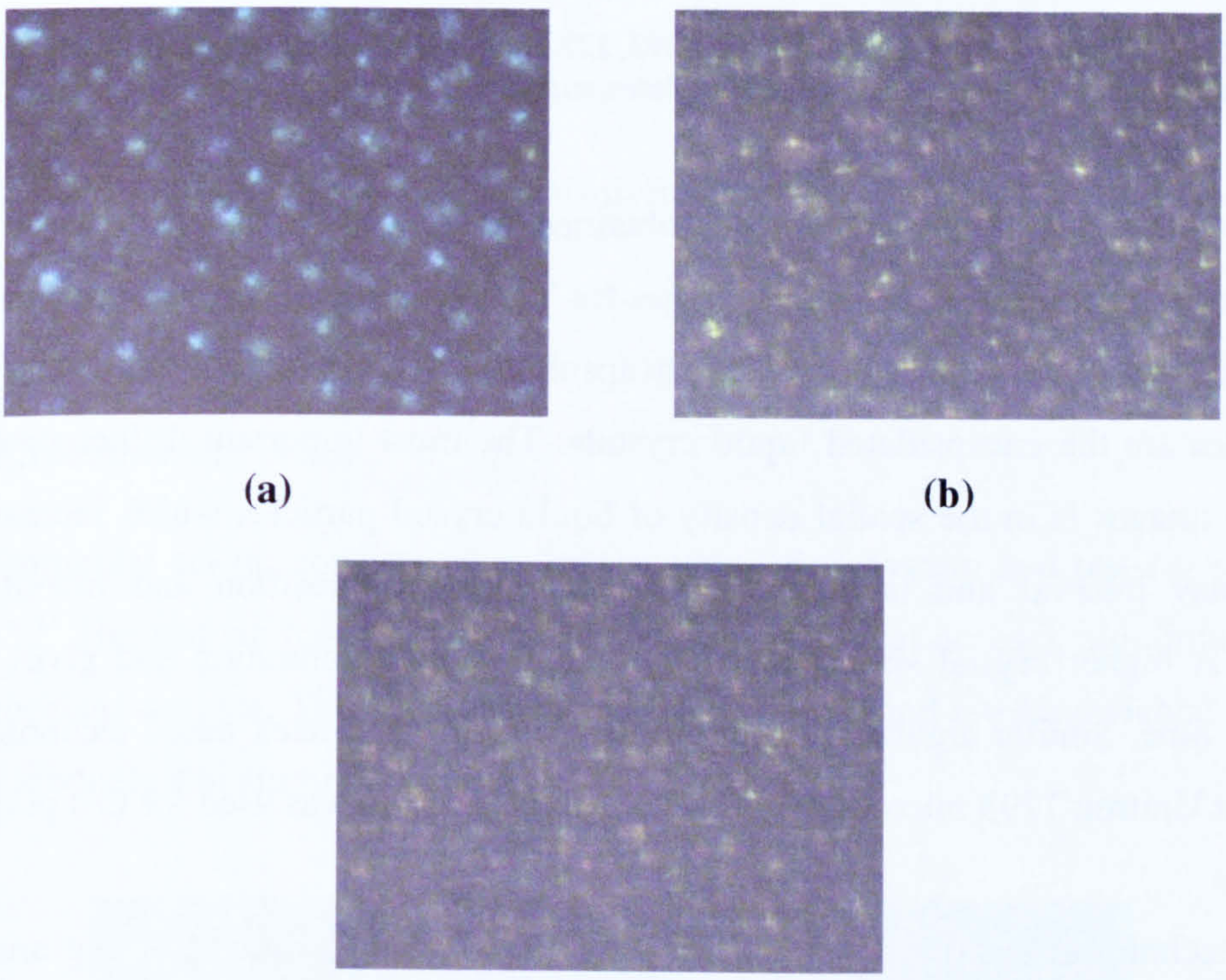

**(a)** **(b)**

**(c)**

**Figure 4-10: Microscopic (Versamet Unitron 7293, 12 X magnifications) images for TLC sheets: (a) R25C5W, (b) R25C10W and (c) R25C15W. Images have a milky appearance and each coloured spot is an encapsulated liquid crystal.**

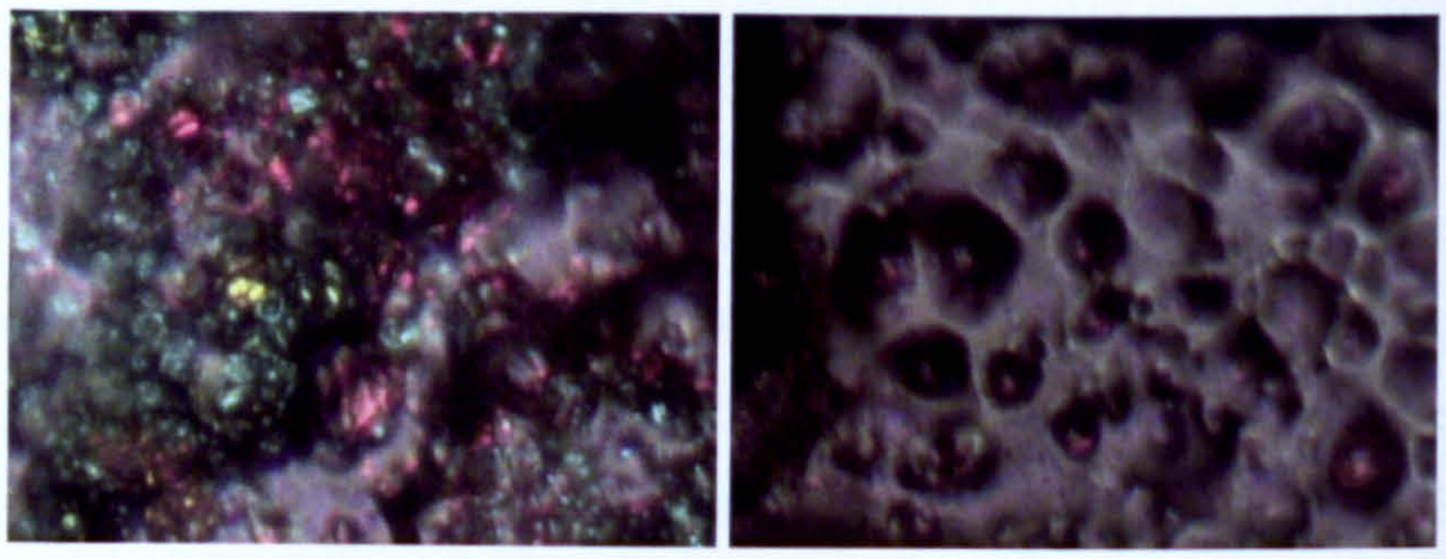

(a) (b)

**Figure 4-11: Microscopic (Versamet Unitron 7293, 12X magnification images for (a) R25C10W TLC emulsion applied by air brush and (b) TLC on latex support .**

Figures 4-10 and 4-11 provide images obtained under the microscope for the various TLC formulations used in the study. Images for TLC sheets have a milky appearance due to the binding material and polyester encapsulation. The coloured spots with blurred boundaries are the encapsulated liquid crystals. The most important difference between the three images is in the spatial density of liquid crystal particles which increases with colour play interval and is controlled by chemical composition and manufacturing process. A higher crystal spatial density improves colour saturation and gives a faster response time. Similar arguments apply to the emulsion and latex based technologies. A Versamet Unitron 7293 microscope with 12X magnification was used for this purpose.

Several techniques such as brush painting, rolling, dipping, spray painting and screen printing are used to apply liquid crystals. These techniques determine thickness and uniformity of TLC material. The microscopic images suggest a random size of microencapsulated liquid crystal for TLC on latex support. The bigger size of liquid crystals affects the colour brightness of the material (Massi 2004); hence, poor colour and thermal resolution for the TLC on latex support. Microscopic analysis confirms these findings.

These microscopic images suggest poor sample to sample repeatability (especially for emulsion and latex based TLC materials), indicating that TLC sheets may be the best choice for intended application. From the calibration data above, it will be better to use a single calibration sheet to obtain all the in vivo data in order to avoid sample to sample variability. However, it is important to consider the pressure sensitivity and hysteresis of TLC materials before implementing any TLC into the final system design.

## 4.2.3 Evaluation of pressure sensitivity of TLC polyester sheets

### *4.2.3.1 Introduction*

The methodology adopted for pressure sensitivity assessment of the TLC materials is now presented.

### *4.2.3.2 Experimental setup*

The experimental set up consists of an image acquisition system and test rig shown in figure 4-12. The test rig has a polycarbonate base (for optical access), aluminium block and appropriate weights. The TLC sheets are self adhesive and are sandwiched between the Polycarbonate and aluminium block.

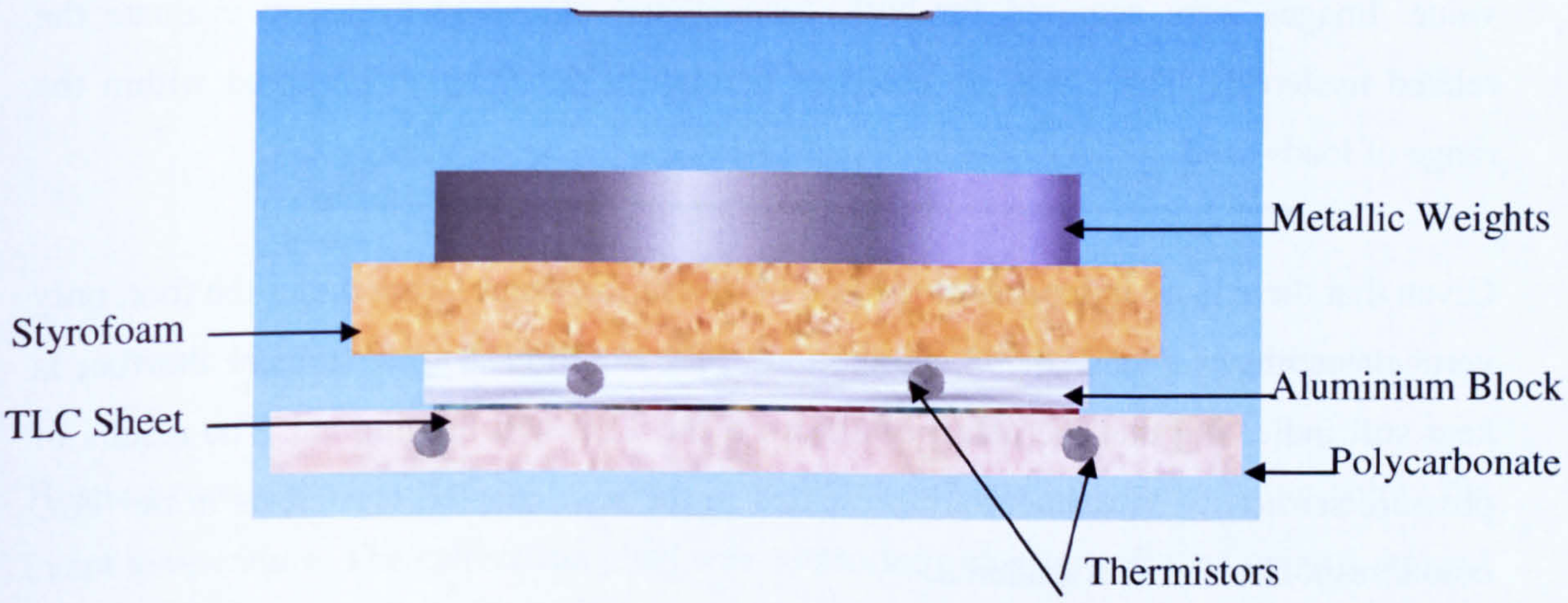


**Figure 4-12: Apparatus for pressure sensitivity testing.**

A similar image acquisition system to that presented in the preceding section was used to investigate the effects of vertical loading on the TLC sheet and latex formulations. The TLC emulsions were not evaluated due to problems with containment. However, the camera and light source were re-located at the bottom of the rig to obtain images through the transparent polycarbonate face. This revised setup was then consistent with the intended method of loading for the clinical LCT system being developed.

Constant temperature was maintained for both aluminium and polycarbonate using a heated water bath and circulator to feed a series of pipes embedded in the polycarbonate and aluminium. Two thermistors were bonded with thermal epoxy at the inlet and outlet terminals of the aluminium and polycarbonate respectively. These thermistors were connected to a digital multimeter HP33401A[12] to record temperature at 1s intervals during the pressure sensitivity tests. A period of 30 minutes was found appropriate for the system temperature to stabilise prior to testing.

The range of weights selected for the load sensitivity experiments was 0-68 Kg applied over an area $0.01m^2$. The pressures (0-70 KPa) in selected range is consistent with the physiologically relevant range (0-200 KPa while stance). Fifteen weight blocks were stacked incrementally each weighing (4.5 Kg) resulting in a pressure range of nearly 0-7000 $Kg/m^2$. Higher loads (>70 Kg) could not be used due to limitations in system design and safety. At each weight, 10 images were acquired and averaged to obtain a mean hue value. Images were acquired for both, loading and unloading cycles to evaluate the related hysteresis. There was no creep or permanent deformation observed within the range of loads used.

Given that there is no independent method of measuring shear forces under the foot, only vertical loading was considered. Furthermore, for the clinical measurement the foot is kept still indicating that the affect of shear on the TLC will be minimal. The results of pressure sensitivity assessment are presented in the next chapter. Hysteresis in the TLC colour response is now considered.

---

[12] **By Agilent Technologies Inc., Santa Clara, CA, USA**

## 4.2.4 Evaluation of hysteresis of TLC polyester sheets

### *4.2.4.1 Introduction*

Hysteresis evaluation for TLC material is now considered.

### *4.2.4.2 Experimental setup*

Using the basic experimental setup described previously in figure 4-2, hue versus temperature calibration curves were generated for both heating and cooling runs. Figure 4-13 illustrates typical hysteresis behaviour in TLC.

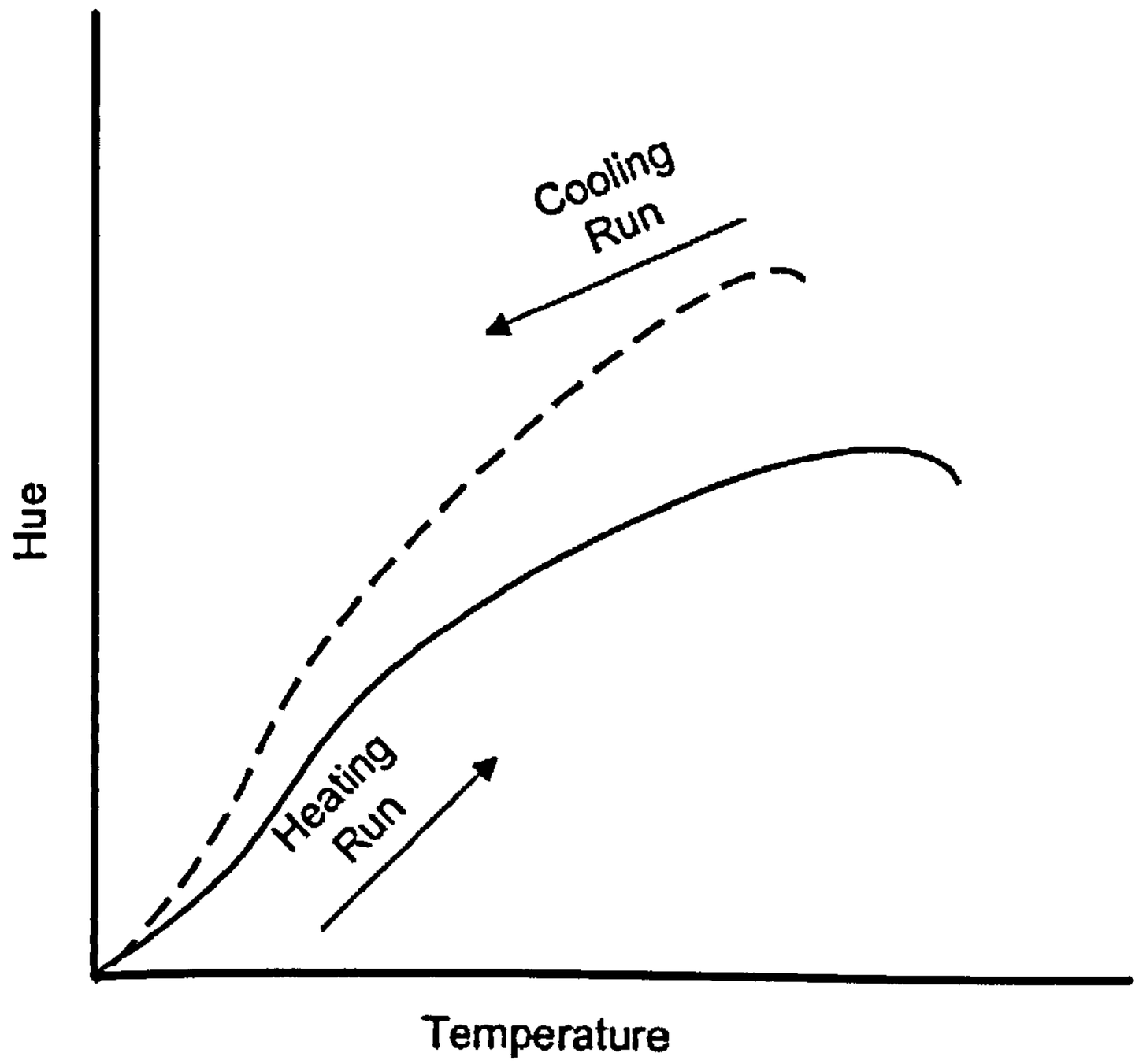


**Figure 4-13: Typical profile of the hysteresis behaviour in thermochromic liquid crystals.**

Heating runs were initiated by bringing the calibration plate to a temperature below the event temperature. The calibration plate was controlled either by software using a manual set point or a ramp input dependent on whether a static or transient test was being

performed. Images were recorded 10 seconds after the set point temperature was reached i.e. soak time setting of 10s was used in the LABVIEW interface. This value was based on knowledge of the response times of the materials based on manufacturer's data (typically, 1-2 seconds). It should be noted that in the past TLC formulations exhibited response times of >60s (Anbar 1998). However, better chemical formulations and manufacturing techniques have led to availability of faster TLC (Armstrong 2004). The physiological changes in temperature are known to be relatively slow from other studies (Anbar 1998; Jung and Zuber 1998), therefore assessing this characteristic was not critical in the context of the clinical application. Two types of cooling run were performed: (a) heating to a temperature equal to the clearing point temperature and (b) to a temperature in excess of the clearing point temperature (in practise a 5°C above the clearing temperature was found to be sufficient to induce hysteresis effects).

Detailed results of hysteresis are presented in the next chapter. Evaluation of calibration, pressure sensitivity and hysteresis was helpful in selecting the best TLC material for the clinical system. However, an alternative TLC calibration approach is discussed in the following section, with the intent of comparing the benefits of each technique for clinical use.

### 4.2.5 Novel calibration approach using neural network

#### *4.2.5.1 Calibration procedure*

The TLC calibration procedure outlined earlier in this chapter provided acceptable results under conditions where accurate control of the illumination source and ambient light conditions were possible i.e. under carefully controlled laboratory conditions. However the required conditions were stringent for practical calibration of the TLC sheets in the clinical setting prior to in vivo data collection. Therefore, a novel automated calibration procedure based on a neural network was used to compensate for differences in the calibration light level.

A multi-layered feed-forward back propagation network was constructed using MATLAB's Neural Network toolbox. The network had one input layer, one hidden layer and one output layer as shown in figure 4-14. The training was performed by the Levenberg-Marquardt method (Mathworks 2002), chosen for its speed and suitability for moderate sized networks. Methods like gradient descent and gradient descent with momentum were also implemented, but found to be more time consuming (Mathworks 2002).

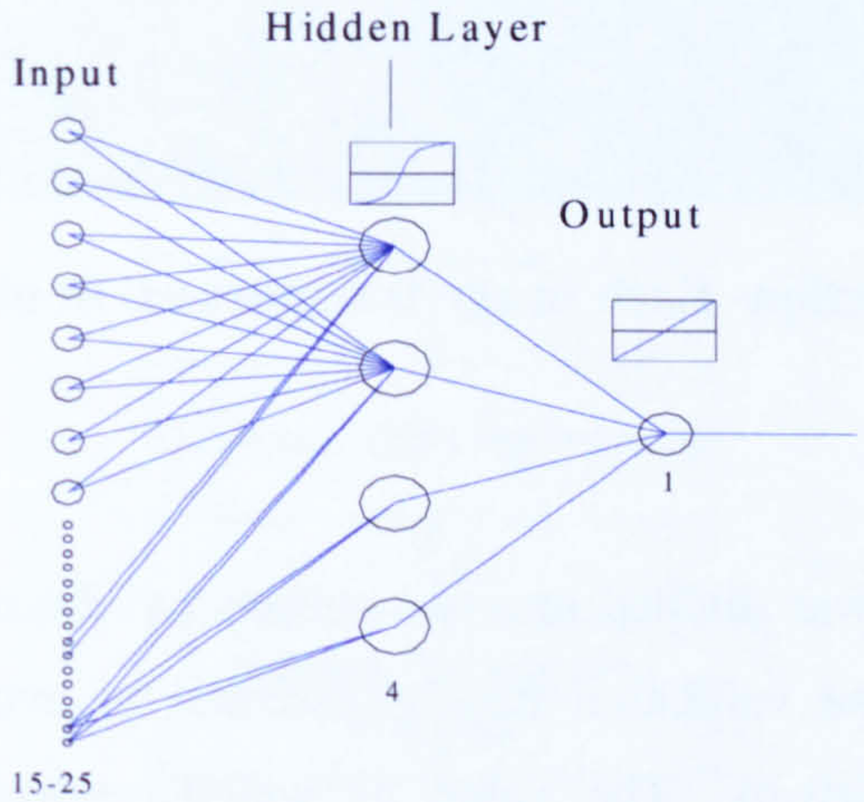


**Figure 4-14: Neural network architecture.**

Neural networks require a large number of training sets for successful training and generalisation. A region of interest (ROI) of 120x120 pixels was marked on the acquired image and was then segmented into blocks of 10x10 pixels as shown in figure 4-15. For each block, 100 RGB triplet values were extracted and stored for the network training. Thus each acquired image contributed to 144 training sets. This enables an input dimensionality for the network of 300 (3x100 for RGB triplet). Such a large input dimensionality if fed to a neural network would involve excessive training time and computational effort to learn. Thus, principal component analysis (PCA) was implemented to reduce input dimensionality. Sometimes the information held in a data set is redundant in nature, especially where the entire image has the same RGB and H values as in the present case. Under such circumstances, the purpose of PCA is to extract principal components from a data set whilst maintaining the essential information (Bharath and Drosen 1994; Bishop 1995).

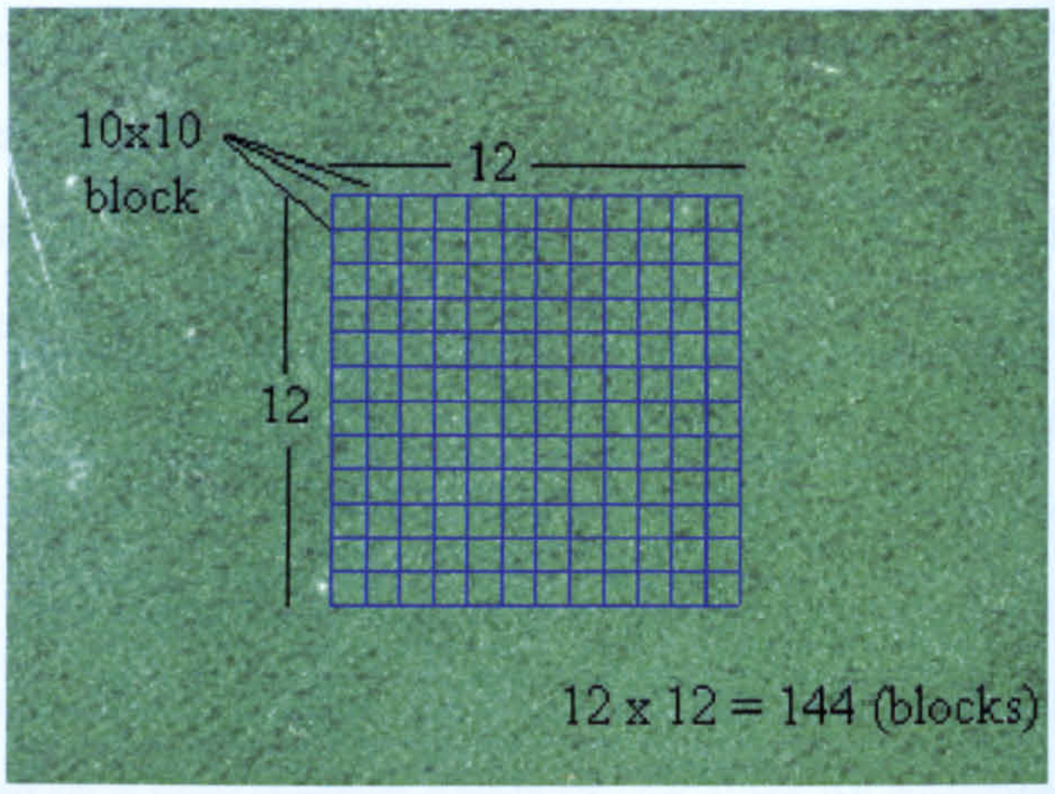


**Figure 4-15: Data extraction- Each image is segmented in blocks of 10x10, to make 144 blocks.**

The total data extracted was divided into two subsets i.e. the input data (95%) and the validation data (5%). The validation data is essential to avoid over fitting or poor generalisation of the network. The value of weights selected affects the rate of convergence for the network, since the error surface is unpredictable. Thus, the network was trained for 50 different weights and results were presented for the weights with least root mean square error. The flow chart in figure 4-16 shows the step by step procedure from image acquisition to the testing of data.

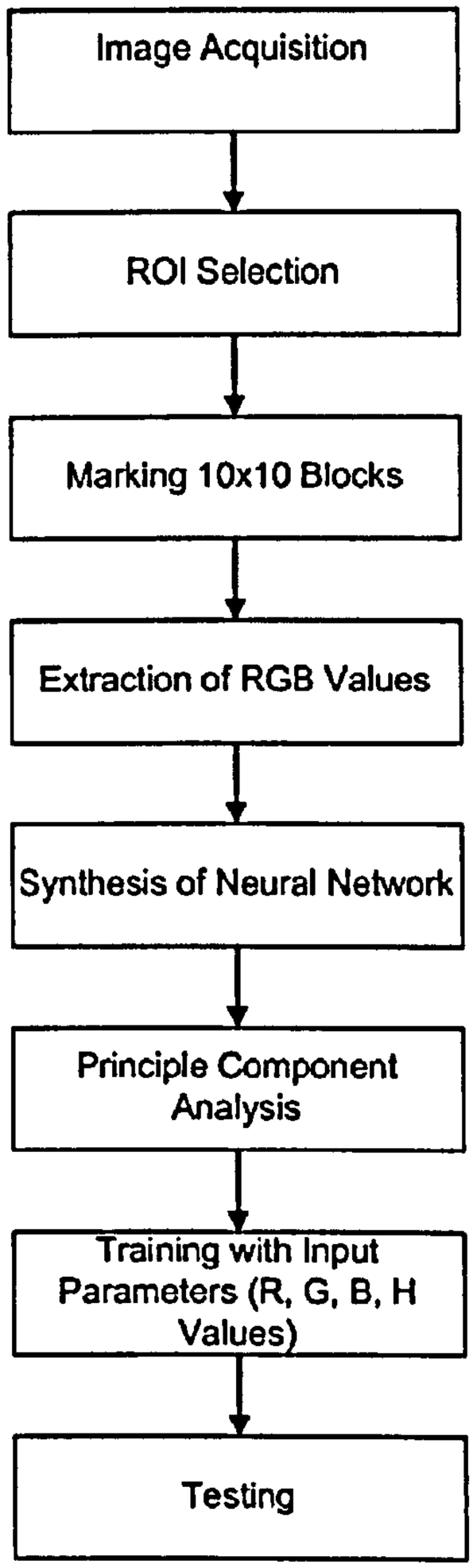


**Figure 4-16: Flowchart of the implemented neural network.**

A more detailed description of this novel calibration procedure is available in the literature (Grewal, Bharara et al. 2006). The results presented in Appendix E, support the idea that this technique has several advantages over the conventional technique for calibration of the TLC. This is further considered in chapter 6. In the context of the current study, automated calibration via the neural network provided the possibility of reduced constraints on the measurement environment simplifying clinical data capture. However, before this is possible further work is required on refining the neural network calibration approach by considering other available training methods and parameters.

Consequently, all data discussed in subsequent chapters was acquired using a system calibrated with the conventional hue-temperature calibration approach.

### 4.2.6 Summary of the characterisation tests

The main objective of characterisation of the three commonly available forms of TLC material was to investigate the linearity of the response across the physiological range of plantar foot temperatures. Furthermore, it tests the TLC materials for insensitivity to pressure and hysteresis effects, which are an essential requirement for the current work. There is no standard reference technique for satisfying these requirements in a single test; partially, because most common applications of LCT do not involve significant loading of the TLC material and hysteresis is application specific. It was, therefore, decided to carry out independent assessment of these requirements using hue temperature calibration curves and tests described in the preceding sections.

Qualitative analysis of microscopic images suggests that spatial density of TLC capsules may play a role in altering the performance of TLC. This variation in spatial density may also explain the operational tolerance during various colour transitions of the colour play interval. These are summarised in table 4-3.

| Transition | Tolerance |
|---|---|
| Red start temperature | ±0.5°C or ±10% of the colour bandwidth (whichever is greater) |
| Green start temperature | |
| Blue start temperature | ±1.0°C or ±20% of the colour bandwidth (whichever is greater) |
| Clearing point temperature | |
| Mild Green temperature | |

**Table 4-3: The operational tolerance for different transitions within the colour play of thermochromic liquid crystals (Hallcrest 1991).**

The exact changes in TLC performance are not documented in the literature. However, retrospective analysis of the calibration datasets for narrow band and wide band TLC

materials provide useful justification that 'higher spatial density may be an essential requirement to induce larger colour range for the TLC'. This is an important finding and may provide basis for selection of a particular TLC formulation for a desired application. In the present study, physiological range of temperatures under the plantar feet was the dominant factor in selecting the specific TLC formulation for clinical evaluation. There is supporting evidence from the calibration data that this larger colour range is mapped onto a limited hue range, affecting the temperature resolution of wideband TLC. This is a fundamental issue with the chemical formulation of the TLC. Results may improve when using a high sensitivity camera and better image processing techniques. The manufacturer's data does not address the above issues. The microscopic analysis was however, most useful in determination of the quality of TLC material.

The experimental results from characterisation tests (presented in the following chapter) were useful for selecting the appropriate TLC material for the intended application. Encapsulated liquid crystals on latex produce poor colour response, attributed to the spatial distribution of liquid crystals. The hue temperature relation cannot be linearly described by a polynomial. Use of emulsion based TLC formulation is limited by poor calibration performance and ethical issues involved in applying them to the anatomical site. The need for skin preparation using black paint (for enhancing colour contrast) and toxicity issue due to application of TLC paint discount further consideration for the current study. Both emulsion and latex based TLC materials are therefore, inappropriate for use with the intended protocol.

TLC sheets offer higher stability and better colour response than the other two formulations. The R25C5W TLC sheet was considered to be most appropriate for use in the clinical LCT system based on the repeatability, calibration, pressure sensitivity and hysteresis tests. Furthermore, this formulation is widely available from the manufacturer and does not require a custom order, thereby lowering the overall system cost. The other two TLC sheets i.e. R25C10W & R25C15W tested were discounted as they have a larger colour bandwidth near the event temperature which must be eliminated before a polynomial fit is successful. This approach limits the temperature range which can be

used for the intended application. However, using an alternative calibration approach such as neural networks (Grewal, Bharara et al. 2006) may solve this problem. Both these TLC sheets may have higher sensitivity to the surface temperatures due to higher spatial density of capsules as revealed by the microscopic images. All proposed issues for R25C10W & R25C15W TLC sheets require further scientific testing and were not within the scope of the present work.

The following section describes the design of the final LCT system (with R25C5W TLC sheet as the thermal sensor), implementation, data collection and processing requirements.

## *4.3 LCT – Clinical system implementation*

### 4.3.1 Final system design

Figure 4-17 illustrates a block diagram representation of the final prototype system. The camera was connected to the laptop computer as shown in figure 4-17, using the Personal

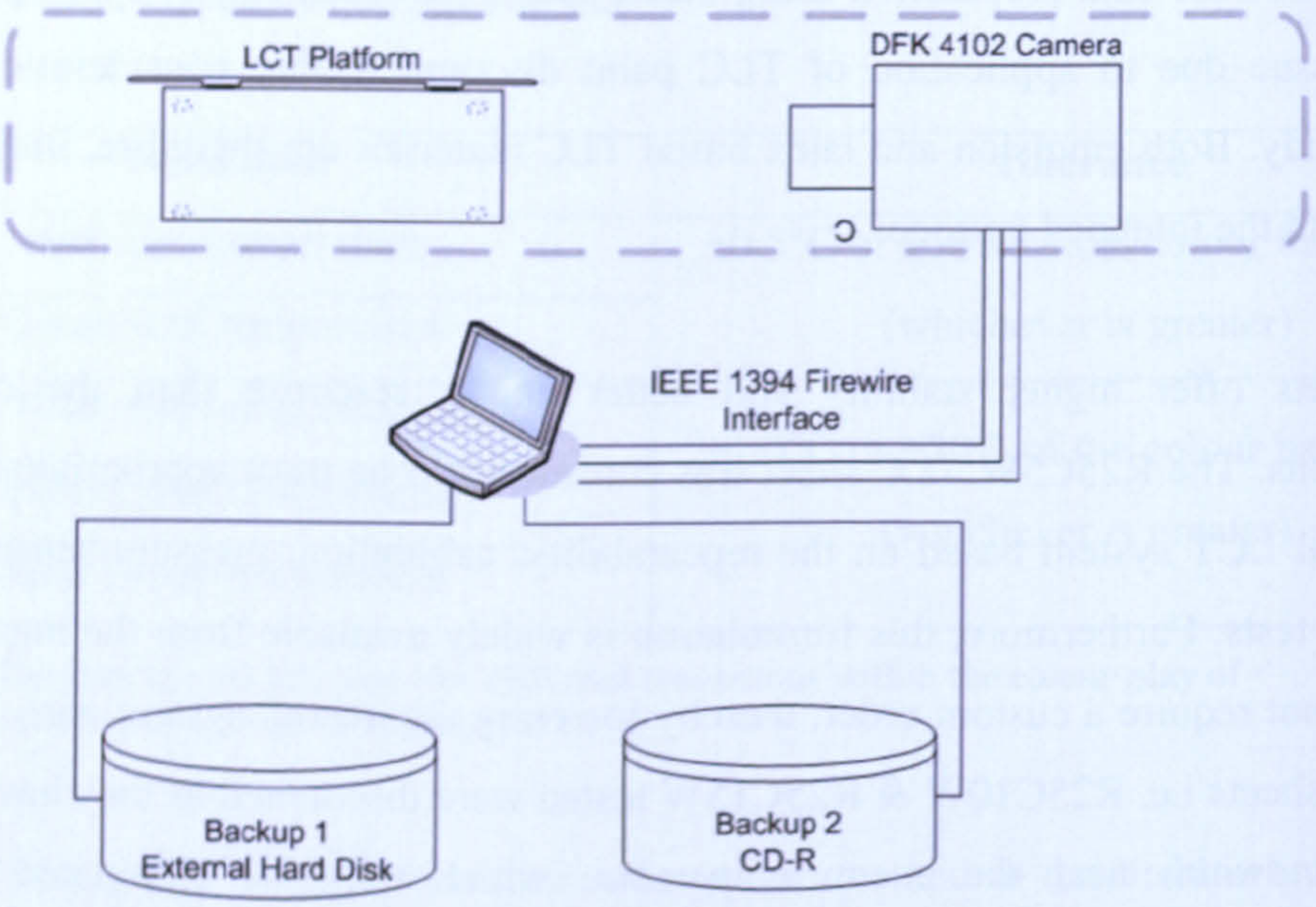


**Figure 4-17: Block diagram representation of the clinical LCT system.**

Computer Memory Card International Association (PCMCIA) card and 6 pin cable for IEEE 1394 devices. Figure 4-18 illustrates the set up for in vivo calibration unit.

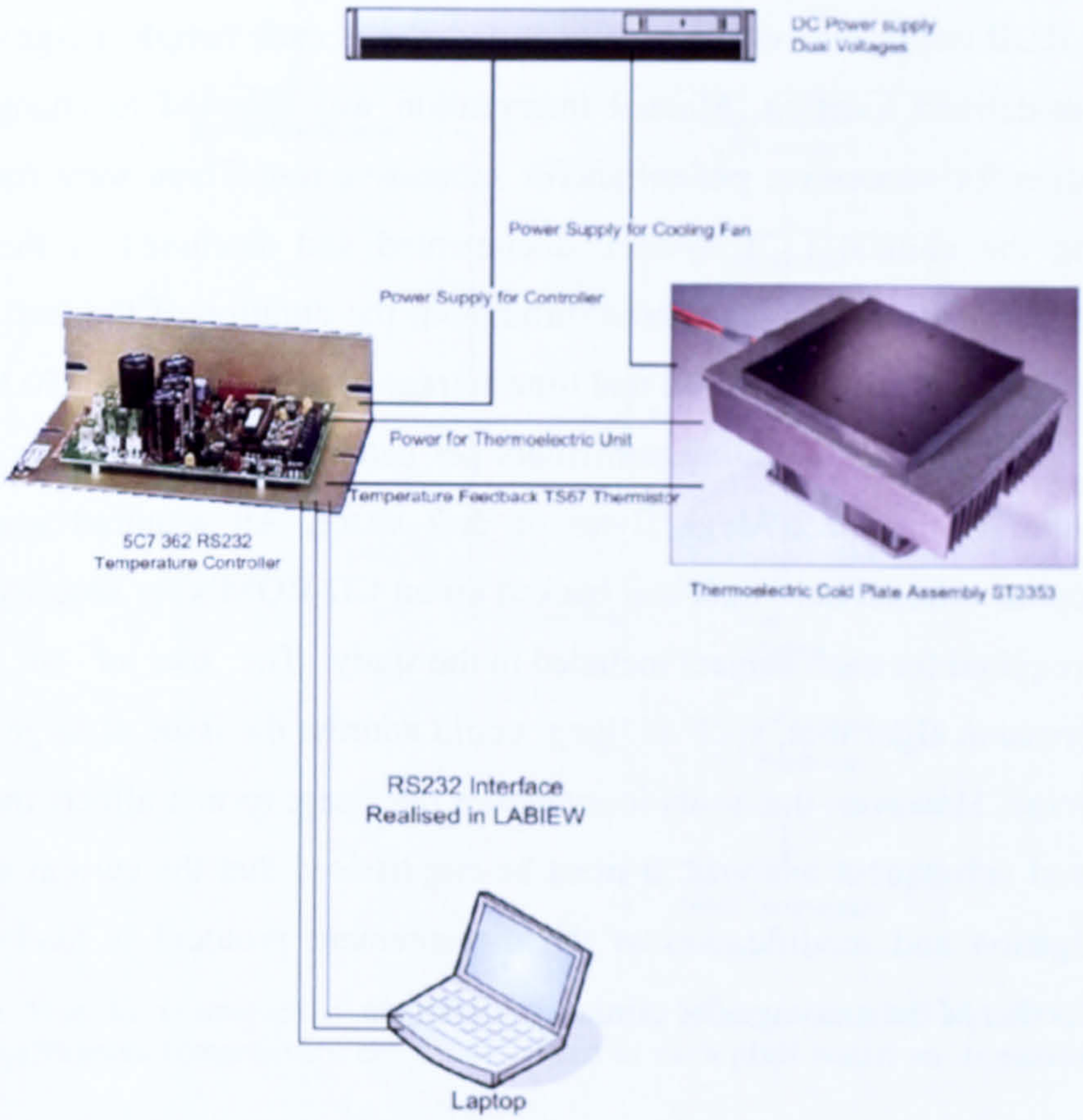


**Figure 4-18: Block diagram representation for the in vivo calibration of R25C5W TLC material.**

The in vivo calibration unit was an independent module and could be connected to the camera when performing calibration of the clinical LCT system. Details about the RS232 interface realised in LABVIEW and calibration algorithm are provided in Appendix F.

### 4.3.2 Data acquisition and image processing

Independent software components were realised for data acquisition and image processing of the data. Manual intervention was required to deal with static and dynamic data. Data acquisition of the clinical thermal images was performed using the IC Capture[8] version 2.0.0.277 (easy image acquisition) software provided by the manufacturer. Before

starting the acquisition, imaging device properties such as exposure, white balance, gain, brightness and saturation were checked to maintain consistency. These parameters were also consistent with the in vivo calibration settings. The 'Sequence Timer Dialog' sampled the RGB image at every five seconds and stored each sample image on the hard disk at a pre-defined location. Manual intervention was required to change the data storage location for successive patient and/or successive test. There were four tests per subject using the clinical LCT system, documented and discussed in the following section. Data acquisition was supervised throughout the duration of the test. The above approach for data acquisition allowed real time storage of approximately 950 Mega Bytes of test data and a text file detailing particulars per patient. Each image was stored as a 'bmp' file and required 2.2 Mega Bytes of disk space. All acquired was manually transferred on an external hard disk and backed up on CD-ROM's for security. Two CD-ROM were required for each subject included in the study. The use of an appropriate image compression algorithm, such as 'jpeg' could address the issue of large image size and data storage. However, due to its lossy nature the 'jpeg; format affects the quality of calibration and subsequent analysis. It must be emphasised that the current study was a pilot investigation and modification of the measurement protocol is likely to further reduce the burden of data storage for clinical acceptance.

Computation of temperature was based on the in vivo hue temperature calibration of the R25C5W TLC sheet used for the tests. A diagram of the algorithm is given in figure 4-19.

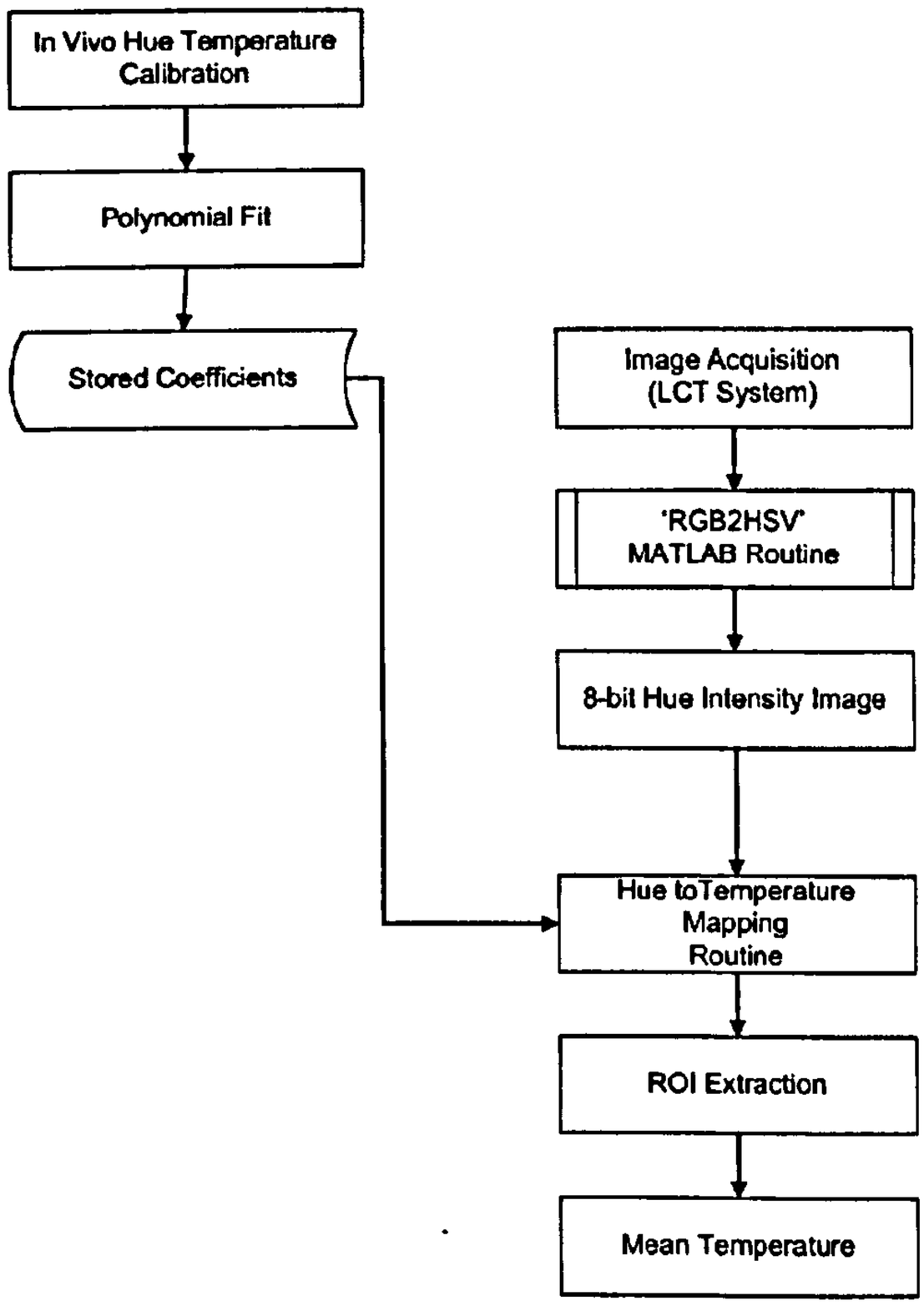


**Figure 4-19: Hue to temperature mapping algorithm implemented in MATLAB. Using the polynomial coefficients, temperature can be generated at each pixel based on its corresponding hue value.**

The calibration procedure was validated through detailed tests described in the following chapter. A total of thirty in vivo calibrations were performed and mean hue was calculated at each set point temperature. An appropriate polynomial fit was then used to describe the hue temperature relation. Each LCT image must be converted into 8-bit intensity image before applying the hue to temperature mapping algorithm in MATLAB using its pre defined 'rgn2hsv' routine in the image processing toolbox. The stored coefficients of the polynomial were then used to calculate temperature at each pixel in the image by using its corresponding hue value. Following this, a ROI can be drawn across desired anatomical site to monitor mean temperature at any instant through the duration of the test.

## *4.4 Clinical assessment of the LCT system*

### 4.4.1 Introduction

This section defines the clinical measurement protocol and presents the formulation of study group and its pre-clinical assessment. A clinical study involving 90 subjects in three study groups was completed at the MV Hospital for Diabetes and Diabetes Research Centre, at Chennai India. Ethical approval for a preliminary clinical evaluation of the system on diabetic subjects with and without neuropathy was obtained from the local ethics committee at MV Hospital for Diabetes and Diabetes Research Centre for this clinical study (WHO accredited).

### 4.4.2 Study group

This research is a pilot study in evaluation of plantar foot temperature for patients with type 2 diabetes mellitus and clinically diagnosed peripheral neuropathy. The main objective of the clinical evaluation of the liquid crystal thermography system was to verify its application in a clinical setting, verify system safety in vivo and collect in vivo data for analysis. A larger prospective study is required to establish statistical significance and correlation between measured values and underlying neuropathic condition, but this is beyond the scope of the present study. Additionally, a longitudinal study to follow up patients at a fixed interval is required to see if the prediction of risk is borne out in practise.

Dr. Vijay Viswanathan, the consultant diabetologist and joint director of the hospital accepted that a diverse type 2 diabetic (minimum duration 12 months) patient group be assessed, excluding patients with active foot ulceration, peripheral vascular disease, Charcot's foot deformity or any physical disability. All the subjects were native of Chennai and of Indian origin. Excluding patients with PVD differentiated current work from previous LCT studies (Stess, Sisney et al. 1986; Benbow, Chan et al. 1994), which did not consider peripheral vascular disease for exclusion criterion. These studies also considered patients with previous history of ulceration.

There was a total of three independent study groups including (a) Diabetics with neuropathy (n=30), (b) Diabetics without neuropathy (n=30) and (c) Healthy controls (n=30). For the neuropathic diabetic group, mean age was 58 years (range 41-71 years) approximately; whereas, for the non neuropathic diabetic group, mean age was 50 years (range 33-63 years) approximately. For healthy normals, mean age was 32 years (range 20-51 years) approximately. This group was not well matched in terms of age to the other two groups due to difficulty in recruiting age matched subjects. A summary of the composition of study group and important parameters such as age, sex, duration of diabetes, %HbA1c and body mass index (BMI) is given in Table 4-4.

| Patient Group/Parameters | Diabetic with Neuropathy | Diabetic without Neuropathy | Healthy Normals |
|---|---|---|---|
| No. of subjects (n) | 28* | 23* | 30 |
| Male\Female | 24/4 | 15/8 | 8/22 |
| Age (in years; mean±SD) | 57.92±7.08 | 50.35±9.79 | 32.43±7.3 |
| Duration of Diabetes(in years; mean±SD) | 14.75±6.8 | 9.45±5.8 | n/a |
| HbA1c (%mean±SD) | 9.01±1.81 | 8.79±1.82 | n/a |
| BMI (in $Kg/m^2$; mean±SD) | 25.24±3.77 | 25.31±3.48 | 25.07±4.16 |
| **Note: A total of '30' subjects per group were included in the clinical study. Two (male) neuropathic diabetic subjects and 7 (3 male/4 female) non neuropathic diabetic subjects were excluded from the final analysis, as they were either recently diagnosed with diabetes or had duration less than 12 months.* | | | |

**Table 4-4: Summary of the composition of study group for the clinical study.**

Patients were mainly selected from the outpatient department of MV Hospital and appointments were scheduled for in patients considering their schedule for other routine diagnostic tests. All subjects were given a prior verbal and written description of the test objectives and test procedure. Informed written consent was obtained from all patients before the thermographic examination. All the measurements were performed under controlled conditions in the foot laboratory at MV Hospital for Diabetes and in accordance with the test protocol approved by the ethical committee.

### 4.4.3 Pretest clinical assessment of the study group

A qualified research nurse from the foot care laboratory at MV Hospital, who was well versed in the regional language assisted during the in vivo data collection throughout the study. A comprehensive evaluation of the patient's foot was performed, typical of the routine foot care programme at the hospital. Visual inspection of the foot followed by sensory neuropathy tests using 10g Semmes Weinstein monofilament and biothesiometer were performed by trained nurses. Both tests have been validated in previous studies (Viswanathan, Snehalatha et al. 2002; Miranda-Palma, Sosenko et al. 2005). Both tests were made at five sites on the foot and a vibration perception threshold for neuropathy was taken as 30V. Insensitivity to a graded 10g nylon monofilament at 3 or more sites was considered as clinical neuropathy. Furthermore, peripheral vascular disease was assessed by determination ABPI, with values at or above 0.9 considered as normal (Pendsey 2003; NHS 2004). Data for mean glycosylated haemoglobin HbA1c which indicates glycaemic control over previous three months was also recorded and is documented in Table 4-4 for the study groups. Two subjects in the non neuropathic group presented current evidence of oedema in the measured foot. This is further discussed in Appendix J.

In order to standardise the patient recruitment process, a clear classification and staging system for the patients was adopted using the exclusion criteria as discussed. Therefore, the diabetic subjects were classified into one of the two groups depending on the results of tests for sensory neuropathy and PVD. An independent test for autonomic neuropathy was performed for diabetic with neuropathy (n=26) and diabetic without neuropathy group (n=17). The detailed results are discussed in Appendix I.

### 4.4.4 Measurement protocol

The testing procedure commenced with a 20 minutes rest period in order for the plantar temperature to equilibrate with the room temperature. The room temperature and humidity were consistently maintained at 24°C and less than 50% respectively with air

conditioning. A total of four different measurements were performed for each patient with 15 minutes in between each test i.e. baseline, repetitive stress, cold immersion recovery and warm up recovery. During the waiting period, patient was seated on a chair with the feet flat on ground. All patients were barefoot, with feet resting on their footwear. The plantar foot temperature was measured using a digital thermometer at the first metatarsal head and the heel before each test. These were used as a baseline reference measurement for each site. The patient feet were then located on the measurement platform using consistent alignment with reference markers. All subjects were advised to avoid movement during the duration of the test and use support from the handrail along the adjacent wall.

For the baseline measurement, 60 static images of the right foot were recorded over a continuous five minute period. The sampling rate was one image every five seconds. Following a resting period of 15 minutes, subjects were advised to walk for 20 minutes for repetitive stress measurements. Following the walking, 60 static images of the right foot were recorded for five minutes, capturing images every five seconds.

During the thermal cycling tests, the right foot for each subject was placed in water at controlled temperature. When skin is wet its temperature can be altered by evaporation. To prevent this problem, the foot was dried thoroughly using a pre-sterilised towel prior to placing on the measurement platform for the thermal cycling measurements. Patients with active foot ulcers, foot infection (toe nail infection, fungal infection) or wounds were excluded and therefore, any sterilisation procedure for the measurement platform was not considered. For the cold immersion test, the patient's foot was placed in a water bath at 18-20°C for three minutes. This variation in temperature did not affect the measurements, as the main purpose was to cool the foot below the ambient temperature at 24°C. Following 15 minutes resting period after the cold immersion test, the foot was placed in a water bath at 37°C for three minutes for the warm up recovery test. The temperature of the non insulated water bath was maintained at 37°C by a ceramic water heating rod with a thermostat. In order to ensure patient safety, the ceramic rod was removed from the bath prior to placing subject's foot inside. Thermal changes during

both the tests were recorded for 10 minutes, capturing static images every five seconds giving a total of 120 images.

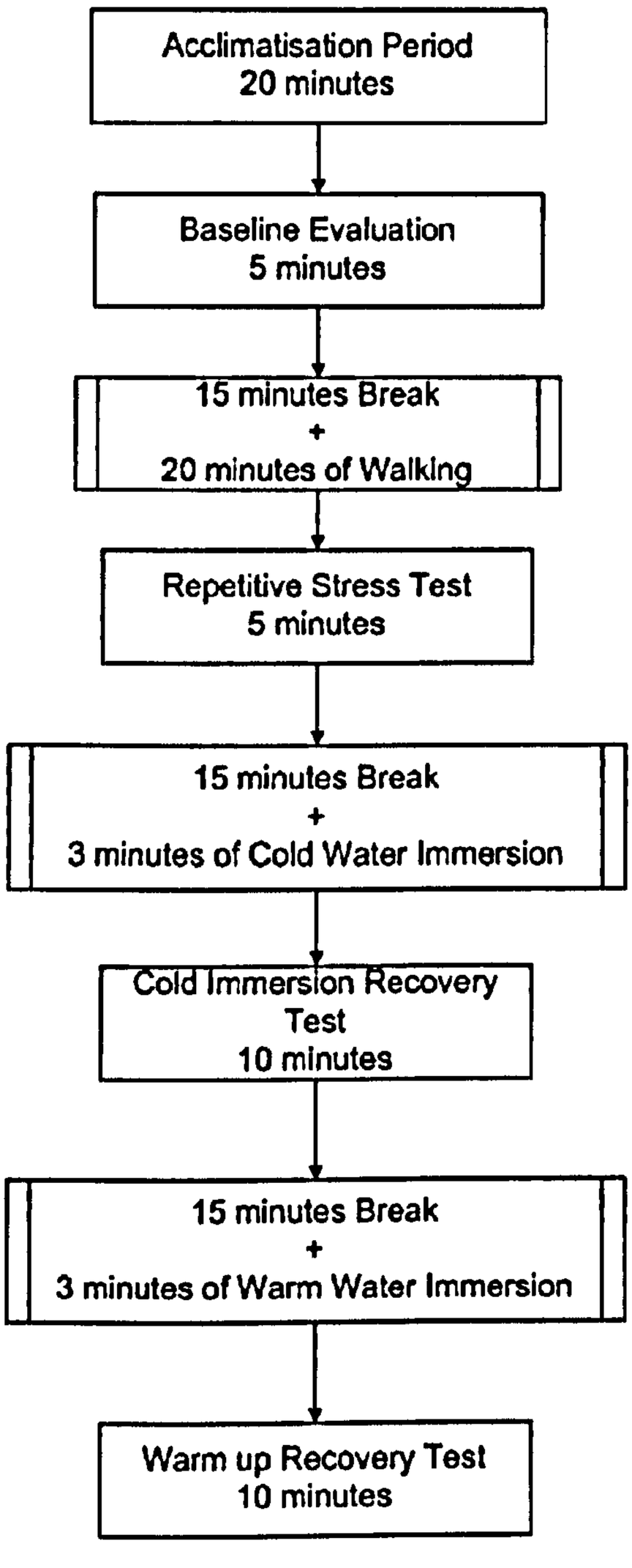


**Figure 4-20: Step by step procedure adopted for the clinical protocol for four tests including baseline evaluation, repetitive stress tests and thermal cycling tests.**

Figure 4-20 illustrates a step by step procedure used for the four tests. Data was not acquired beyond 10 minutes for the thermal cycling tests due to the limited capacity of the recording equipment. It was not possible to analyse the data in real time due to

limitation of the analytical interface into the camera acquisition software. After completion of the test sequence, the light source was switched off (to prevent heating effects on the TLC sensor) and the foot was carefully removed from the platform to avoid any physical damage to the patient.

# Chapter 5 In vitro characterisation and clinical results

## *5.0 Introduction*

In this chapter, results from in vitro characterisation of TLC material, pre-clinical in-vivo assessment of the system and results from the clinical evaluation of the liquid crystal thermography system are presented. A clinical study involving 90 subjects in three study groups was completed at the MV Hospital for Diabetes and Diabetes Research Centre, at Chennai India.

## *5.1 In vitro results*

### 5.1.1 Introduction

Results from the in vitro characterisation of three physical forms of TLC material are now presented.

### 5.1.2 R25C5W TLC sheet

In the remaining analysis of in vitro calibration data, all results are illustrated for n=5 samples of the calibration runs. This constraint was imposed by the time taken for each calibration run (45 minutes). Given the high repeatability (5%) of the TLC measurements established using n=30 sets it was considered that the smaller data set was acceptable for the purposes of the current study.

Figure 5-1 presents a typical calibration curve for the TLC sheet material assessed in the study. In practise the data for this type of curve was obtained over a wider temperature range, i.e. from the event temperature to the clearing point temperature. This was found to be necessary to avoid possible errors due to application of a rapid thermal transient at the start temperature. Thus the calibration range of the system was typically ±3°C greater

than that of the TLC sheet. Typical data obtained over this extended range is shown in figure 5-2.

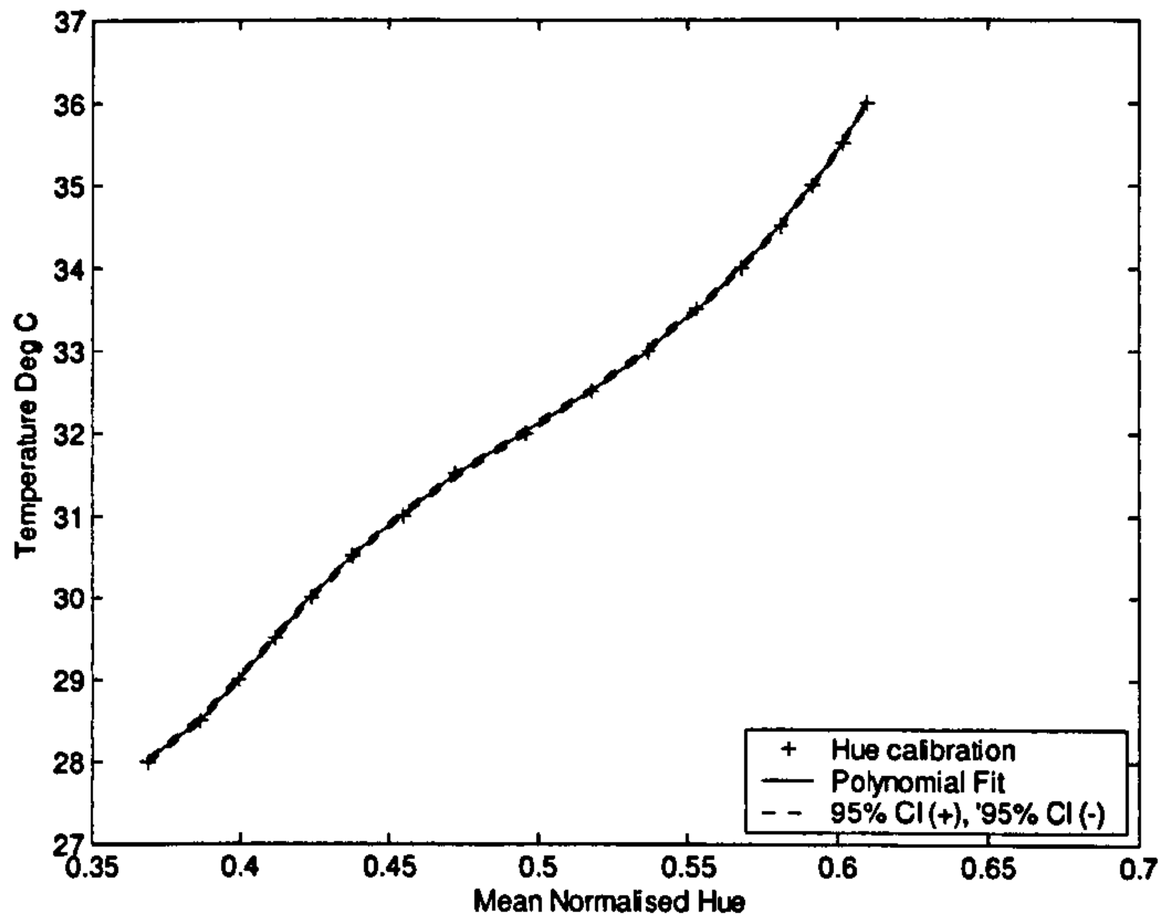


**Figure 5-1: Typical calibration curve for a TLC sheet material R25C5W. Due to discontinuities in the response, the sensor is only useful over a part of the hue range and within this range hue is approximately linear. Here the mean normalised hue is based on n=5 samples.**

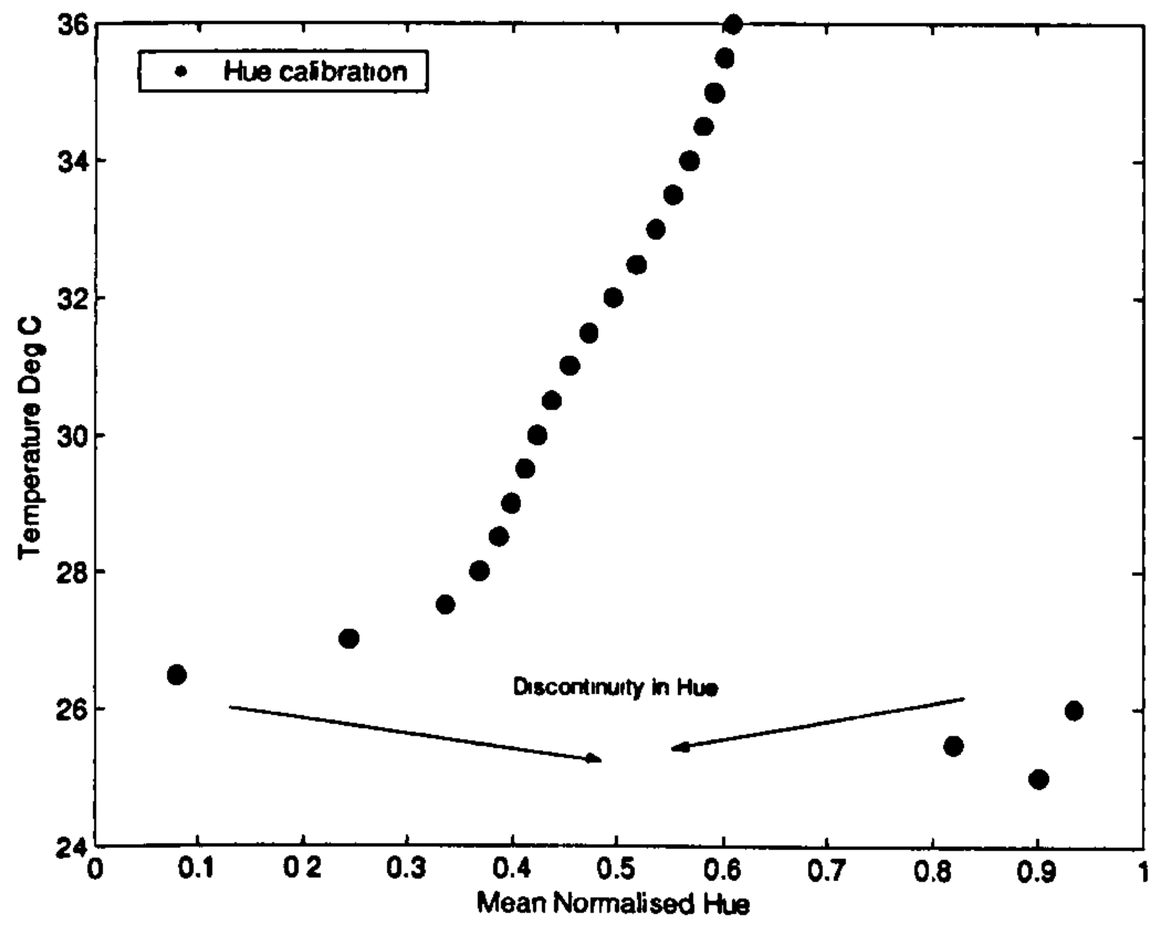


**Figure 5-2: Illustration of discontinuity in hue. This must be removed before fitting an appropriate polynomial.**

It is clear that a discontinuity in the data occurs at the low temperature end of the range whereas at the high temperature end of the range, useful data can still be obtained. This

latter finding was important in the context of the current study as it suggested the possibility of using a single wide band TLC sheet over the full physiological test range. This is better than using two or more sheets each covering a different temperature band within the overall operating range. Note that the discontinuity at the lower end of the temperature range had to be removed before a calibration function was fitted to the data.

Figure 5-3 illustrates the standard deviation of the hue for the samples evaluated in figure 5-1. This figure also shows the affect of introducing a median filter. Using a 3x3 median filter reduces the standard deviation by a maximum of 30 %. Filtering is a task dependent process. Median filtering is typically used for eliminating data dropouts and salt and pepper type noise and has the important advantage over averaging filter, that it does not degrade edges or sharp gradients. Filtering operation should not be performed on hue due to its periodicity, but rather should be done on RGB intensity images used to calculate hue (Anderson 1999). However, this can decrease the spatial resolution of the image. Therefore, filtering was discounted for use in the in vivo calibration and the analysis of clinical data. It must be emphasised that image enhancement and image restoration techniques may be more useful for emulsion based TLC applications, where higher variation exists in the number of crystals per pixel. TLC sheets on the other hand have a uniform distribution due to better manufacturing technique.

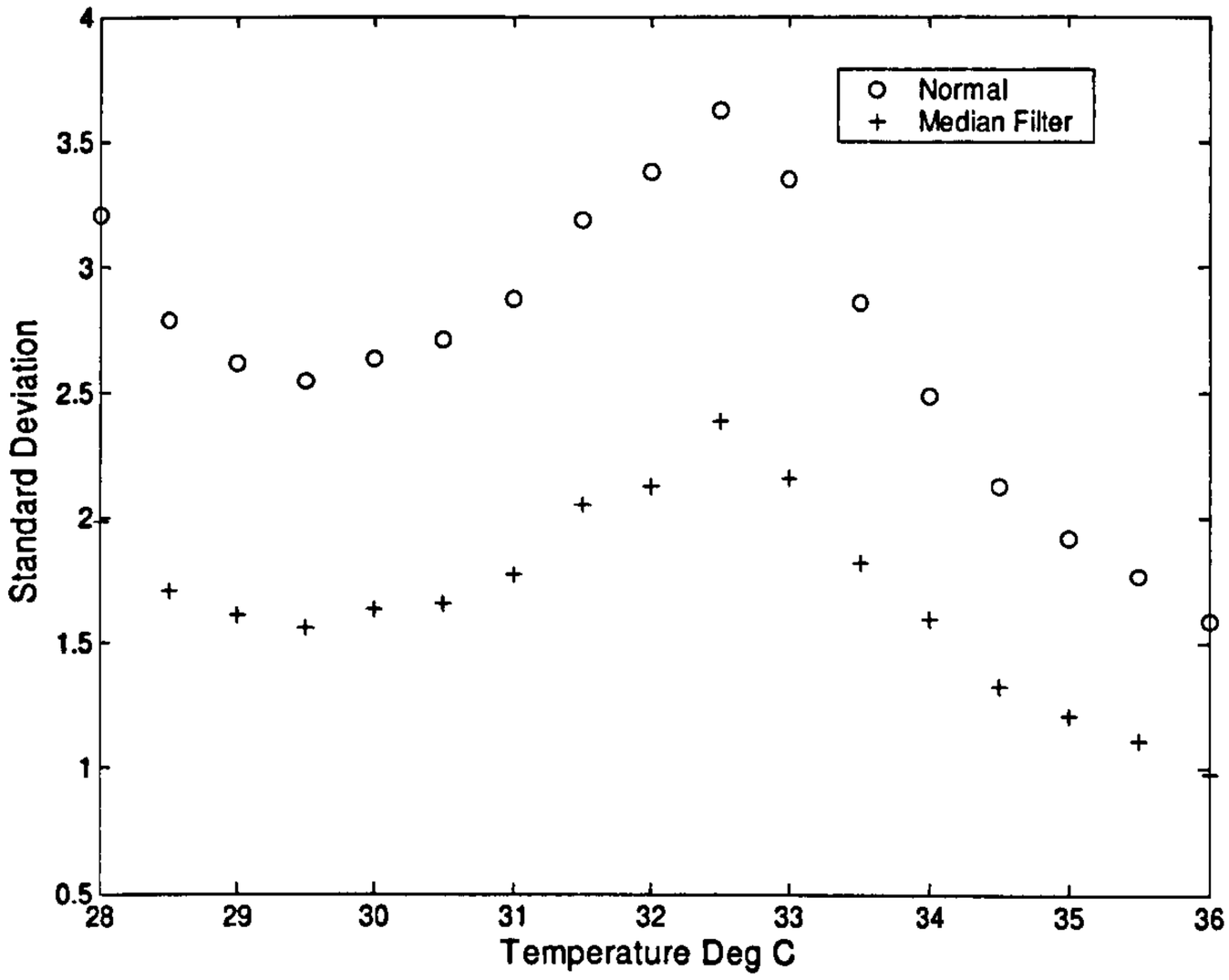


**Figure 5-3: Standard deviation in the mean normalised hue values used to produce figure 4-14. An increase in the measured variance is seen to occur at the colour transition temperature.**

The inherent spatial variations in the TLC have been considered using the microscopic analysis of samples. The coverage area which determines number of crystals per pixel is a significant factor in determination of spatial resolution and temperature resolution. This is however; a limitation of the TLC's and therefore, cannot be resolved by imaging device or image processing.

The following section addresses the dependence of TLC colour response on the illumination source intensity.

### 5.1.3 Effect of source light intensity

It is now appropriate to consider the effect of changes in light intensity on the hue-temperature calibration. Figure 5-4 shows the effect of illumination intensity on hue temperature calibration for the R25C5W TLC sheet specimen.

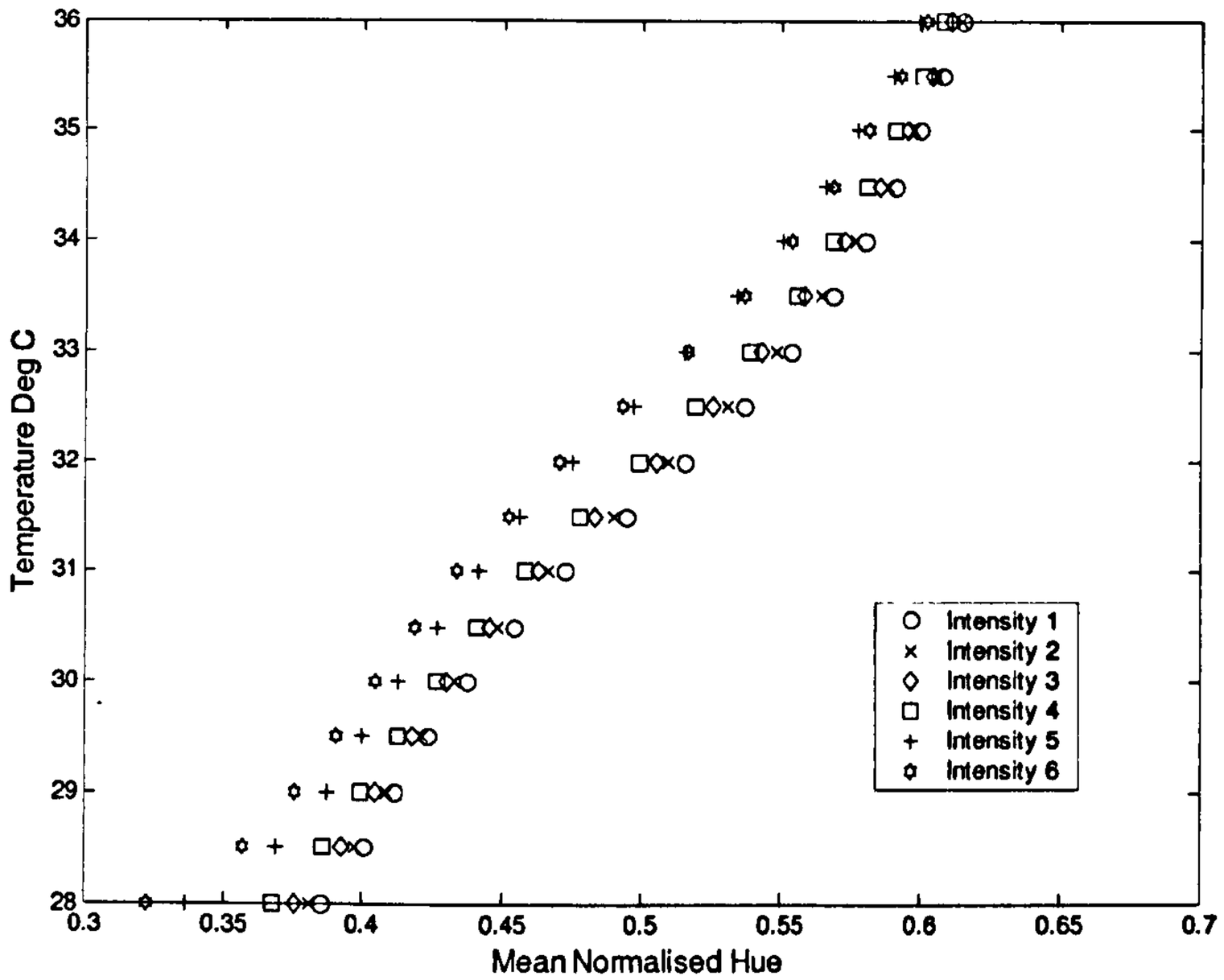


**Figure 5-4: The effect of different values of source intensity on the hue versus temperature calibration for R25C5W TLC sheet.**

The incident light intensity ('L') was changed by changing the power knob and F-stop setting ('F') on the camera lens. F-stop indicates the size of the aperture and is inversely proportional to the indicated number i.e. a smaller number like F3.5 means big aperture size and vice versa. For each light intensity setting, an image was acquired from the test surface with liquid crystals outside their colour play interval. The images were used to extract the mean pixel intensity and corresponding standard deviation from a similar region of interest. The order of the incident light intensity (maximum to minimum) is listed in Table 5-1.

| Light description | Arbitrary intensity | Standard deviation |
|---|---|---|
| L90 F3.5 (maximum) | 31.41 | 3.85 |
| L90 F5.6 | 24.81 | 3.22 |
| L90 F8.0 | 19.49 | 2.61 |
| L80 F3.5 | 19.53 | 2.53 |
| L80 F5.6 | 16.65 | 2.30 |
| L70 F53.5 (minimum) | 15.62 | 2.17 |

**Table 5-1: Incident light intensity settings.**

Figure 5-4 suggests that there is a 10-12% change in hue when light intensity is changed by 50%. There is an upward shift in hue when light intensity is increased resulting in a different calibration curve. This shift in hue produces a corresponding shift in the measured temperature producing an error. This error was assessed by comparing it with an independent measurement of the calibration plate achieved using a thermistor (uncertainty 0.1°C), which confirmed that the effect was not due to the source temperature increasing with light level (bulb self heating). This change in hue corresponds to a maximum error in measured temperature of up to 1°C.

The preceding investigation confirmed the necessity for calibration of the TLC material to include a means of compensating for possible variations in the intensity of the light source. To address this problem, a novel neural network based calibration approach was considered. Results of this study have been published (Grewal, Bharara et al. 2006) and are further considered in Appendix E.

Wideband TLC sheets, emulsion based TLC and latex based TLV were also considered and their results are presented in Appendix D. A noticeable difference between the wideband and narrow band versions of this TLC material is the higher discontinuity in hue towards the event temperature for the former. This was significant to selection of the optimum TLC material for the intended final application. The higher the discontinuity in

hue, the lesser will be the useful colour bandwidth of the corresponding TLC material in relation to the required physiological test range.

Results of pressure sensitivity assessment of R25C5W TLC sheet are now presented in the following section.

### 5.1.4 Results of pressure sensitivity experiments

Figure 5-5 illustrates a typical hue versus load graph for the R25C5W TLC sheet. A consistent light setting (L90 F8.0) and water bath at constant temperature (at 30°C) were used throughout pressure sensitivity experiments. At each load, mean hue was calculated from 10 images captured one second apart.

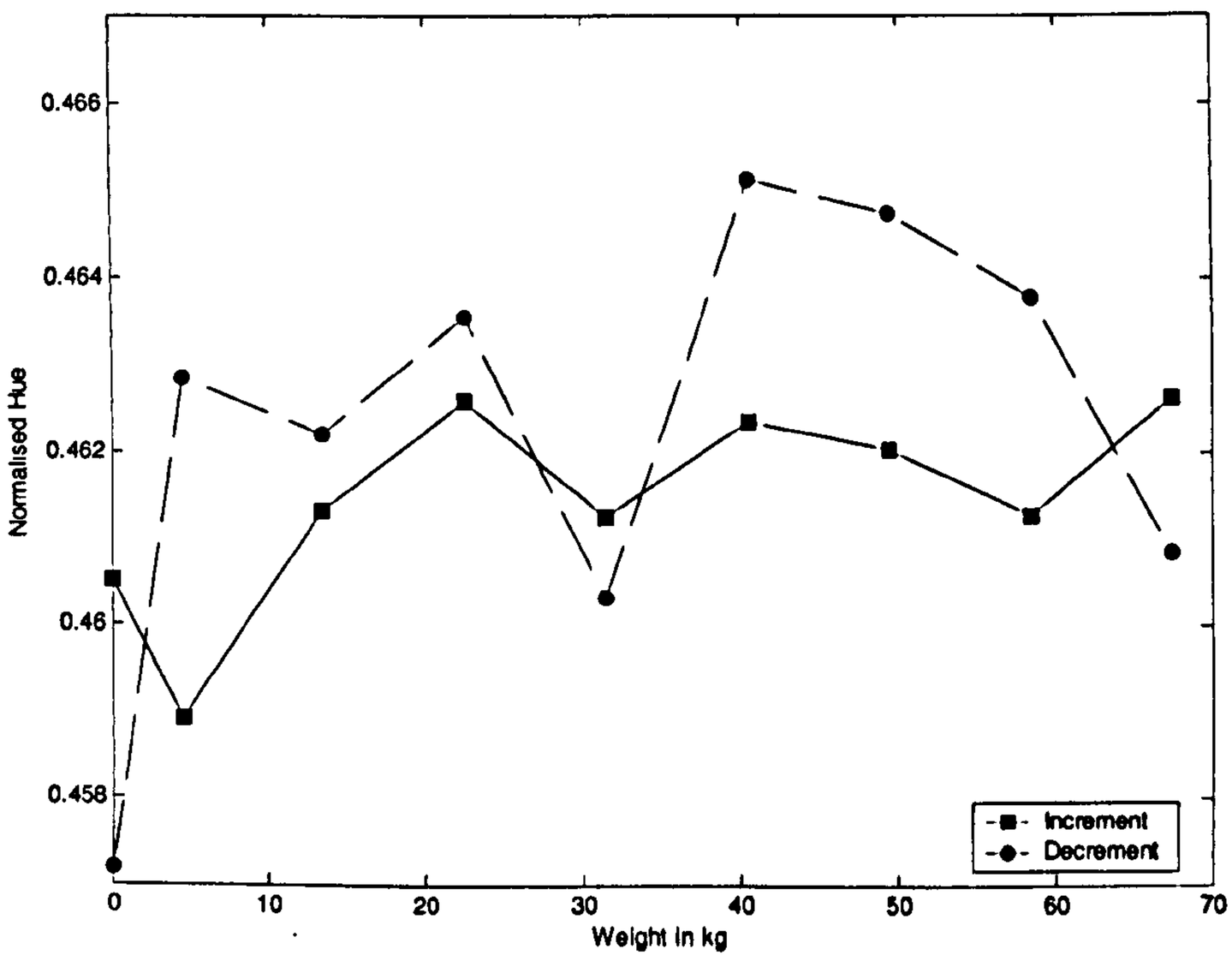


**Figure 5-5: Typical hue versus load dataset for R25C5W TLC sheet. At each load, mean hue is averaged from 10 images. All data was collected under similar light intensity setting and constant temperature.**

Figure 5-6 illustrates a similar graph for a repeated dataset obtained at the same settings of the camera, light intensity and temperature to evaluate the repeatability of the

experimental setup. The hue range has shifted upwards at the same temperature for similar range of loads used. This test was performed after two hours of the previous test to provide sufficient time for the TLC sheet to recover. Therefore, this shift in response is not a short term effect.

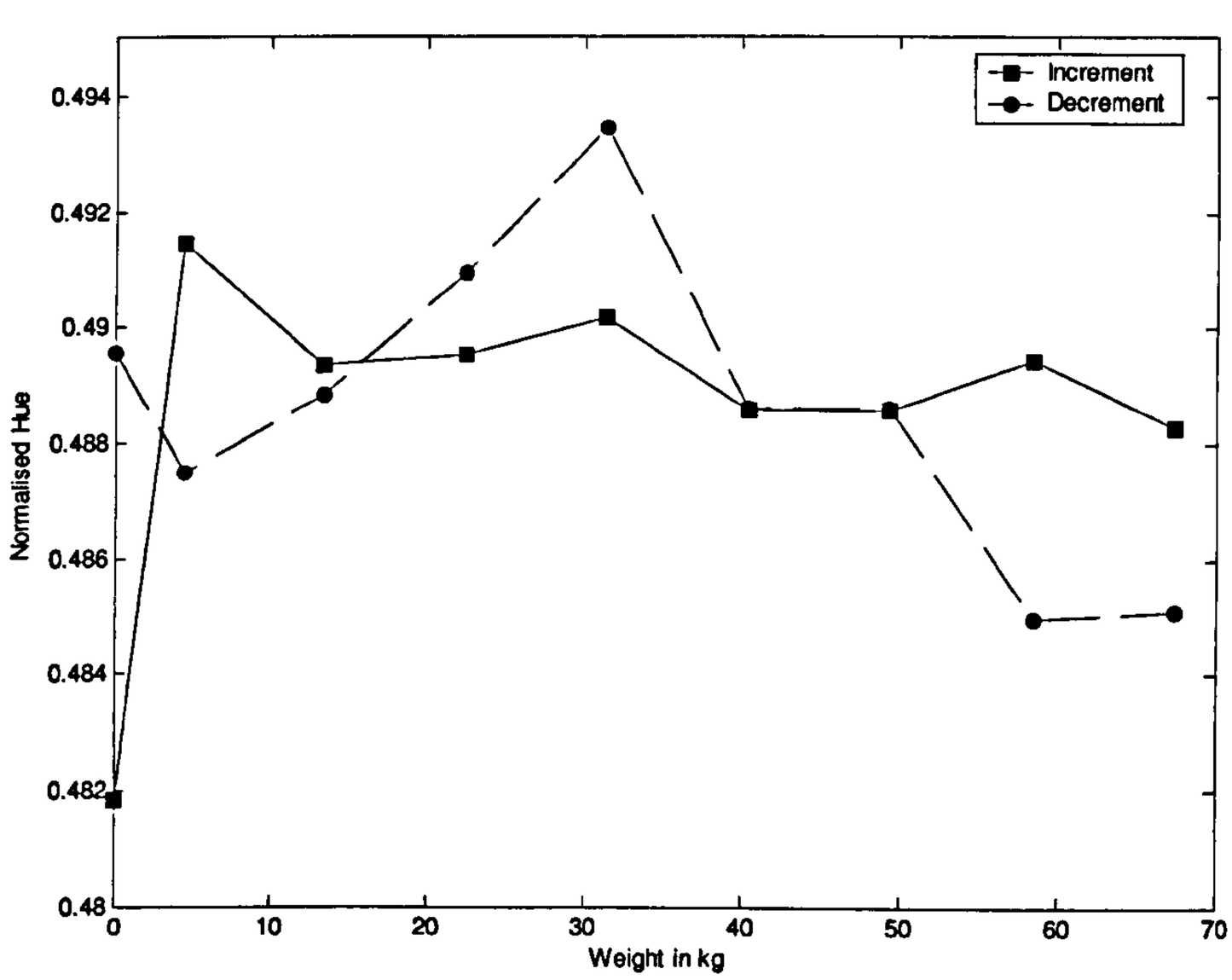


**Figure 5-6: Poor repeatability of the measured hue due to drawbacks in experimental setup. Movement between the aluminium and polycarbonate and physical damage to TLC material leads to poor repeatability of the test.**

This is due to two reasons:

(a) The TLC material is sandwiched between the aluminium block and polycarbonate. Relative movement between the aluminium and polycarbonate causes physical damage to the TLC material as shown in figure 5-7. Each image is representative of damage caused during one increment and decrement cycle. All tests were carried on a single day. Furthermore, this leads to poor image quality and results in a different hue value. This relative problem was an inherent problem of the design and was addressed by altering the design. The clinical sheets were manually inspected after pressure sensitivity test to check for any signs of slip of the liquid crystals which would have important

consequence for the clinical measurement. But there were no signs of slip seen on the TLC sheet.

(b) Due to different thermal conductivities of the aluminium and polycarbonate, there is a thermal gradient (over the aluminium surface) which directly affects the measured hue. This cannot be a time issue i.e. a time lag as the temperature reaches the correct value as sufficient time (30 minutes) was allowed for temperature stabilisation. Therefore, the actual value of the hue should be the same after this lag, independent of the load. However, it must be emphasised that temperature was only measured at the inlet and outlet of the aluminium block. Therefore, this issue could be addressed by having more thermistors over the aluminium block. This could not be implemented in the design under consideration, due to possibility of physical damage to the thermistors.

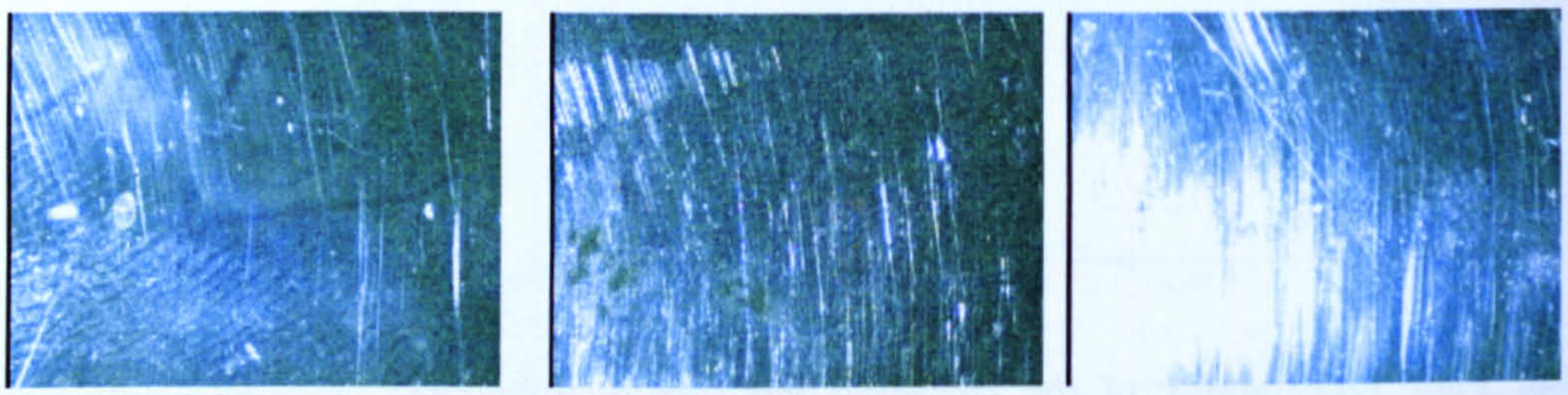

(a) (b) (c)

**Figure 5-7: Images of R25C5W TLC sheet showing progressive physical damage due to movement between the aluminium and polycarbonate when testing for pressure sensitivity.**

To reduce the problem of movement between the aluminium and polycarbonate an industrial strength single sided adhesive tape (duct tape) was used between the two. In order to prevent scratches, a thin polyester film was introduced between the polycarbonate and TLC sheet. However, using polyester film changes the hue values significantly for the images as seen in figure 5-8 (a). This may be primarily due to the change in refractive index and therefore, reflection of the incident illumination. Besides, it changes the camera focus leading to blurring in the image.

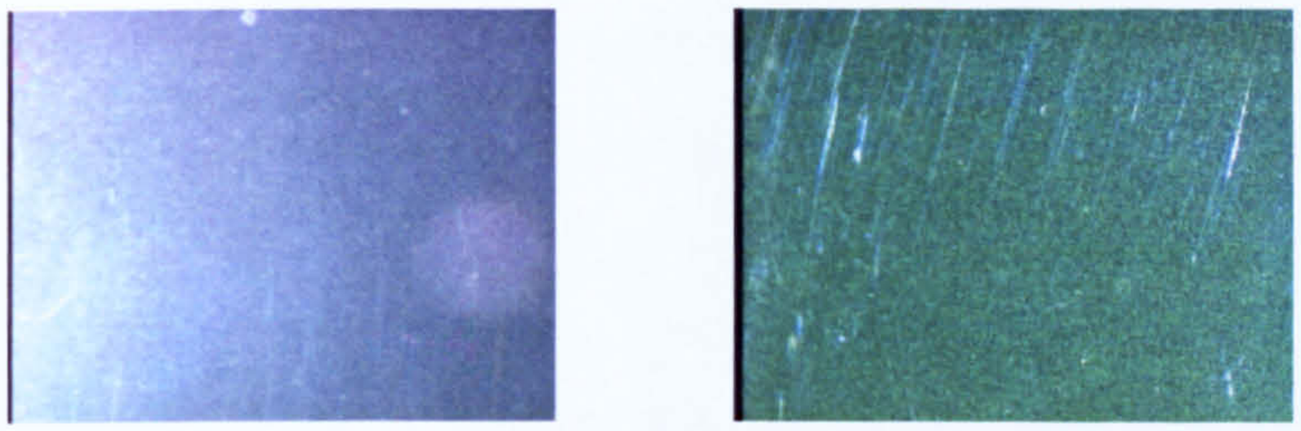

(a) (b)

**Figure 5-8: Change in colour information by using polyester film. Note the change in hue and blurring in image (a) due to change in refractive index and camera focus respectively.**

Therefore, the use of polyester film was discounted from further data collection. Figure 5-9 illustrates the effect of using the duct tape in improving the image quality and overall experimental setup. Figure 5-10 illustrates the hue versus load graph for the R25C5W TLC sheet using the improved setup. The standard deviation in hue calculation from the region of interest is illustrated in figure 5-11. The standard deviation is higher than the value obtained from the calibration runs in section 5.1.2. This may be due to better thermal contact of the TLC sample in the experimental setup for calibration runs.

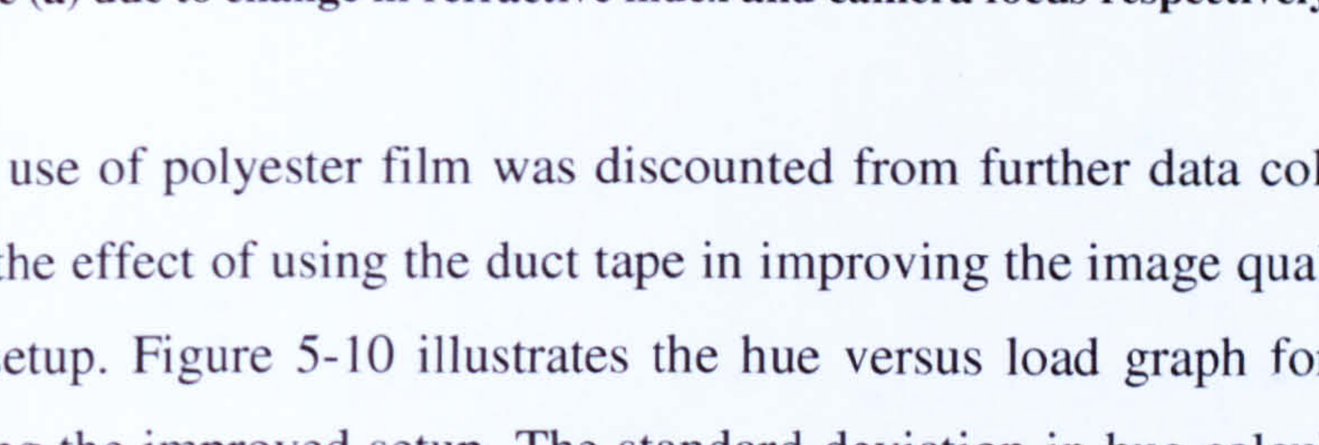

(a) (b)

**Figure 5-9: Comparison between TLC images, illustrating the effect of improved pressure sensitivity setup. Image (b) illustrates the inherent problem of relative movement inducing physical damage to the TLC sheet.**

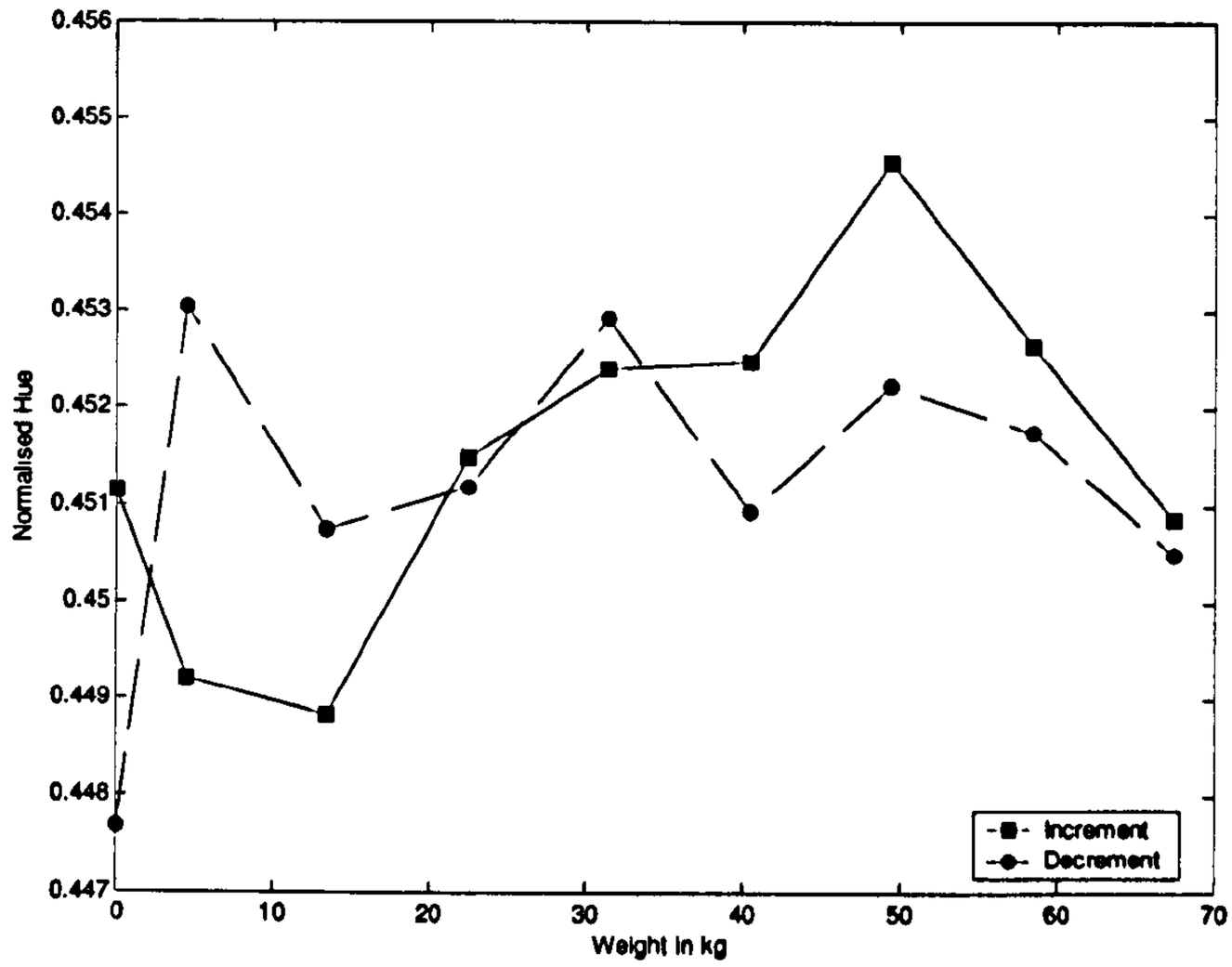


**Figure 5-10: Hue versus load dataset for R25C5W TLC sheet. Data illustrated here is collected from improved pressure sensitivity setup.**

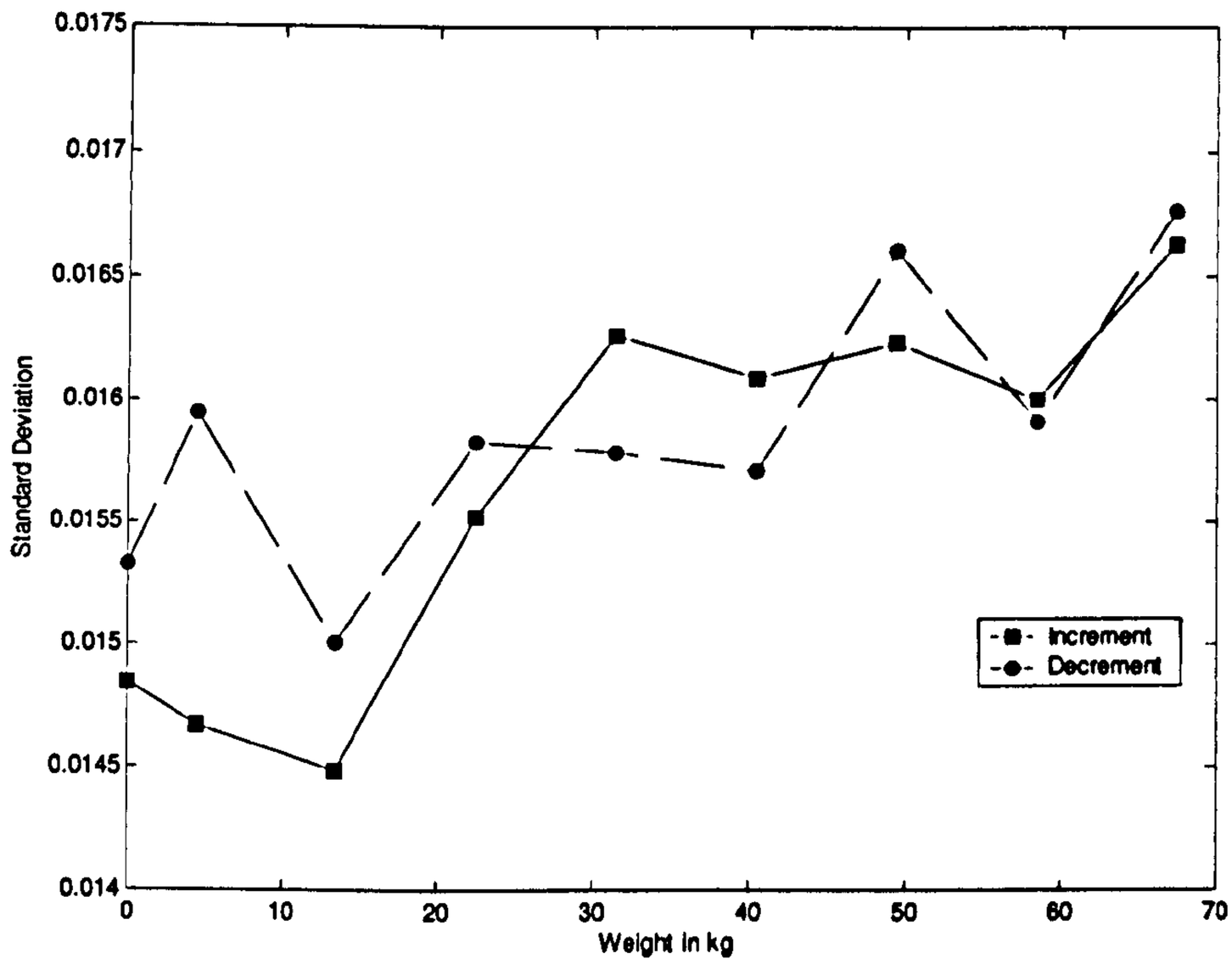


**Figure 5-11: Standard deviation versus load illustrated for both loading and unloading cycle during pressure sensitivity testing. The standard deviation in measured hue is slightly higher than the value during calibration runs.**

For an independent assessment of pressure sensitivity of TLC, it was important to consider the effects of different field of view of the camera, different region of interests

for hue calculation and different physical size of the TLC sheet sample. By changing the field of view of the camera, it is possible to discount any changes due to thermal gradient on the aluminium surface. Intuitively, thermal gradient will be largest at the inlet and outlet and smallest at the centre of the aluminium. By evaluation of the hue versus load dataset for different regions of interest, changes due to variable loading at different areas of the sheet can be separated. Loads were applied sequentially as increment and decrement cycles to investigate pressure sensitivity.

Table 5-2 lists the mean hue values and standard deviation (SD) for pressure sensitivity tests. 'SD' is the standard deviation measured as shown in figure 5-12. Ideally, the hue should be independent of changes in load. Practically, there is a nonlinear behaviour of hue in a very narrow range with respect to the load as seen from the hue versus load graph in figure 5-12. Thus, 'SD' gives a measure of the extent of this nonlinear hue behaviour. Figure 5-12 shows mean hue (average hue for all loads) and standard deviation for the increment steps for one of the datasets. Table 5-3 also shows the mean hue and standard deviation for multiple hue versus temperature calibration runs performed under similar lighting conditions. The hue and SD values are compared at the same load during the increment and decrement cycle. It can be seen that mean hue values for all the three fields of view are different. This may indicate non uniformity in temperature distribution. Temperature was only measured at the inlet and outlet of the aluminium block. Interestingly, the mean and 'SD' values for the three fields of view follow a similar pattern except for the 'SD' value in the left corner during decrement (this is an outlier).

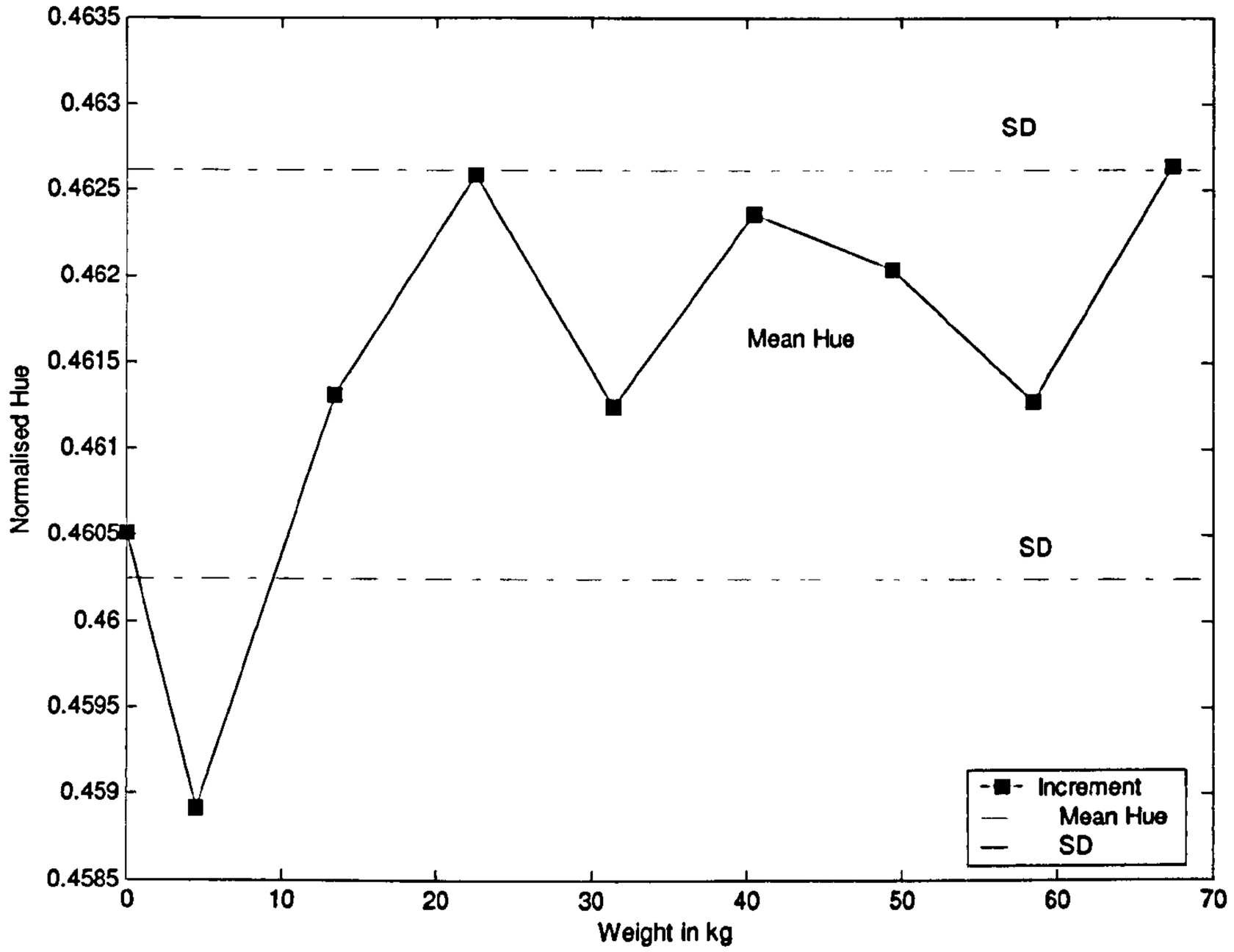


**Figure 5-12: Pressure sensitivity for R25C5W TLC sheet. Mean hue and 'SD' values are calculated from different hue values at different loads to consider the spread of hue.**

| ROI | Left Corner | | Right Centre | | Centre | | Calibration | |
|---|---|---|---|---|---|---|---|---|
| | *Increment* | *Decrement* | *Increment* | *Decrement* | *Increment* | *Decrement* | *Hue* | *St. Dev* |
| Mean | 117.2 | 117.6 | 124.6 | 124.6 | 115.1 | 115.1 | 110.42 | 3.0 |
| SD | 0.56 | 1.18 | 0.69 | 0.68 | 0.45 | 0.41 | 0.43 | n/a |

**Table 5-2: Pressure sensitivity results for R25C5W TLC sheet for different field of views.**

It was important to evaluate pressure sensitivity for a different TLC sample size, in order to discount the effect of thermal non-uniformities on the aluminium surface. Two sample sizes were used (25.4mm x25.4mm and 100mm x 100mm). Results are listed in Table 5-3.

| Sample Size | Small | | Large | | Calibration | |
|---|---|---|---|---|---|---|
| | *Increment* | *Decrement* | *Increment* | *Decrement* | *Hue* | *St. Dev in hue* |
| Mean | 117.7 | 117.9 | 115.1 | 115.1 | 110.42 | 3.0 |
| SD | 0.30 | 0.64 | 0.45 | 0.41 | 0.43 | n/a |

**Table 5-3: Pressure sensitivity results for R25C5W TLC sheet for different TLC sample size.**

However, all the 'SD' values from tables 5-2 and 5-3 are of similar order as the standard deviation in hue calculation during routine calibrations of the same TLC material, confirming pressure insensitivity over the range of loads considered. This is a key point, justifying the use of TLC sheets in the clinical system for evaluation of thermal patterns under the plantar foot. It must be emphasised that contact thermography using TLC is the only method of measuring skin temperature under the influence of load.

### 5.1.5 Results for hysteresis assessment of TLC

Both narrowband and wideband TLC material were tested for hysteresis effects. A representative of the image taken from the heating and cooling runs is shown in figure 5-13. Note that the images are shown at 30°C and the image is at uniform temperature. One of the noticeable things in the images is the reduction in intensity during the cooling run. The RGB graphs shown later in figure 5-17, also exhibits this phenomenon. The heating run started at 25°C and using the ramp mode of the temperature controller was raised until 46°C i.e. the clearing point temperature of R25C5W TLC sheet.

(a) (b) (c)

**Figure 5-13: Sample images at T=30°C for hysteresis tests. There is a decrease in intensity from left to right, during cooling run (b and c) as against heating run (a).**

There is a significant decrease in R, G and B intensities when cooled rather than heated. The magnitude of this decrease is a function of peak temperature prior to cooling; the higher the temperature the greater is the decrease. This can be attributed to the decrease in reflectivity of TLC during cooling run, consistent with other studies (Bakrania and Anderson 2002; Anderson and Baughn 2004).

A small ROI was selected at the centre of the image, converted to HSV domain and hue was determined using MATLAB. The graph in figure 5-14 illustrates hue versus temperature dataset for the R25C5W TLC sheet.

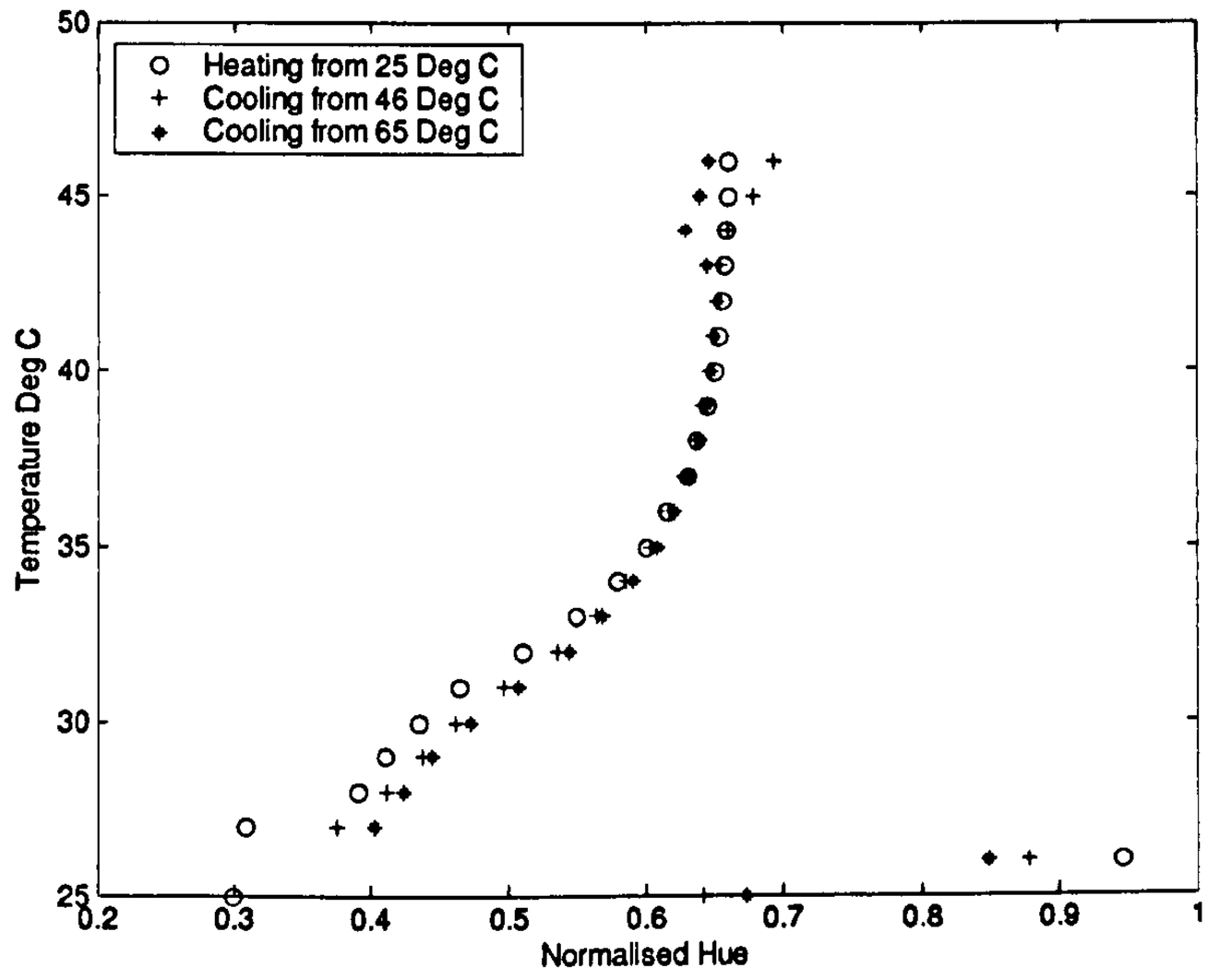


**Figure 5-14: Results for hysteresis tests on R25C5W TLC sheet. The graphs show hue versus temperature curves for heating and cooling runs.**

Figure 5-15 illustrates standard deviation in hue calculation at each temperature increment, throughout the colour play interval and within the useful colour bandwidth (bottom) for the R25C5W TLC sheet. The standard deviation values are consistent with the calibration dataset.

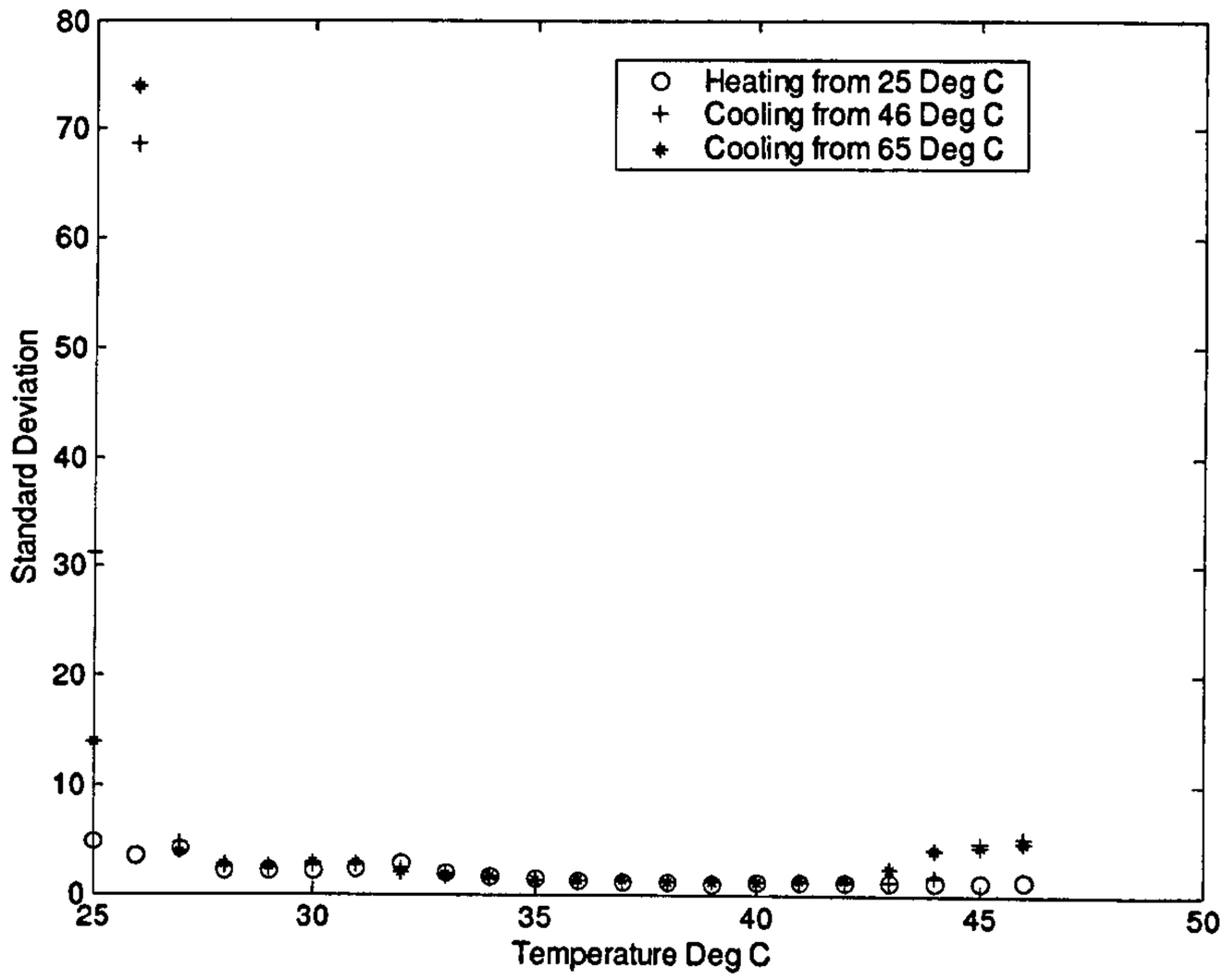


**(a)**

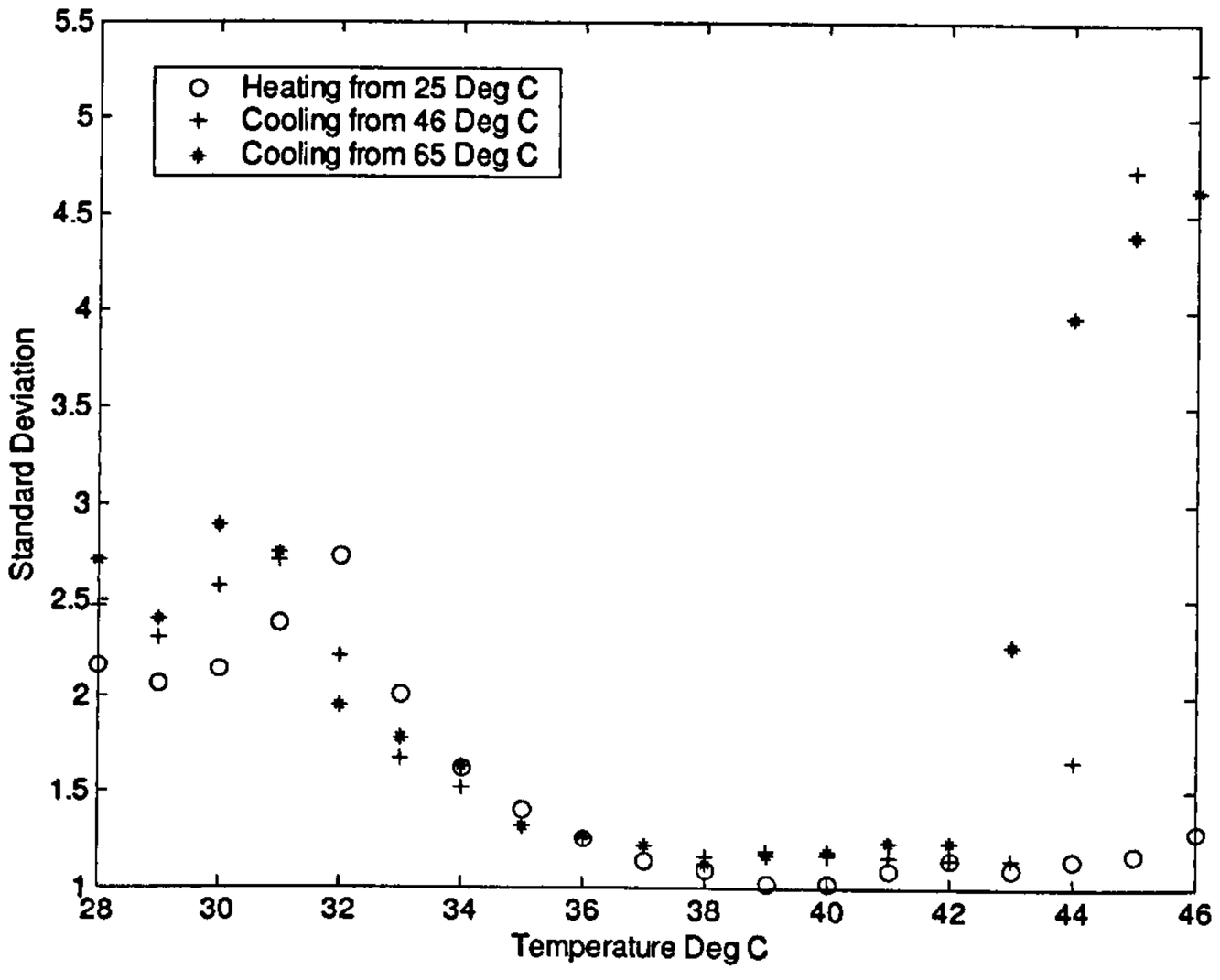


**(b)**

**Figure 5-15: Standard deviation in hue calculation for the hysteresis tests on R25C5W TLC sheets. The graphs illustrate standard deviation in hue values for complete (top) and useful colour bandwidth (bottom).**

Note the abnormally high standard deviation at the event temperature (25°C) in figure 5-15 (a) due to misalignment of the crystalline structure during cooling run.

The first indication of hysteresis is the decrease in R, G and B intensities when cooled rather than heated as seen in figures 5-16 and 5-17.

**Figure 5-16: Calibration bars for the heating and cooling runs. Notice the reduction in intensity of colours throughout the colour play interval for the cooling runs.**

Figure 5-16 illustrates the calibration bars for the hysteresis tests. These results are consistent with the current published literature for the TLC hysteresis (Anderson 1999; Bakrania and Anderson 2002; Anderson and Baughn 2004). A complete history of the testing order for R25C5W TLC sheet is presented in Table 5-4.

| Direction of calibration | Maximum or minimum temperature °C |
|---|---|
| Heating | 25 |
| Cooling | 46 (Clearing point temperature) |
| Cooling | 65 |

**Table 5-4: Testing order for R25C5W TLC sheet.**

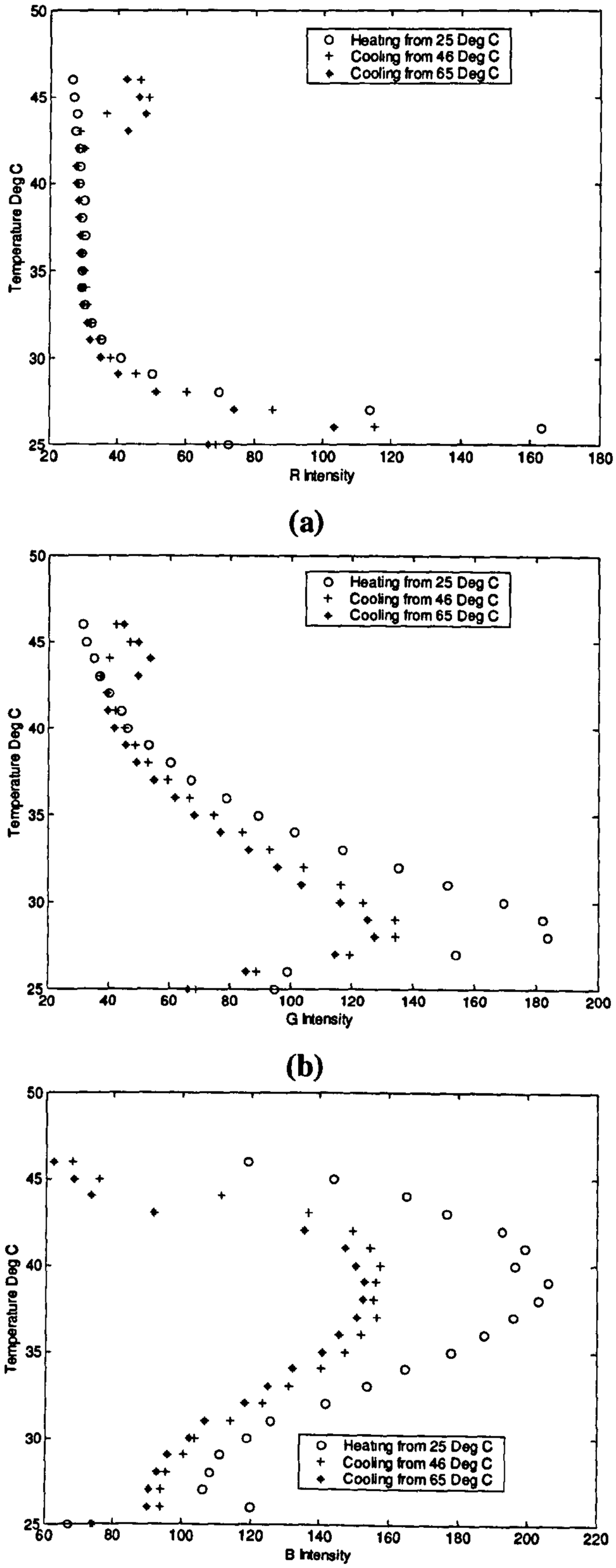


(a)

(b)

(c)

**Figure 5-17: Results for hysteresis tests on R25C5W TLC sheet. The graphs show R, G and B intensities versus temperature curves for heating and cooling runs.**

Wideband TLC and emulsion based TLC materials also show decrease in RGB intensities upon cooling, similar to narrow band TLC material. Results from the wideband TLC material (R25C15W polyester sheet) and emulsion based TLC material (R25C10W paint) are presented in Appendix H.

Table 5-5 summarises the results of the hysteresis measurements for the TLC sheet and emulsion formulations that were found to exhibit significant hysteresis.

| TLC | R | G | B |
|---|---|---|---|
| R25C5W Sheet | 37% | 31% | 26% |
| R25C15W Sheet | 6% | 3.5% | 4% |
| R25C10W Paint | 39% | 36% | 25% |

**Table 5-5: Maximum percentage decrease in R, G and B intensities for TLC sheet and emulsion.**

## *5.2 Results of the clinical study*

### 5.2.1 Introduction

Results from the clinical study at MV Hospital for Diabetes, Chennai (India) are now presented.

### 5.2.2 Processing and analysis of test data

Design of the clinical protocol and the test duration were limited by capacity of the LCT system, available disk space, acquisition software and patient ease. The LCT system design and its implementation are discussed in the preceding chapter. A total of 950 Mega Bytes of data was generated per patient and could be immediately transferred to the external hard disk from laptop.

There was no pre-processing algorithm or filtering applied to the data to prevent any smoothening of the raw data. However, there was a routine check to determine any corrupted files/images. Loss of mains supply and malfunctioning of the data acquisition

software caused corrupted files. During the measurement, the timing sequence was regularly monitored by the timer settings from the data acquisition software. The hue to temperature mapping algorithm was then applied to covert RGB colour images into hue plane, where hue at each pixel was used to represent temperature. By selecting an appropriate region of interest, the mean temperature at the respective anatomical site could be determined.

Patient movement was observed throughout the test duration as any movement of the foot being measured can alter measured temperature, especially during recovery tests. Patient movement alters the temperature in the field of view of the camera leading to measurement errors. All patients were comfortable with the study times (up to 10 minutes) and no movement in the feet was recorded except, in one patient who stepped off the platform due to discomfort. This subject was excluded from the final analysis.

The recording of data from all subjects was within ±10 seconds, relative to the acclimatisation time before starting the measurement. This variation occurred because of the time taken to manually position the feet on the platform with reference to markers.

Figures 5-18, 5-19 and 5-20, illustrate the mean temperatures and standard deviations in the measured temperatures at the first metatarsal head using the digital thermometer prior to each of the four clinical tests.

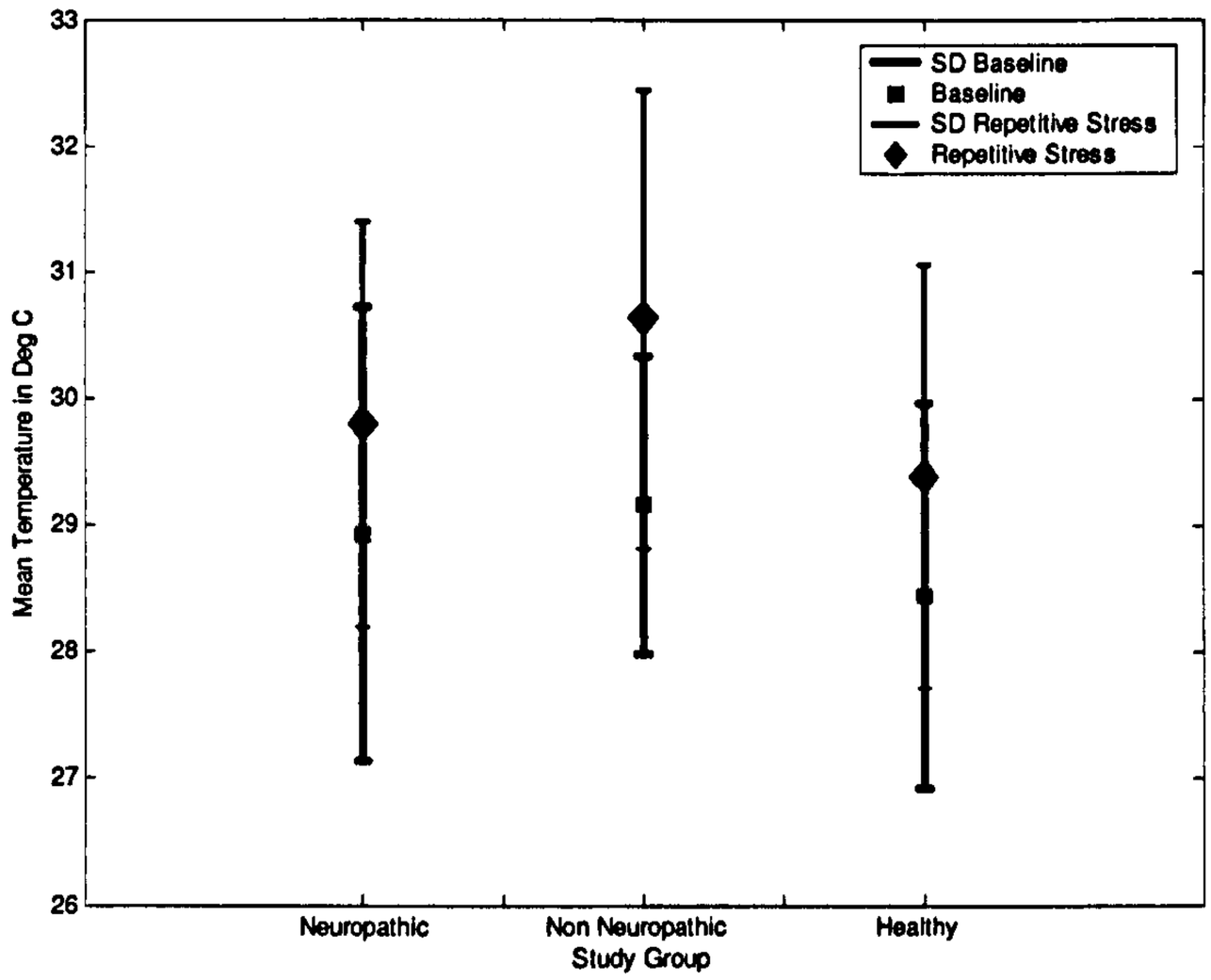


**Figure 5-18: Preclinical temperatures measured using digital thermometer, prior to the baseline and repetitive stress tests. The upper and lower limits of the error bars represent standard deviation in measured temperatures.**

Figure 5-18 represents the mean temperature for three study groups prior to the baseline and repetitive stress tests.

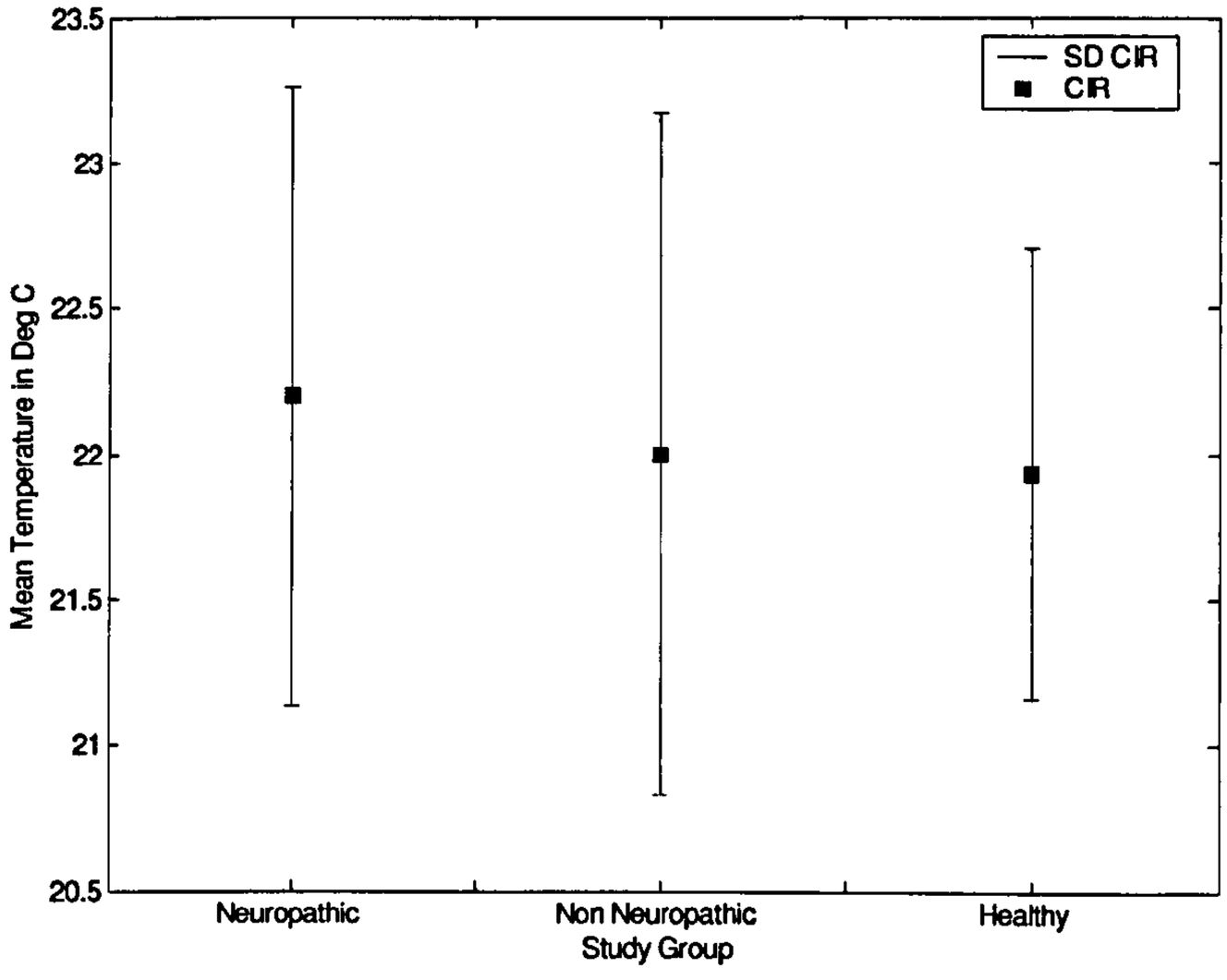


**Figure 5-19: Preclinical temperatures measured using digital thermometer, prior to the cold immersion recovery (CIR) test. The upper and lower limits of the error bars represent standard deviation (SD) in measured temperatures.**

Figure 5-19 represents the temperatures measured using digital thermometer after the 15 minutes resting period following the repetitive stress test and prior to the assessment of cold immersion recovery. The measurements were taken immediately after the foot was taken out from cold water (at 18-20°C) and dried thoroughly to prevent damage to the TLC sheet. All subjects had the foot cooled below the room temperature i.e. 24°C.

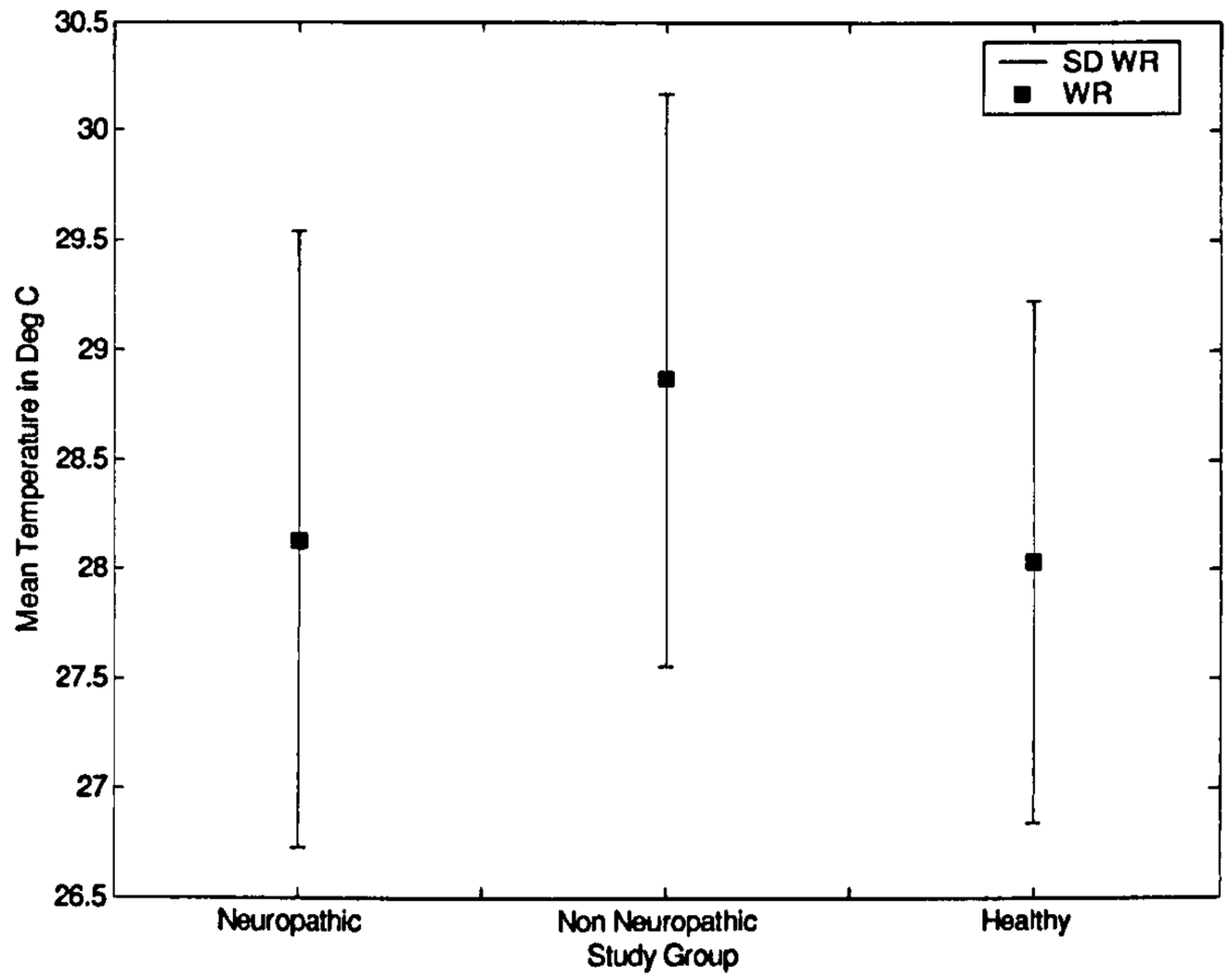


**Figure 5-20: Preclinical temperatures measured using digital thermometer, prior to the warm up recovery (WR) test. The upper and lower limits of the error bars represent standard deviation in measured temperatures.**

Figure 5-20 represents the temperatures measured using digital thermometer after the 15 minutes resting period following the cold immersion recover test and prior to the assessment of warm up recovery. The measurements were taken immediately after the foot was taken out from warm water (at 37°C) and dried thoroughly.

Table 5-6 and 5-7 list mean temperatures (measured using a digital thermometer) and standard deviations for all study groups, measured at the first metatarsal head and the heel. The magnitude of the increase is highest in the non neuropathic group. However, no statistical inference can be drawn for the following reasons, (a) limited number of samples in each group and (b) poor accuracy of the digital thermometer (±1.5 °C). These results are indicative and considered as a reference measurements in the subsequent discussion.

| Study Group | Baseline | Repetitive Stress | Cold Immersion Recovery | Warmup Recovery | Measurement Units |
|---|---|---|---|---|---|
| **Neuropathic** | 28.93 | 29.80 | 22.20 | 28.13 | Mean (°C) |
| | 1.80 | 1.61 | 1.06 | 1.41 | Standard Deviation |
| | | | | | |
| **Non Neuropathic** | 29.17 | 30.63 | 22.00 | 28.87 | Mean (°C) |
| | 1.18 | 1.81 | 1.17 | 1.31 | Standard Deviation |
| | | | | | |
| **Healthy** | 28.45 | 29.39 | 21.94 | 28.03 | Mean (°C) |
| | 1.52 | 1.67 | 0.77 | 1.20 | Standard Deviation |

**Table 5-6: Preclinical temperatures measured at the first metatarsal head using digital thermometer, prior to the clinical tests using LCT system. The mean temperatures in °C and standard deviation are shown for all study groups.**

| Study Group | Baseline | Repetitive Stress | Cold Immersion Recovery | Warm up Recovery | |
|---|---|---|---|---|---|
| **Neuropathic** | 28.87 | 29.63 | 22.17 | 27.80 | Mean (°C) |
| | 1.76 | 1.47 | 1.09 | 1.35 | Standard Deviation |
| | | | | | |
| **Non Neuropathic** | 29.10 | 30.50 | 22.10 | 28.60 | Mean (°C) |
| | 1.30 | 1.94 | 1.18 | 1.22 | Standard Deviation |
| | | | | | |
| **Healthy** | 28.26 | 29.35 | 21.77 | 27.90 | Mean (°C) |
| | 1.55 | 1.60 | 0.88 | 1.14 | Standard Deviation |

**Table 5-7: Preclinical temperatures measured at the heel using digital thermometer, prior to the clinical tests using LCT system. The mean temperatures in °C and standard deviation are shown for all study groups.**

For the thermal cycling tests, the measurements in the above tables suggest that the foot cools down successfully below the ambient temperature at 24°C following immersion in cold water. The detailed response measured using the LCT system is discussed in the following sections. The foot was immersed in warm water at 37°C for three minutes to evaluate its response following this induced thermal hyperaemia. Warming of the plantar tissue (to temperatures up to 44°C) is used as a vasodilatory stimuli for TcPO2 assessment (Gaylarde, Fonseca et al. 1988).

### 5.2.3 Results of baseline tests

The results for evaluation of baseline temperatures in all study groups are presented in this section. Following the preclinical tests to categorise patients as neuropathic or non-neuropathic, detailed verbal description of the test procedure was given to all subjects. Efforts were made to comfort the patient throughout testing procedures to minimise study time and any motion artefacts. Figures 5-21 to 5-23, show the mean baseline temperatures in °C at three regions of interest i.e. first metatarsal head, second metatarsal head and the heel respectively.

All measurements are shown for the complete five minutes of the baseline study. Figure 5-21 (b) illustrates the mean temperature and standard deviation under the first metatarsal head at the start and after five minutes of the baseline test for all study groups. This is the typical error bar representation and the quantitative values are presented in tables 5-10 to 5-12. The response of the diabetic groups is faster at all the regions and attains higher temperature at the end of five minutes. The response for the diabetic groups has similar start temperatures; however the non-neuropathic diabetic group exhibits a higher rate of increase post one minute leading to a maximum difference of 0.5 °C in final temperature at the first metatarsal head.

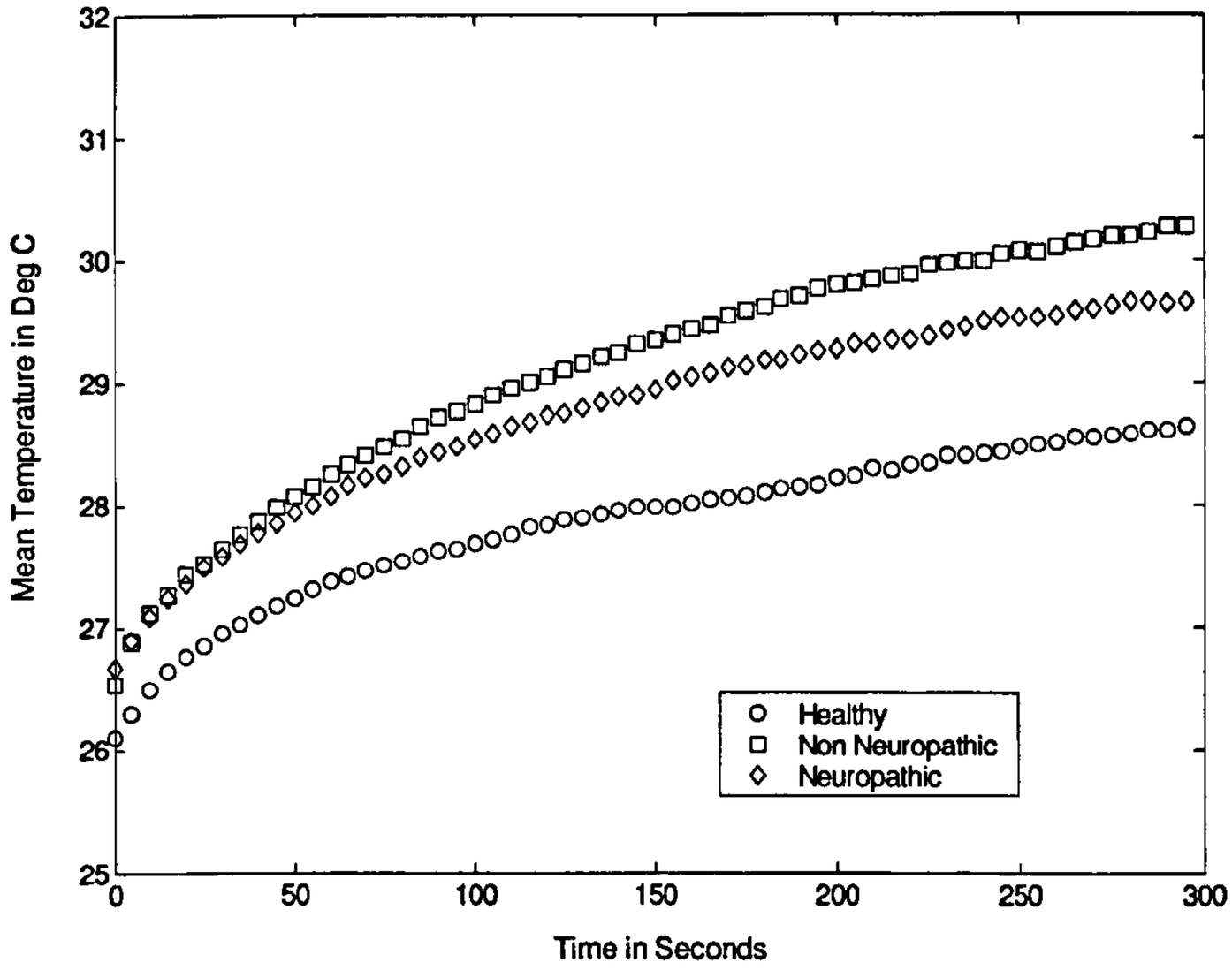


**(a)**

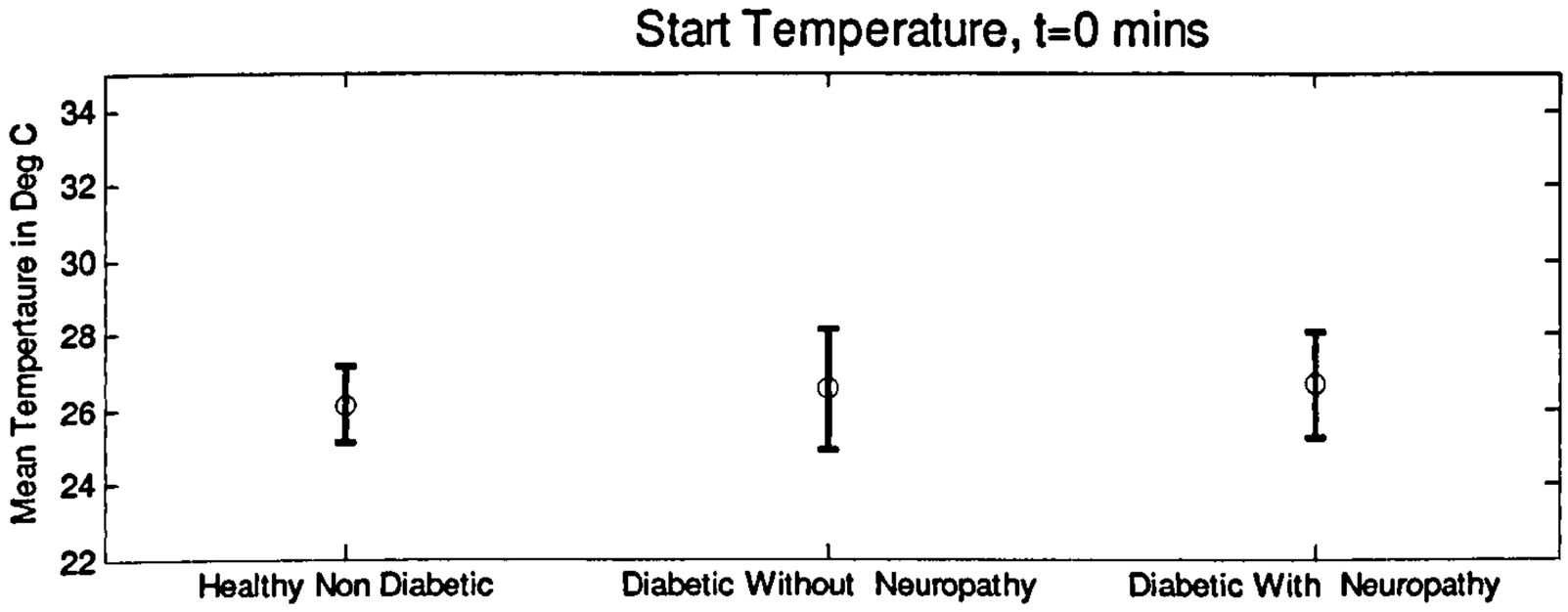


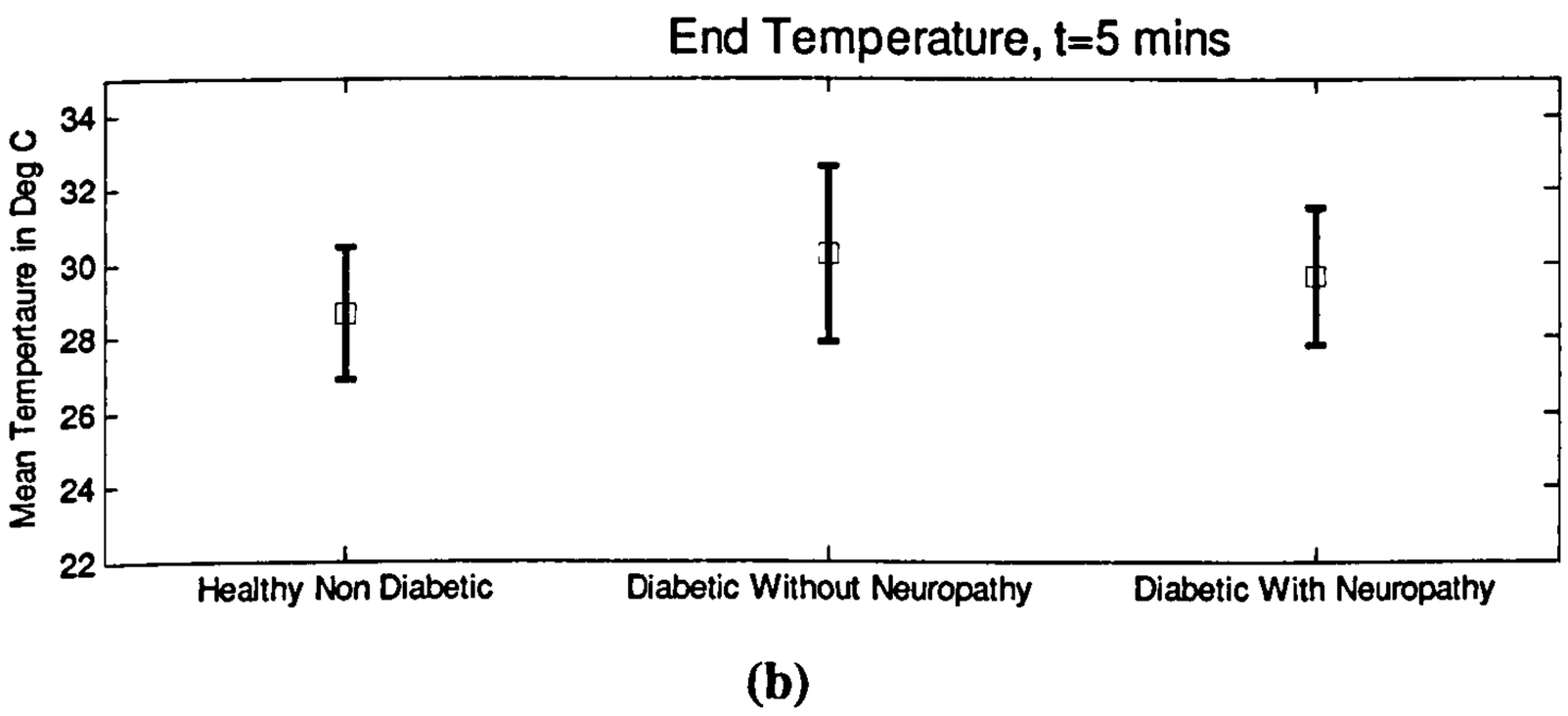


**(b)**

**Figure 5-21: (a) Baseline mean temperature (°C) under the first metatarsal head for all three study groups, healthy non-diabetics, diabetics with neuropathy and diabetics without neuropathy. (b) Error bar curve representing the mean tempertaure and standard deviation under the first metatarsal head for all three study groups at the start and after five minutes of baseline test.**

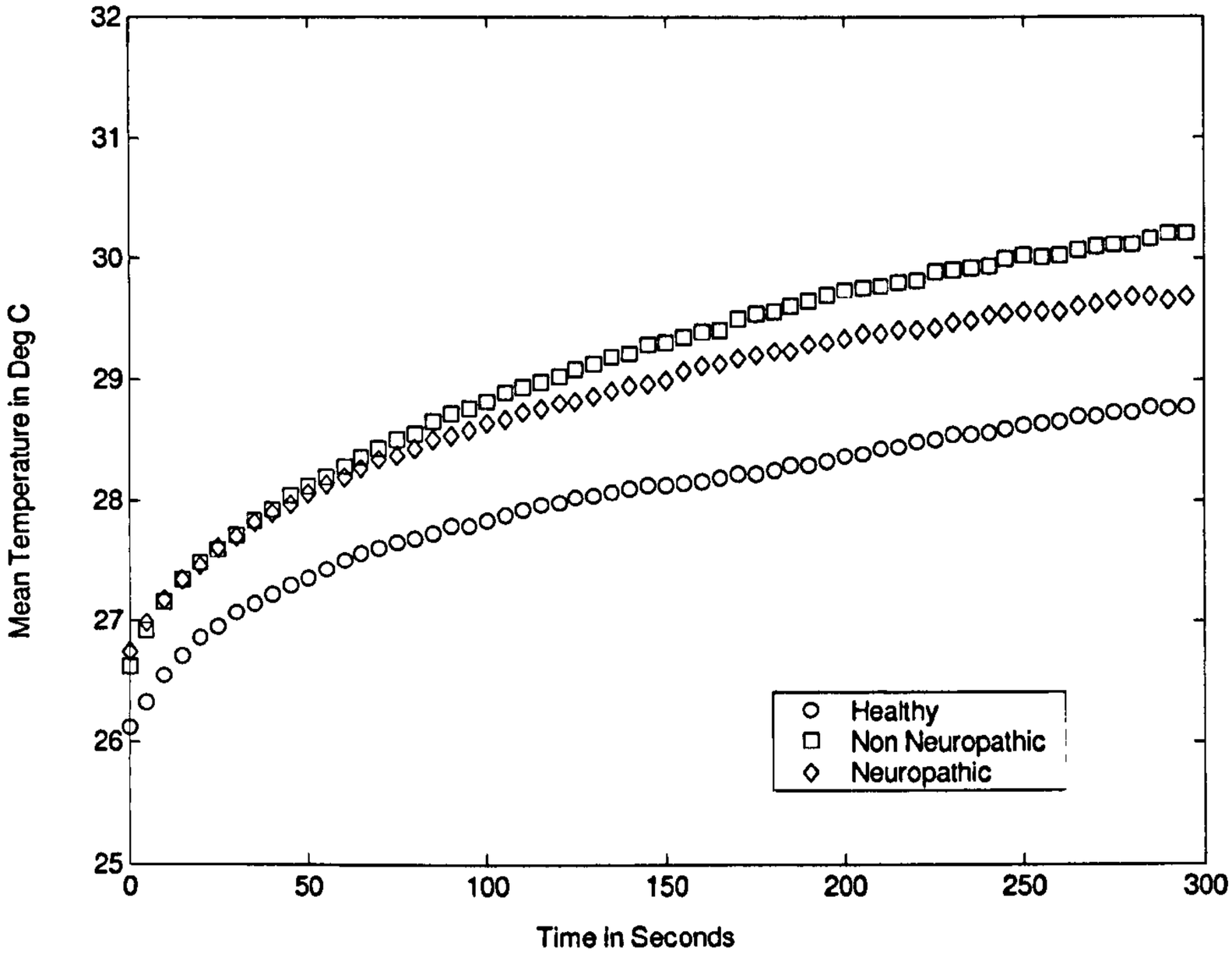


**Figure 5-22: Baseline mean temperature (°C) under the second metatarsal head for all three study groups, healthy non-diabetics, diabetics with neuropathy and diabetics without neuropathy.**

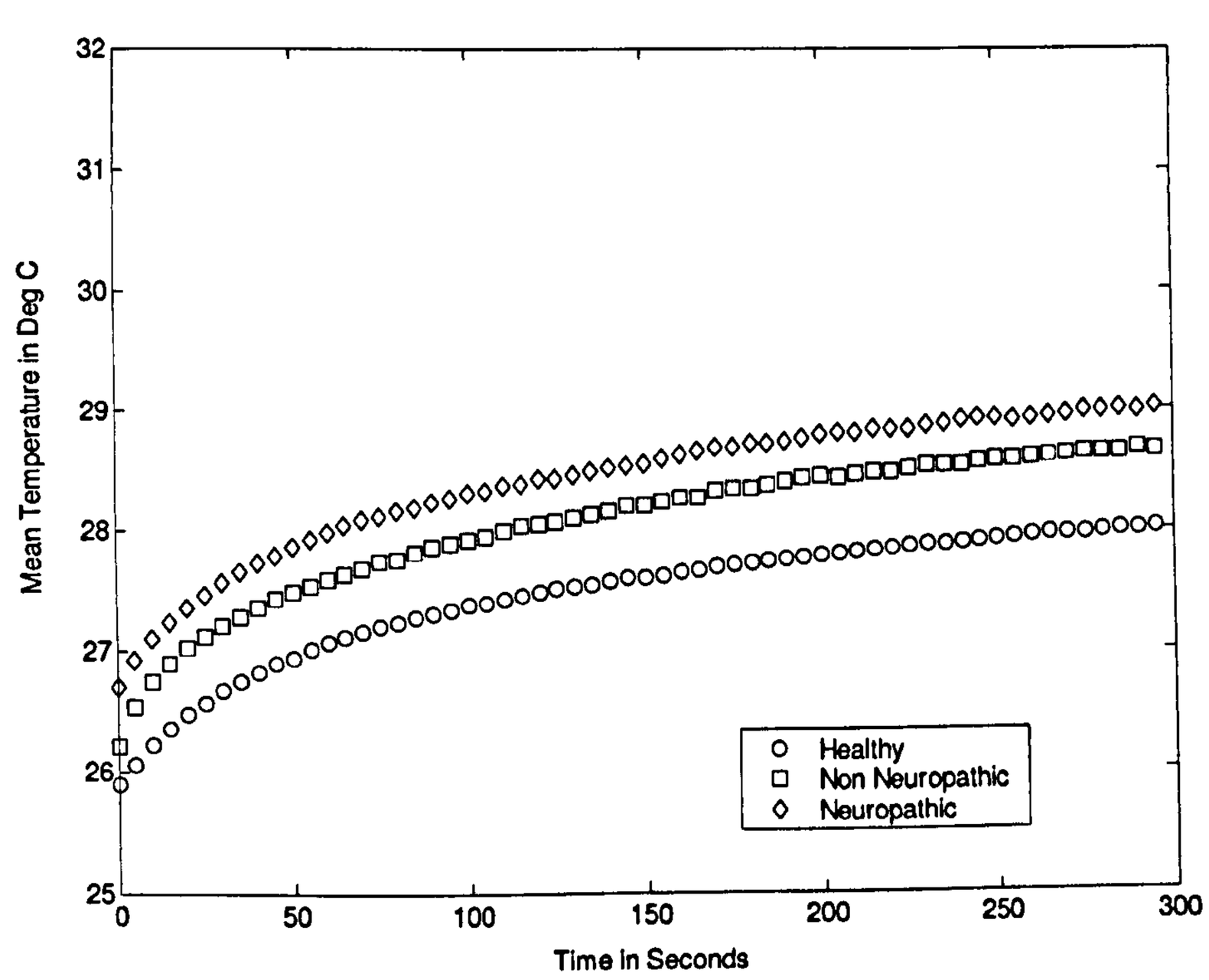


**Figure 5-23: Baseline mean temperature (°C) under the heel for all three study groups, healthy non-diabetics, diabetics with neuropathy and diabetics without neuropathy.**

Figures 5-24 to 5-26, illustrate the temperature and temporal information for all subjects in each study group with the mean temperature represented as a solid line through the data. All measurements in the figures are at the heel for the complete five minutes duration of baseline tests. Figure 5-27 illustrates the start and end temperatures for all subjects in each study group, represented in the form of histograms. The histograms clearly show that only 23% of the healthy non diabetics achieve the final temperature post five minutes above 30 °C, compared to 43% and 46% of diabetics without neuropathy and diabetics with neuropathy, respectively. The temperature threshold of 30°C used in analysis of current data, was based on values stated in published literature (Stess, Sisney et al. 1986; Benbow, Chan et al. 1994).

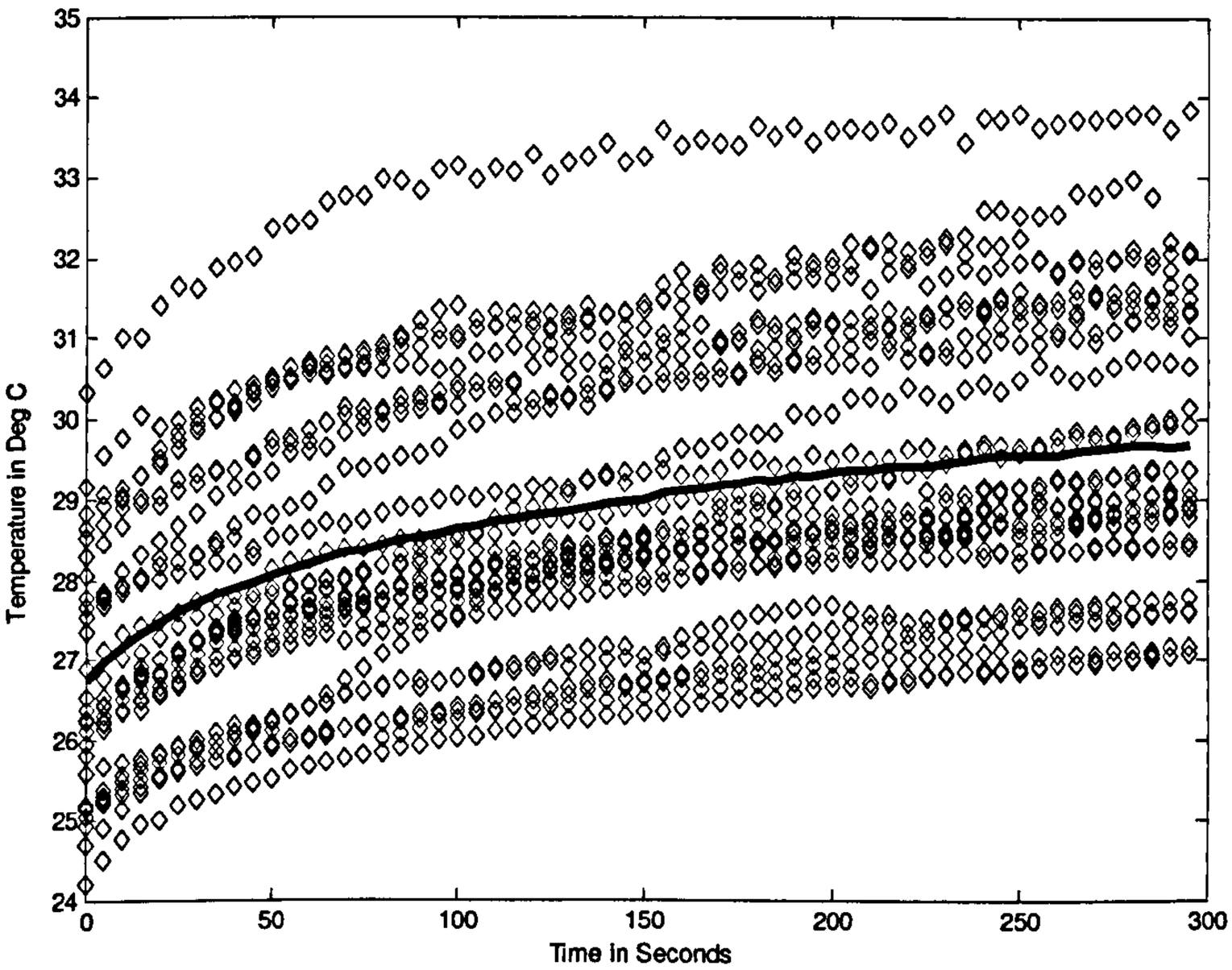


**Figure 5-24: Baseline temperature (°C) under the heel measured for five minutes for n=30 healthy non-diabetic subjects. The solid line represents the mean temperature for the group.**

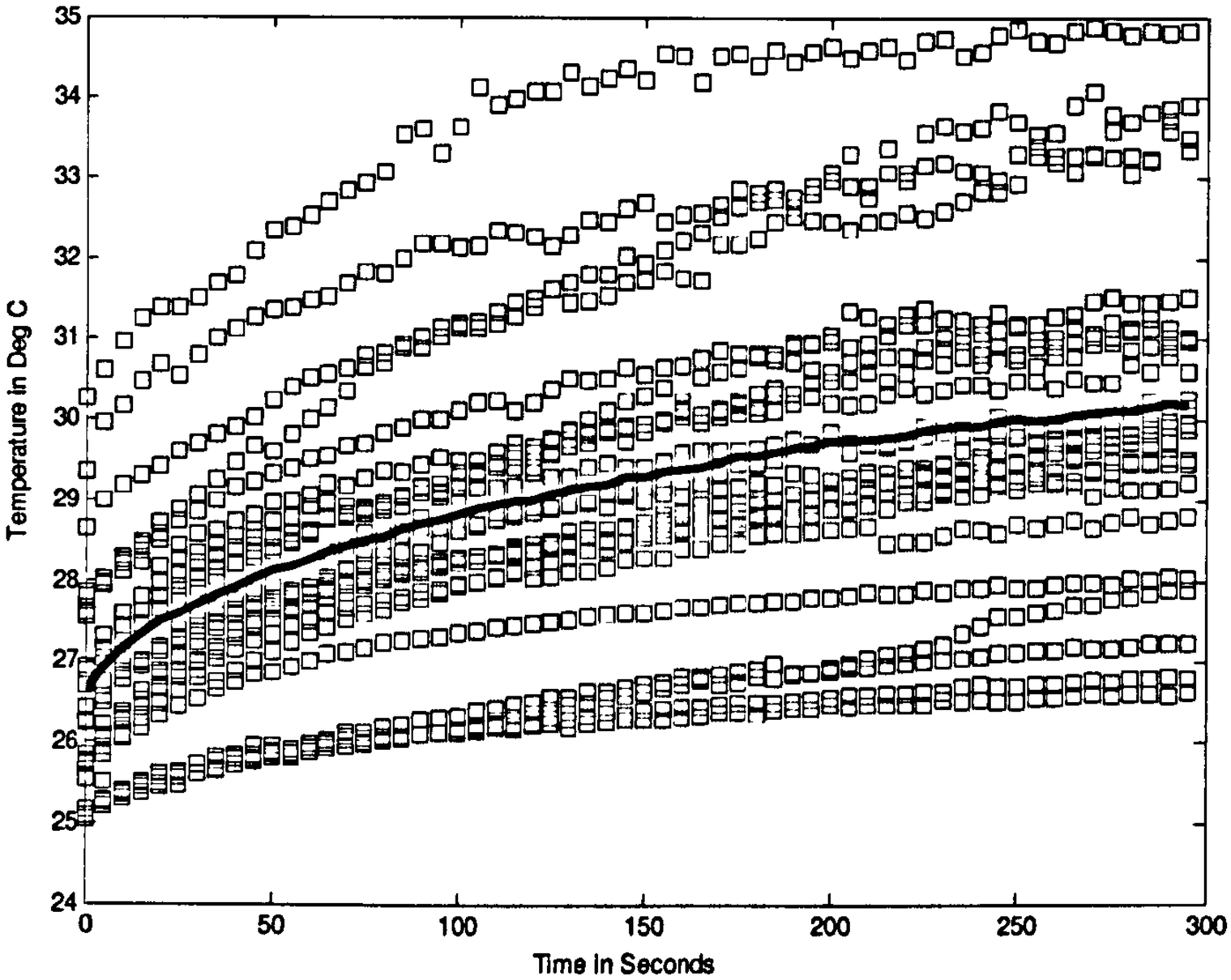


**Figure 5-25: Baseline temperature (°C) under the heel measured for five minutes for n=23 diabetics without neuropathy. The solid line represents the mean temperature for the group.**

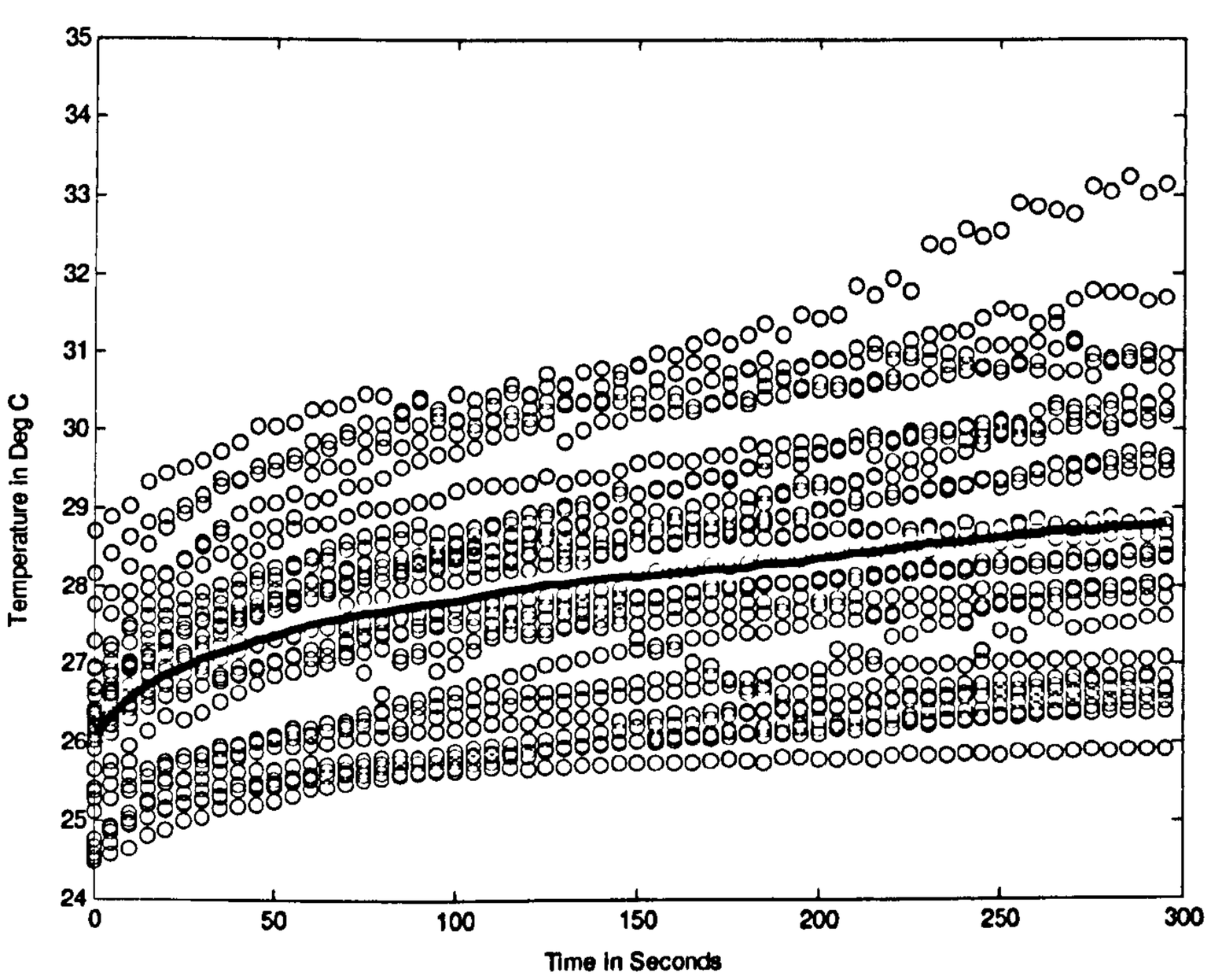


**Figure 5-26: Baseline temperature (°C) under the heel measured for five minutes for n=28 diabetics with neuropathy. The solid line represents the mean temperature for the group.**

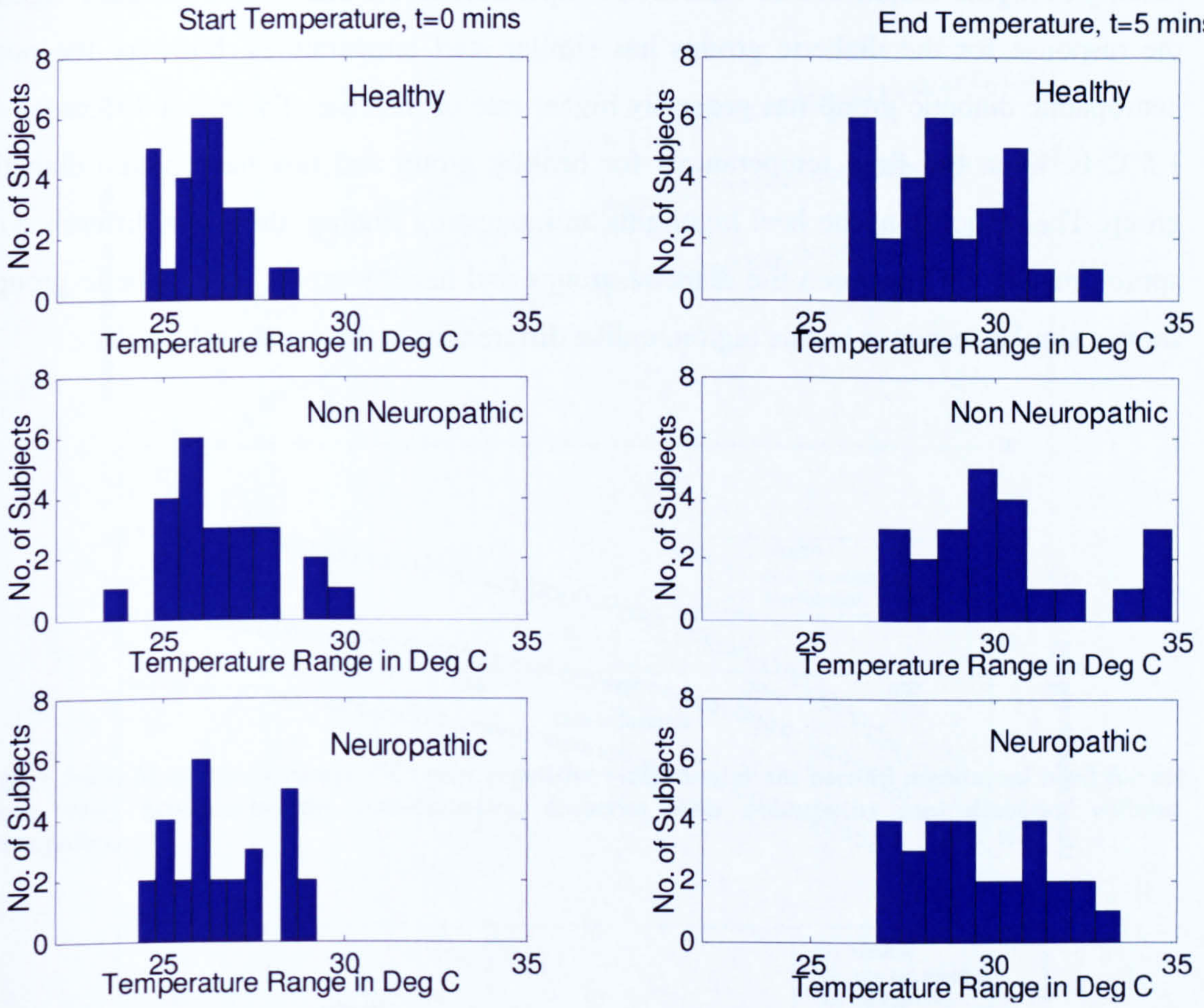


**Figure 5-27: Histogram representation of the start and end baseline temperatures for all study groups at the first metatarsal head. The graphs are indicative of percentage of people above a certain temperature threshold in all study groups.**

## 5.2.4 Results of repetetive stress tests

The results for evaluation of plantar temperatures post repetitive stress in all study groups are presented in this section. Figures 5-28 to 5-30, show the mean temperatures in °C at three regions of interest i.e. first metatarsal head, second metatarsal head and the heel respectively.

All measurements are shown for the complete five minutes of the repetitive stress study. The response of the diabetic groups is consistent with the pattern in baseline study,

leading to higher magnitude of measured temperature at the end of five minutes. Again, the response for the diabetic groups has similar start temperatures, however the non-neuropathic diabetic group has generally higher rate of increase. There is a difference of 1.5°C between the final temperatures for healthy group and non neuropathic diabetic group. The response at the heel highlights an interesting finding; there is a difference of approximately 1°C between the diabetic groups and healthy group. The diabetic groups show a similar response in this region, unlike differences in the metatarsal heads.

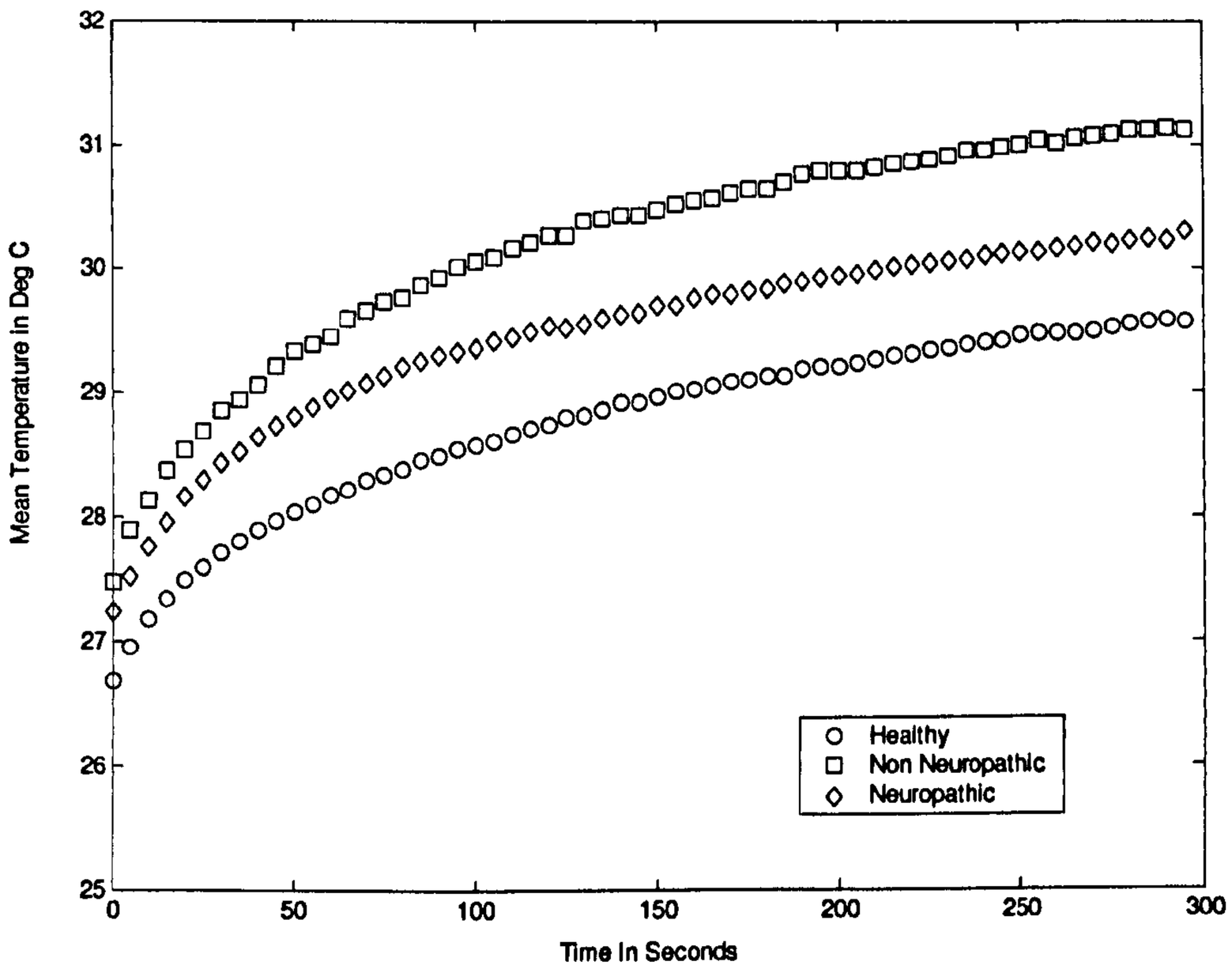


**Figure 5-28: Mean temperature (°C) post repetitive stress under the first metatarsal head for all three study groups, healthy non-diabetics, diabetics with neuropathy and diabetics without neuropathy.**

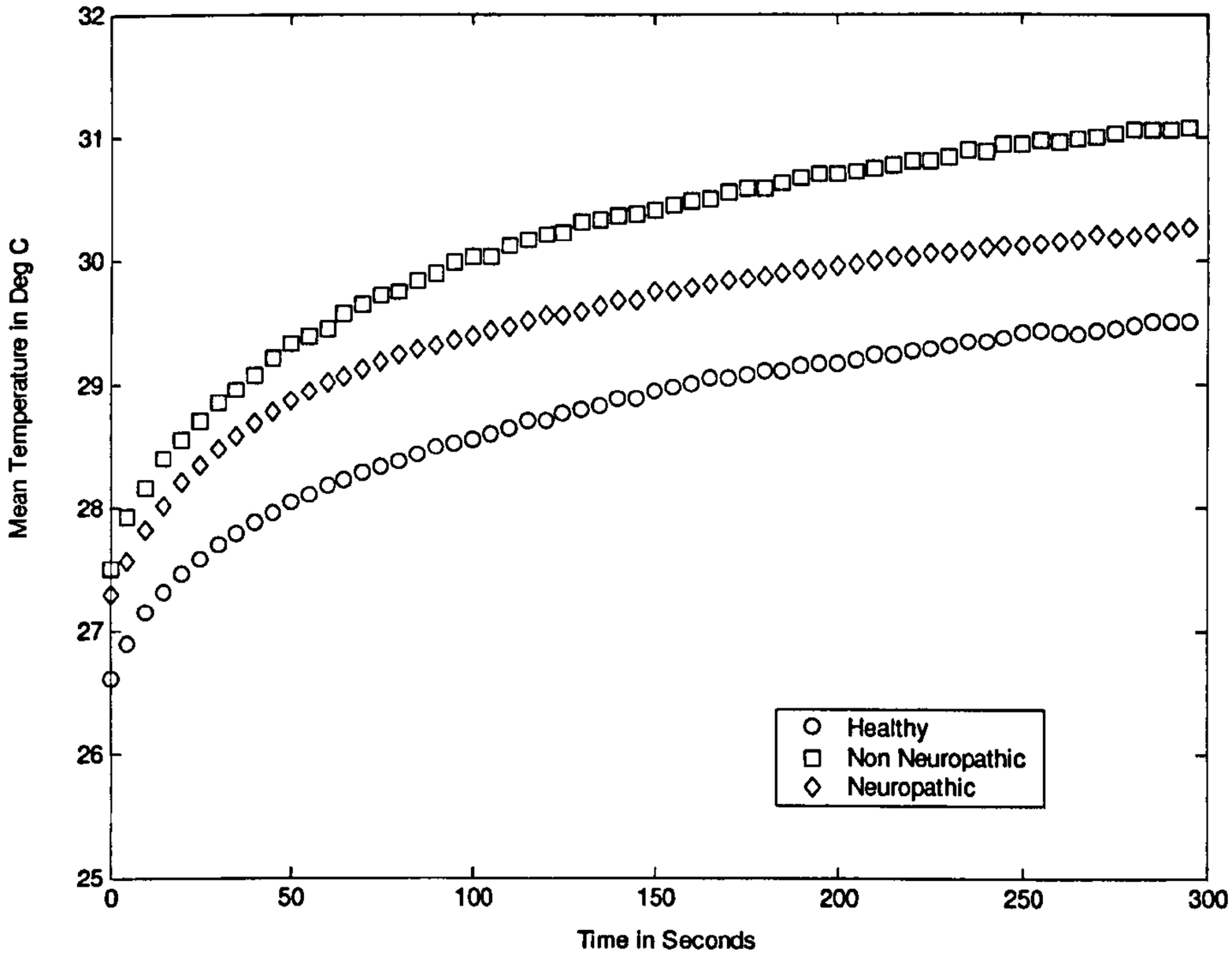


**Figure 5-29: Mean temperature (°C) post repetitive stress under the second metatarsal head for all three study groups, healthy non-diabetics, diabetics with neuropathy and diabetics without neuropathy.**

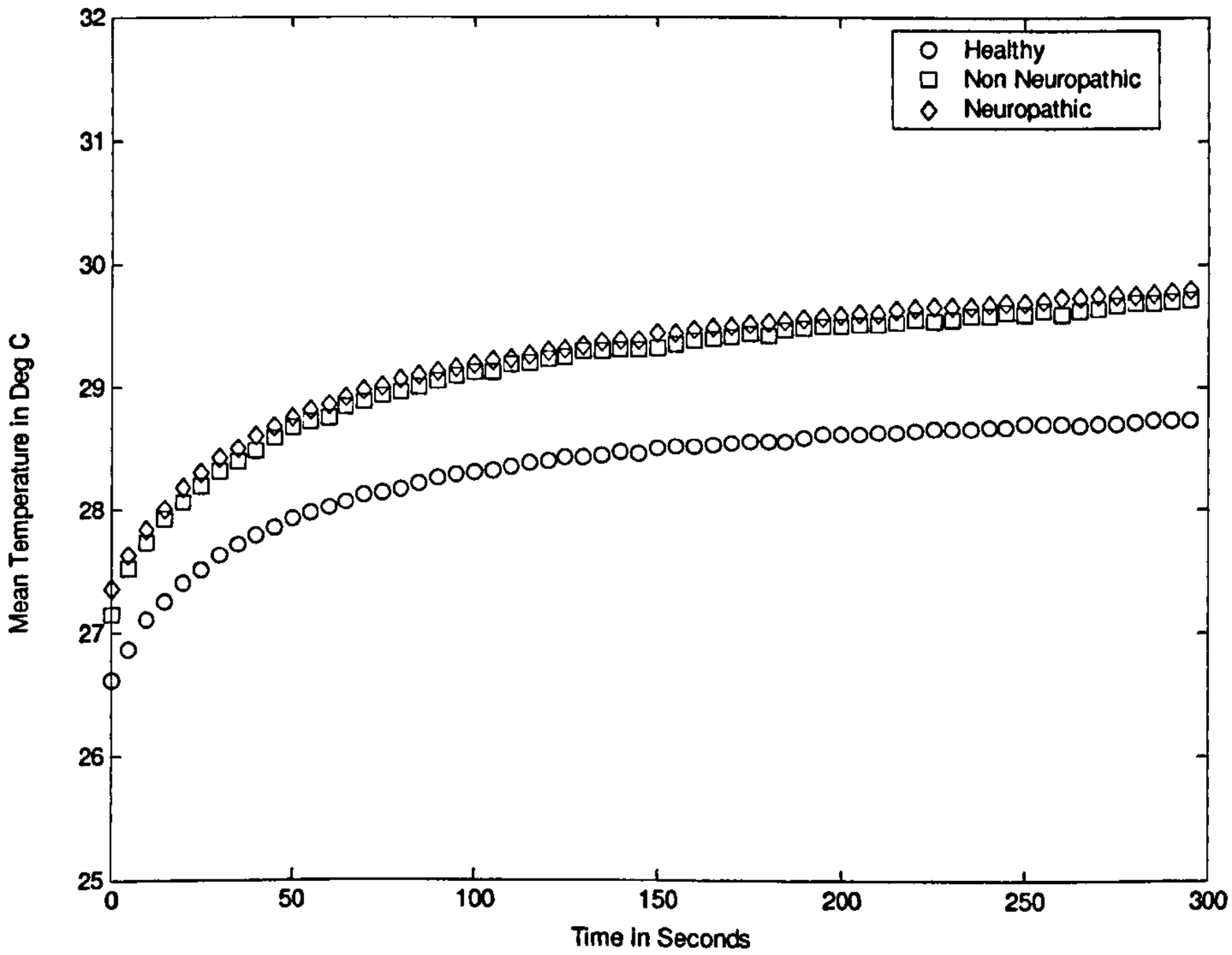


**Figure 5-30: Mean temperature (°C) post repetitive stress under the heel for all three study groups, healthy non-diabetics, diabetics with neuropathy and diabetics without neuropathy.**

The temperature and temporal information for all subjects in each study group is not illustrated in further analysis, as there is a similar distribution as shown in figures 5-24 to 5-26. The results for all clinical tests are summarised in tables 5-10 to 5-12 and discussed in terms of mean and standard deviation. Figure 5-31 illustrates the start and end temperatures for the repetitive stress test for all subjects in each study group, represented in the form of histograms. The histograms show that 30% of the healthy non diabetics have a final temperature post five minutes above 30 °C, compared to 65% and 54% of diabetics without neuropathy and diabetics with neuropathy. The highest increase in the percentage compared to baseline values is for the non neuropathic diabetic group, followed by the diabetic with neuropathy and healthy group. From a similar histogram analysis at the heel as shown in figure 5-32, only 17% of the healthy group have final temperatures greater than the set threshold, compared to 48% and 46% of the non neuropathic diabetic group and neuropathic diabetic group respectively.

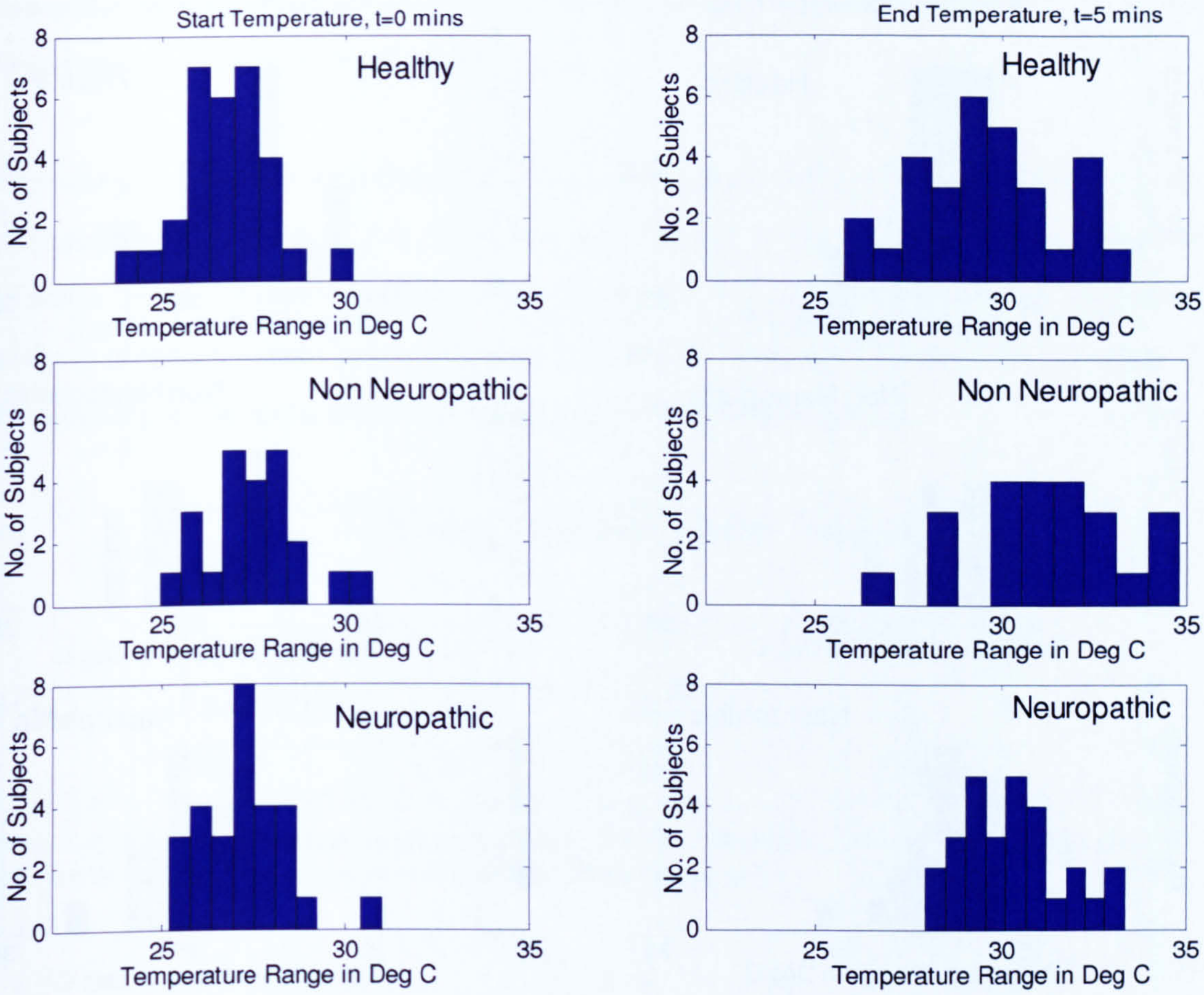


**Figure 5-31: Histogram representation of the start and end temperatures post repetitive stress for all study groups at the first metatarsal head. The graphs are indicative of percentage of people above the 30°C temperature threshold in all study groups.**

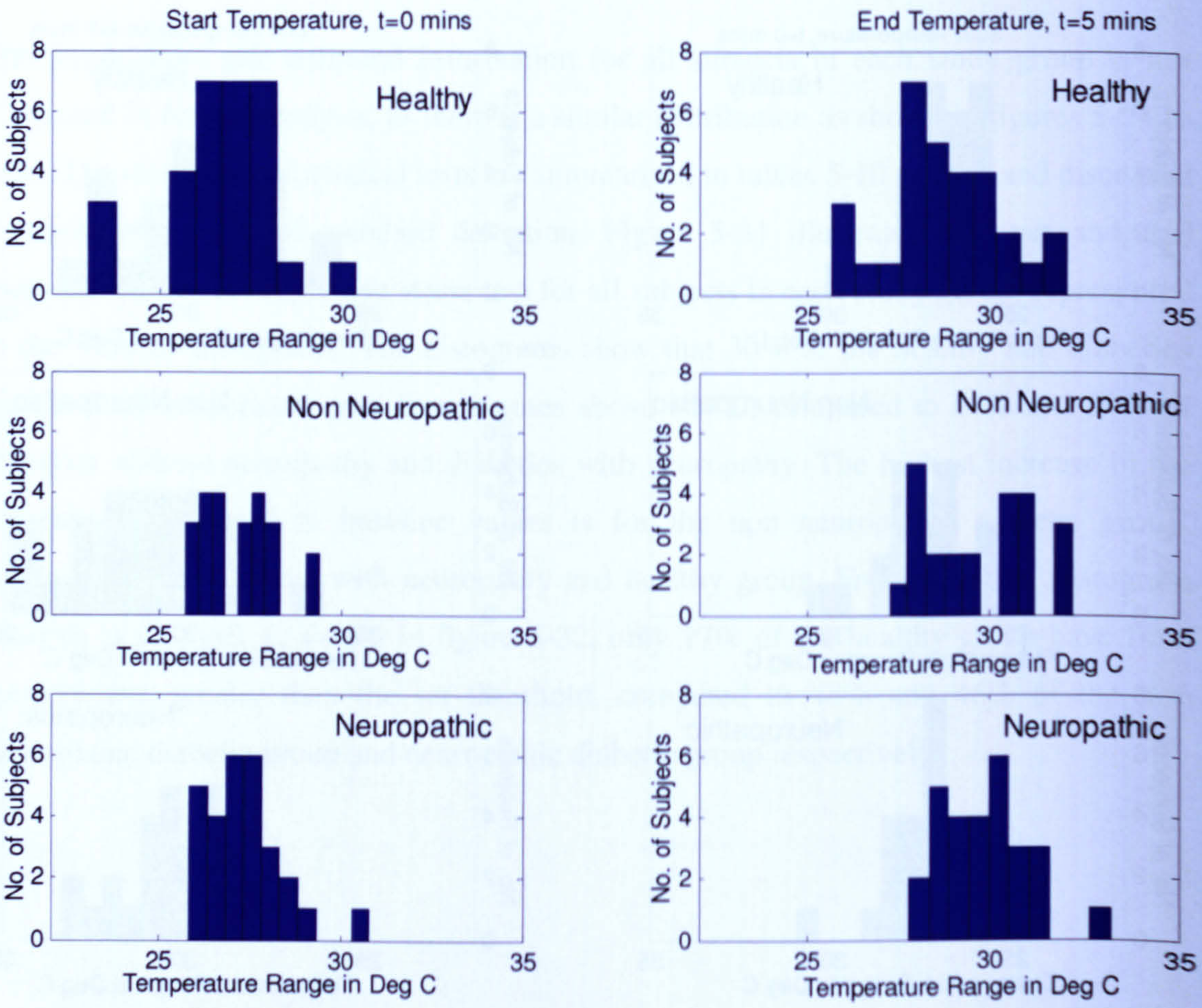


**Figure 5-32: Histogram representation of the start and end temperatures post repetitive stress for all study groups at heel.**

## 5.2.5 Results of thermal cycling

### *5.2.5.1 Cold immersion recovery*

The results for evaluation of plantar temperatures following cold immersion in all study groups are presented in this section. Figures 5-33 to 5-35, show the mean temperatures in °C at three regions of interest i.e. first metatarsal head, second metatarsal head and the heel respectively.

All measurements are shown for the complete 10 minutes of the cold immersion study. Table 5-8 lists the differences between final temperatures post 10 minutes during cold

immersion recovery test and final temperatures post five minutes of baseline tests, at the three regions of interest for all study groups.

Interestingly, diabetics with neuropathy show the highest differences at all the three sites, indicated in bold in table 5-8. This is a key clinical finding suggesting the impaired response of the thermoreceptors. This finding is further strengthened by qualitative analysis of the recovery curves in figures 5-33 and 5-34, which illustrate the saturation of the recovery at the metatarsal head region for the neuropathic group.

| | **Healthy** (°C) | **Non Neuropathic** (°C) | **Neuropathic** (°C) |
|---|---|---|---|
| **1st MTH** | 1.46 | 3.09 | **3.46** |
| **2nd MTH** | 2.44 | 2.29 | **3.01** |
| **Heel** | 2.29 | 2.55 | **2.82** |

**Table 5-8: Differences between mean temperature post 10 minutes for cold immersion recovery test and baseline temperatures post five minutes for all study groups.**

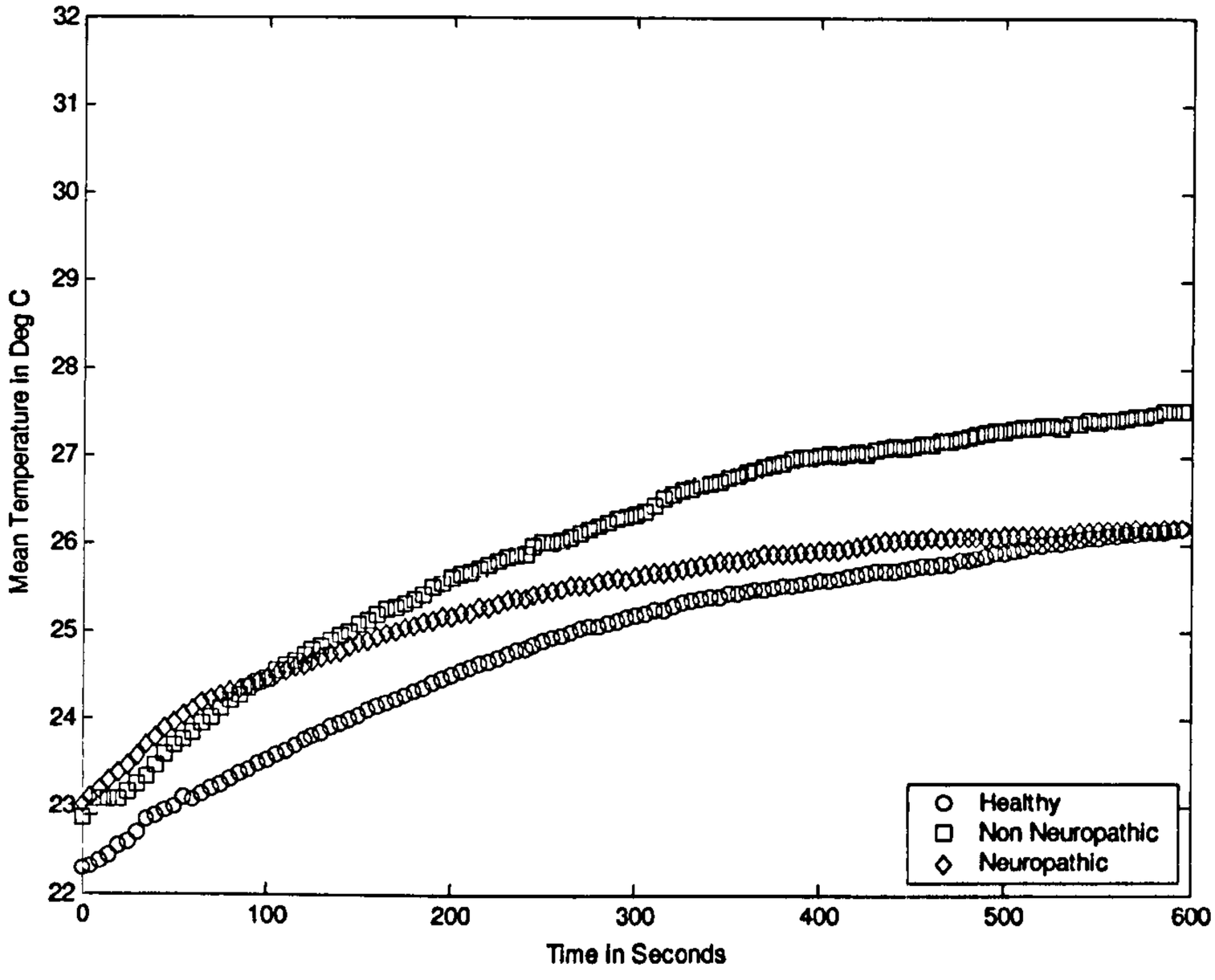


**Figure 5-33: Mean temperature (°C) following cold immersion under the first metatarsal head for all three study groups, healthy non-diabetics, diabetics with neuropathy and diabetics without neuropathy.**

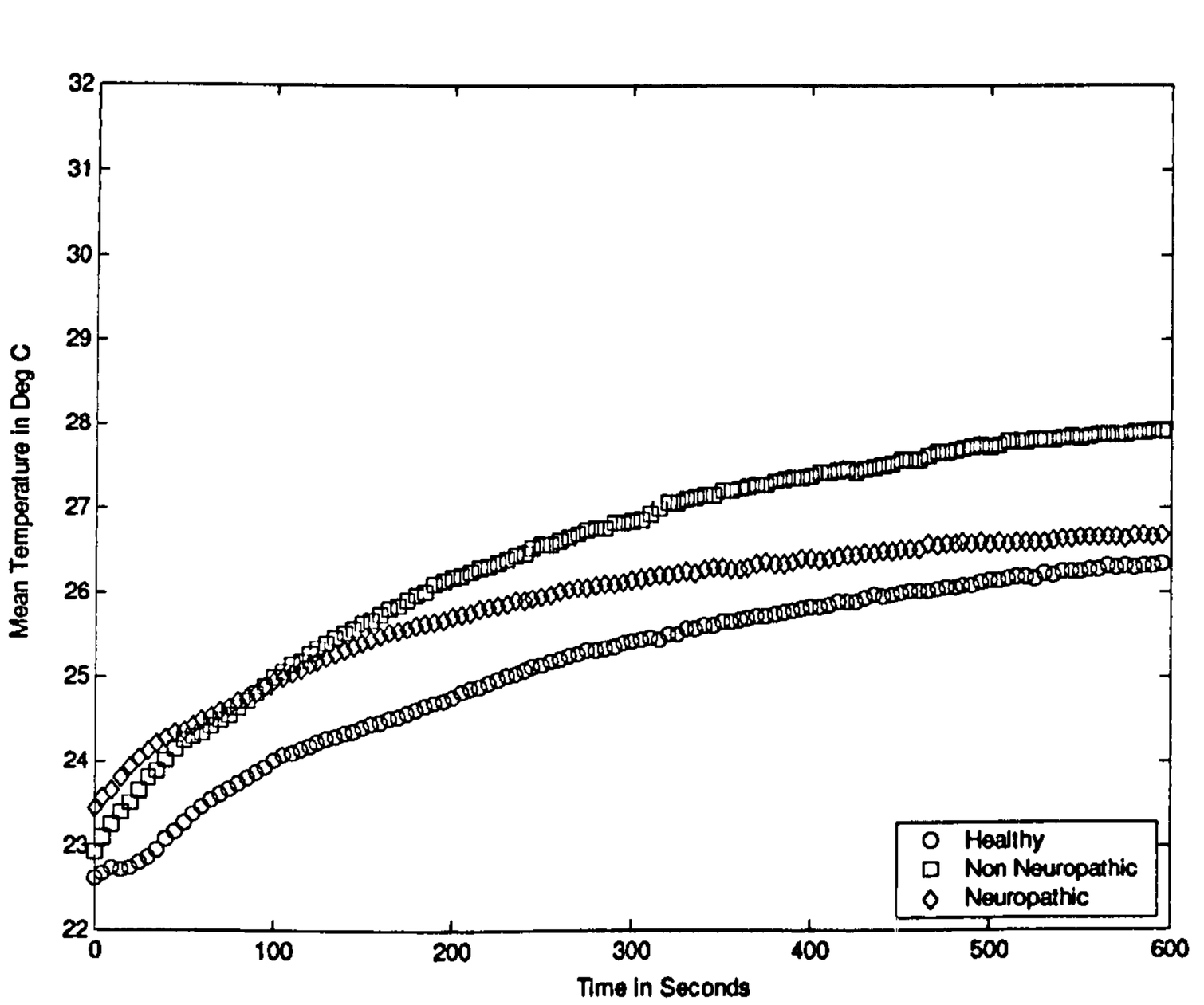


**Figure 5-34: Mean temperature (°C) following cold immersion under the second metatarsal head for all three study groups, healthy non-diabetics, diabetics with neuropathy and diabetics without neuropathy.**

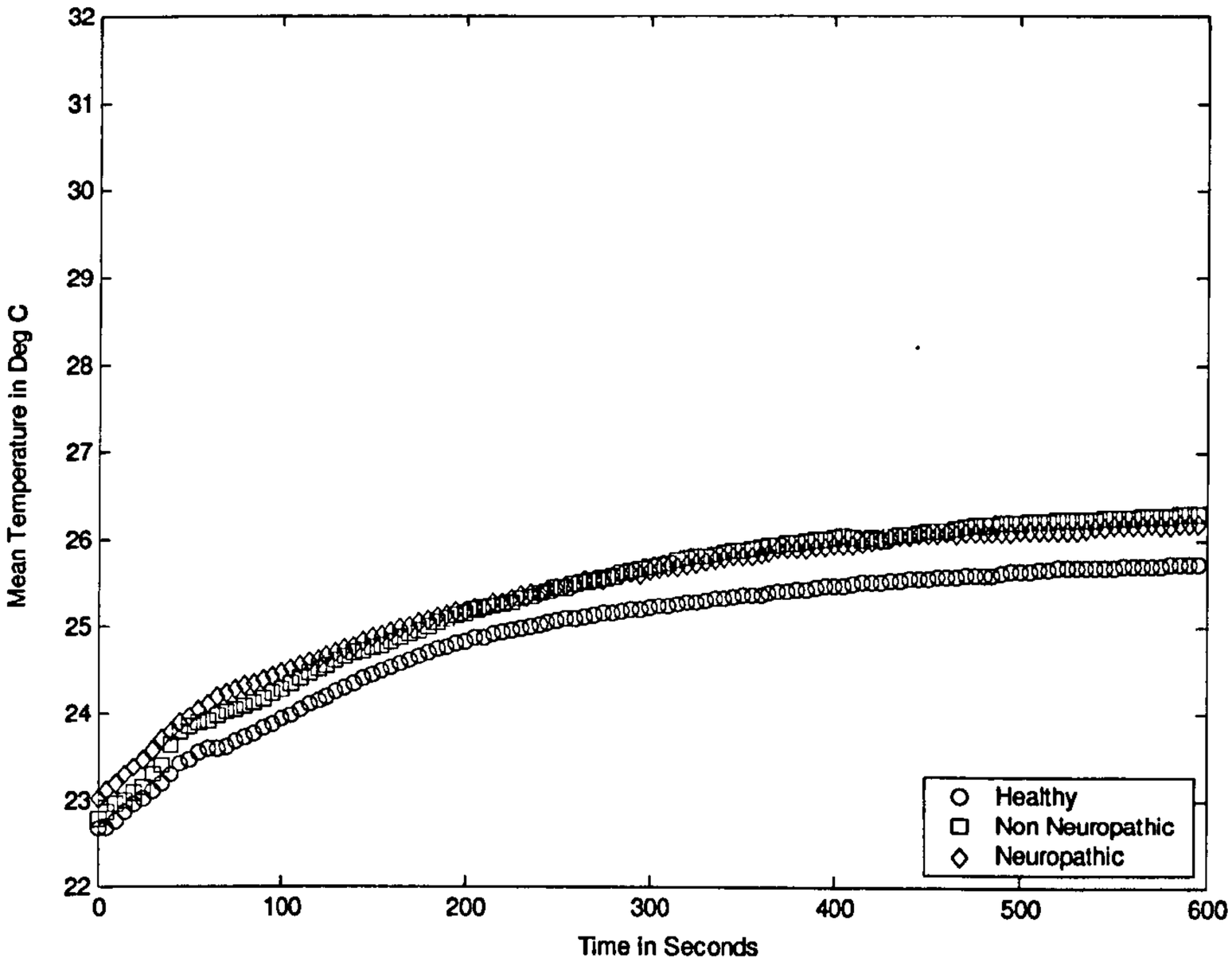


**Figure 5-35: Mean temperature (°C) following cold immersion under the heel for all three study groups, healthy non-diabetics, diabetics with neuropathy and diabetics without neuropathy.**

### *5.2.5.2 Warm up recovery*

The results for evaluation of plantar temperatures following warm water immersion in all study groups are presented in this section. Figures 5-36 to 5-38, show the mean temperatures in °C at three regions of interest i.e. first metatarsal head, second metatarsal head and the heel respectively.

All measurements are shown for the complete 10 minutes of the warm water immersion study. Table 5-9 lists the differences between final temperatures post 10 minutes during warm up recovery test and final temperatures post five minutes of baseline tests, at the three regions of interest for all study groups. Again, diabetics with neuropathy show the highest differences at all the three sites, indicated in bold in table 5-9.

| | Healthy (°C) | Non Neuropathic (°C) | Neuropathic (°C) |
|---|---|---|---|
| **1st MTH** | 0.37 | 0.22 | **1.29** |
| **2nd MTH** | 0.47 | 0.22 | **1.19** |
| **Heel** | 0.9 | 0.27 | **1.33** |

**Table 5-9: Differences between mean temperature post 10 minutes for warm up recovery test and baseline temperatures post five minutes for all study groups.**

Consider the histogram analysis at the first metatarsal head for all study groups as shown in figure 5-39. Approximately, 30% (n=7) of the non neuropathic diabetic subjects show the final recovery temperatures ranging from 32-35 °C.

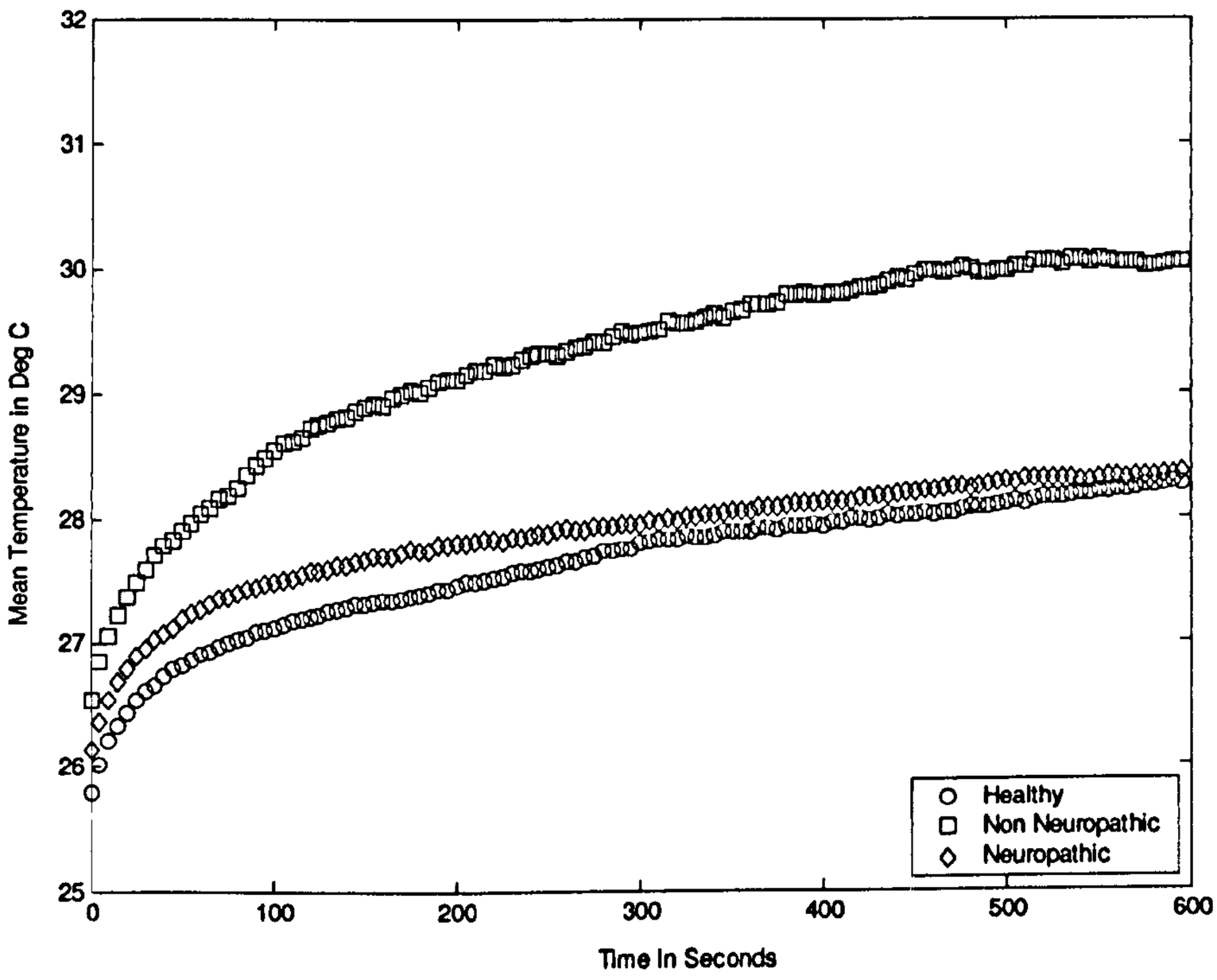


**Figure 5-36: Mean temperature (°C) following warm water immersion under the first metatarsal head for all three study groups, healthy non-diabetics, diabetics with neuropathy and diabetics without neuropathy.**

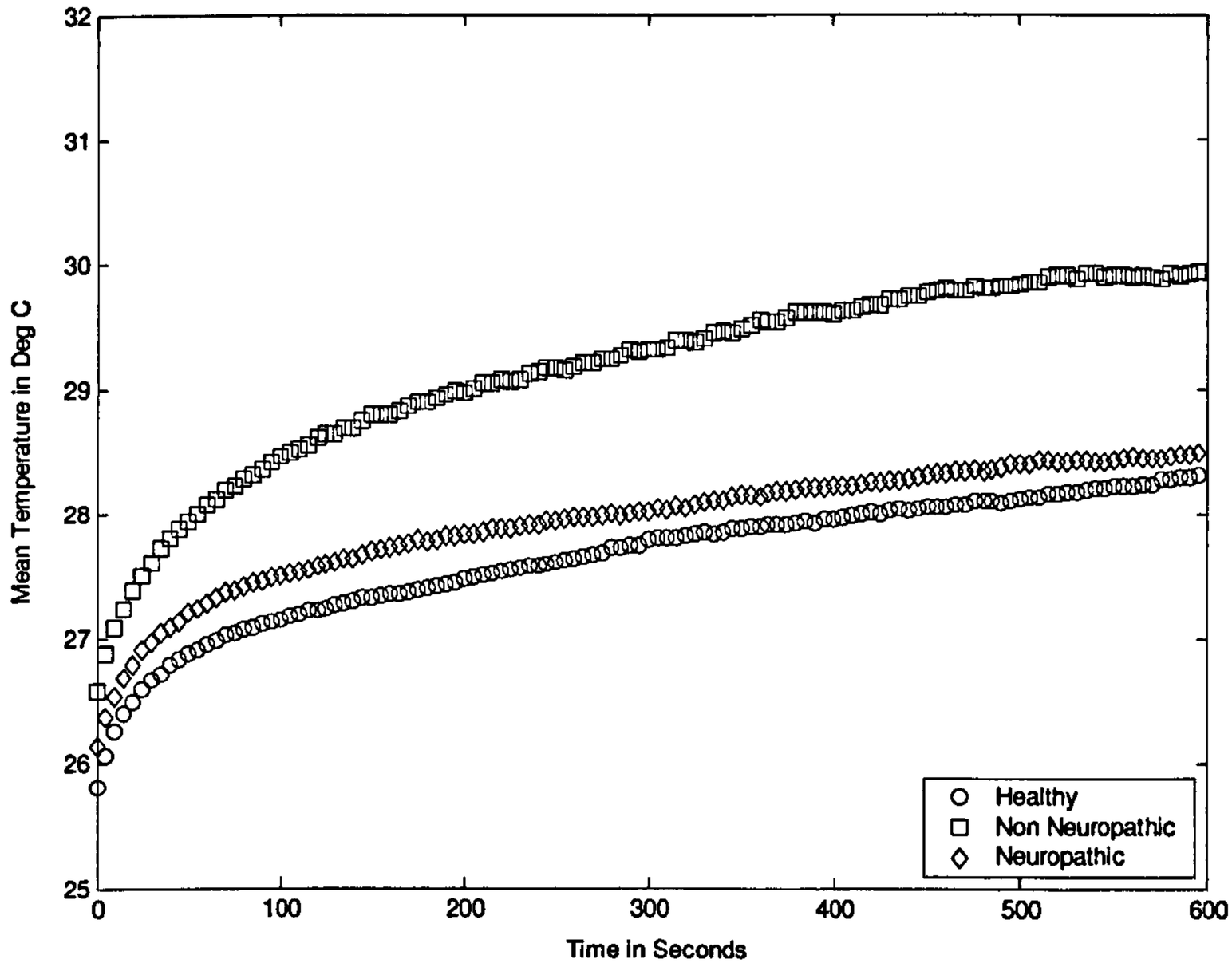


**Figure 5-37: Mean temperature (°C) following warm water immersion under the second metatarsal head for all three study groups, healthy non-diabetics, diabetics with neuropathy and diabetics without neuropathy.**

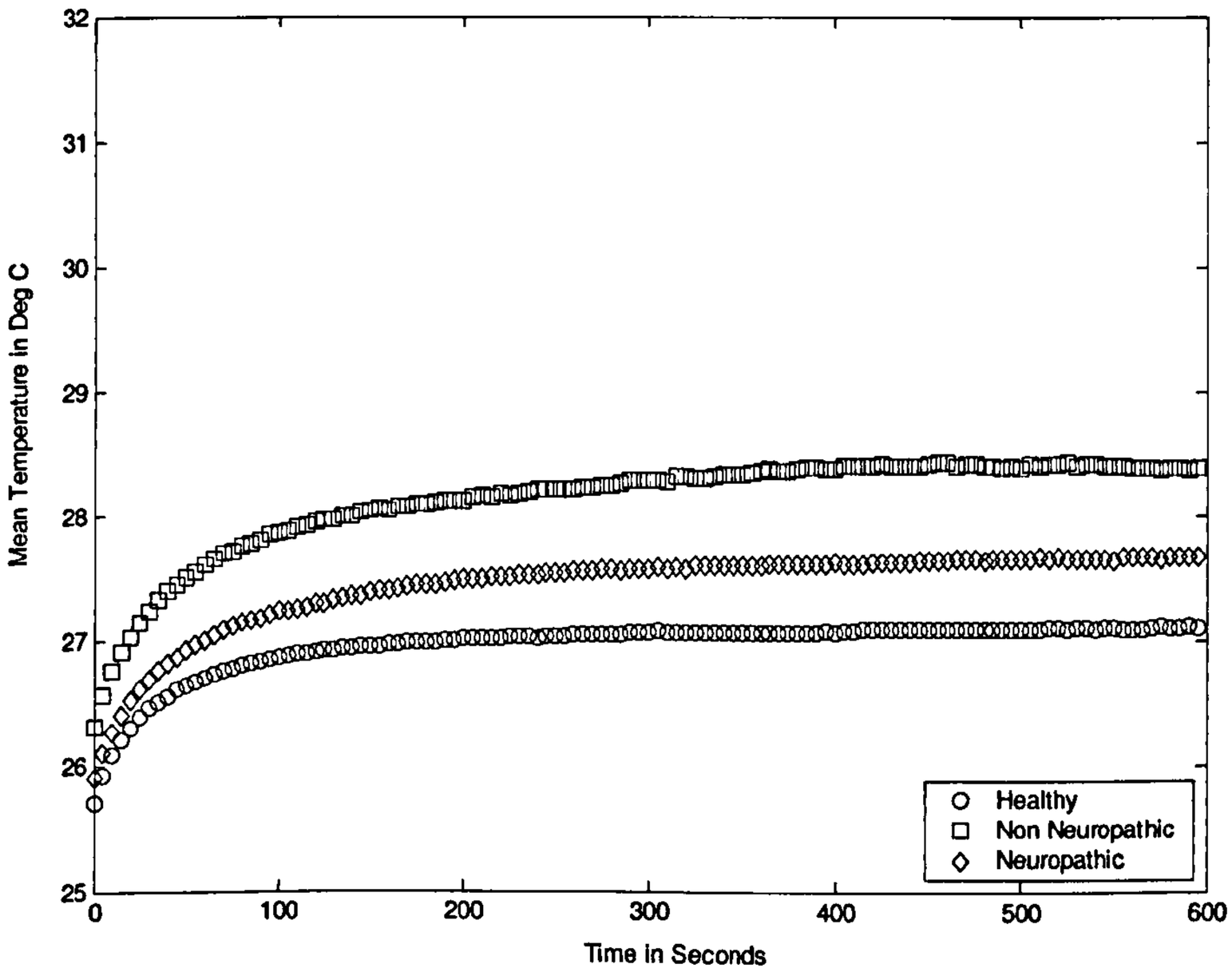


**Figure 5-38: Mean temperature (°C) following warm water immersion under the heel for all three study groups, healthy non-diabetics, diabetics with neuropathy and diabetics without neuropathy.**

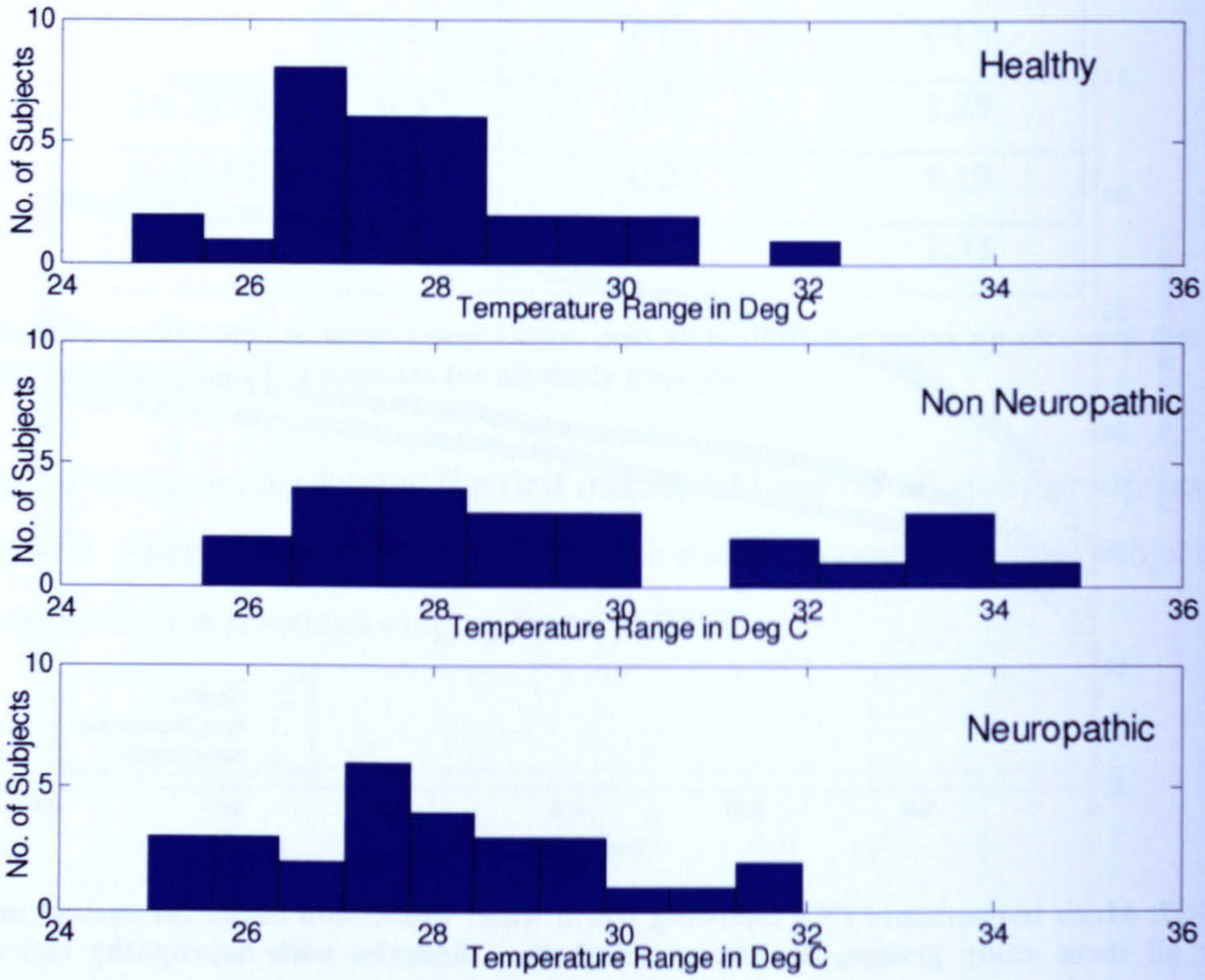


**Figure 5-39: Histogram representation of the final temperatures post ten minutes warm up recovery test for all study groups at first metatarsal head. The arrow indicates a band of subjects with highest recovery temperatures.**

## 5.2.6 General features of the results

The mean plantar temperatures under the effect of load for all study groups were well defined within the active range of the liquid crystal sensor. The temperature data was characterised by comparing the trends in mean temperatures, start temperatures (at time t=0 minutes) and final temperatures (at time t=5/10 minutes). Complete dataset for all study groups was analysed, according to the clinical protocol. Consistent data storage and image format helped accessibility and processing. Each stored data file represented a whole field image of the plantar foot. The extraction of hue plane and mapping of hue to temperature (at each pixel) was straightforward to code into the software. Tables 5-10, 5-11 and 5-12 summarise the mean temperatures at the start and end of each clinical test.

The data is listed for three regions of interests (right corner) in the form of mean and standard deviation for all study groups i.e. non diabetic healthy group (n=30), non neuropathic diabetic group (n=23) and neuropathic diabetic group (n=28).

| | Baseline | | Repetitive Stress | | Cold Immersion Recovery | | Warm up Recovery | | |
|---|---|---|---|---|---|---|---|---|---|
| Start | 26.11 | 1.02 | 26.69 | 1.26 | 22.29 | 0.47 | 25.80 | 0.98 | 1st MTH |
| End | 28.64 | 1.77 | 29.57 | 1.92 | 26.18 | 2.20 | 28.27 | 1.83 | |
| | | | | | | | | | |
| Start | 26.12 | 1.05 | 26.62 | 1.27 | 22.61 | 0.83 | 25.82 | 0.96 | 2nd MTH |
| End | 28.78 | 1.80 | 29.50 | 1.99 | 26.34 | 2.00 | 28.31 | 1.82 | |
| | | | | | | | | | |
| Start | 25.90 | 1.27 | 26.62 | 1.49 | 22.66 | 0.84 | 25.71 | 1.02 | Heel |
| End | 28.01 | 1.39 | 28.73 | 1.66 | 25.72 | 1.40 | 27.11 | 1.46 | |
| | | | | | | | | | |
| | Mean Temperature | Standard Deviation | Mean Temperature | Standard Deviation | Mean Temperature | Standard Deviation | Mean Temperature | Standard Deviation | |

**Table 5-10: Summary of the mean temperature measurement at three regions of interest for the non diabetic healthy group. The start and end temperatures for all four clinical tests are listed.**

| | Baseline | | Repetitive Stress | | Cold Immersion Recovery | | Warm up Recovery | | |
|---|---|---|---|---|---|---|---|---|---|
| Start | 26.54 | 1.60 | 27.47 | 1.32 | 22.87 | 1.10 | 26.55 | 1.15 | 1st MTH |
| End | 30.26 | 2.36 | 31.12 | 2.17 | 27.17 | 3.38 | 30.04 | 2.93 | |
| | | | | | | | | | |
| Start | 26.63 | 1.44 | 27.50 | 1.35 | 22.924 | 0.93854 | 26.59 | 1.10 | 2nd MTH |
| End | 30.20 | 2.21 | 31.08 | 2.10 | 27.91 | 3.06 | 29.93 | 2.64 | |
| | | | | | | | | | |
| Start | 26.21 | 1.48 | 27.16 | 1.04 | 22.78 | 0.87 | 26.32 | 0.83 | Heel |
| End | 28.66 | 1.73 | 29.71 | 1.49 | 26.11 | 1.48 | 28.39 | 1.85 | |
| | | | | | | | | | |
| | Mean Temperature | Standard Deviation | Mean Temperature | Standard Deviation | Mean Temperature | Standard Deviation | Mean Temperature | Standard Deviation | |

**Table 5-11: Summary of the mean temperature measurement at three regions of interest for the non neuropathic diabetic group. The start and end temperatures for all four clinical tests are listed.**

| | Baseline | | Repetitive Stress | | Cold Immersion Recovery | | Warm up Recovery | | |
|---|---|---|---|---|---|---|---|---|---|
| Start | 26.67 | 1.41 | 27.25 | 1.22 | 23.01 | 1.01 | 26.14 | 1.28 | 1st MTH |
| End | 29.65 | 1.84 | 30.29 | 1.42 | 26.19 | 1.40 | 28.36 | 1.93 | |
| | | | | | | | | | |
| Start | 26.75 | 1.54 | 27.30 | 1.26 | 23.43 | 1.13 | 26.15 | 1.31 | 2nd MTH |
| End | 29.68 | 1.82 | 30.27 | 1.31 | 26.67 | 1.40 | 28.49 | 1.97 | |
| | | | | | | | | | |
| Start | 26.71 | 1.23 | 27.36 | 1.08 | 23.01 | 1.01 | 25.92 | 0.99 | Heel |
| End | 29.01 | 1.43 | 29.79 | 1.24 | 26.19 | 1.40 | 27.68 | 1.21 | |
| | | | | | | | | | |
| | Mean Temperature | Standard Deviation | Mean Temperature | Standard Deviation | Mean Temperature | Standard Deviation | Mean Temperature | Standard Deviation | |

**Table 5-12: Summary of the mean temperature measurement at three regions of interest for the neuropathic diabetic group. The start and end temperatures for all four clinical tests are listed.**

Mean temperatures are comparable at the first and second metatarsal heads for the study groups and non neuropathic diabetic group shows the highest temperature followed by the neuropathic group.

The results of this study allowed an evaluation of temperature measurements under tissue loading using a low cost LCT system and rigorous clinical protocol. By restricting the regions of interest to three, it was possible to obtain detailed analysis of the dataset in each group with the intent of identifying useful parameters to assess the neuropathic diabetic foot.

## *5.3 Summary*

All three physical forms of commercially available TLC were evaluated for the intended application and TLC sheets were found to be most appropriate based on the characterisation tests. TLC sheets have shown to be repeatable, easily calibrated, pressure insensitive and free from hysteresis effects for desired temperature range.

Results for pressure sensitivity show that TLC sheets are insensitive to vertical pressure in the range of loads tested i.e. 0-70KPa. Current literature suggests that the pressure range for stance and walking are 0-200 KPa and 0-1000 KPa. Extreme pressures may lie

in the range of 2000-3000 KPa. TLC on latex support was found to be pressure sensitive. Due to the nature of the latex, upon flexing it results in uncertainties in measured hue values. This may be the reason for its limited temperature resolution.

In vivo calibration of the TLC sheet used in the LCT system has been identified as the best approach for assessing the plantar foot temperatures. A well studied and validated calibration technique was employed for calibration of the TLC sheet used for the LCT system. Independent assessment of LCT pressure sensitivity proved that the TLC polyester sheets are insensitive to vertical loading within the physiological range of interest. Therefore, the measured response is only indicative of the changes in skin surface temperature in contact with the sensor.

A consistent clinical protocol and pre-clinical tests were used for the present study approved by the clinician and foot care team. The protocol was approved by the local ethical committee. This protocol includes four clinical tests i.e. baseline evaluation, repetitive stress evaluation, cold immersion recovery and warm up recovery.

All the measurements are useful in assessing the neuropathic diabetic foot. Given the current findings, the LCT system appears to be capable of assessing plantar foot temperatures under loading. Further clinical data is required to investigate some of the questions raised regarding the physiological factors for the findings and identify if these findings will be of clinical use in furthering the role of thermal measurements in assessing the diabetic foot.

# Chapter 6 Discussion

## *6.0 Introduction*

This chapter considers the implications of the methodology adopted for the current study and focuses on discussion of results of the clinical study based on the physical and physiological issues, including current knowledge of the diabetic foot.

## *6.1 In vitro characterisation*

The simple calibration uses hue as a parameter, monotonically increasing with temperature. When the RGB data is converted into HSV, only the hue component is included for further processing in the calibration approach adopted. Ideally, choosing other available hue models such as HSI (hue, saturation and intensity) and HLS (hue, lumination and saturation) will not affect the calibration. As the image processing was done using MATLAB, an HSV model was employed due to ease of use. The light source used was placed at an angle of 15-20 degree with the axis of the camera. This angle/placement of the light source was maintained constant for all the tests. There was no distortion observed at this angle. In the context of the clinical study, this is not directly relevant as a different arrangement for illumination and camera was used in the LCT system.

The in vitro characterisation tests were performed with the intention of justifying the use of a specific TLC material for the liquid crystal thermography system. However, the results presented may also be useful for developing LCT for other biomedical applications such as orthopaedic assessment, Raynaud's syndrome and Hansen's disease (leprosy). TLC sheets offer higher stability and better colour response than the other two formulations. Characterisation of commonly available TLC material demonstrates that TLC sheets have a monotonically increasing response of hue across the physiological range of plantar foot temperatures, as intended for the clinical LCT system. The wideband TLC sheets (R25C10W and R25C15W) are discounted for use in a clinical

system as they have a larger colour bandwidth near the event temperature which must be eliminated before a polynomial fit is successful. This approach limits the temperature range which can be used for the intended application. However, initial tests using an alternative calibration approach based upon neural networks appears to offer a solution to this problem although a more comprehensive study is required to confirm this. Encapsulated liquid crystals on latex produce poor colour response, attributed to the spatial distribution of liquid crystals.

There is a shift in the calibration curve during cooling leading to temperature bias in both narrow band and wide band TLC sheets. Hysteresis is only an issue when the crystals are heated above their clearing point temperature. If the liquid crystals are used within their colour bandwidth, the calibrations are repeatable. No permanent hysteresis effects were observed for the TLC polyester sheets and emulsion based TLC over relatively short time scales of two weeks.

## *6.2 Neural network calibration*

With numerous emerging applications of neural networks in heat transfer, a new calibration approach was considered for thermochromic liquid crystals which has not been achieved by the conventional techniques. The neural network used the RGB intensities as training data for accurately calibrating the TLC under varying lighting conditions. The advantages of using neural networks over the traditional hue temperature calibration are:

(a) It merges the different hue calibration curves from different lighting conditions into a single curve.

(b) It is inclusive of the distribution of RGB intensities within the region of interest unlike the mean or median value of hue which can be significantly affected by the lighting condition, coverage factor and the TLC bandwidth.

(c) The entire colour bandwidth can be used without the need to remove discontinuities in the hue. However, the results are shown to improve when considering only the useful colour bandwidth of the TLC.

(d) The shift in hue with the varying light intensity requires regular calibration checks during LCT measurements, this in turn will require a different colourmap (or Lookup Table) to produce accurate temperature measurements using the conventional techniques. Calibration using neural networks provides a more robust approach following the computing effort required for training.

However, it should be emphasised that this technique is not intended as a replacement for conventional techniques. It offers significant advantages over manual hue temperature calibration that may be useful in certain research or industrial applications. For example, accurate determination of temperature distribution in complex geometries is dependent on highly stable illumination. Since, neural networks have been successfully used to deduce convective heat transfer coefficients in thermo-fluid applications (Jambunathan, Hartle et al. 1996), it is envisaged that by using this technique a completely automated and stand-alone system can be developed to map the TLC colour response and evaluate the heat transfer coefficients.

The results obtained for the TLC polyester sheet are encouraging. However, better understanding of neural network calibration on wideband TLC materials and other physical types of TLC materials (i.e. emulsion based TLC and latex based TLC) with a similar trend of hue versus temperature curve is required to generalise the calibration technique. It will also be necessary to refine the procedure by taking into consideration TLC hysteresis and pressure sensitivity effects. This will require significant additional investigation and therefore was considered outside the scope of the current study. The conventional calibration approach was used for the analysis of clinical study results.

## 6.3 Liquid crystal thermography system

The aim of the LCT system was to examine means of measuring thermal changes in the plantar skin of patients with diabetes and neuropathy. Vascular changes due to abnormal neuronal control involve changes that can be identified and monitored through their effects on the dynamics of thermal behaviour on human skin (Anbar 1998). Previous studies of diabetic neuropathy have utilised several instruments to detect lack of protective sensation in the foot. However, there has not been any instrument designed specifically for evaluation of thermal patterns under the foot and other temporal parameters, such as rate of change of vascularity and thermal hyperaemia. Ideally, there should be an instrument to evaluate neuropathy independently, objectively, easy to use, readily available, sensitive and specific. It would appear that limitations exist resulting from the thermal techniques themselves.

Diabetic foot ulcers occur due to irregularities in underlying microangiopathy and neuropathy. Therefore, either measurements should be made at several discrete locations or a whole field technique such as LCT or IR thermography should be used. Electrical contact thermometry or cutaneous thermal perception need more time to make point measurements over the same surface area. Therefore, both techniques were discounted from use in current study. LCT is a factor of magnitude cheaper than IR thermography systems (Anbar 1998; Bharara, Cobb et al. 2005). Derived techniques using IR imaging, such as, DAT study thermal behaviour in the time domain and are therefore, less sensitive to reflection artefacts (Anbar and Milescu 1998). The technique may be suitable for speciality diagnostic centres and research teams. Additionally, neurogenic modulation of perfusion are exhibited at lower frequencies (Anbar and Milescu 1998). A low cost thermal technique such as LCT offers the potential to measure static and dynamic parameters under foot.

## 6.4 Physiological interpretation of the measured response

The present study involves assessing the plantar foot temperatures when the foot is loaded. Evidence from other studies suggest that reperfusion of tissue following removal

of load is of clinical interest, especially in the diabetic group (Rayman, Hassan et al. 1986a; Rayman, Williams et al. 1986b; Cobb 2000). Mean blood flow into the tissue, plantar pressure, duration of loading and dynamic response of perfusion has all been evaluated. However, there has been no study related to temperatures under the normally loaded foot. Thermometry has an important role in furthering current understanding of the pathogenesis of diabetic foot ulceration (Bharara, Cobb et al. 2006).

During standing, the foot sole is exposed to high static pressure, resulting in changes in the microcirculation. It is suggested that the temperature response during the loading period is likely to be dominated by local metabolic factors, perfusion status and physical characteristic of the plantar tissue in contact with the TLC sheet. This increase is linked to a complex interplay between all these factors and their association can only be established by independent assessment of these factors. Vertical loading has a higher impact on superficial blood flow in contrast to shear, which affects perfusion deeper in dermis (Tsay 1991). The measured response is consistent with the above finding and only considers vertical loading of the foot.

Microcirculation involves surface capillary loops which serve nutritional demands and deeper located AV shunts for body temperature regulation. Both nutritional and thermoregulatory blood flow is of interest in the current study. Considering nutritional capillaries only account for 15% of total blood flux (Fagrell 1984), it is reasonable to assume that thermoregulatory blood flow contributes to the majority of the thermal changes in the current study. However, it must be stressed that it is not possible to separate changes in blood flow from the thermal images acquired using the LCT system. The difficulty of making this distinction is further complicated by the fact that when the skin temperature is increased extrinsically the metabolic demands of the tissue also increase and therefore both nutritional and thermoregulatory flow will increase. Besides, when these changes are considered under the influence of load as in the present study, there is a rise in capillary pressure causing vasoconstriction to prevent oedema formation (Flynn and Tooke 1995). This is a strong additional control mechanism overriding the normal thermoregulatory response (Meinders, Lange et al. 1996). However, a precise

determination of interaction between the underlying pressure, its effect on microcirculation and associated thermal changes is not within scope of this study.

Although it is clear, that the hyperaemic response compensates for the ischaemic state of tissue upon loading (Flynn, Edmonds et al. 1988; Meinders, Lange et al. 1996; Cobb 2000), there is no evidence suggesting whether any such response is induced when the duration of loading is longer. Current analysis was restricted to five minutes for baseline and repetitive stress tests and ten minutes for thermal cycling tests. This was due to limited capacity for data recording. However, the recording time is consistent with the commonly used cold stress test for Raynaud's syndrome where 10 minutes recovery period is observed (Ring 1988; Ring 1995; Jung and Zuber 1998). The response during all four tests had one similarity; there is an increase in temperature throughout the duration of the test with the rate of increase falling with time. Therefore, further analysis only considers measured temperatures, temporal changes and comparison for three study groups.

Intuitively, thermal stimulus to plantar tissue will result in recruitment of thermoregulatory shunt flow mediated by the hypothalamus to maintain homeostasis. In the diabetic groups, this ability is compromised due to degeneration of thermoreceptors and autonomic neuropathy. The temperature values after immersion in warm water at 37°C for all groups indicate temperatures much lower than the temperature of the water. This may be due to two reasons, (a) heat exchange with the surroundings at 24°C when the foot is taken out from water and wiped using a pre-sterilised towel and (b) withdrawal of nutritive blood supply following thermal vasodilation. The first reason results in hypothalamus mediated activity which counteracts the preceding thermal stimulus i.e. changes in ambient temperature could affect thermoregulatory blood flow independent of the temperature of water. The time difference between removal from water bath and LCT measurement was less than 60 seconds. The second reason can be physiologically justified with the findings of Flynn and Tooke (1995) and Meinders et al. (1996) as discussed above. It is suggested that blood flow remained uninfluenced by heating when measured in a dependent position. The importance of these physiological effects on

interpreting results from current study is affected by the extent of underlying neuropathy and impairment of microvascular system.

Both sensory neuropathy and autonomic neuropathy can affect perfusion to lower extremities (Flynn and Tooke 1995) and hence, temperature (Bharara, Cobb et al. 2006). Both neuropathies coexist and therefore, it is not possible to establish an independent correlation between measured thermal response and each form of neuropathy using the current protocol. It is important to state that the patients were allocated to either of the three study groups, based on the results of monofilament testing and vibration perception threshold testing. Detailed information on the microcirculatory status of the feet was unavailable and therefore, the comparison between three study groups was based on the responses to thermal stimulus and physical stress on the plantar foot. It is shown that by assessing the thermal parameters at the same sites as that of sensory testing we are able to distinguish between both clinical and sub-clinical forms of neuropathy.

### 6.4.1 Thermal assessment of the diabetic foot

The remaining analysis problem relates to quantifying the results from the clinical LCT system. There is no 'gold standard' method of validating in vivo LCT measurements and responses, therefore, in vivo calibration of the TLC sheet was considered appropriate for the clinical assessment. Simple measurements from a digital thermometer were however, used as reference and were consistent with the LCT system measurements. The importance of a whole field thermal image using LCT must be emphasised, when considering use of appropriate thermal modality for plantar foot assessment.

Assessment of foot temperature under load resulted in a rise in temperature throughout the duration of the test, suggesting a compensatory physiological response of the tissue following loading. Temperature distribution under the plantar surface of the foot is determined by the heat conductivity of muscular and adipose tissues and heat emissivity of the skin. The highest increase in temperature was consistently observed for the non-neuropathic group, an important finding for sub-clinical neuropathy. This increase may

be physiologically justified by thinning of the adipose tissue, which is known to occur in the patients with diabetes (Kao, Davis et al. 1999; Cavanagh, Ulbrecht et al. 2001). Adipose tissue typically acts as a heat resistance and scatters the heat flux. Thickness of adipose tissue affects the heat transport from inner tissues (Jung and Zuber 1998). Being nearer to skin surface, the pathologic changes in the adipose tissue can be visualised in the thermogram as inflammatory responses, especially in the diabetic groups.

Generally, the neuropathic group shows higher temperatures in all tests at all measured sites when compared with the healthy group. This is consistent with the generally increased blood flow in other studies (Stess, Sisney et al. 1986; Benbow, Chan et al. 1994), attributed to autonomic neuropathy affecting the sympathetic regulation of blood flow (Tanenberg, Schumer et al. 2001). The difference is smallest at the heel between the neuropathic group and non neuropathic group. This may be due to the influence of adipose tissue, which affects the thermal conductance from deeper vessels. The high prevalence of autonomic neuropathy in the diabetic group without detectable sensory neuropathy (tested independently using the Ansiscope, Appendix I), may be the underlying cause for the high temperatures under the plantar foot.

### 6.4.2 Repetitive stress test

The overall higher increase in the percentage of subjects above threshold, compared to baseline values for the diabetic groups (neuropathic and non neuropathic), may be of clinical interest, as this may indicate the underlying high plantar pressures experienced by the diabetic group leading to inflammatory responses at the areas of increased loading i.e. metatarsal heads and heel. High plantar pressures in the neuropathic diabetic subjects is clinically accepted and well documented (Lord, Reynolds et al. 1986; Cavanagh, Ulbrecht et al. 2001). A similar thermal trend in the non neuropathic foot provides a useful diagnosis of sub-clinical neuropathy.

The above finding at the heel supports the claim that this may arise due to thinning of the adipose tissue in diabetic subjects. Structural alterations to the plantar skin and sub-

tissues are associated with the long term type 2 diabetes (Cavanagh, Simoneau et al. 1993). The clinical importance of these changes lies in the fact that repeated mechanical stresses can exceed the damage threshold of the tissue (Kao, Davis et al. 1999). There is evidence of positive correlation between applied pressure and measured temperature (Goller, Lewis et al. 1971; Guy, Clark et al. 1985). This is also verified from the results of the current study during the repetitive stress test.

The results from this test suggest the foot warms up after exercise presumably due to increased blood flow owing to increased metabolic requirement, especially at the high pressure areas. This is evidenced by the heat radiated from the foot in the thermal images. The effect of cooling due to evaporation of sweat was not dominant under the controlled ambient conditions (both temperature and humidity were consistently maintained at 24°C and less than 50% respectively with air conditioning). It must also be stressed that the ability to sweat is typically compromised due to autonomic neuropathy (Tanenberg, Schumer et al. 2001).

### 6.4.3 Thermal cycling tests

A linearly increasing recovery response for the healthy and non neuropathic groups, suggests that the response of thermoreceptors is intact. Both groups show good recovery post 10 minutes to baseline temperatures (consistent with the commonly used cold stress test studies), except the non neuropathic group assessment at the first metatarsal head. This may be due to selective degeneration of thermoreceptors in the foot. Thermal cycling tests provide a useful justification of the diminished or absent response of the thermoreceptors for the neuropathic group. The group shows poor recovery to baseline temperatures at all measurement sites indicating the failure of the hypothalamus mediated recovery under the foot following an event of thermal stimulus. These subjects have no clinical evidence of peripheral vascular disease but clinical evidence of sensory neuropathy, therefore the response is dominated by the function of thermoreceptors or related signalling pathways.

The response is more pronounced at the metatarsal head region for cold immersion recovery due to punctuate distribution of the sensory receptors. This is evidenced by considering the examples in Appendix J, where the images show that recovery starts in the metatarsal head region in all the study groups.

For the warm up recovery test, the neuropathic diabetic group shows the highest differences in the recovery towards baseline temperature at all the three sites i.e. first metatarsal, second metatarsal and heel. This may be indicative of sub-clinical neuropathy and failure of the thermoreceptors to regulate perfusion to the foot following an event of warm immersion. This is consistent with the findings from cold immersion recovery test.

From the histogram analysis of the non neuropathic group during the warm up recovery test, 30% of the subjects reach maximum temperatures above 32°C. The response of non neuropathic diabetic group leads to the overall high mean temperatures for this group.

The recovery response at the heel is comparatively slower which is likely to be due to the presence of adipose tissue which provides thermal insulation. Besides, the geometrical condition of the skin surface may itself modify the processes of emission and absorption of heat (Jung and Zuber 1998).

## *6.5 Summary*

There was a consistent trend for all measurements, where the temperature increased linearly over time and finally saturates. This may be indicative of underlying changes in perfusion due to posture and plantar pressure leading to changes in temperature. This is an important finding, but unfortunately the direct implications of changes in load distribution in terms of thermal coupling from foot to TLC sheet are unknown. Due to practical difficulties of using a simple thermometer simultaneously with the LCT measurement, it was not possible to confirm if temperature did increase with constant loading under constant temperature.

As shown in the data, there is a shoulder region with the highest rate of increase of temperature within the first two minutes, followed by a slower rate of increase of temperature. Typically, there is a reduction in perfusion under load due to compression of the tissue, followed by a hyperaemic response to provide tissue nutrition when unloaded (Cobb 2000). However, the skin surface temperature is affected by ambient temperature, tissue perfusion, internal metabolism and any pathophysiology. Considering, there was a consistent (similar temperature patterns during tests) response for all subjects, ambient temperature and pathophysiological factors (as patients with PVD and foot infection were excluded) can be ruled out as causative factors. Both tissue perfusion and metabolic activity are interlinked and the measured temperature under load can therefore, be considered as a function of both. It must be emphasised that lack of an independent study of tissue perfusion under load over time is a limitation of present study. Availability of results from a similar study can supplement the thermal measurement results and further the association between load and thermal changes.

The histogram analysis of the clinical datasets provides an underlying bell shaped curve of the start/end temperatures for all study groups. The mechanism for this distribution is unknown and therefore, can be addressed in a larger clinical study. However, bell shape distribution implies a normal model (Bland 2004) and may be explained by assessing the independent factors identified during the current study.

Higher temperatures for the diabetic groups may be due to the fact that, 65% subjects in non neuropathic diabetic group and 88.5% of the subjects in neuropathic diabetic group, show either late or advanced stage neuropathy (Appendix I). The temperature at the heel is consistently less than the temperature at metatarsal heads in each group for all clinical tests, indicative of the influence of adipose tissue. This is also supported by the fact that more than 50% of the subjects in the diabetic groups wear their footwear for less than 8 hours a day. Barefoot walking directly affects the plantar tissue, especially the heel. However, this comment is limited to the natives of the state in India, where the study was performed.

The high standard deviation in the measured temperatures and unmatched subjects in the study groups complicated the statistical analysis of the dataset. The mean temperature data shows poor correlation with the age, duration of diabetes, BMI and HbA1c percentage, with the exception of neuropathic diabetic group which shows a 40% correlation between the measured temperature at first metatarsal head and BMI. However, the consistency in the measured temperatures and temporal variation at three measurement sites are useful indications for the patterns associated with diabetes and subsequent neuropathy, which may be clinically asymptomatic but visible when testing the response of thermoreceptors.

# Chapter 7 Conclusions

## *7.0 Introduction*

A critical review of the development and clinical application of the liquid crystal thermography system is presented in summary form. Results of the in vivo clinical evaluation of the system are discussed. Recommendations for improvement of the current system and further work are given. In the final section, the overall contribution of the present work in considered.

## *7.1 Summary*

The project is reconsidered in terms of the theoretical background and review of the literature; assessing the feasibility of the initial proposal and its clinical adaptation. Justification is given of the plantar temperature assessment under load by liquid crystal thermography using an appropriate protocol. Such a thermological assessment could not be performed using existing techniques or systems and the requirement of a LCT system is identified. The contact thermography approach provides the ability to measure foot temperature under load, critical to the neuropathic diabetic foot (Bharara, Cobb et al. 2006). A review of the development of such a contact thermography system is discussed in the following sections.

### 7.1.1 Review of justification for the study

From the previous studies, perfusion related complications in the diabetic foot at both macrovascular (Shaw and Boulton 1997) and microvascular (Jaap and E 1995; Tooke 1996) levels are well presented and understood. This has led to a clear distinction between ischaemic and neuropathic complications in the diabetic foot disease. Several techniques such as ankle brachial perfusion index, Doppler ultrasound and laser Doppler are used both clinically and in the research domain to assess peripheral vascular disease

(Williams , Picton et al. 1993; Hurley, Jung et al. 2001; Ouriel 2001). These techniques have also provided clinical evidence of elevated blood supply in the neuropathic foot. Routine assessment of risk of ulceration in the diabetic foot involves measurement of plantar pressure and determination of the extent of sensory neuropathy. However, it should be emphasised that these techniques alone cannot be used to predict mechanisms that lead to tissue damage and initiate ulceration. Limited lack of consensus on appropriate threshold values leading to plantar ulceration further complicate the problem (Cavanagh and Ulbrecht 1995), suggesting the need for supplementary techniques and evidence based diagnosis. Poor nutritional supply to compensate for higher tissue metabolism (due to excessive plantar pressures) and degeneration of sensory receptors are common factors leading to neuropathic ulceration. However, there is no conclusive evidence. Autonomic neuropathy further leads to impaired regulation of perfusion and depletion of the nutritive supply (Lord, Reynolds et al. 1986). The other important requirement of any supplementary evidence is the ability to diagnose neuropathic condition at an early stage (Perkins and Bril 2002).

Careful investigation of the current techniques for assessing the neuropathic diabetic foot suggests a bias in measuring the response of mechanoreceptors. This bias is inappropriate in the opinion of the author and therefore, a clear requirement exists to asses the response of thermoreceptors. Thermal changes at the plantar surface reflect vascular status, skeletal changes, and inflammation at the site under consideration, all of which can be attributed to diabetic neuropathy. Considering clinical evidence suggesting dynamic loading leading to foot ulceration in diabetes, it is useful to measure foot temperature under load.

Contact thermography is suitable for assessing the plantar temperatures in the neuropathic diabetic foot and considers the affect of neuropathy on regulation of blood flow. The findings of such an evaluation provide a whole field analysis of the plantar foot, identifying any localised event of neuropathic complication. The most important benefit of such an evaluation is the assessment of the foot under the influence of load.

Furthermore, it can be useful to validate the nutritional deficit's (during plantar loading and thermal stimulus) contribution in foot ulceration.

### 7.1.2 Re-evaluation of objectives

Justification for the focus of the present study on assessing thermal patterns under the diabetic neuropathic foot is discussed in the preceding section. Originally, it was envisaged to conduct a prospective clinical trial in order to relate thermal changes with underlying sensory neuropathy in patients with diabetes. The method of liquid crystal thermography was identified as the most appropriate technique because of low cost, ability to obtain data non-invasively, its non ionising effects and ability to assess the foot under load. This technique has been successfully used to assess the diabetic foot in other studies (Stess, Sisney et al. 1986; Benbow, Chan et al. 1994) and is typically, used in breast thermography and sports injury assessments (Leinidou 2003). One major limitation of previous studies was pressure dependence on the colour response. In the current study, pressure insensitive formulation was used. The commercial LCT system was considered unsuitable for current study due to higher cost, inability to assess the foot under load and inability for quantitative data analysis. The in vitro characterisation confirms these findings.

Consequently, the aim of the study shifted from a rigorous clinical evaluation to constructing, characterising and validating a LCT system for assessing the diabetic feet responses to thermal stimulus.

### 7.1.3 Limitations of the system design

The LCT system was designed with the intention to provide a comprehensive justification for the potential clinical benefit in performing a contact thermographic assessment of the diabetic foot. Currently, the calibration unit was independent of the measurement platform and calibration data was acquired with the LABVIEW interface and analysis performed in MATLAB. Clinical data acquisition was realised using the camera

manufacturer's software and subsequent analysis performed in MATLAB. In order to account clinical acceptability, the calibration unit should be integral part of the measurement platform and data acquisition and analysis should be more streamlined, possibly using a simpler user interface. This could be accomplished using the software development kit available from the manufacturer but required significant implementation effort and therefore, was considered outside the scope of current study.

The two hour duration for the measurement protocol is not suitable for routine clinical investigation. It must be stressed however, that the focus of current study was to prove diagnostic benefit for the high-risk foot and further current understanding of the association between thermal patterns under the foot and sensory neuropathy. In future studies, the measurement protocol can be modified to reduce the total time required for clinical investigation.

A laptop computer was used to collect and store the clinical data from each patient. This data was transferred on an external hard drive and backed up on CD-ROM's. It would however, be beneficial to have a stand alone dedicated workstation for data collection, storage and processing. This will further provide benefits of real time data analysis and automated backup on an external drive.

## *7.2 Recommendations for further work*

Thermal measurement of the diabetic foot has been shown to be a useful technique in clinical management of the diabetic foot. Various parameters of interest and measurement techniques have been identified to study pathophysiology of the vascular system and neuronal control in diabetic foot disease. At the start of this project it became evident that limitations of liquid crystal technology prevented application to assessment of diabetic foot disease. This study has demonstrated methods for successful deployment of LCT technology for assessment of the diabetic foot.

Application of the plantar monitoring system for a full clinical trial requires additional in vivo assessment of response time and shear sensitivity of the TLC sheets. The response time measured should be significantly less than the physiologically relevant times for the changes that are intended to be determined.

An appropriate physiological model indicating changes in the perfusion based on clinical protocol can be further used to correlate perfusion and thermal changes post stress and application of thermal stimulus. Such a model can be realised by assessment of microcirculatory changes using a suitable modality. To the author's knowledge no such model has been postulated by other groups. The data provided by the current study allows such a model to be produced and then investigated by a future study. This model may be limited by localisation of measurements, unlike the whole field capability of contact thermography. However, local measurements at the most prevalent sites of ulceration i.e. metatarsal heads, great toe and heel can be clinically useful.

Shear sensitivity assessment provides two major benefits. Firstly, it can be used to identify motion artefacts when evaluating elderly group of diabetic patients. Secondly, it renders the system's adaptation into a dynamic measurement system (such as one proposed in Appendix K), where the motion needs to be resolved into shear and vertical loading. The important benefit of such a system would be in identifying focal areas under the foot that are prone to repetitive stress due to cyclic loading, inflammation and skin breakdown.

Furthermore, there is a need for refining currrent assessment protocol. Following recommendations are considered useful for future clinical studies:

(a) For repetetive stress measurements, a treadmill may be more suitable in order to use consistent distances, speed and run time. For the current clinical study, it was unavailable and hence, subjects were asked to walk within the premises.

(b) Ideally, repetitive stress tests should have been the last test as the time to recover from exercise is unknown and could affect the thermal cyclic tests. An independent assessment of the recovery times, post physical stress may also be useful to improve the assessment protocol.

(c) When evaluating patients with foot deformity or Charcot's foot, the maximum study time may need to be reduced as the normal balance mechanism during standing for these patients is significantly affected (Cavanagh, Ulbrecht et al. 2001; Pendsey 2003).

(d) Use of an insulated water bath for thermal cyclic tests is appropriate for standardisation of the temperatures. Besides, if the foot is immersed in warm water there is often creep of the dermis. This was not investigated in the current study and therefore, must be considered for future clinical studies as it may affect the thermal coupling to the TLC sheet.

(e) The measurement platform should be pre-sterlised using appropriate method (for example, Milton's fluid) to prevent any cross infection. This is an essential permissive factor for evaluating patients with active wounds or foot ulcers.This approach may be useful in assessing wound healing since tissue around the wound is often at higher temperature.

(f) While evaluating the physiological differences between the diabetic group (with/without neuropathy) and the healthy group, the age/sex related differences in thermoregulatory mechanisms must also be determined. Furthermore, the incidence of type 2 diabetes increases with age and it is therefore, an important factor to be considered (Ha and Lean 1998; World Health Organization 1999).

(g) For the cold stress test, it is recommended to use a plastic bag before immersion in cold water. This is a standard procedure in cold stress tests for Raynaud's phenomenon and prevents water retention by the plantar skin (Howell, Kennedy et al. 1997; Cherkas, Howell et al. 2001). In the current study, the patient foot was towel dried, to prevent

water retention by the skin and any physical damage to the TLC. However, water retention by the skin is likely to affect the temperature measurements as heat exchange in water is eight times faster than in air.

It is recommended that the camera used in the current study is retained and a stand alone system is developed that provides an easy user interface for data acquisition and data analysis. This may also address the data storage issue, by using appropriate algorithms to eliminate the redundant data and only record incremental changes in the TLC images. Further image processing may help to remove background noise from the typical LCT images (Appendix J) and standardise the colour scale, consistent with the infrared thermography i.e. inverting the conventional colour scheme for TLC such that blue represents cold and red represents hot.

The results from the past two LCT studies (Stess RM, Sisney PC et al. 1986; Benbow, Chan et al. 1994) and current study cannot be directly compared as they are different in many ways. This indicates the need for standardised guidelines for thermal assessment of the diabetic foot. There has been a growing interest in home monitoring and ambulatory measurements of the foot temperatures in diabetic neuropathic foot to prevent foot ulceration using simple digital thermometers (Lavery, Higgins et al. 2004), LCT technology (Kantro 2006) and smart insoles[13]. However, a clinical thermometry system with a standardised assessment protocol can further current knowledge about diabetic foot (and infections/ulcers) and provide evidence based diagnosis of symptomatic or asymptomatic neuropathic condition. The use of home monitoring devices is further strengthened by the clinical evidence that neuropathic thermal patterns are not constant from day to day, described as autosympathectomy (Clark, Goff et al. 1988). Using LCT over IR thermography to assess diabetic neuropathic foot may yield useful diagnostic information (at a lesser cost) at the expense of thermal accuracy (Cavanagh, Ulbrecht et al. 2001). There is clearly a need for rigorously controlled studies.

---

[13] **Zephyr Technology Ltd., Auckland, Newzealand**

## 7.3 Contribution

A liquid crystal thermography system has been developed and applied in a clinical setting to assess its performance and implications on the clinical management of the diabetic foot. A new multi-centre collaboration was established for furthering the role of thermography in assessment of the diabetic neuropathic foot. The LCT system extends application of contact thermography in assessment of plantar temperatures under the influence of load which is essential for assessment of the diabetic foot. The important advantages of this system are safety of examination, non-invasive technique, simplicity, speed and low cost. Such a system promotes a coupling between prevalent sensory testing modalities and itself, aimed to characterise the diabetic neuropathic foot. Clinical application on a small study group has demonstrated that the system has the capability to provide supplementary evidence, in detecting neuropathic complications which may be symptomatic and asymptomatic, arising due to sensory neuropathy (most specifically thermoreceptors). This clinical study demonstrated for the first time, the evidence of poor recovery times for the diabetic foot with neuropathy when assessing the foot under load.

The TLC sensors employed in the LCT system have been independently characterised and shown to be repeatable, pressure insensitive and free from hysteresis. A key finding from this study provides insight into the relationship between spatial density of TLC and colour bandwidth. The analysis of characterisation data suggests that higher spatial density may be an essential requirement to induce larger colour range for the TLC. A novel neural network based calibration technique has been developed, which can be potentially useful in thermological applications, after addressing the identified limitations. In vivo calibration has been shown to be most suitable for measuring plantar temperatures. Initial results for a small study group (n=90) indicate raised plantar temperatures for the diabetic group at baseline and post stress indicating the intact vascular status of the foot. Furthermore, a temperature deficit (due to poor recovery to baseline temperature) suggests degeneration of thermoreceptors leading to diminished hypothalamus mediated activity in the diabetic neuropathic group.

# Appendices

# Appendix A St. Vincent's Declaration

**The Saint Vincent Declaration, St. Vincent, Italy (1989)**

The 'Saint Vincent Declaration' is a model for prevention self care and is used as guidelines for national diabetes related service development. A joint initiative by the World Health Organisation (WHO) and International Diabetes Federation (IDF) is aimed at garnering support at local, regional and national level to tackle the socio-economic burden of diabetes and its complications. The goals of St. Vincent Declaration focus on diagnosis, treatment and prevention of diabetes and its complications such as retinopathy, nephropathy, neuropathy, amputation, cardiovascular disease and pregnancy related complications.

Since its origin, a number of European meetings have been organized (Hungary-1992, Greece-1995, Portugal-1997, Turkey-1999). European Association for Study on Diabetes (EASD) and IDF conduct regular meetings for disseminating information on research, management and medical services in diabetes and its serious health problems.

St. Vincent Declaration aims to promote:

- detection and control of diabetes and of its complications with self-care and community support.
- awareness in the public, patients and clinical professionals of the present opportunities and the future potential for prevention of the diabetic complications.
- training and teaching in diabetes management and care for people of all ages with diabetes.
- specialised paediatric care for children with diabetes.
- Reinforcement of existing centres of excellence in diabetes care, education and research and creation of new centres.
- independence, equity and self-sufficiency for all people with diabetes.
- fullest possible integration of the diabetic citizen into society.

- Prevention of serious diabetic complications by use of effective measures, thereby:

  - reducing new blindness due to diabetes by one third or more.
  - reducing numbers of people entering end-stage diabetic renal failure by at least one third.
  - reducing by one half the rate of limb amputations for diabetic gangrene.
  - cutting morbidity and mortality from coronary heart disease in the diabetic by vigorous programmes of risk factor reduction.
  - achieving pregnancy outcome in the diabetic woman that approximates that of the non-diabetic woman.

- establishment of modern information technology for quality assurance of diabetes health care provision and for laboratory and technical procedures in diabetes diagnosis, treatment and self-management.
- European and international collaboration in diabetes research and development through appropriate agencies and in active partnership with diabetes patients organisations.
- urgent action in the spirit of the WHO programme, "Health for All" to establish joint machinery between WHO and IDF, European Region, to initiate, accelerate and facilitate the implementation of these recommendations.

# Appendix B Technical drawings

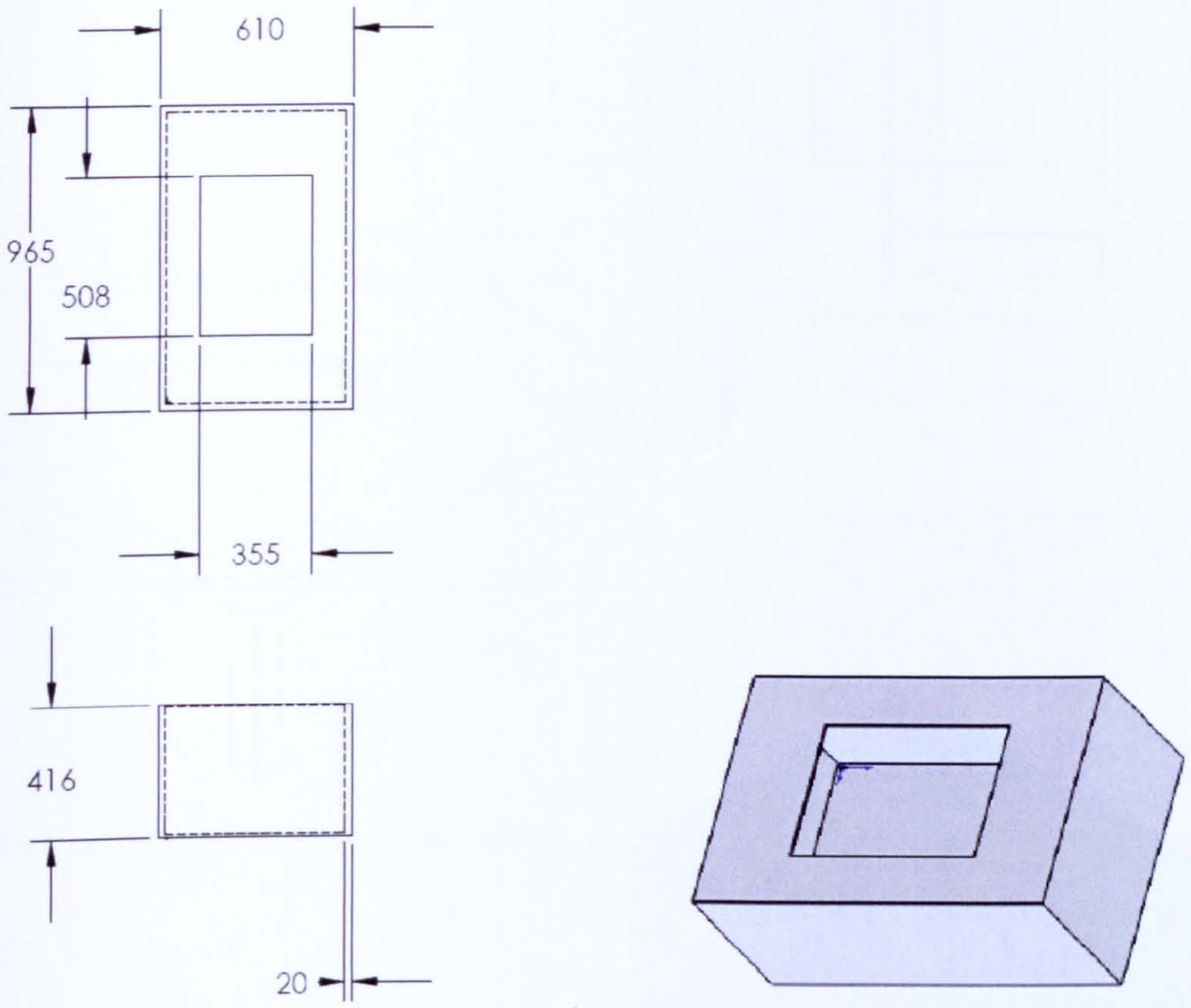


**Figure B-1: Technical drawing for the first prototype of measurement platform.**

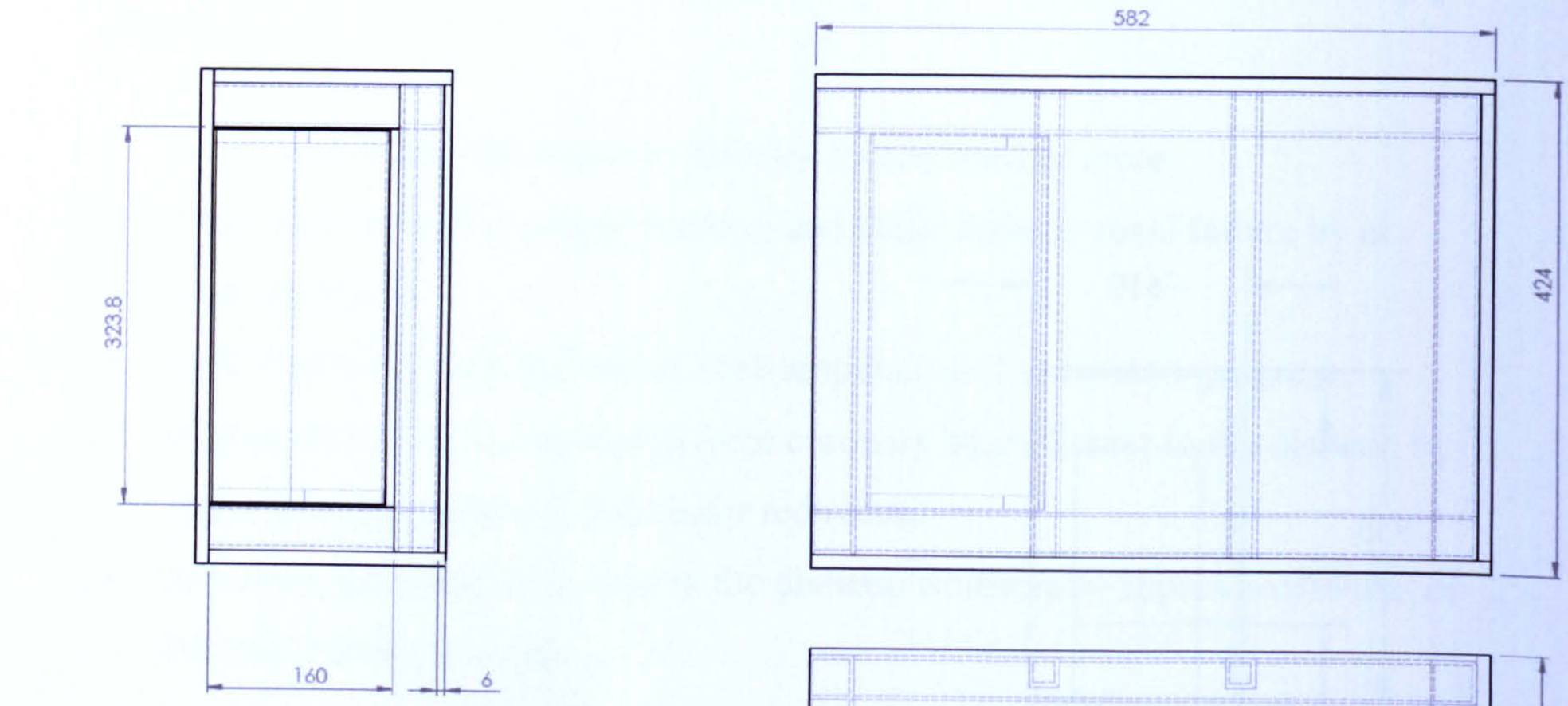


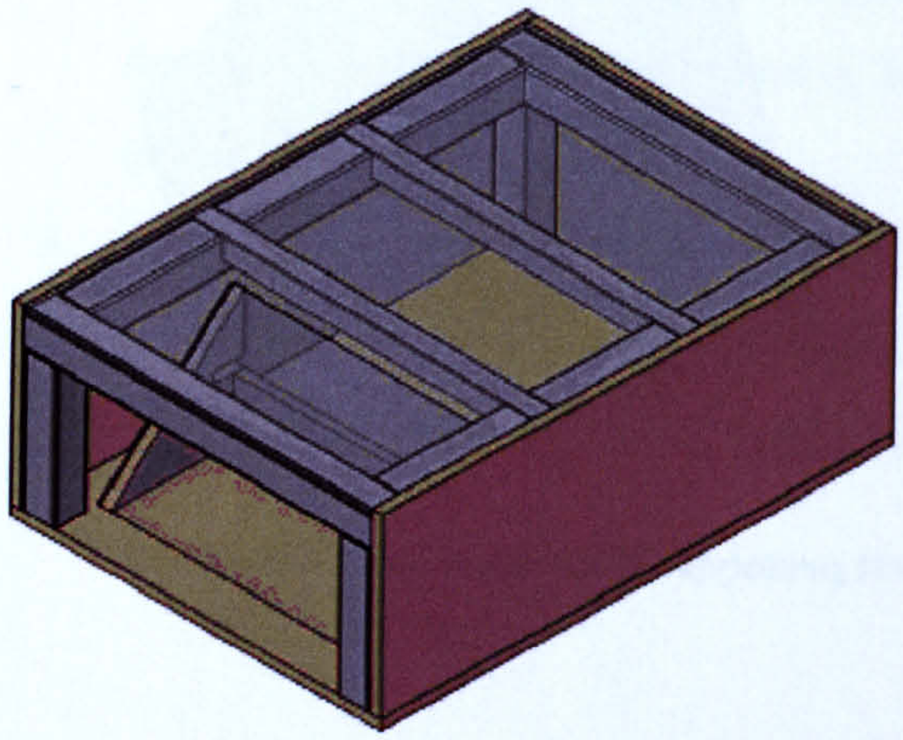

**Figure B-2: Technical drawing for the second prototype of measurement platform.**

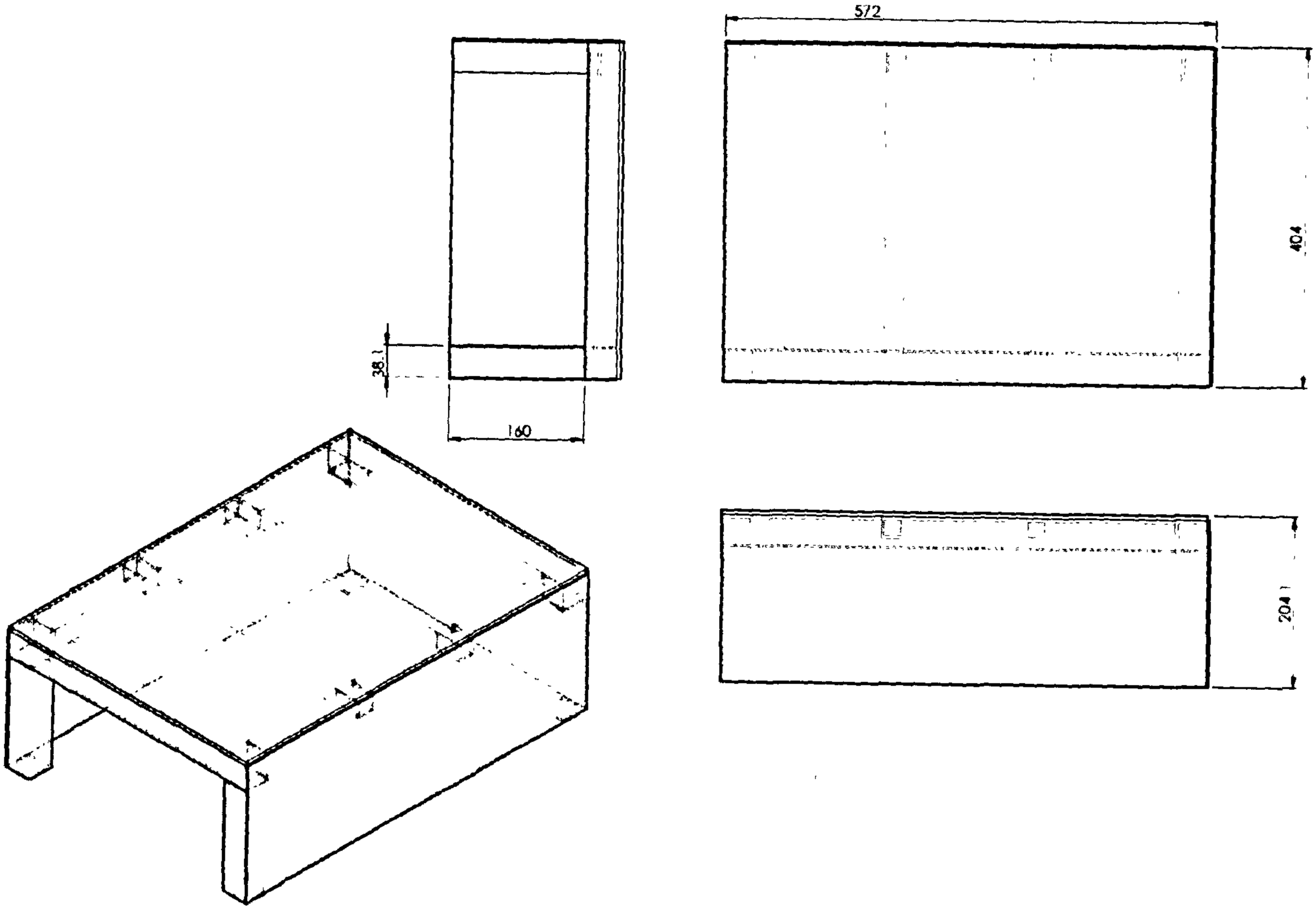


**Figure B-3: Technical drawing for the metallic stand for second prototype of measurement platform.**

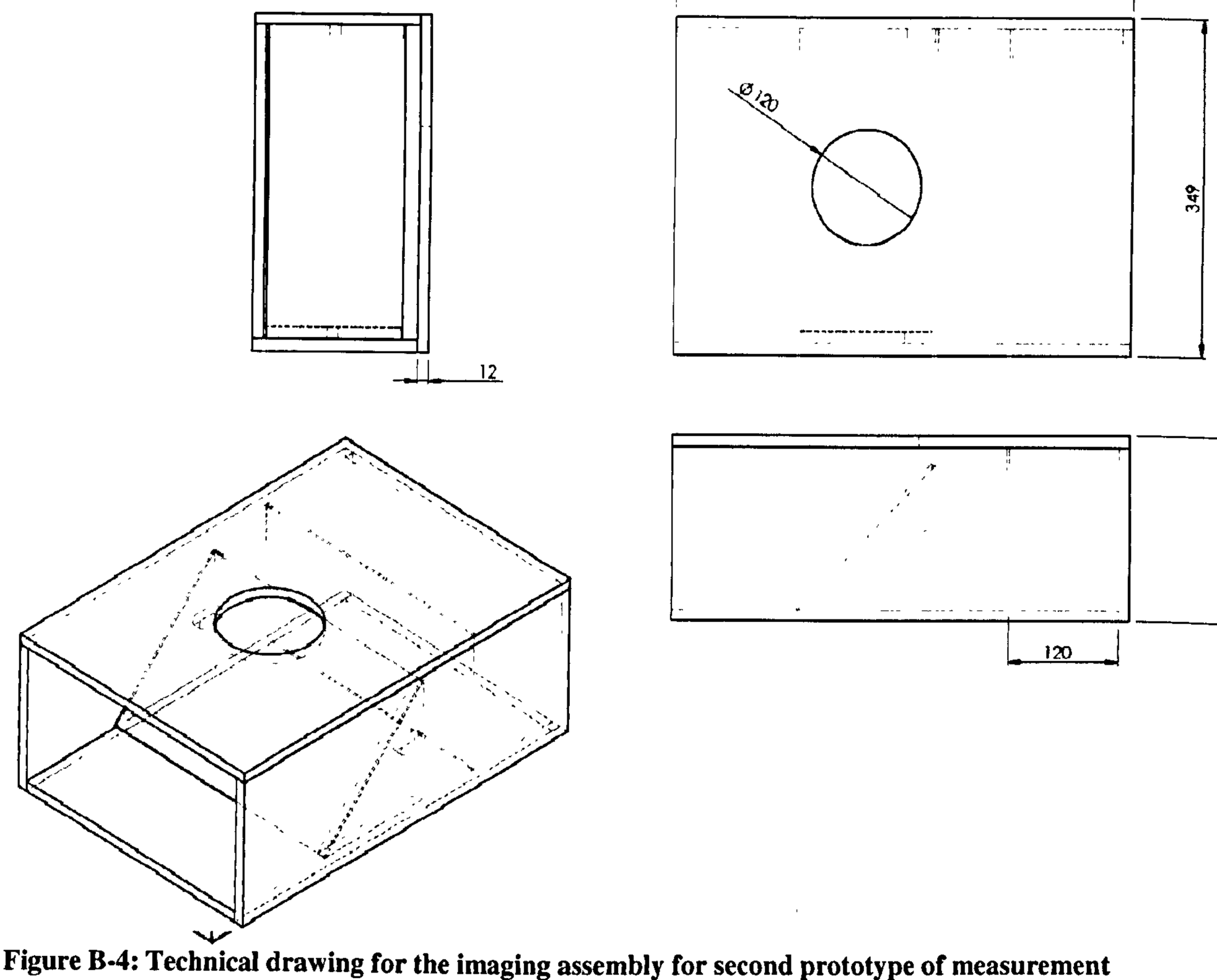


**Figure B-4: Technical drawing for the imaging assembly for second prototype of measurement platform.**

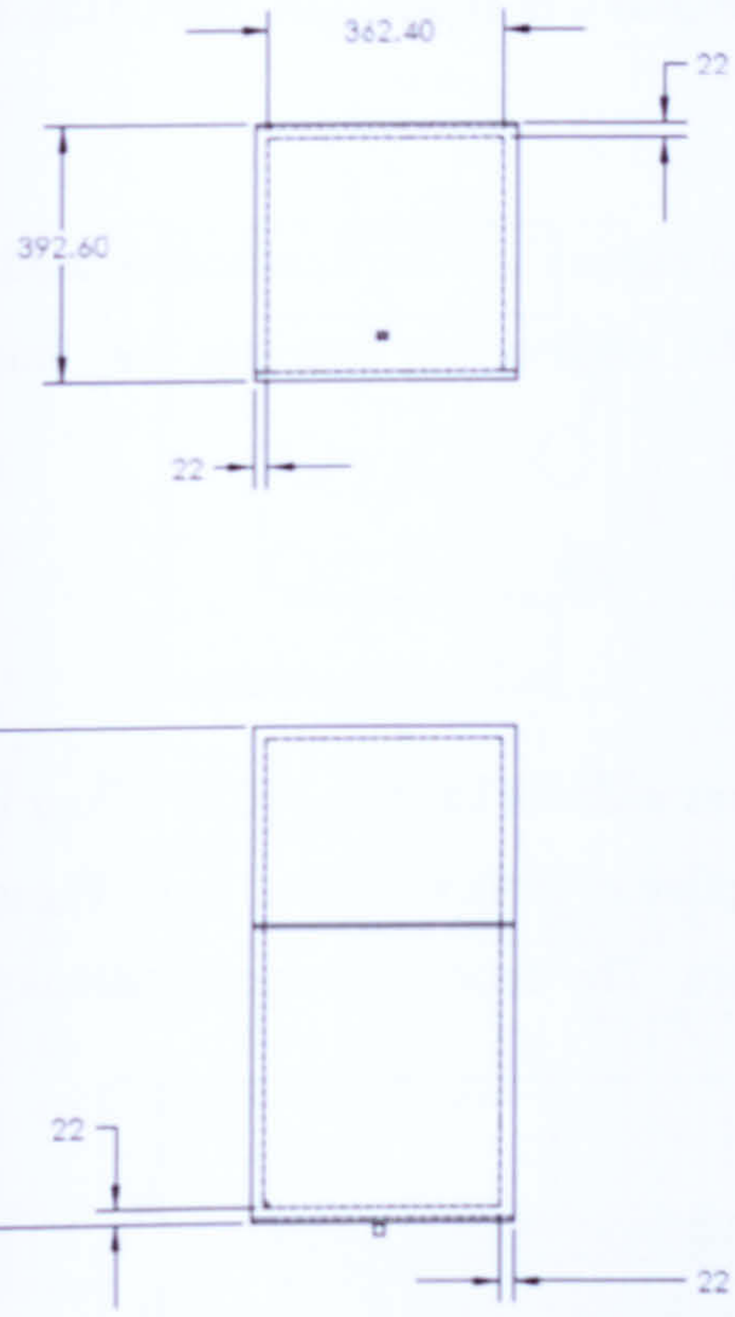


**Figure B-5: Technical drawing for the final prototype of measurement platform.**

# Appendix C Camera and light source specifications

This section provides the technical details of the camera and the light source used in the final prototype of the LCT system. Photographs, engineering drawings and functional specifications are provided.

## DFK 41AF02 RGB camera

Photograph C-1 illustrates the camera and the lens used for capturing RGB colour images representing the thermal patterns under the plantar surface of the foot. Figure C-1 provides the technical drawings for the camera. The functional specifications of the camera are provided in table C-1.

**Photograph C-1: Single CCD RGB camera based on IEEE 1394 protocol and its associated mount lens.**

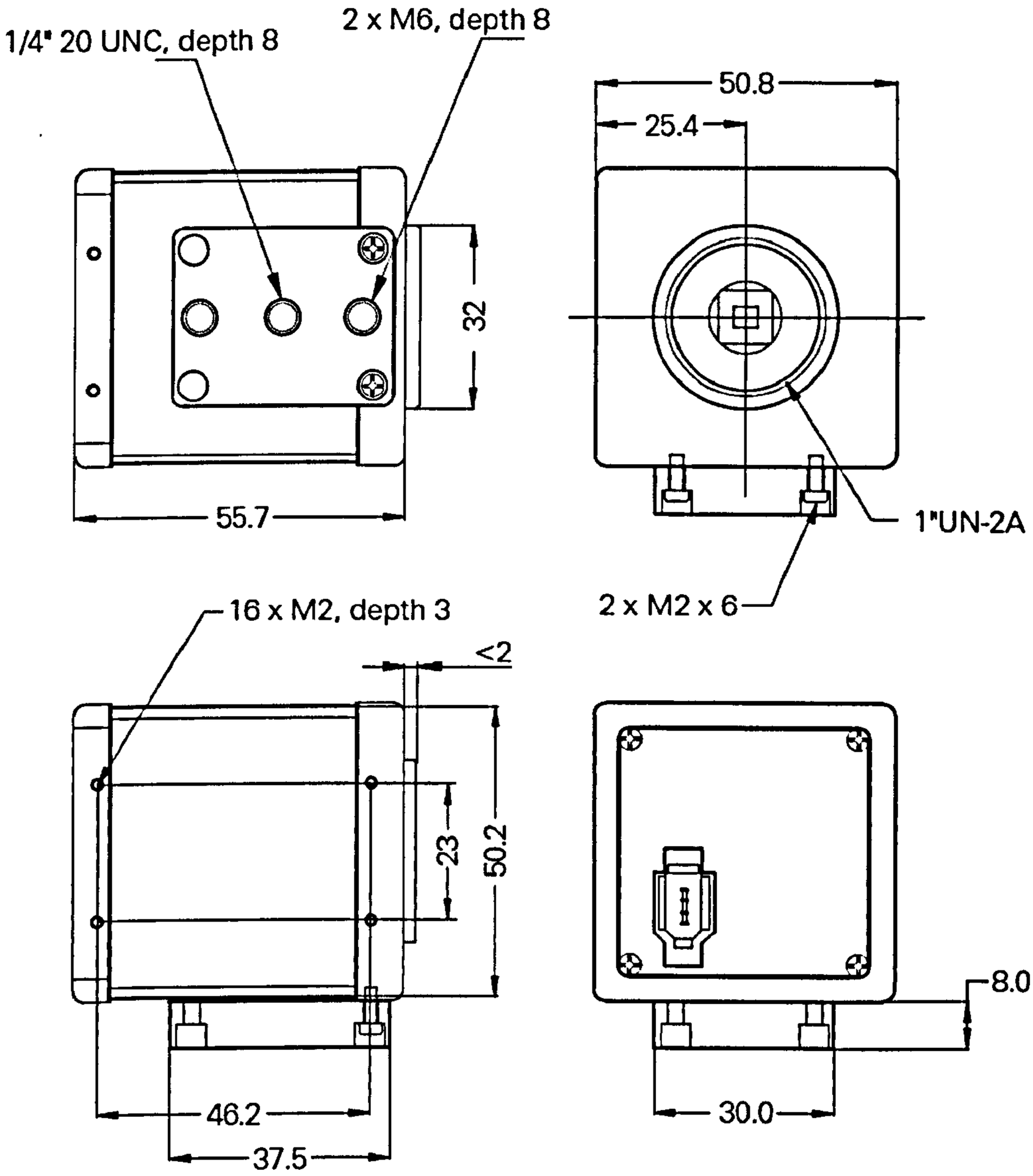


**Figure C-1: Engineering drawings for the DFK 41AF02 RGB camera. All dimensions are in 'mm'.**

| | |
|---|---|
| **General behaviour:** | |
| Video formats @ Frame rate | 1280 x 960 UYVY @ 7.5, 3.75 fps<br>1280 x 960 BY8 @ 15, 7.5, 3.75 fps |
| Sensitivity | 0.5 lx at 1/7.5s, gain 20 dB |
| Dynamic range | ADC: 10 bit, output: 8 bit |
| SNR | ADC: 9 bit at 25 °C, gain 0 dB |
| | |
| **Interface (optical):** | |
| Sensor specification | ICX205AK |
| Type | progressive scan |
| Format | 1/2 " |
| Resolution | H: 1360, V: 1024 |
| Pixel size | H: 4.65 µm, V: 4.65 µm |
| Lens mount | C/CS mount |
| | |
| **Interface (electrical):** | |
| Supply voltage | 8 to 30 VDC |
| Current consumption | approx 200 mA at 12 VDC |
| | |
| **Interface (mechanical):** | |
| Dimensions | H: 50.6 mm, W: 50.6 mm, L: 50 mm |
| Mass | 265 g |
| | |
| Adjustments (man): | |
| Shutter | 1/10000 to 30 s |
| Gain | 0 to 36 dB |
| Offset | 0 to 511 |
| Saturation | 0 to 200 % |
| White balance | -2 dB to +6 dB |
| | |
| Adjustments (auto): | |
| Shutter | 1/10000 to 30 s |
| Gain | 0 to 36 dB |
| Offset | 0 to 511 |
| White balance | -2 dB to +6 dB |
| | |
| **Environmental:** | |
| Max. temperature (operation) | -5 °C to 45 °C |
| Max. temperature (storage) | -20 °C to 60 °C |
| Max. humidity (operation) | 80 % non-condensing |
| Max. humidity (storage) | 95 % non-condensing |
| | |

**Table C-1: Functional specifications for the DFK 41AF02 RGB camera,**

**White light LED array**

The white light LED array (Model No: STP312C-2CW-012V from Ledtronics, California) was used as the illumination source for the final prototype of the LCT system. The chip material for the LED was InGaN. Figure C-2 illustrates the engineering drawing

for the LED strip and photograph C-2 represents the 27 LED's cluster used for the LCT system. The functional specifications of the LED's are provided in tables C-2 and C-3.

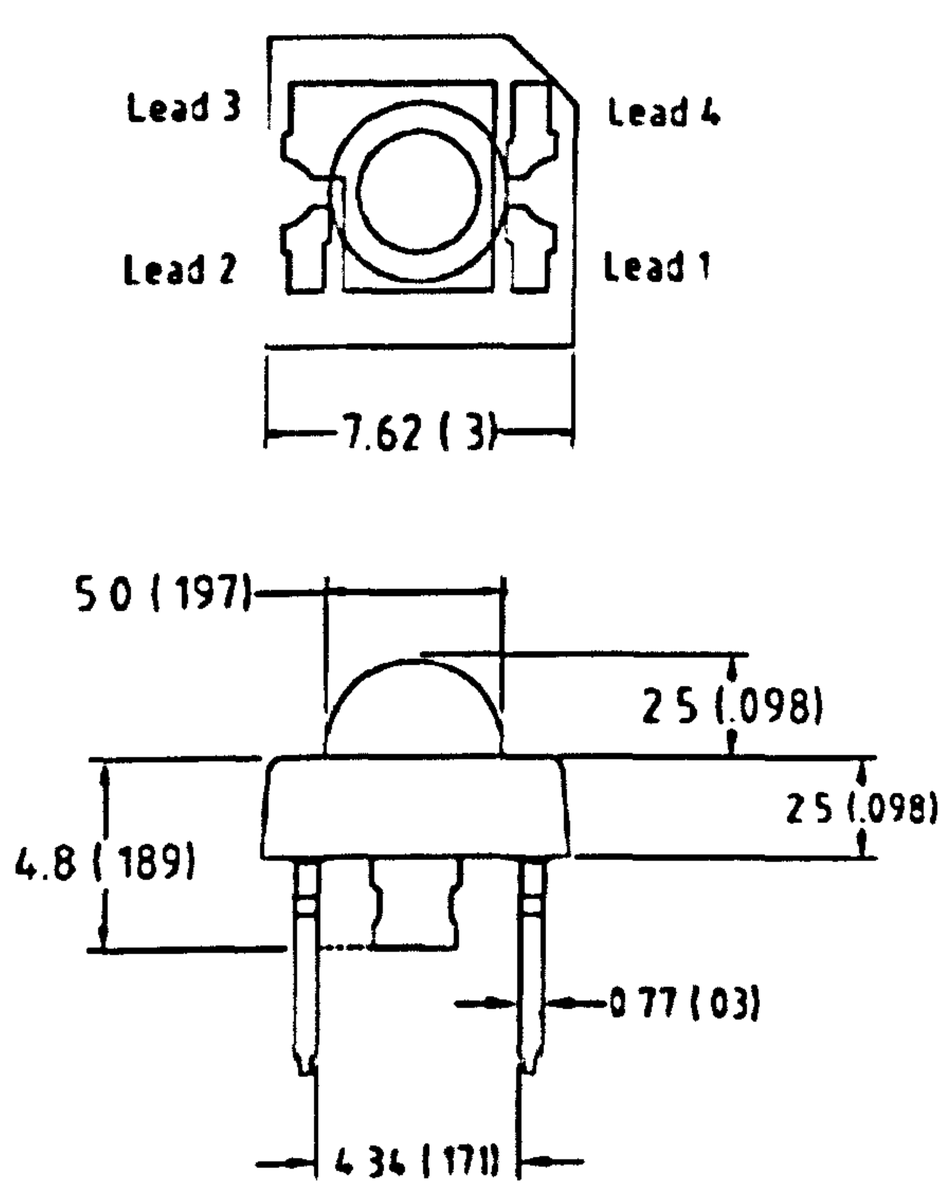


**Figure C-2: Engineering drawings for the STP312C-2CW-012V white light LED array. All dimensions are in 'mm'.**

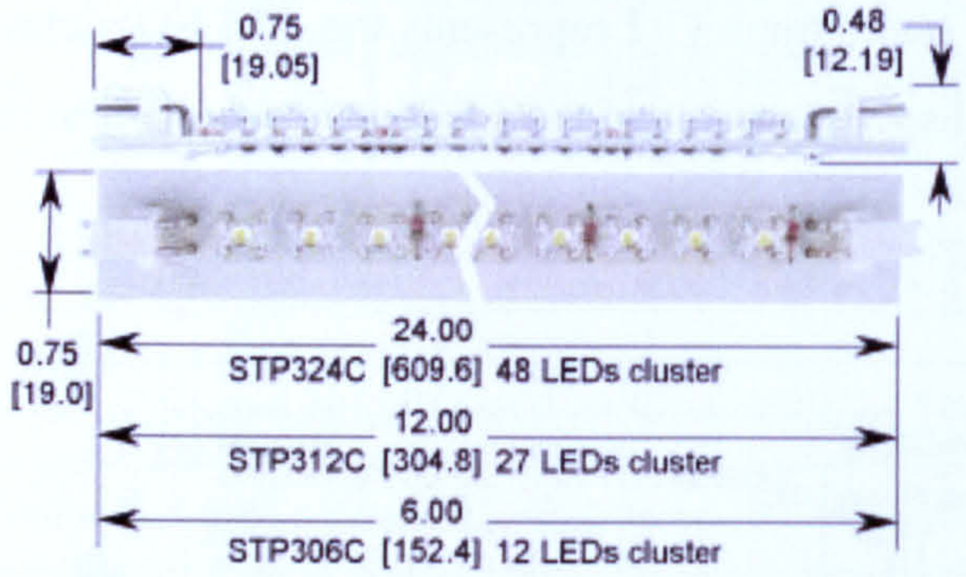


**(a)**

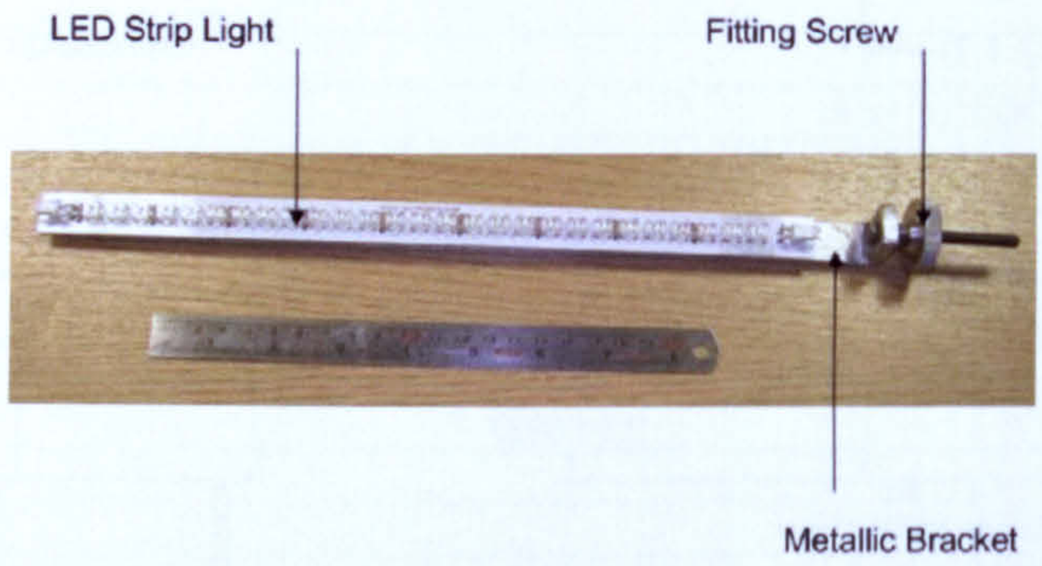


**(b)**

**Photograph C-2: Image for the STP312C-2CW-012V white light LED array.**

| Parameter | MAX. | Unit |
|---|---|---|
| Power Dissipation | 220 | mW |
| Peak Forward Current<br>(1/10 Duty Cycle, 0.1ms Pulse Width) | 100 | mA |
| Continuous Forward Current | 20 | mA |
| Derating Linear From 50°C | 0.4 | mA/°C |
| Reverse Voltage* | 5 | V |
| Electrostatic Discharge (ESD) | 150 | V |
| Operating Temperature Range | -20°C to +80°C | |
| Storage Temperature Range | -30°C to +100°C | |
| Lead Soldering Temperature [4mm (.157") From Body] | 260°C for 5 Seconds | |

* VR rating tested for each individual chip

**Table C-2: Absolute maximum ratings at ambient temperature 25°C for the LED's.**

| Paraın eter | Symbol | Min. | Typ. | Max. | Unit | Test Condition |
|---|---|---|---|---|---|---|
| Luminous Intensity | $I_v$ | 3000 | 3500 | --- | mcd | $I_f$=20mA (Note 1) |
| Viewing Angle | $2\theta_{1/2}$ | --- | 70 | --- | Deg | (Note 2) |
| Forward V oltage | $V_f$ | --- | 9.5 | 11 | V | $I_f$=20mA |
| Reverse Current | $I_R$ | --- | --- | 50 | μA | $V_R$=5V |
| SCP | --- | --- | --- | --- | --- | --- |
| Lumens | --- | --- | --- | --- | --- | --- |
| Radiant Intensity | --- | --- | 11100 | --- | μW/sr | --- |

**Table C-3: Electrical optical characteristics at ambient temperature 25°C for the LED's.**

The choice of the illumination source greatly affects the hue versus temperature calibration of the TLC material. The spectrum for the white light LED illustrated in figure C-3, typically provides high sensitivity of the TLC in the visible range. There is no significant UV component present in the spectrum, this prevents the degradation of the liquid crystal and poor repeatability.

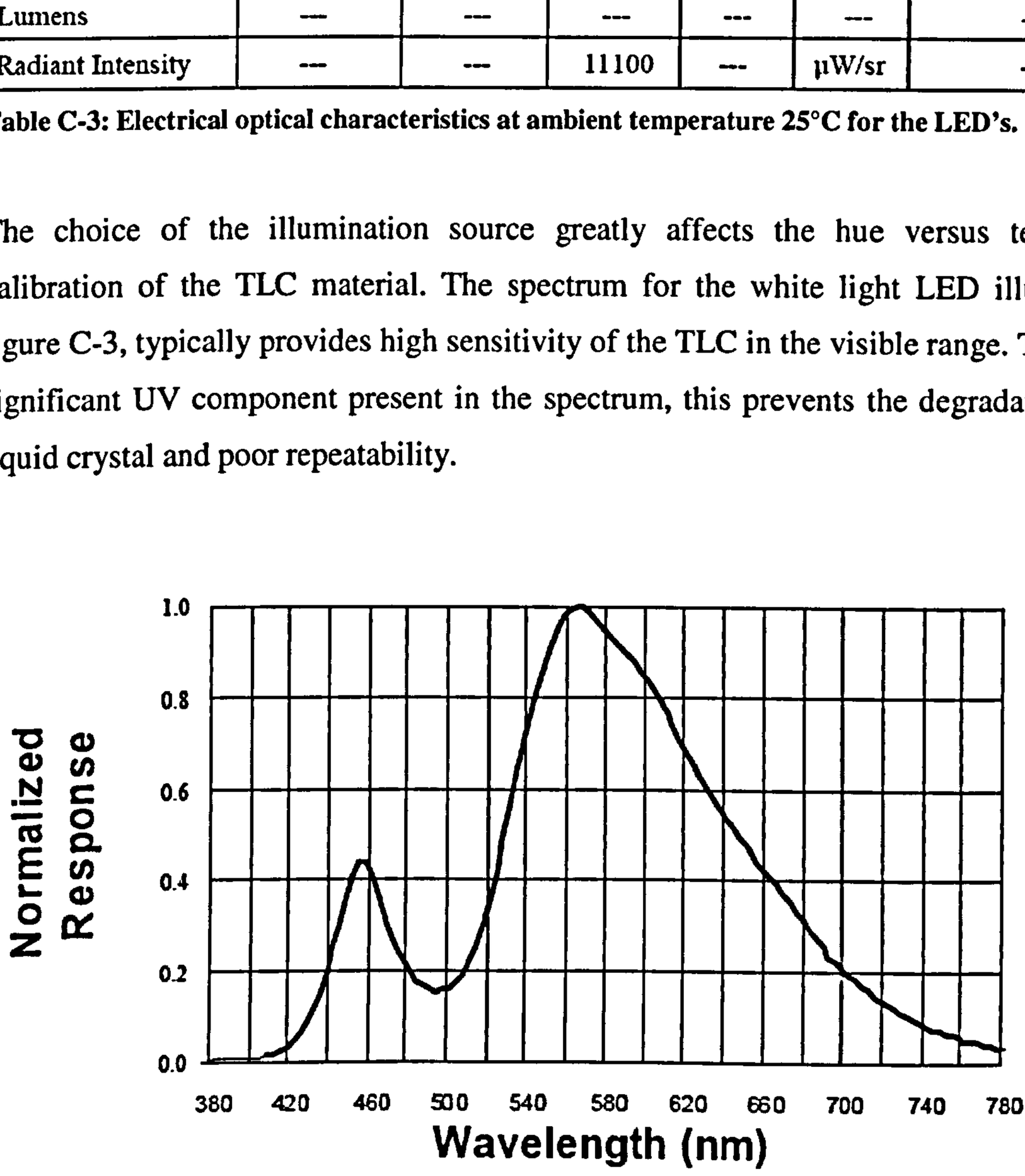


**Figure C-3: Optical spectrum drawings for the STP312C-2CW-012V white light LED array.**

# Appendix D Calibration interface and additional results

## LABVIEW interface for TempView system

This section focuses on the calibration interface realised in LABVIEW for the commercial liquid crystal thermography system, TempView (by ImageTherm Engineering, Waltham, MA, USA). Figure D-1 illustrates the graphical user interface for the calibration of TLC samples. The system is capable of both data acquisition and data processing. However, data processing was accomplished using Image Processing Toolbox in MATLAB for consistency with the calibration of clinical LCT system under consideration.

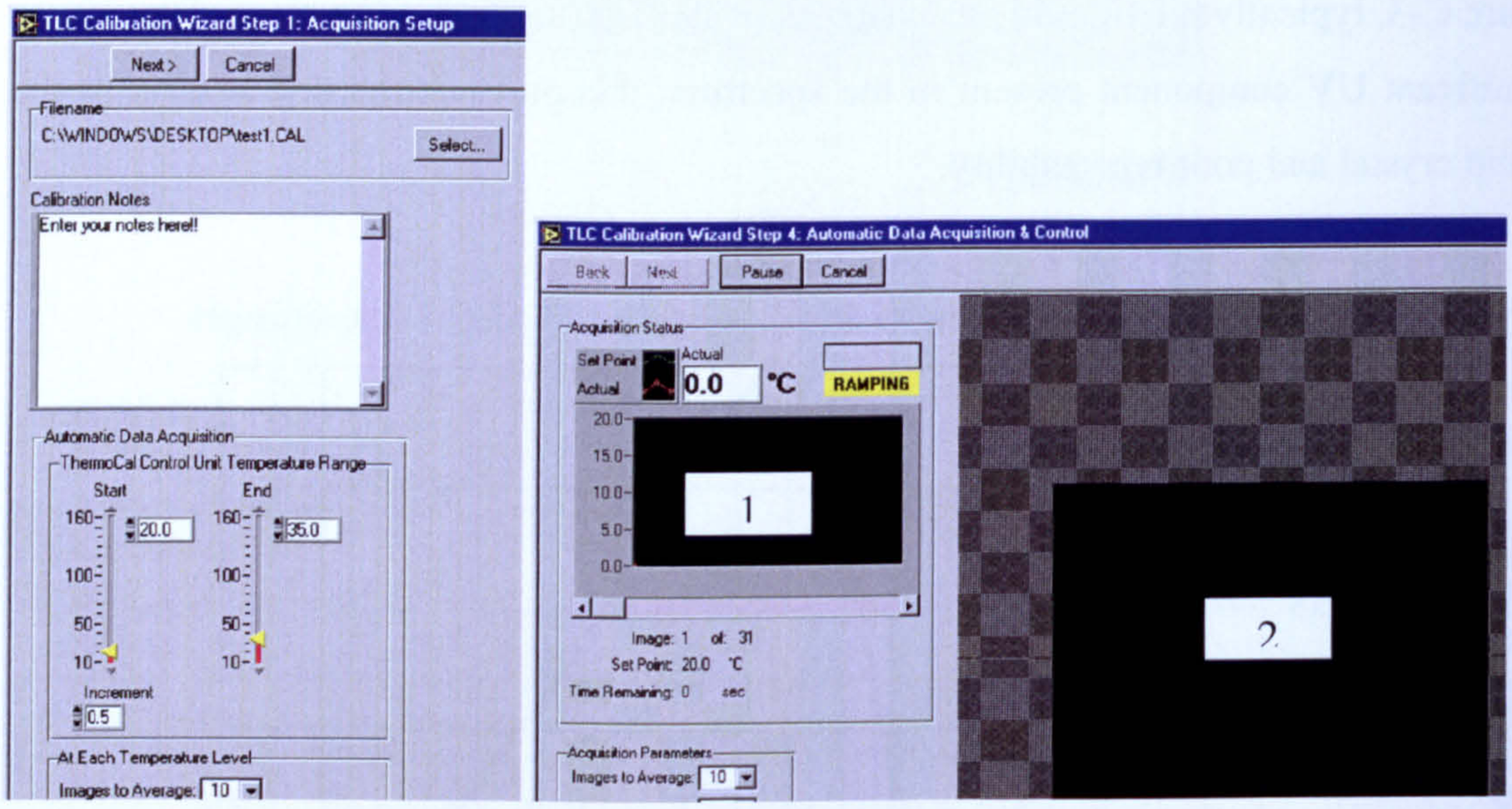


**Figure D-1: LABVIEW based graphical user interface for the thermochromic liquid crystal calibration. Image on the left shows the initial parameters for the calibration and image on the right shows the active window when the calibration is in progress. Label '1' in indicates the real time temperature curve and Label '2' indicates the real time image of liquid crystals.**

Detailed procedure for calibration is discussed in the thesis. However, some important factors are reviewed in this section.

(a) A ramp input is used for the thermoelectric unit to calibrate the TLC sample within the colour bandwidth in appropriate specified increments. The software waits for 10 seconds before capturing the image at the set point temperature for stability reasons.

(b) The time taken for a single calibration run for a TLC sample is dependent on the colour bandwidth of the sample. Typically, using the TempView system it takes 45 minutes for a R25C5W sample, 75 minutes for a R25C10W sample and 90 minutes for a R25C15W sample.

(c) The hue temperature data is made continuous before entry in order to produce a valid polynomial. The order of polynomial fit is different for different colour bandwidths of the TLC material. The order of the fit is chosen by investigating the goodness of fit parameters and analysis of residuals. Typical parameters used to check the goodness of fit are SSE sum squared error (SSE), R-Square error, Adjusted R-Square error, and Root mean square error (RMSE). Ideally, the SSE and RMSE must be zero and R-square values must be 1 for a perfect fit (Mathworks 2002). The 95% confidence intervals are also plotted for the fit. The goodness of fit can also be visually assessed by with width of the 95% confidence intervals.

(d) The usable range of TLC sheets or emulsion is reduced when using the polynomial fitting approach. Secondly, the sensitivity of is not constant and varies in red, green and blue regions of the calibration curve. This is a limitation of TLC and an appropriate formulation can be selected dependent on the application.

## Results for wideband TLC, emulsion based TLC and latex based TLC

### R25C10W TLC sheet

Figures D-2 and D-3 provide hue versus temperature calibration curves for the R25C10W TLC sheet. A noticeable difference between the wideband and narrow band TLC material is the higher discontinuity in hue towards the event temperature for the former. This has a significant role in selecting the optimum TLC material for the intended final application.

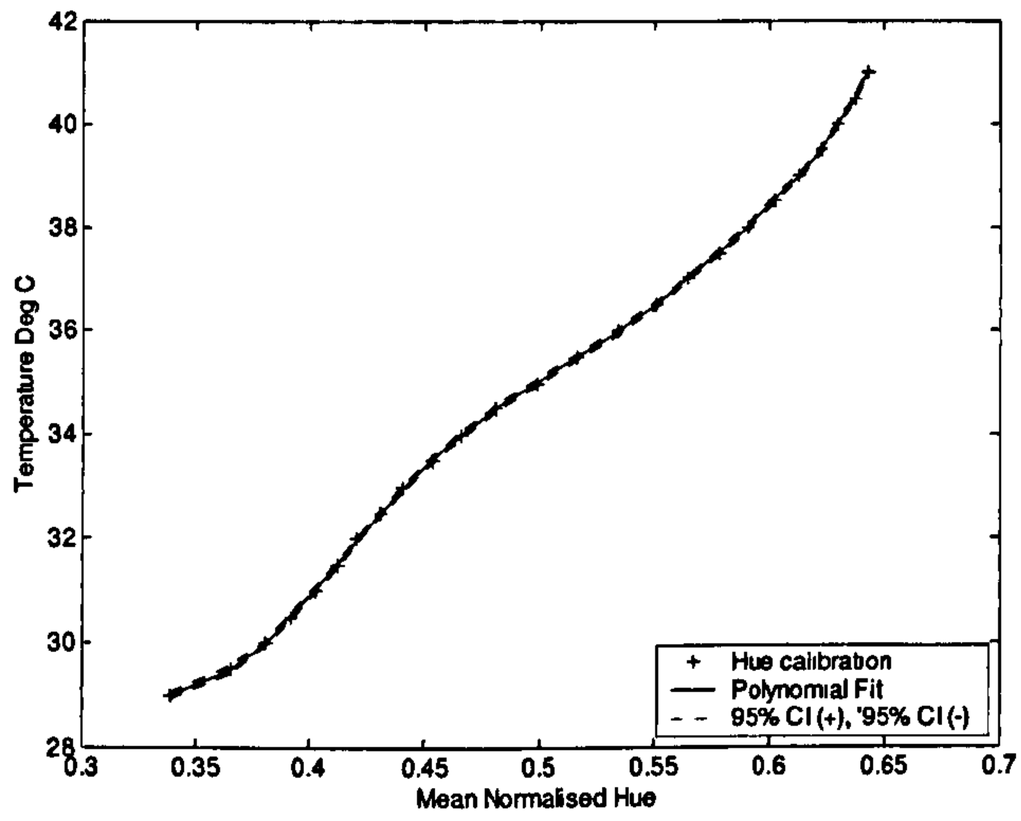


**Figure D-2: Calibration curve for a TLC sheet material R25C10W. Here the mean normalised hue is based on n=5 samples.**

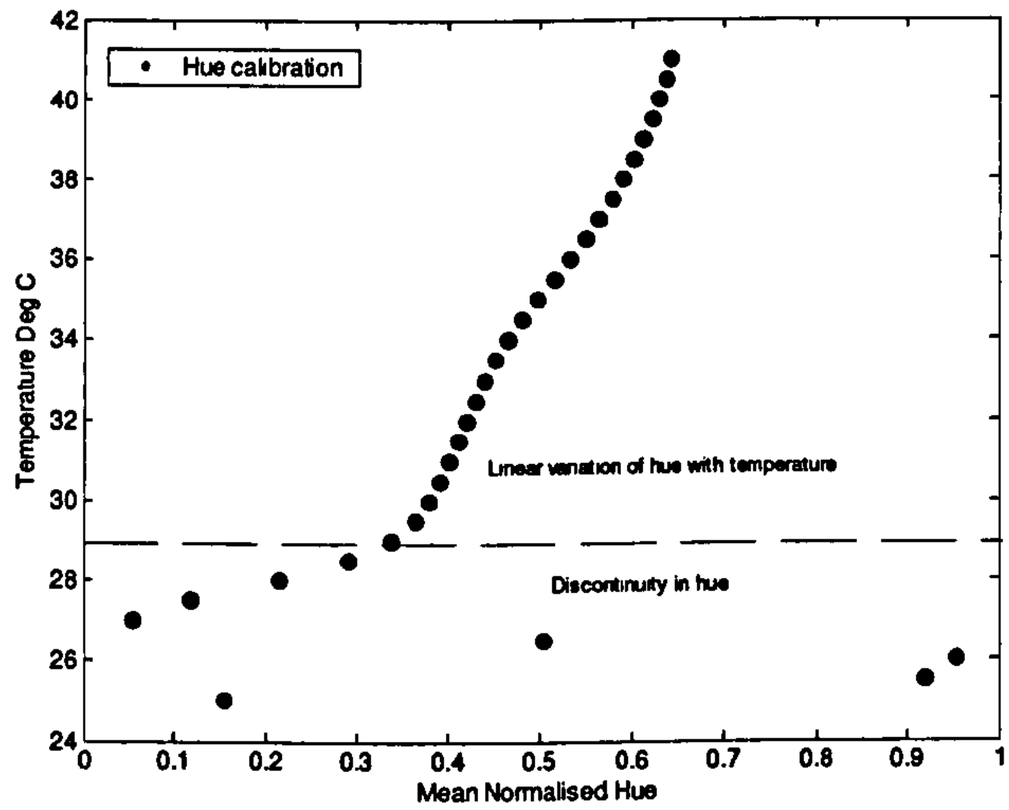


**Figure D-3: Illustration of discontinuity in hue for R25C10W TLC sheet. This must be removed before fitting an appropriate polynomial.**

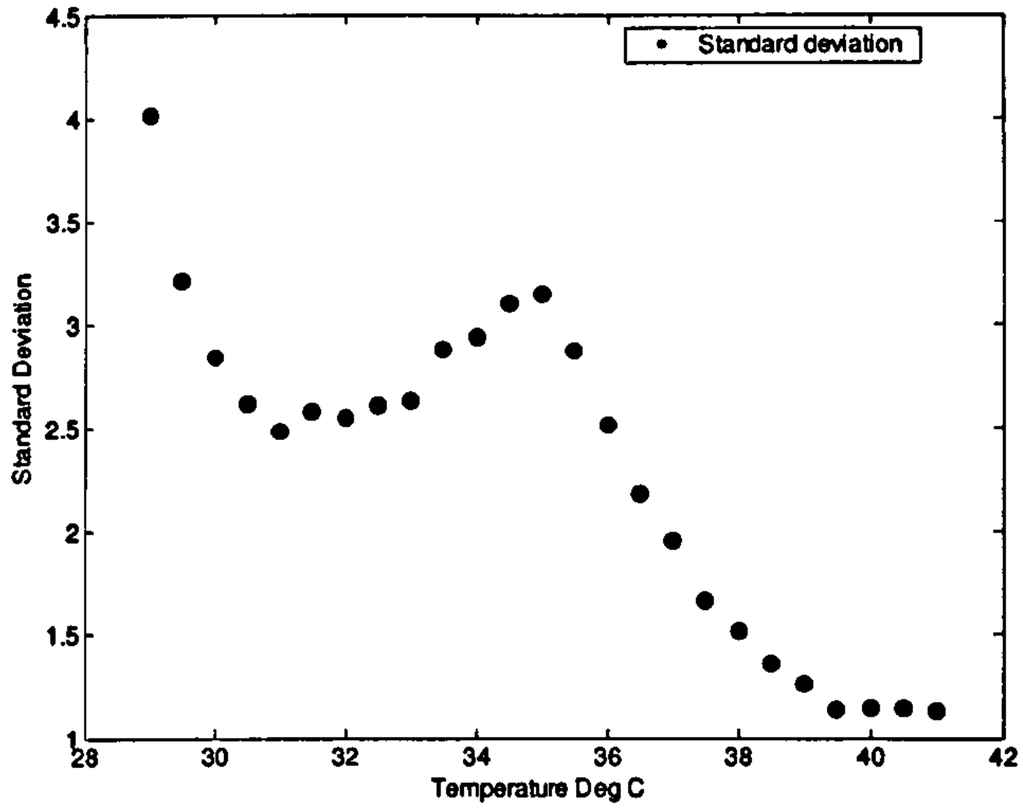


**Figure D-4: Standard deviation in the mean normalised hue values used to produce figure D-2. A similar increase in the measured variance is seen to occur at the colour transition temperature as observed for R25C5W TLC sheet.**

Figure D-4 shows the standard deviation of the hue for 5 samples evaluated in figure D-2.

## R25C15WTLC sheet

Figures D-5 and D-6 provide hue versus temperature calibration curves for the R25C15W TLC sheet. Higher discontinuity in the R25C10W and R25C15W TLC sheets, suggests that these may not be an ideal choice for the intended final application. The poor quality of fit in figure D-5 also supports these findings.

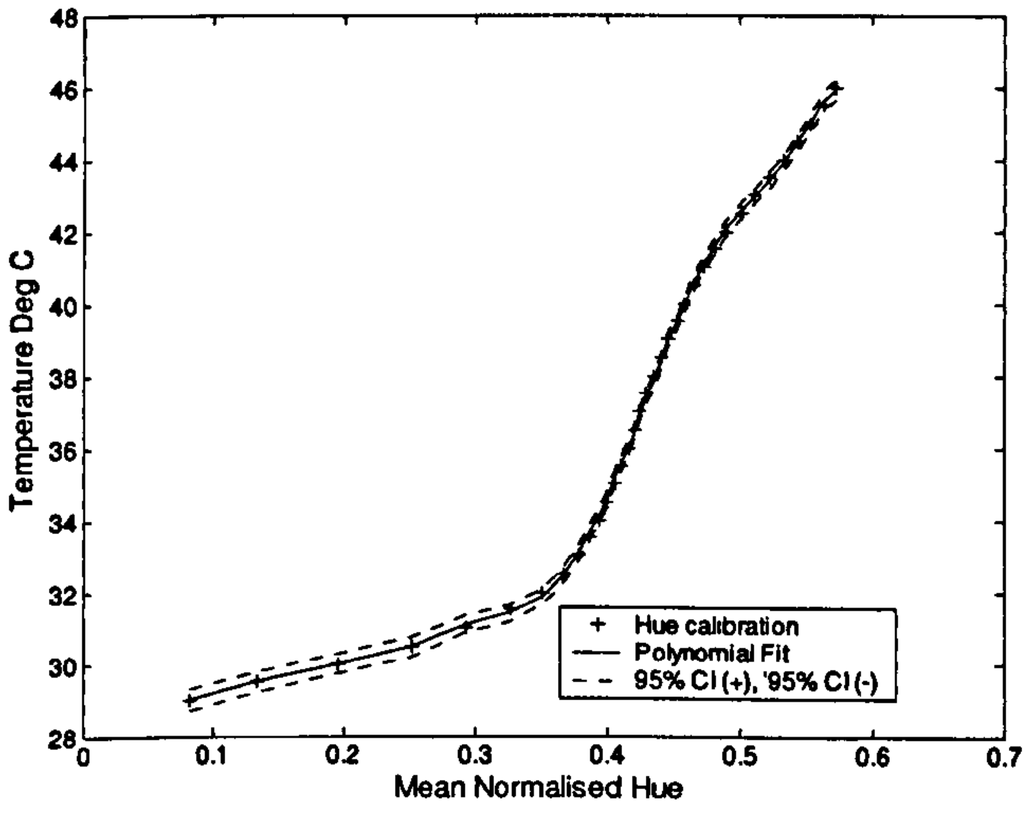


**Figure D-5: Calibration curve for a TLC sheet material R25C15W. Here the mean normalised hue is based on n=5 samples.**

Higher the discontinuity in hue, lesser will be the useful colour bandwidth of the corresponding TLC material. It must be emphasised that hue data points at corresponding temperatures are closely spaced; this may affect the temperature resolution. This is further supported with data in figure D-7 which illustrates the error bar representation of the calibration data. The upper and lower limits of the error bars are the standard deviation in hue as shown in figure D-8.

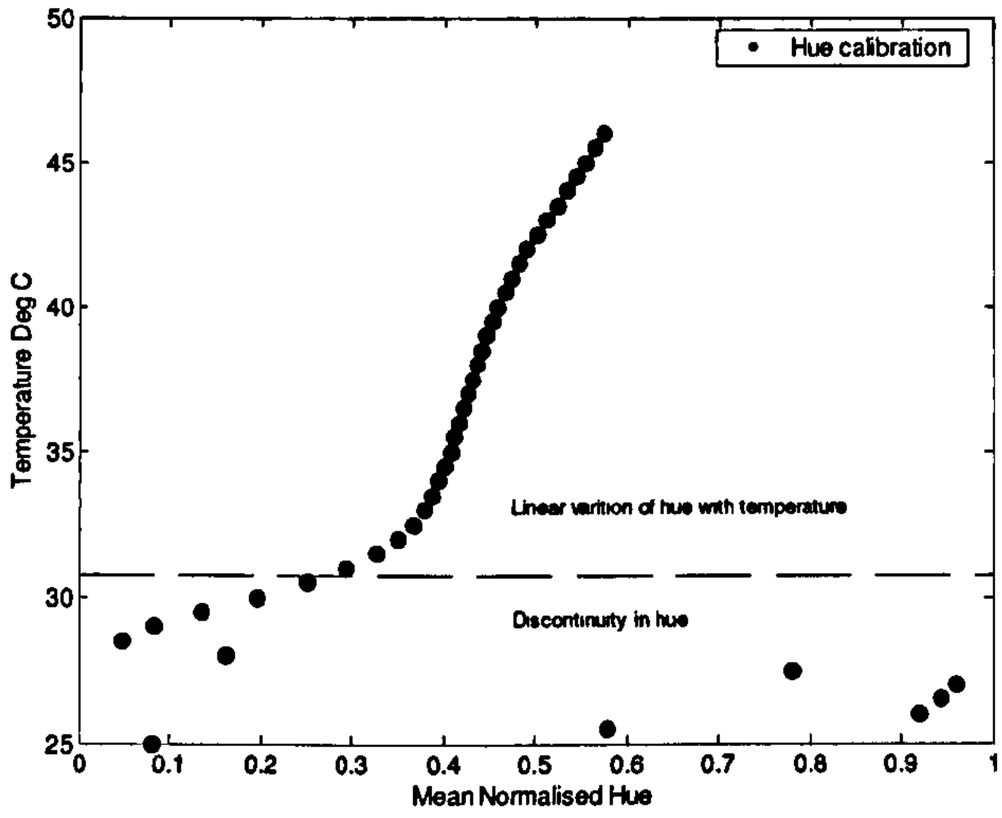


**Figure D-6: Illustration of discontinuity in hue for R25C15W TLC sheet. This must be removed before fitting an appropriate polynomial.**

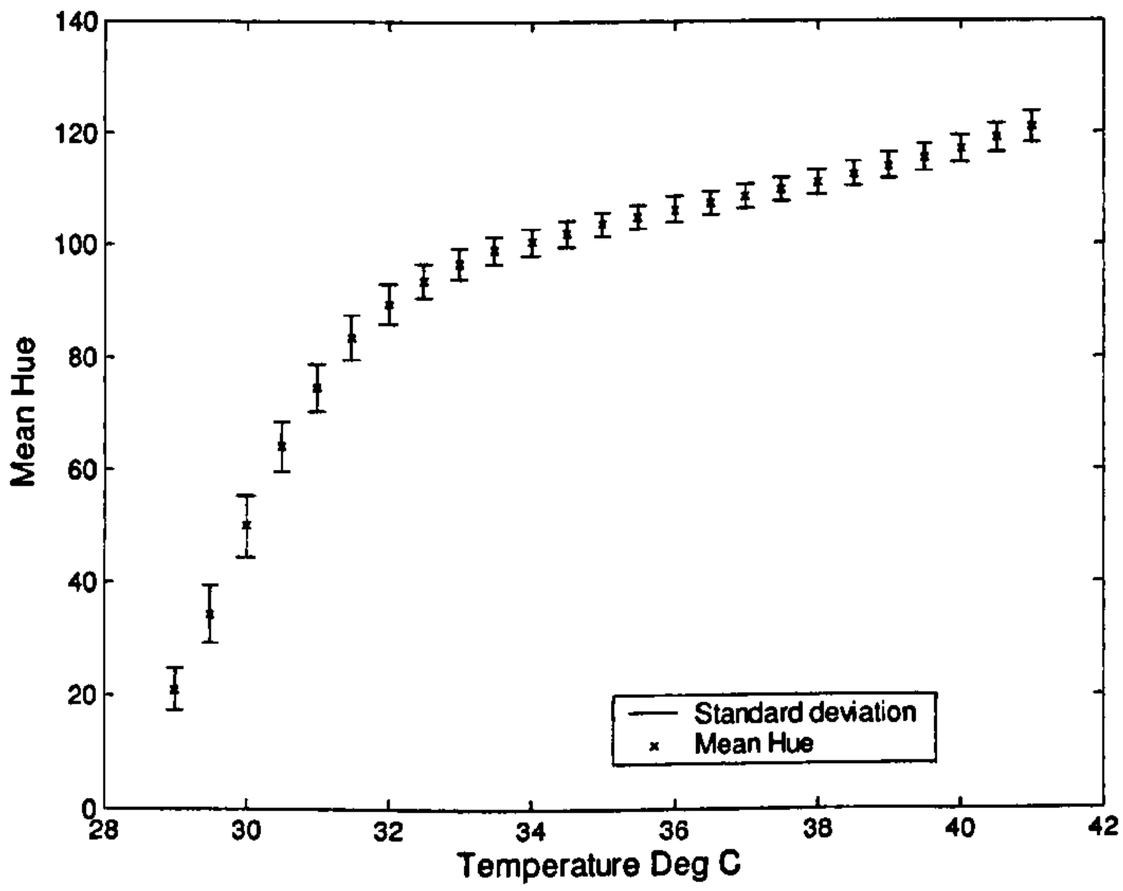


**Figure D-7: Error bar representation of the calibration data for R25C15W TLC sheet.**

Figure 4-24 shows the standard deviation of the hue for 5 samples evaluated in figure D-5.

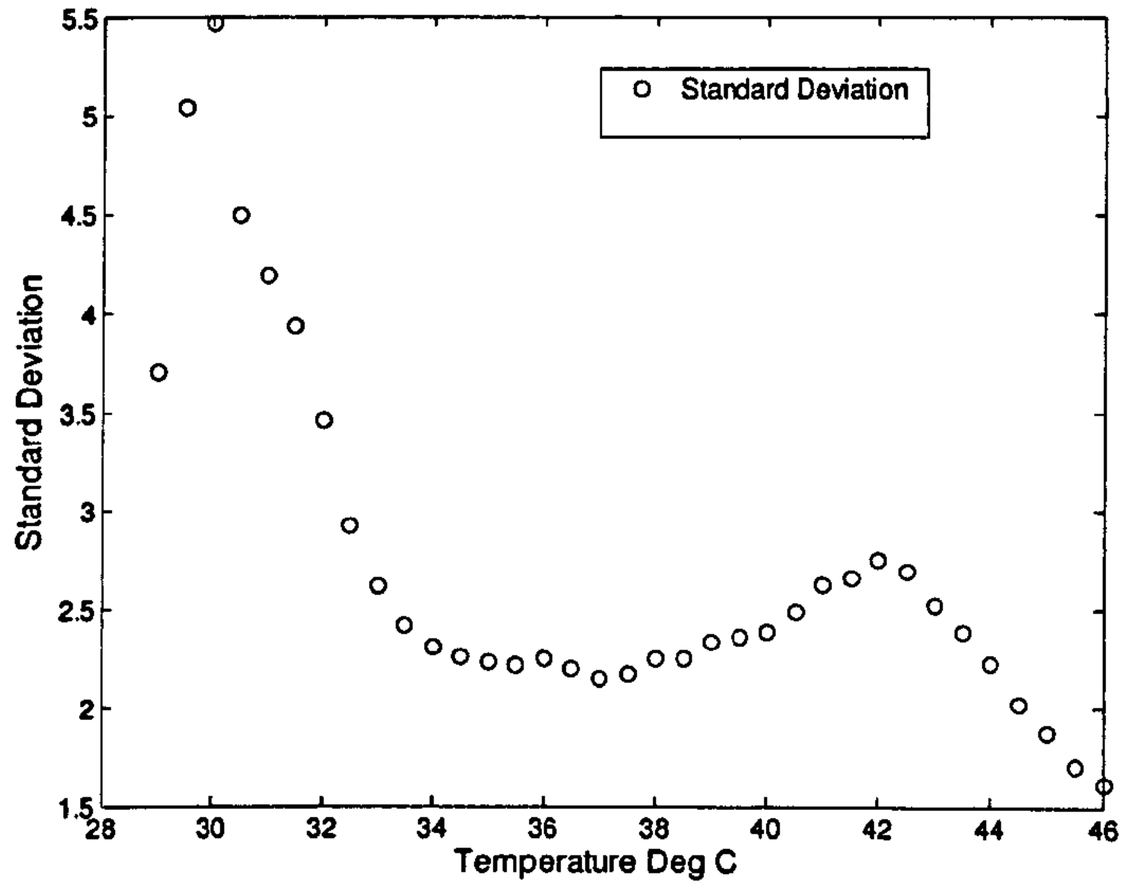


**Figure D-8: Standard deviation in the mean normalised hue values used to produce figure D-5. A similar increase in the measured variance is seen to occur at the colour transition temperature as observed for R25C5W and R25C10W TLC sheets.**

**R25C10W emulsion based TLC**

Figures D-9 and D-10 provide hue versus temperature calibration curves for the R25C10W emulsion based TLC.

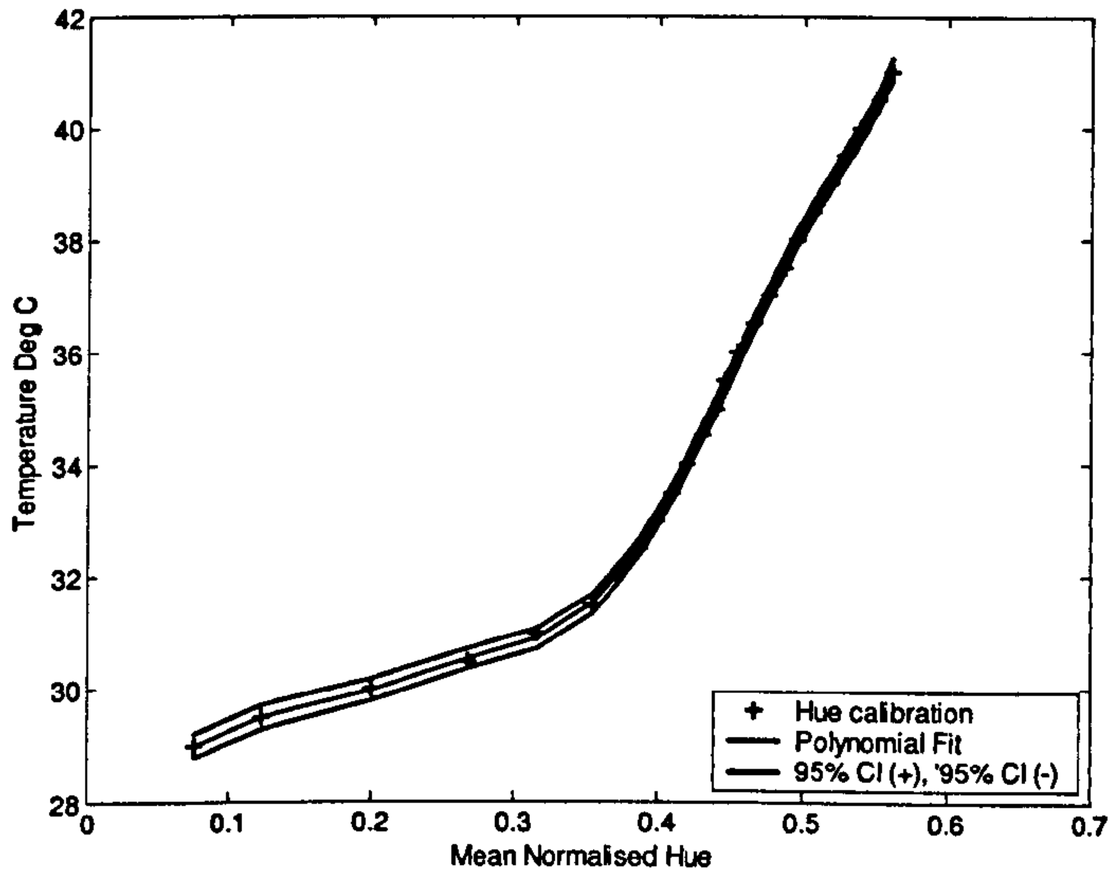


**Figure D-9: Calibration curve for an emulsion based TLC R25C10W. Here the mean normalised hue is based on n=5 samples.**

The poor quality of polynomial fit can be attributed to the high discontinuity in hue as shown in figure D-10. The uncertainty is calibrating the TLC paints is evidenced by the high standard deviation in measured hue as shown in figure D-11.

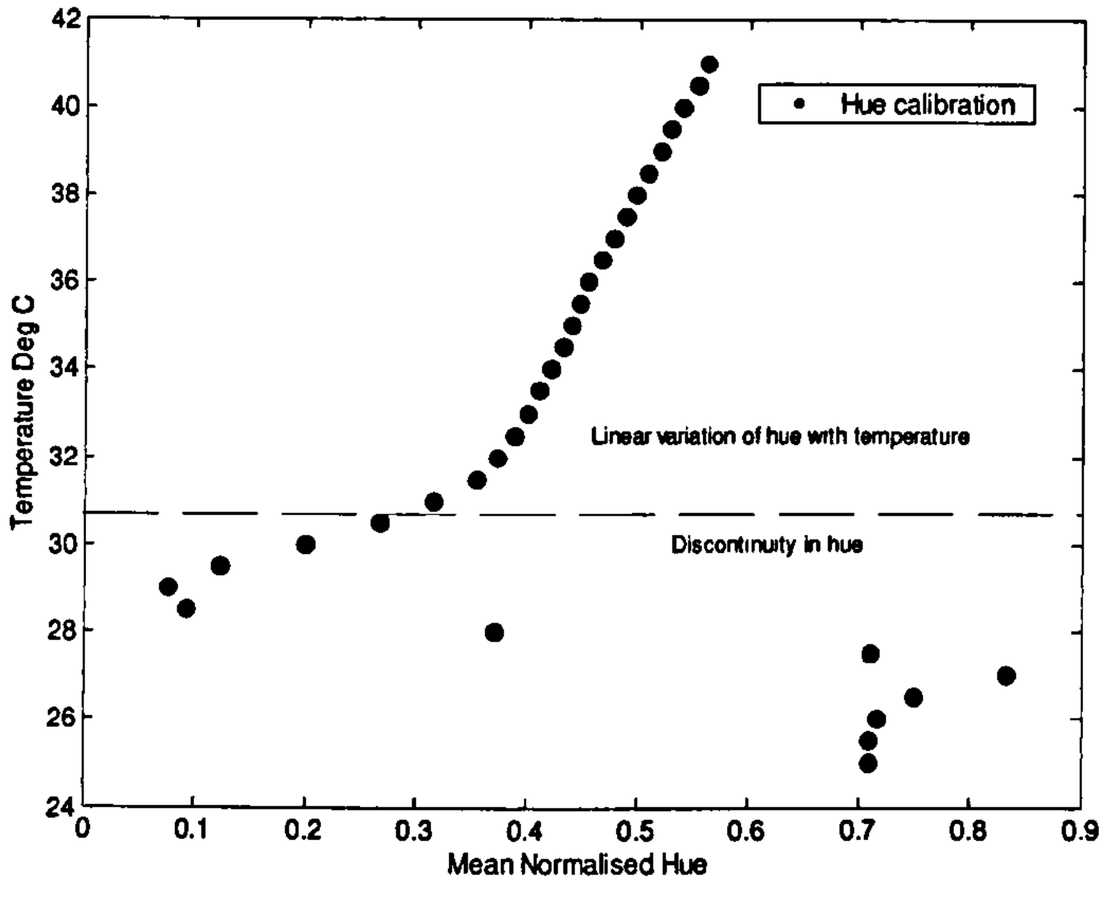


**Figure D-10: Illustration of discontinuity in hue for R25C10W emulsion based TLC. This must be removed before fitting an appropriate polynomial.**

Ideally, all the reflected light recorded by the camera must come from the liquid crystals as the black backing is considered a perfect black body. Therefore, the hue versus temperature calibration is independent of the amount of liquid crystal (spatial density or coverage factor). However, practically a large background component of reflected light can overshadow contribution of liquid crystal component resulting in hue attenuation. The background component comprises of the binder material, encapsulation material and black paint. It must be noted that along with the coverage factor, other factors that contribute the hue versus temperature calibration are illumination source, spectral distribution of background and the camera electronics. Due to these reasons, the colour response for sprayable paint is poor in comparison with the TLC sheet

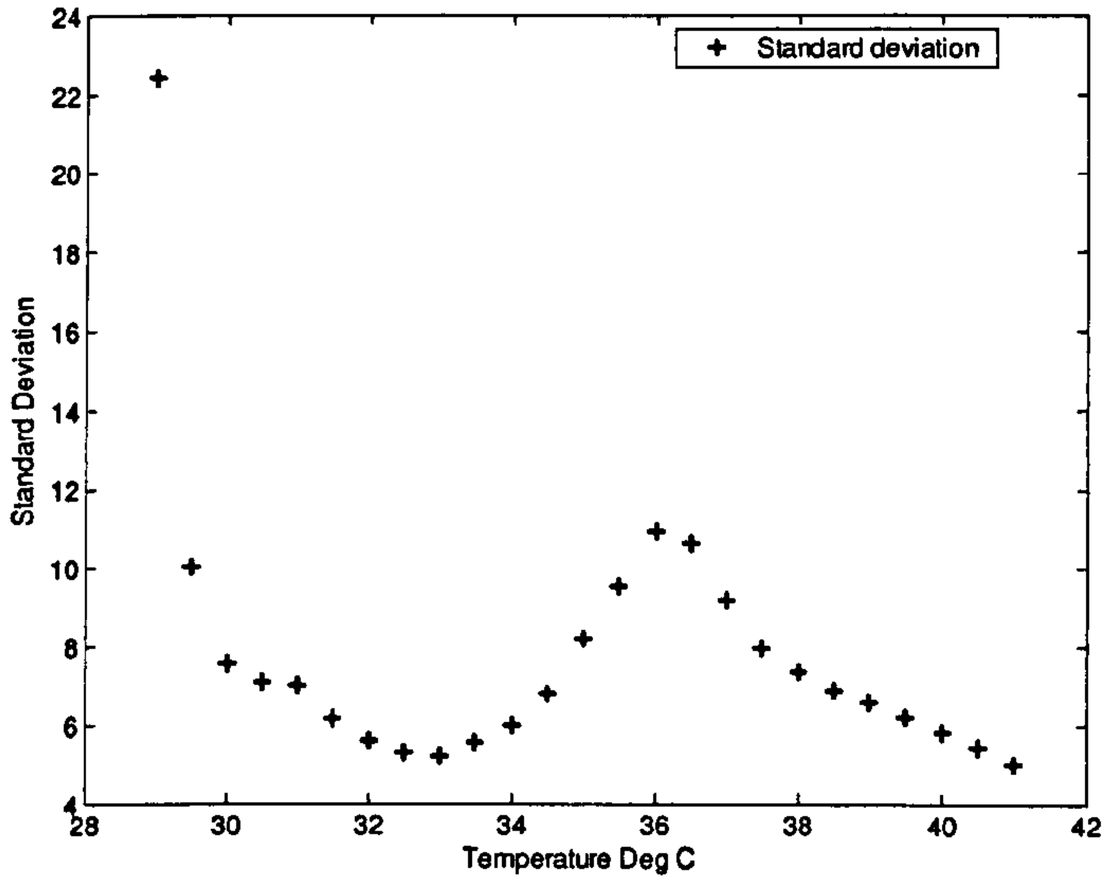


**Figure D-11: Standard deviation in the mean normalised hue values used to produce figure D-9. The standard deviation in numerically higher for the emulsion based TLC as compared to TLC sheets.**

TLC sheets which have better and uniform coverage areas as compared to the TLC surfaces prepared manually. Microscopic analysis can be used to examine the coverage factor as discussed in the thesis. Background subtraction is commonly used to collapse calibrations for regions of differing TLC coverage factors with the same illumination source (Anderson 1999).

**Latex based TLC**

Figure D-12 provide hue versus temperature calibration curves for the latex based TLC material.

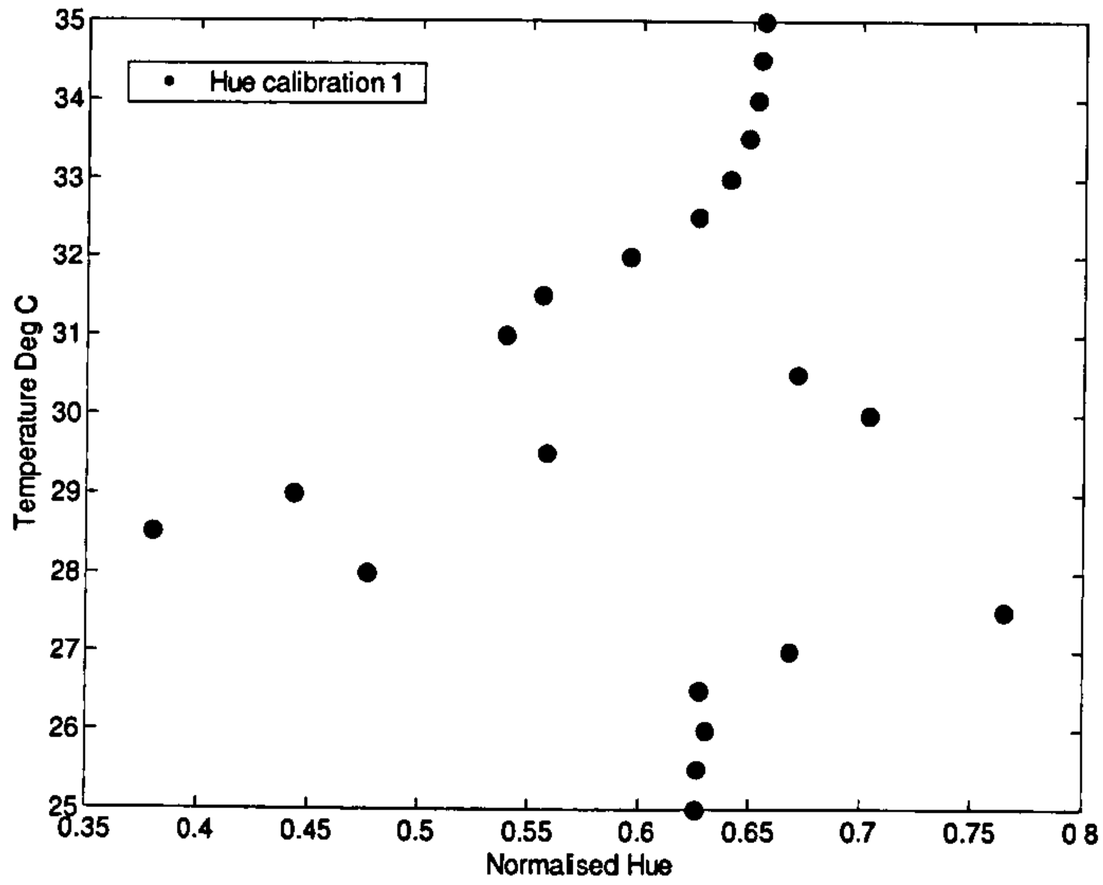


**Figure D-12: Calibration curve for latex based TLC material.**

High standard deviation leads to uncertainty in calibrating latex based TLC using the hue versus temperature approach. The random distribution of hue with respect to temperature can be attributed to the physical properties of latex. This issue is further addressed in the microscopic analysis of TLC materials. Due to the nature of the latex, upon flexing it results in uncertainties in measured hue values. This may be the reason for its limited temperature resolution.

# Appendix E Neural network calibration

In this section, detailed results on neural network calibration approach are presented. The benefit of neural network approach is to achieve a hue measurement by eliminating the dependency on illumination intensity.

**Results for R25C5W TLC sheet**

Figure E-1 shows the hue versus temperature data for the repeated heating runs on single TLC sample and in figure E-2 the mean hue versus temperature for four different lighting conditions are shown. The mean hue was calculated from five different heating runs on the same sample under different lighting conditions. The repeatability of these measurements has been confirmed independently.

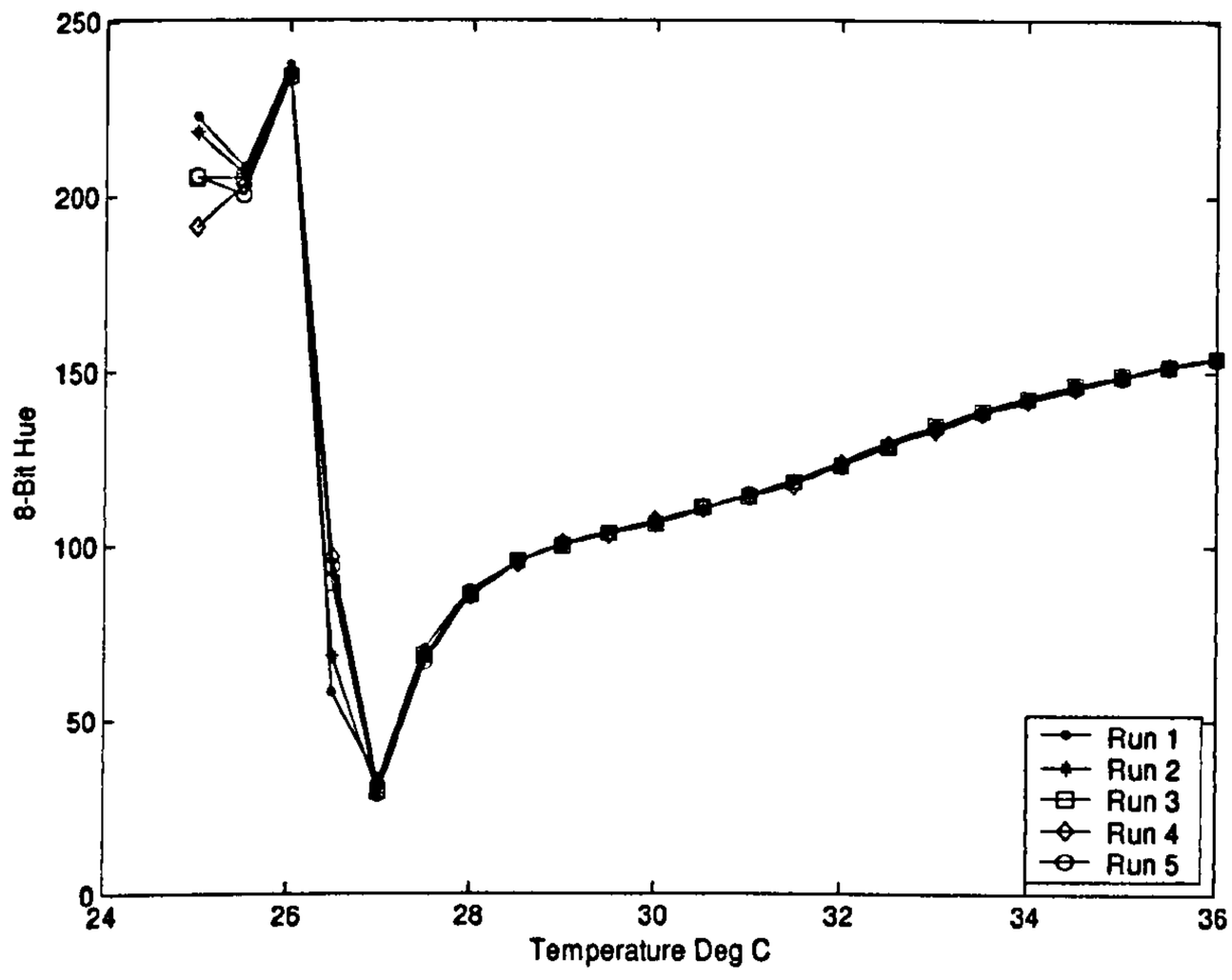


**Figure E-1: Hue versus temperature curves for 5 repeated calibration runs under similar lighting conditions.**

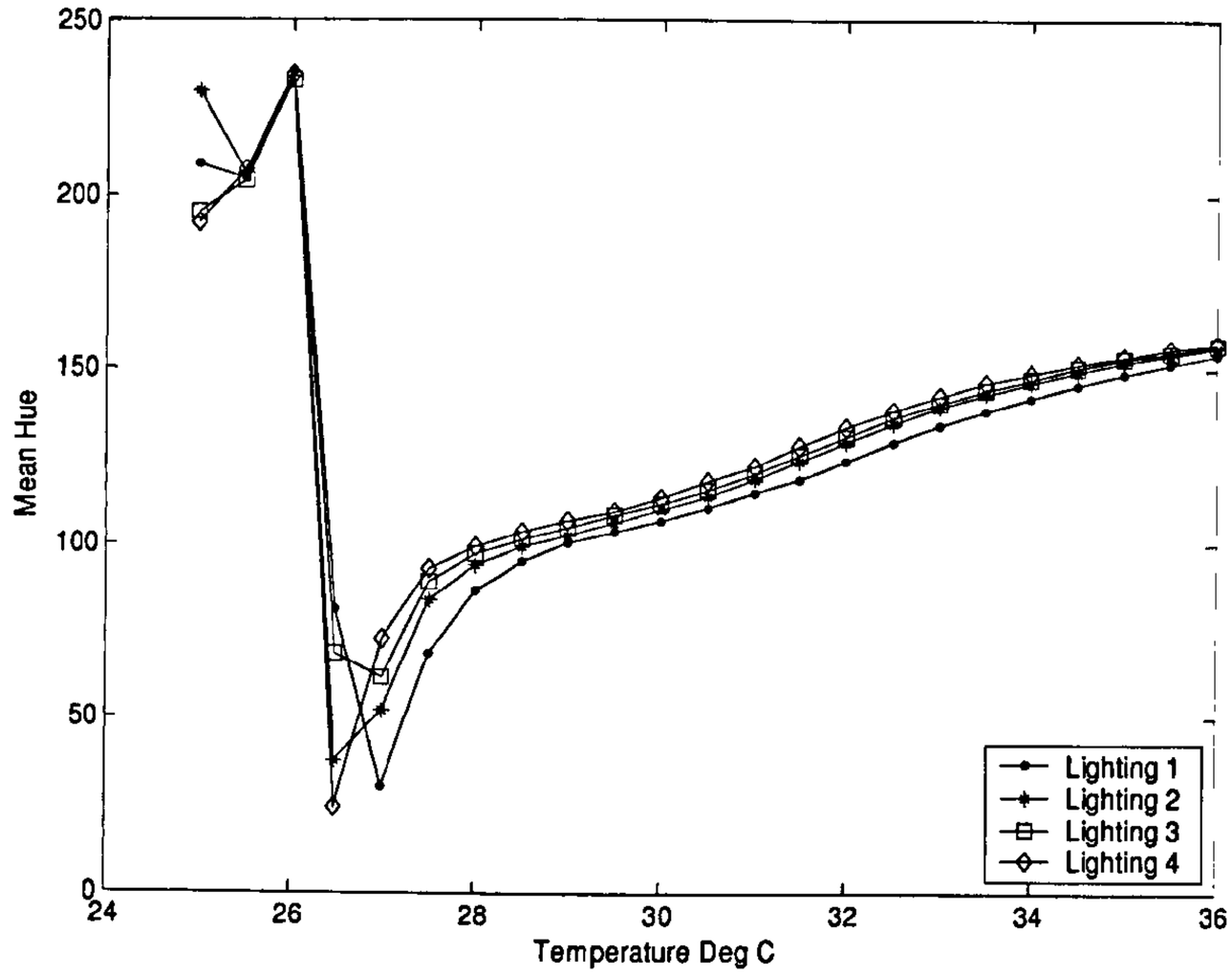


**Figure E-2: Hue versus temperature calibration dataset for four different lighting conditions. At each temperature set point, the hue value is determined from the mean of n=5 samples.**

The change in light intensity settings, spectral content of the illumination source and ambient conditions have been discussed in the thesis.

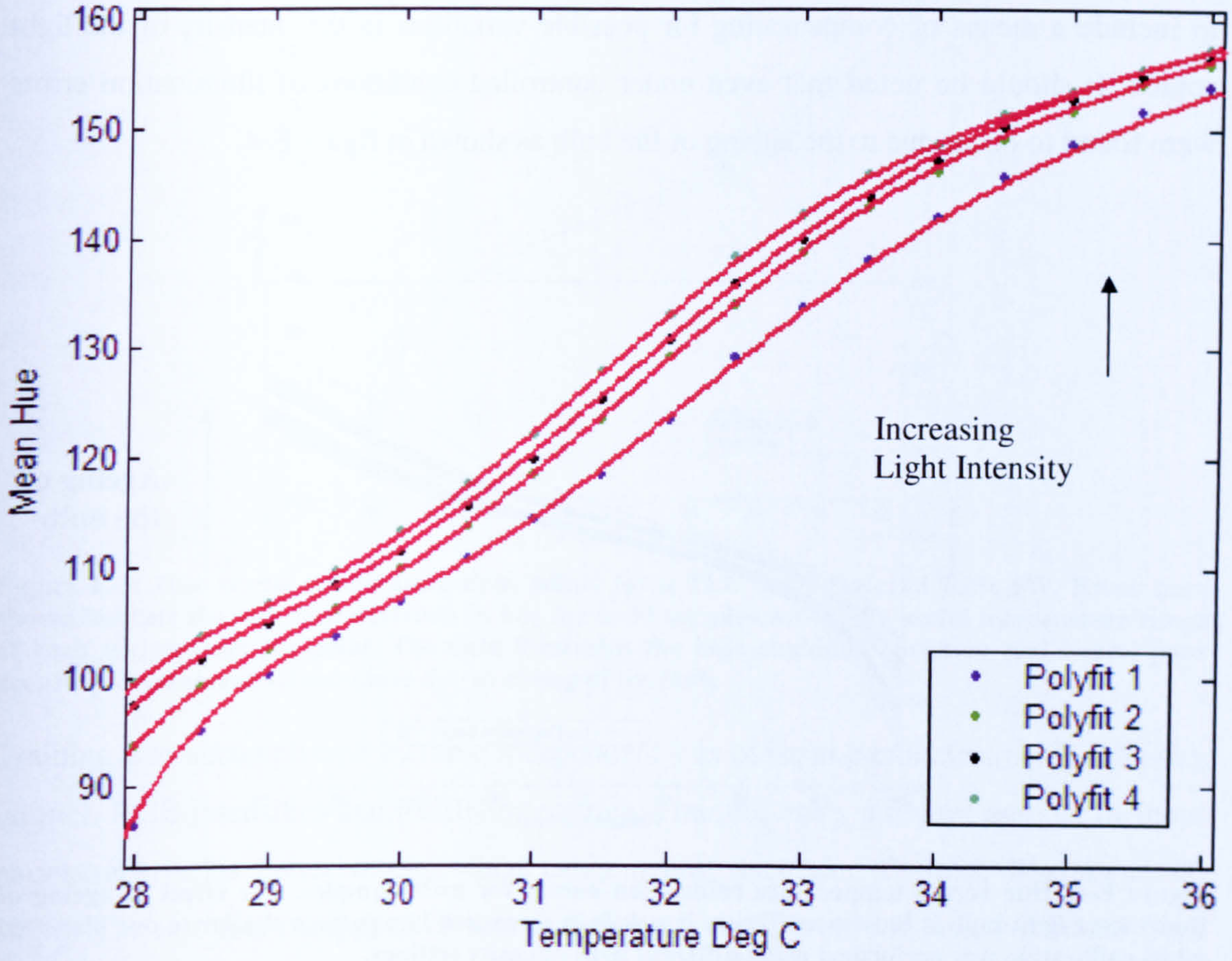


**Figure E-3: Polynomial fit for all four light intensity settings.**

It is evident from the graph in figure E-3 that there is an upward shift in hue when light intensity is increased resulting in a different calibration curve. This may produce inaccurate results as a particular hue value will be mapped onto four different temperatures leading to a maximum error in measured temperature of +/- 1° C. The graph shows that there is a 10-12% change in hue when light intensity is changed by 50%. This shift in hue produces a corresponding shift in the measured temperature producing an error. This error was quantified by comparing it with an independent measurement of the calibration plate achieved using a thermistor (uncertainty 0.1°C), which confirmed that the effect was not due to the source temperature increasing with light level (bulb self heating).

The preceding investigation confirmed the necessity for calibration of the TLC material to include a means of compensating for possible variations in the intensity of the light source. It should be noted that even under controlled conditions of illumination errors were found to occur due to the ageing of the bulb as shown in figure E-4.

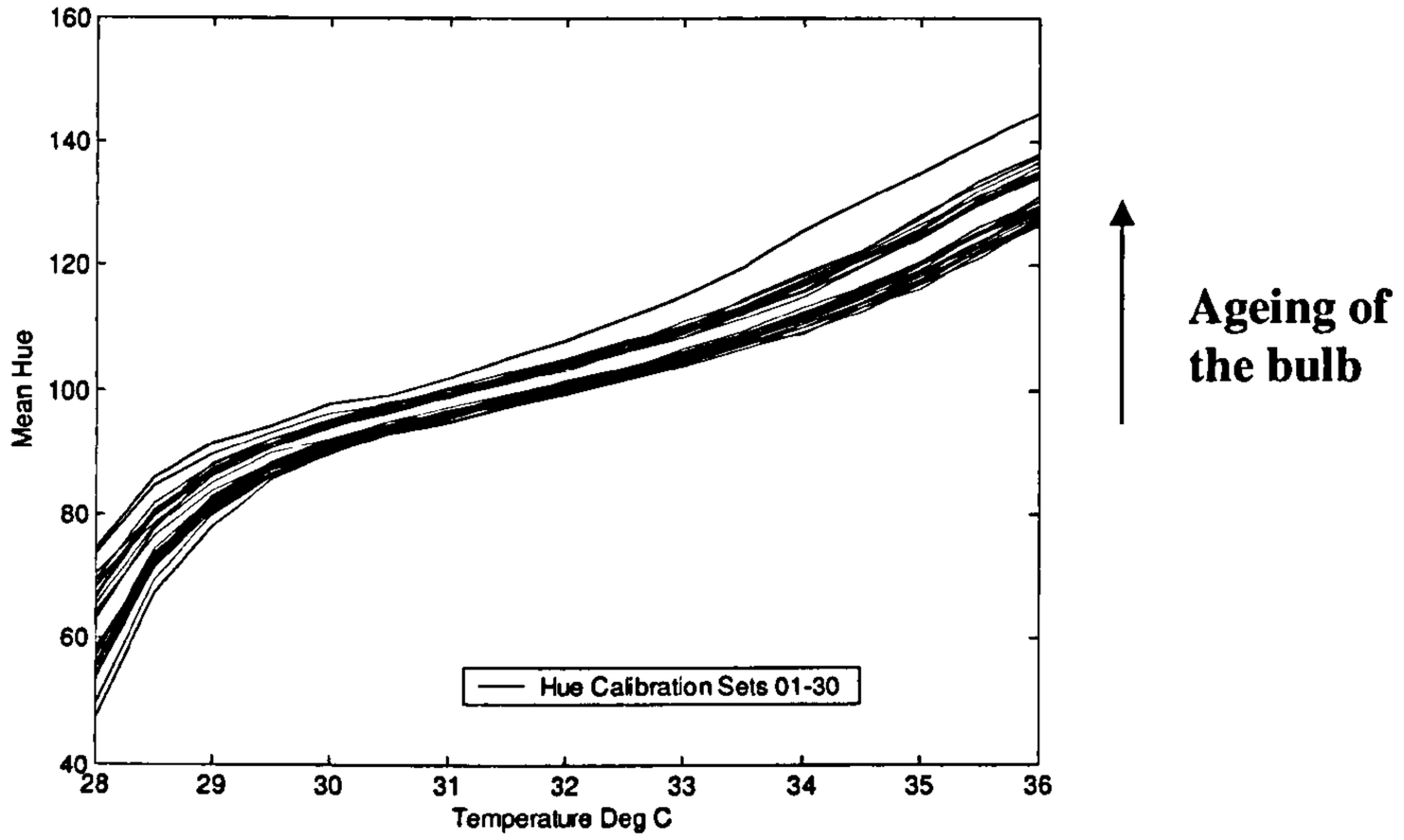


**Figure E-4: Hue versus temperature calibration curves for n=30 samples. The effect of ageing of fluorescent light bulb is illustrated. There is a shift in measured hue pattern similar to one observed when calibration was performed using different light intensity settings.**

Figure E-5 illustrates the error bars for the above data indicating standard deviation in measured hue. The correlation coefficients for n=30 samples from repeatability dataset and n=30 samples for the current dataset (bulb ageing) is 0.52, indicating poor correlation in the measured hue value under similar light intensity setting. This issue can be addressed by replacing the bulb regularly, however this cannot be done cheaply.

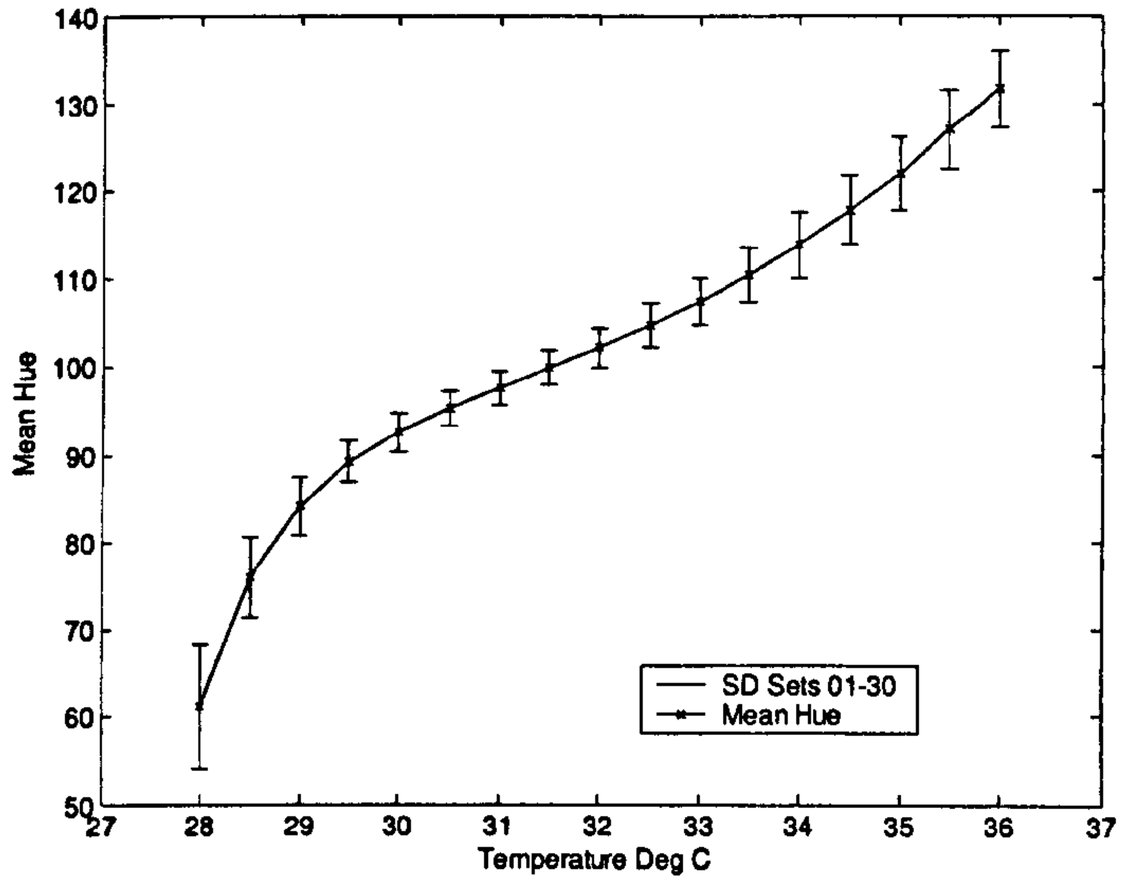


**Figure E-5: Hue versus temperature data points for a TLC sheet material R25C5W. Error bars shown indicate the standard deviation in hue for n=30 samples within the useful temperature range at each temperature set point. The data illustrates the high standard deviation and hence, poor accuracy in measured temperature due to ageing of the bulb.**

Training was accomplished by three independent sets of input parameters i.e. H intensity (alone), RGB intensities and RGBH intensities. Training using a higher number of input parameters yields better results when using neural networks (Grewal, Bharara et al. 2006). The test data comprised of four comprehensive different sets, each obtained from a different light setting to represent the entire data and for the generalisation of the system. The mean percentage errors (deviation from the ideal response), for all test points were calculated for each set of input parameters. Ideal response was defined by a straight line fit between the achieved and target dataset. The percentage error for the current approach is defined as the absolute value of mean difference in target temperature and achieved temperature at each temperature set point used for calibration for each light setting. It can be represented as,

**Percentage Error= Abs [Mean ($dT_{25,25.5,26,.....36}$)]** **Equation E-1**

Therefore, it is a single value describing the quality of calibration at all temperature points used under different lighting conditions. This error was considered to be the figure of merit for each of these input conditions.

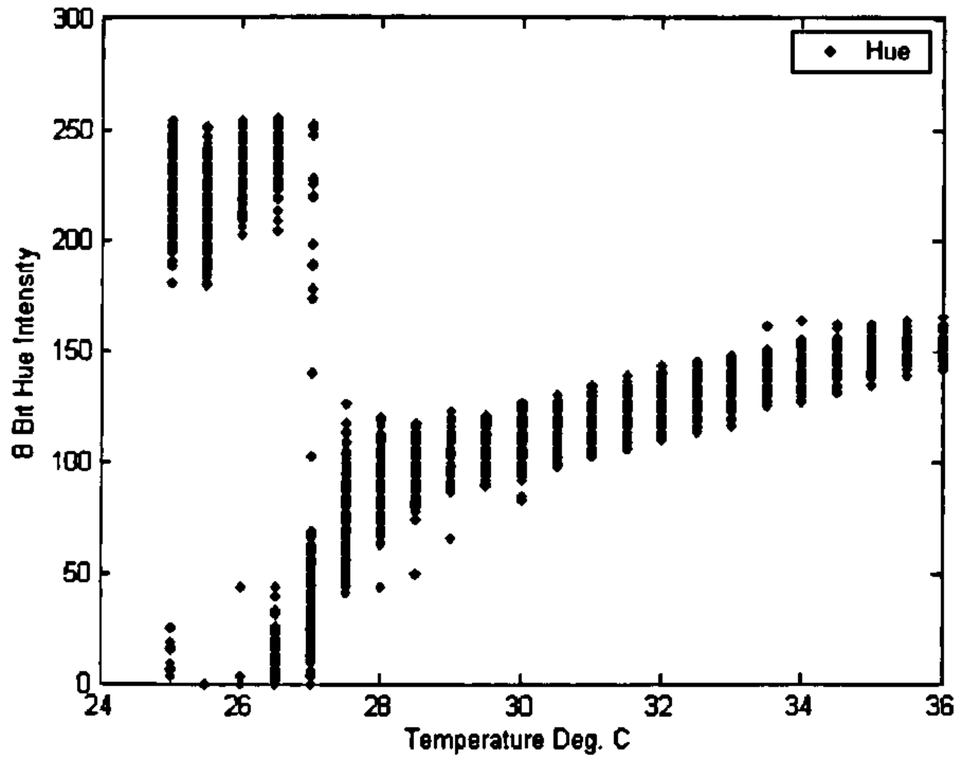


**Figure E-6: 8 bit hue intensity from 23 images each acquired at temperature set point in the 25 °C – 36°C range under one lighting condition. A total of 14400 pixels at each temperature set point were used for the training of the neural network.**

Figure E-6 illustrates the typical training dataset from one lighting condition for the R25C5W TLC sheet. Four calibration datasets from four different lighting conditions were used for training the neural network. Therefore, 8-bit hue intensity for a total of 14400x4 pixels was considered at each temperature set point. Figure E-6 illustrates training data from only one single lighting condition.

Figure E-7 shows the test results when the hue alone was used for the training. The straight line indicates the ideal response between the target output and the achieved output. The plot shows the error in the measured temperature, the total error from four different test data sets was found to be 1.28%.

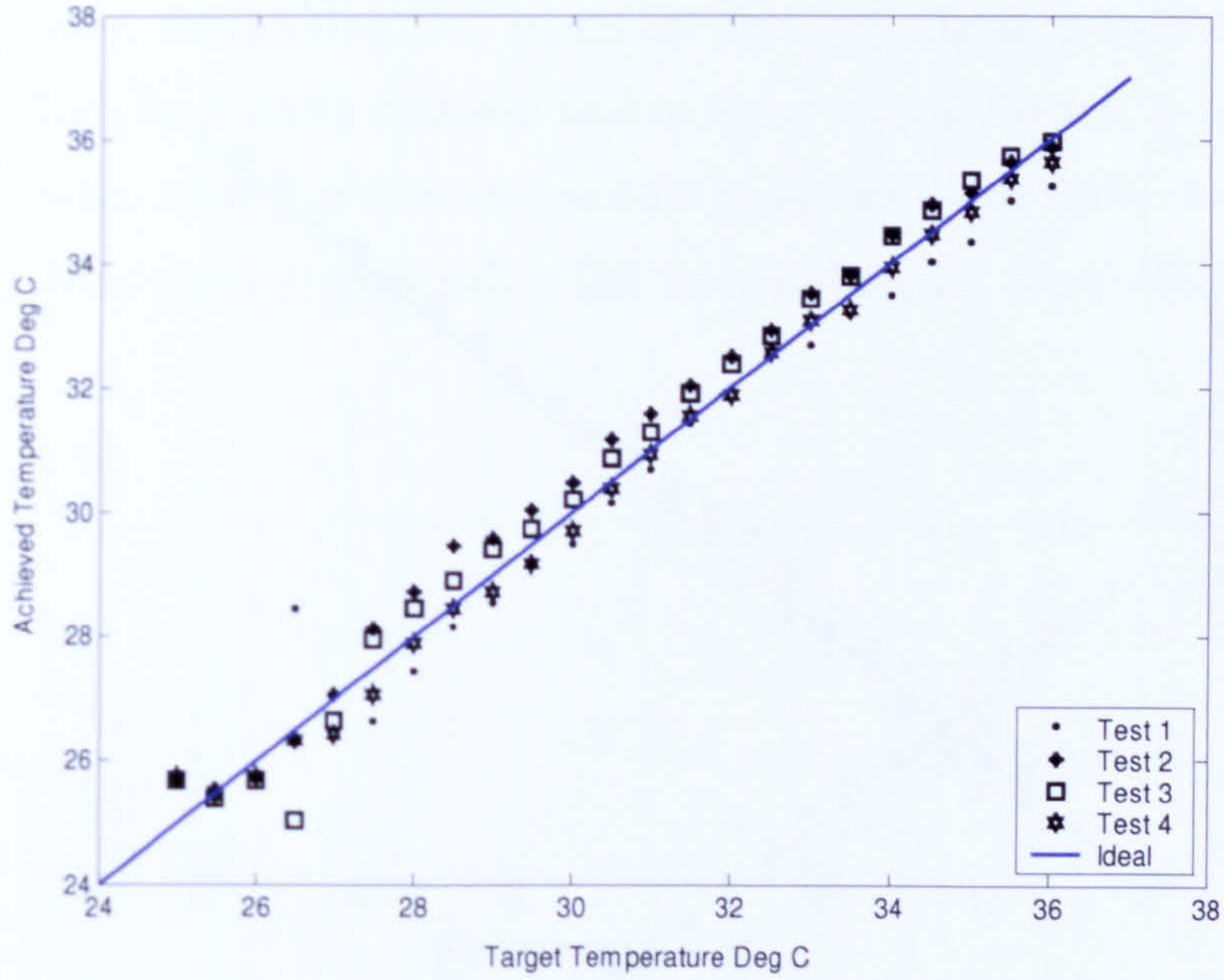


**Figure E-7: Target output versus achieved output using 8 bit hue intensity.**

The effect of increasing the number of parameters from the image data was investigated by using the hue intensity along with the RGB intensities as input data as shown in figure E-8. It is important to note that the high standard deviation in the input parameters (RGB and H) near the event temperature may affect the test results therefore the neural networks were trained only within the useful colour bandwidth of the TLC, figure E-9. The total measured error was reduced from 0.77% for entire colour bandwidth to 0.40% for the usable colour bandwidth.

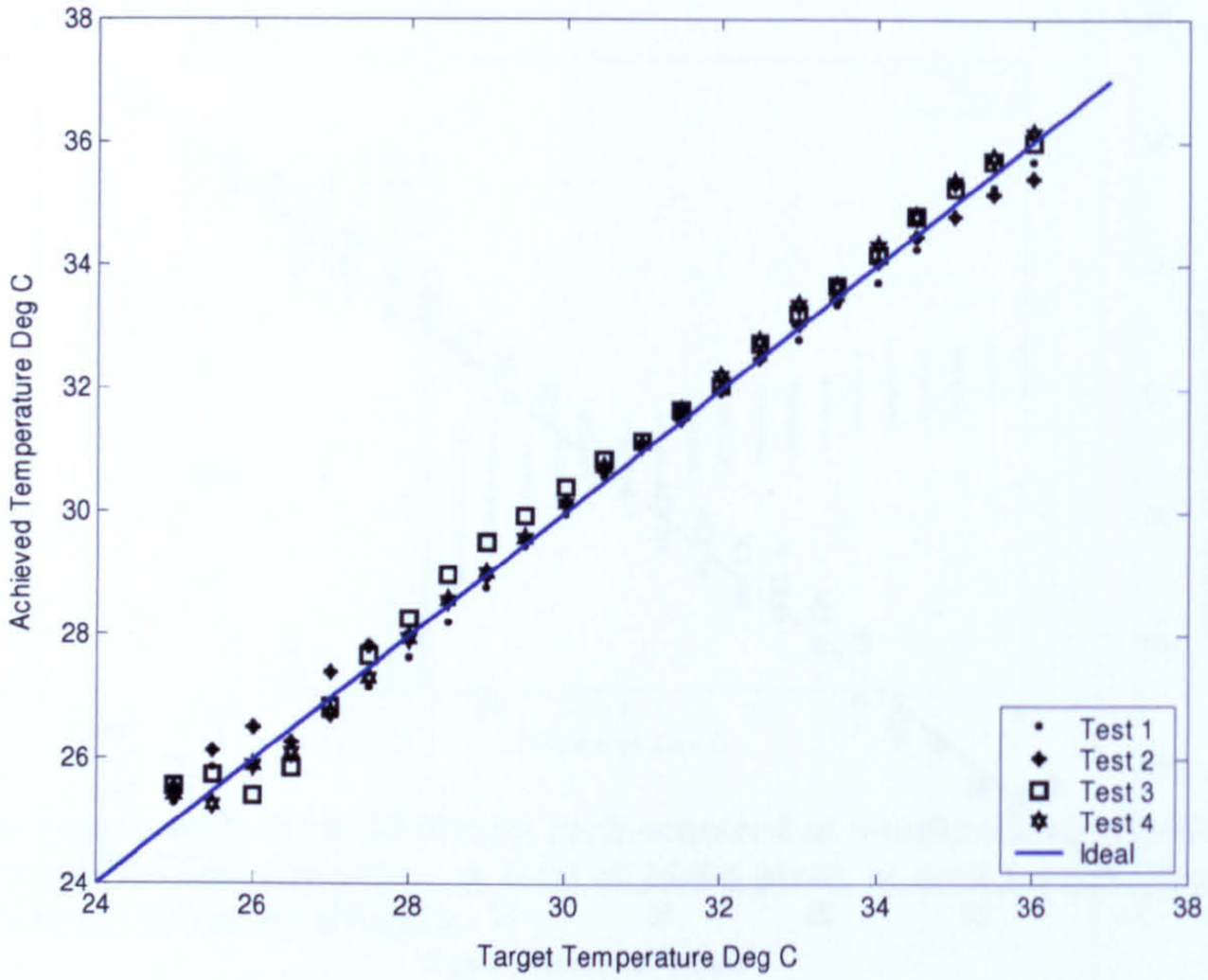


**Figure E-8: Target output versus achieved output using RGBH for entire colour bandwidth 25 °C – 36°C.**

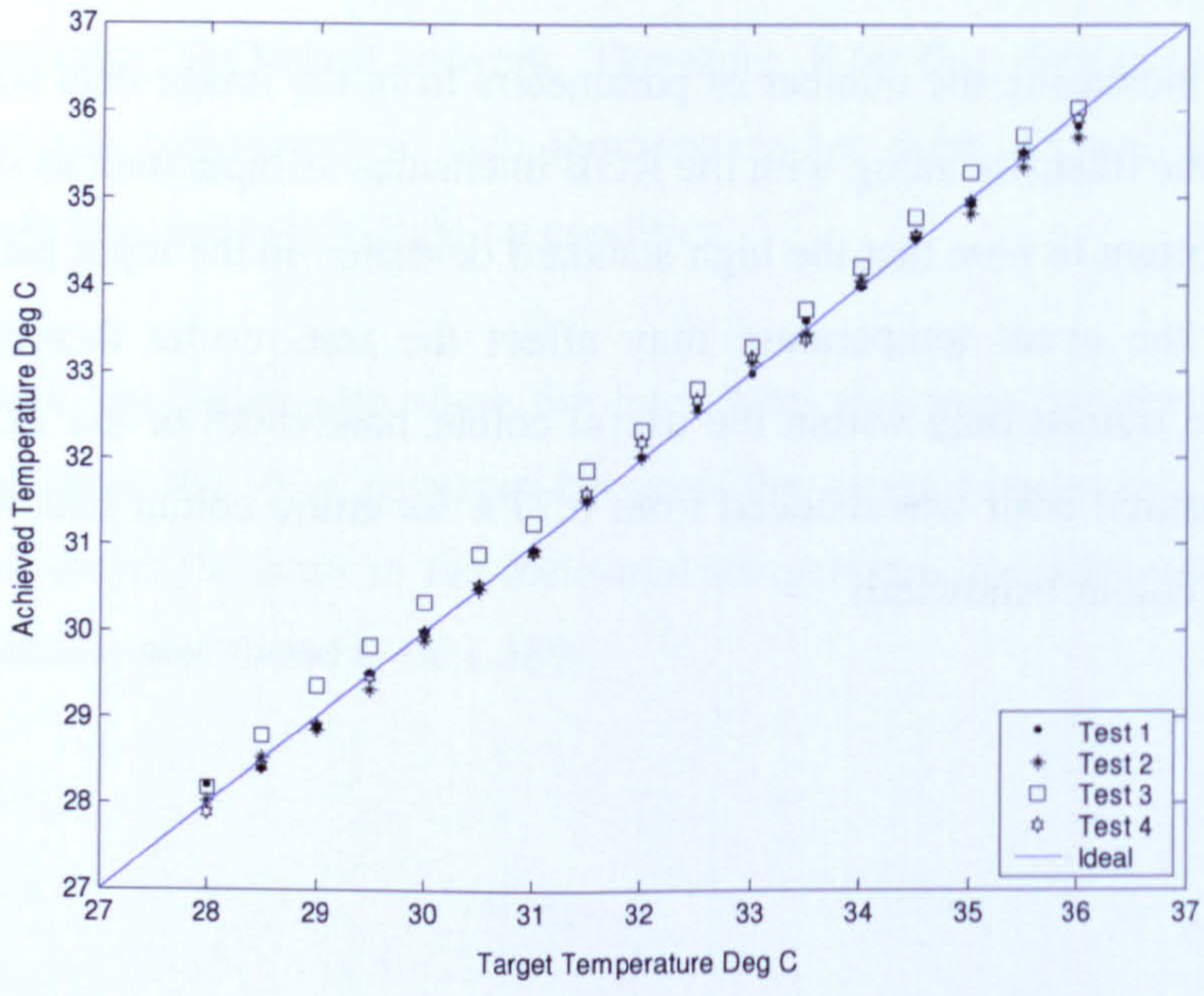


**Figure E-9: Target output versus achieved output using RGBH for useful colour bandwidth 28 °C – 36°C**

The test results from figure E-7 give the highest errors in the measured temperature when the hue alone is used for training and testing. This shows that the hue is susceptible to error in the measured temperature. Furthermore, the same hue value exists for different

temperatures when considering the effect of changing lighting intensity. Therefore, eliminating it from the training data will lead to better results. Figures E-10 & E-11 show the test results when training was done using the RGB intensities within the entire and the useful colour bandwidth respectively. The errors obtained were 0.68% and 0.38% respectively.

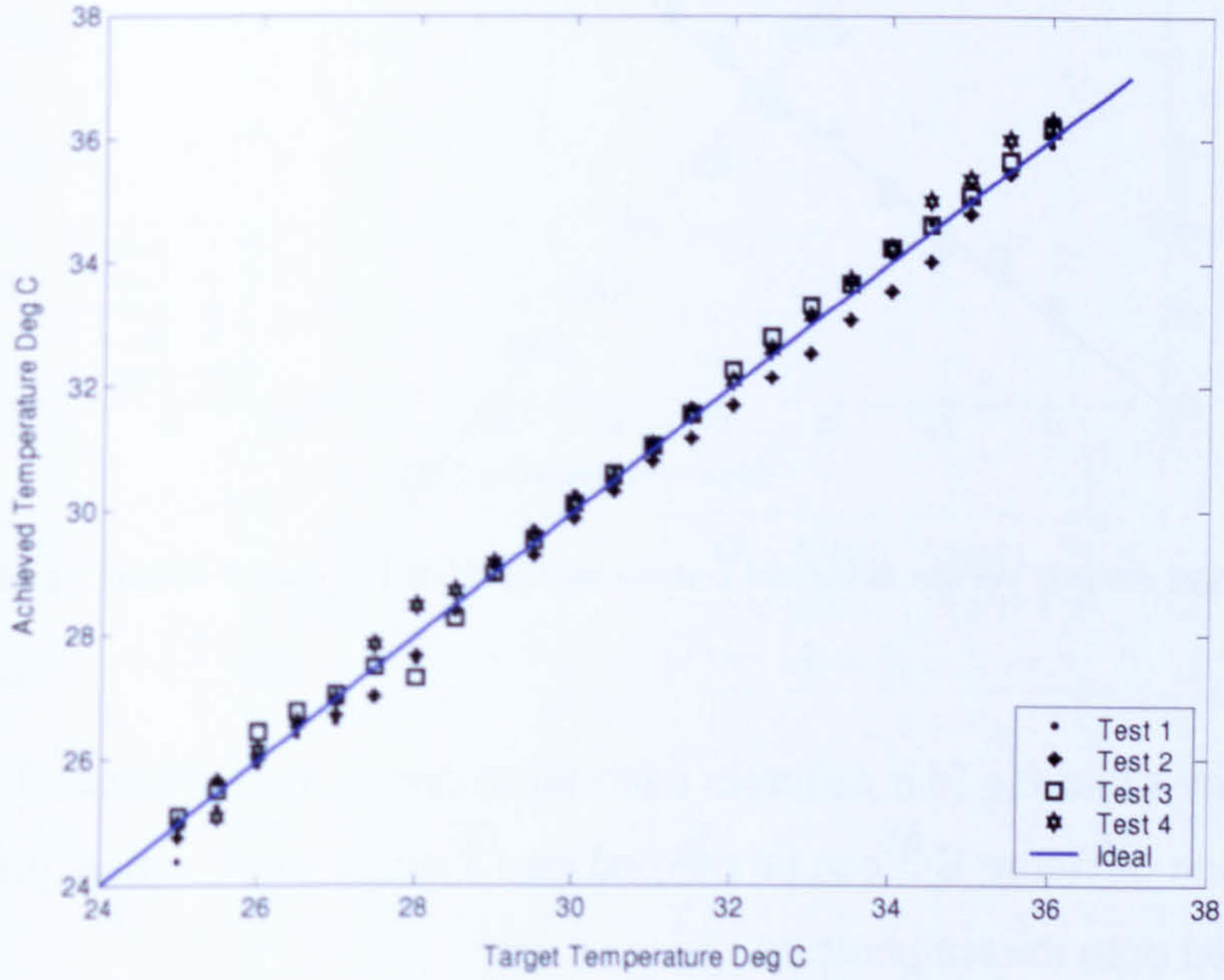


**Figure E-10: Target output versus achieved output using RGB for entire colour bandwidth 25 °C – 36°C.**

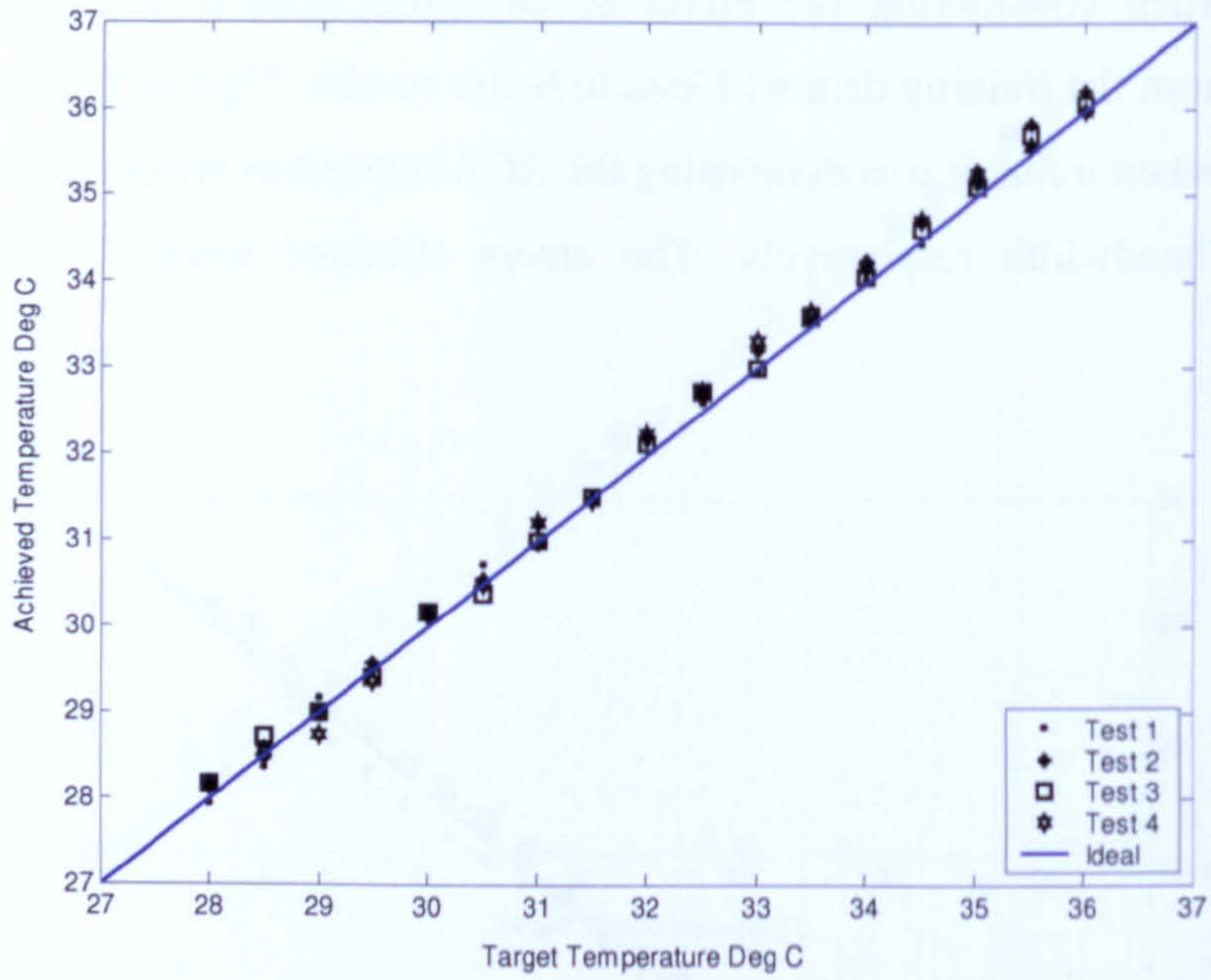


**Figure E-11: Target output versus achieved output using RGB for useful colour bandwidth 28 °C – 36°C.**

Figure E-11 shows that the four different calibration curves, each representing a different lighting condition of figure E-3 can be merged into a single curve, where the RGB triplet has been mapped onto the temperature.

The above plots suggest that the best results are obtained by using the RGB intensities provided training data is within the usable bandwidth of the TLC. Figure E-12 shows the regression analysis for the plot in figure E-11. The x-axis indicates the target temperature and the y-axis indicates the achieved temperature.

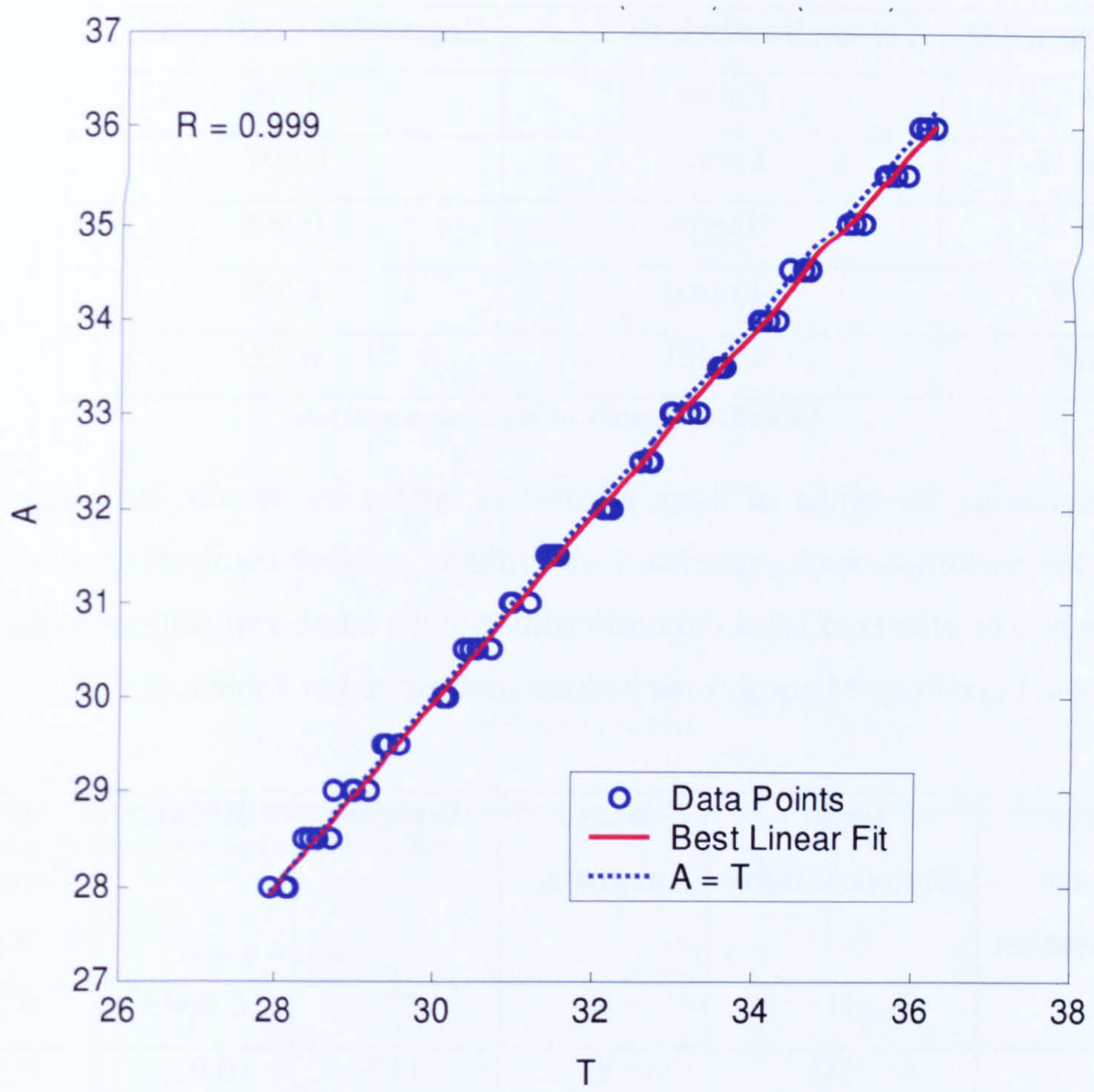


**Figure E-12: Regression analysis on RGB as training data.**

## Summary of results and discussion

Table E-1 lists the results of the regression analysis on the output data from all the independent input parameters considered.

| Input Parameter | Colour Bandwidth | Regression Coefficient |
|---|---|---|
| H | Entire | 0.990 |
| RGB H | Entire | 0.997 |
| RGB H | Useful | 0.998 |
| RGB | Entire | 0.997 |
| *RGB* | Useful | 0.999 |

**Table E-1: Results of regression analysis.**

After considering the effect of input parameters on the test results, it is important to consider the performance characteristics for different network configurations relevant to the analysis. The effects of input dimensionality and the number of neurons in the hidden layer for the Levenberg-Marquardt method are summarized in Table E-2.

| Neural Network Configuration | Input Dimensionality | No. of neurons | Weights | RMSE | Mean Percentage Error |
|---|---|---|---|---|---|
| 1 | 11 | 6 | 72 | 0.0048 | 0.36 % |
| 2 | 13 | 8 | 112 | 0.013 | 0.38 % |
| 3 | 15 | 8 | 128 | 0.015 | 0.34 % |
| 4 | 17 | 3 | 54 | 0.008 | 0.37 % |
| 5 | 19 | 9 | 110 | 0.0038 | 0.39 % |
| 6 | 21 | 7 | 154 | 0.0043 | 0.34 % |
| 7 | 23 | 9 | 216 | 0.0031 | 0.37 % |
| 8 | 25 | 10 | 260 | 0.0044 | 0.36 % |

**Table E-2: Performance of different network configurations.**

The tests confirm that the errors can be reduced by increasing the input dimensionality and the number of neurons in the hidden layer. However, the best performance was obtained with the input dimensionality of 17 and 3 neurons in the hidden layer. This is because the network is generalized with a lower number of neurons and does not result in over fitting of the data, even though the configuration number 6 shows the least error. Figures E-13 and E-14 show results for the sixth network configuration from table E-2.

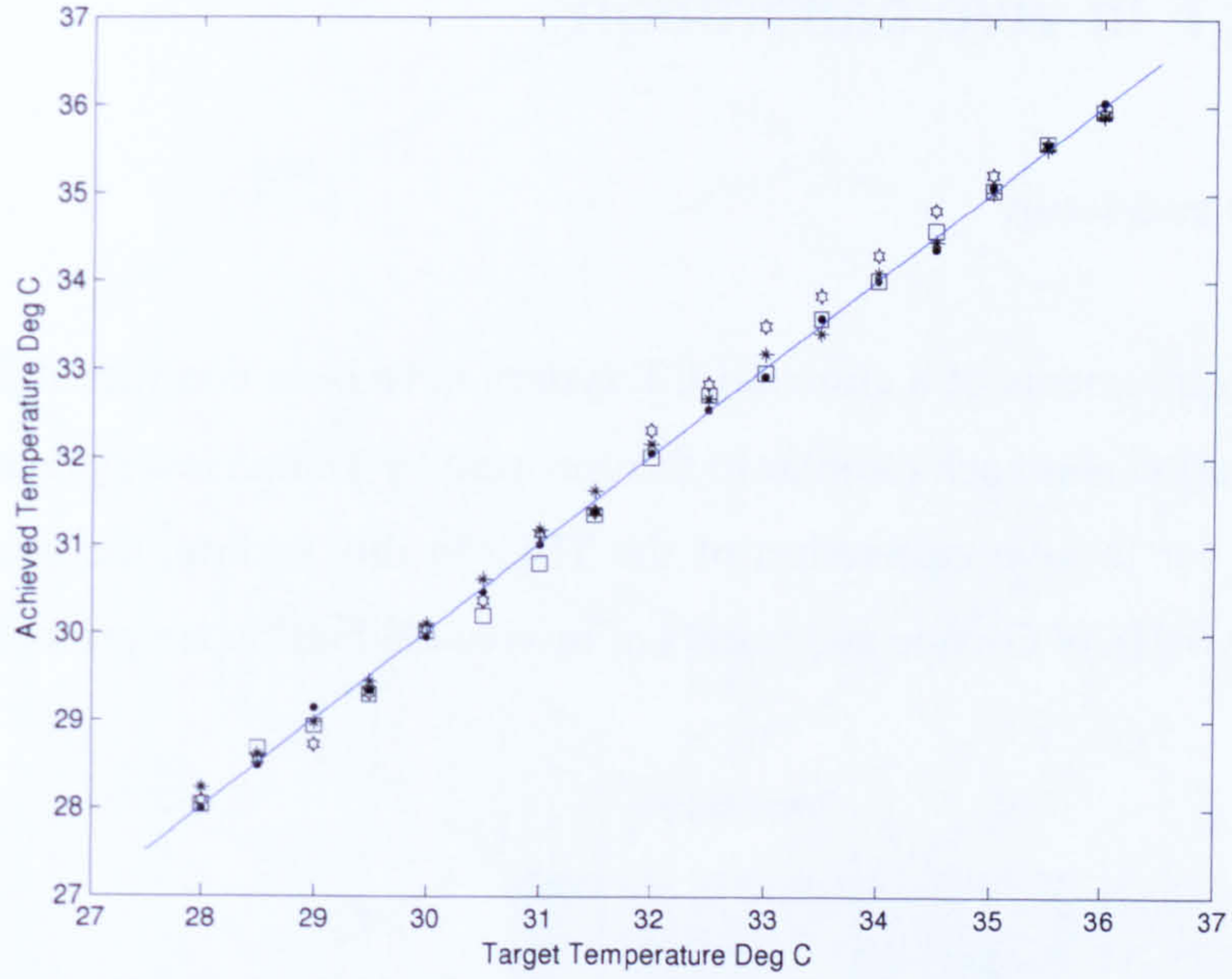


**Figure E-13 : Target output versus achieved output using RGB for useful colour bandwidth (28 °C – 36°C) using the best network configuration.**

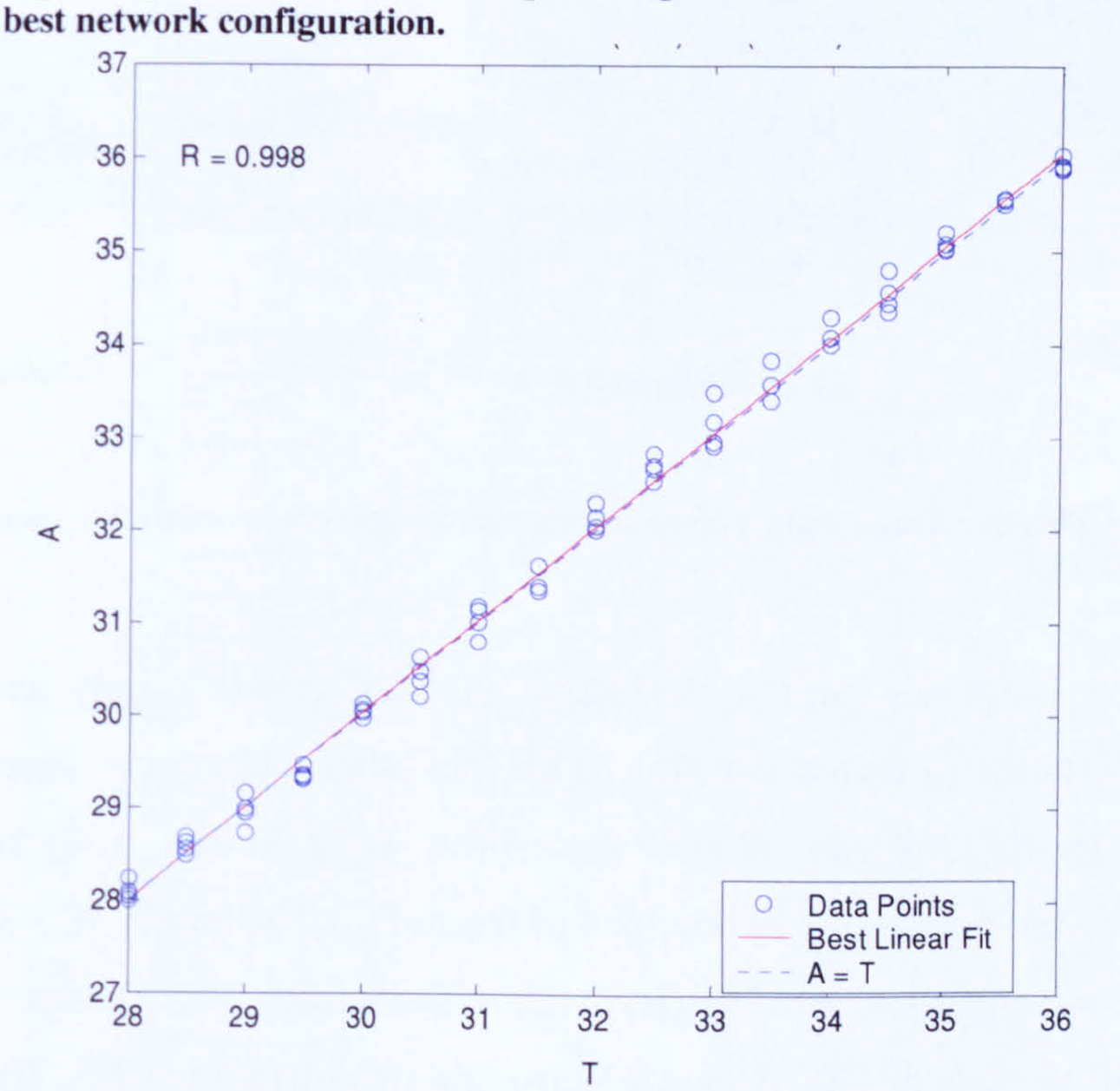


**Figure E-14: Regression analysis using RGB as training data for the best network configuration.**

# Appendix F In vivo calibration

## Requirements and setup

The specific requirements of a clinical LCT system have been considered in the thesis. A low cost calibration approach (similar to the one used by TempView system) was realised in LABVIEW for in vivo calibration of the TLC. In this section, the setup for in vivo calibration, LABVIEW G-code and results of in vivo calibration are presented.

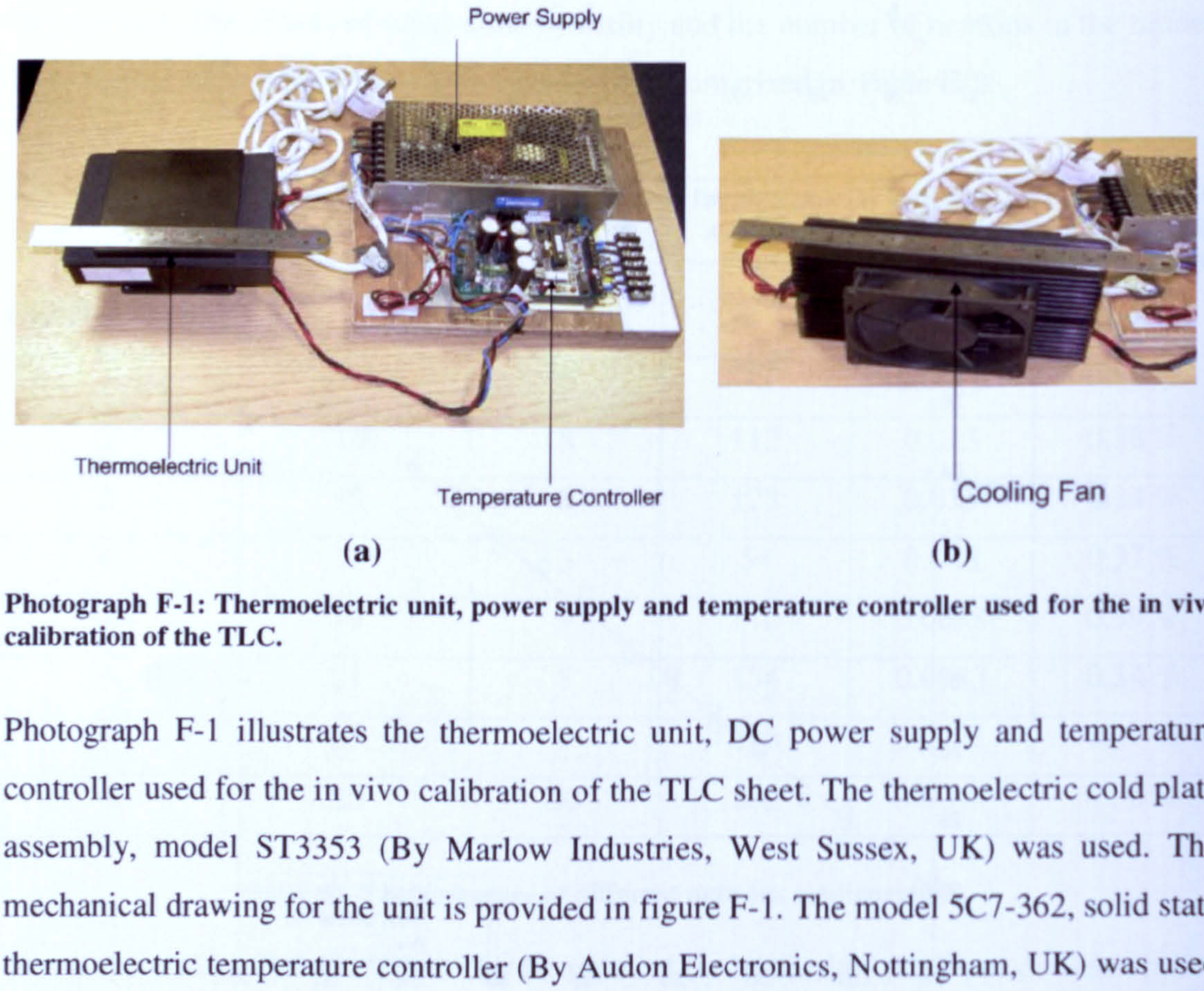


**Photograph F-1: Thermoelectric unit, power supply and temperature controller used for the in vivo calibration of the TLC.**

Photograph F-1 illustrates the thermoelectric unit, DC power supply and temperature controller used for the in vivo calibration of the TLC sheet. The thermoelectric cold plate assembly, model ST3353 (By Marlow Industries, West Sussex, UK) was used. The mechanical drawing for the unit is provided in figure F-1. The model 5C7-362, solid state thermoelectric temperature controller (By Audon Electronics, Nottingham, UK) was used with TS67-170 thermistor (By Audon Electronics, Nottingham, UK). The temperature controller is a bi-directional control for independent thermoelectric modules and its parameters are PC programmable using the RS-232 interface. Typical parameters used for programming the controller are illustrated in figure F-2.

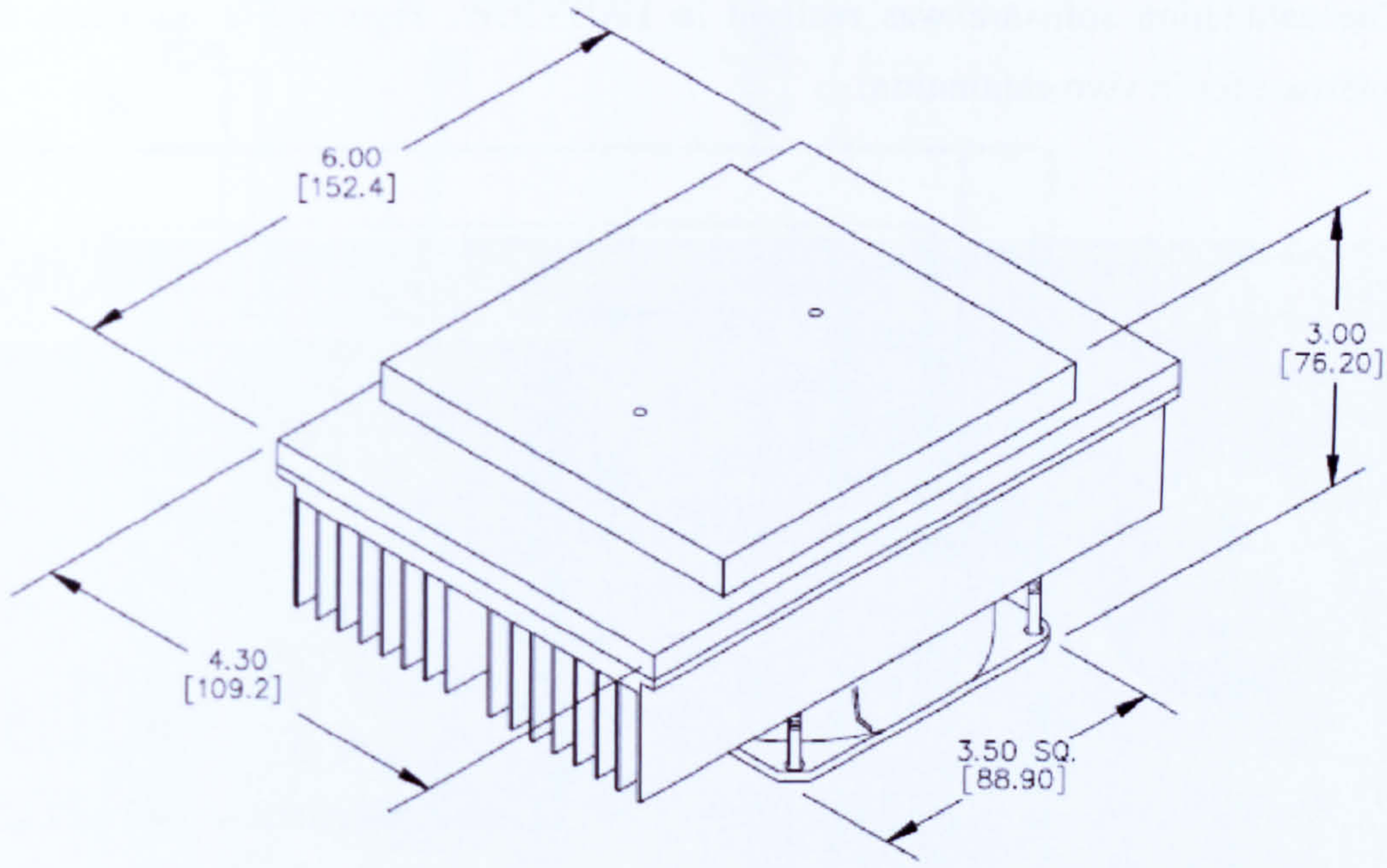


Millimeters are in [ ]

**Figure F-1: The technical drawing for the ST3353 thermoelectric unit.**

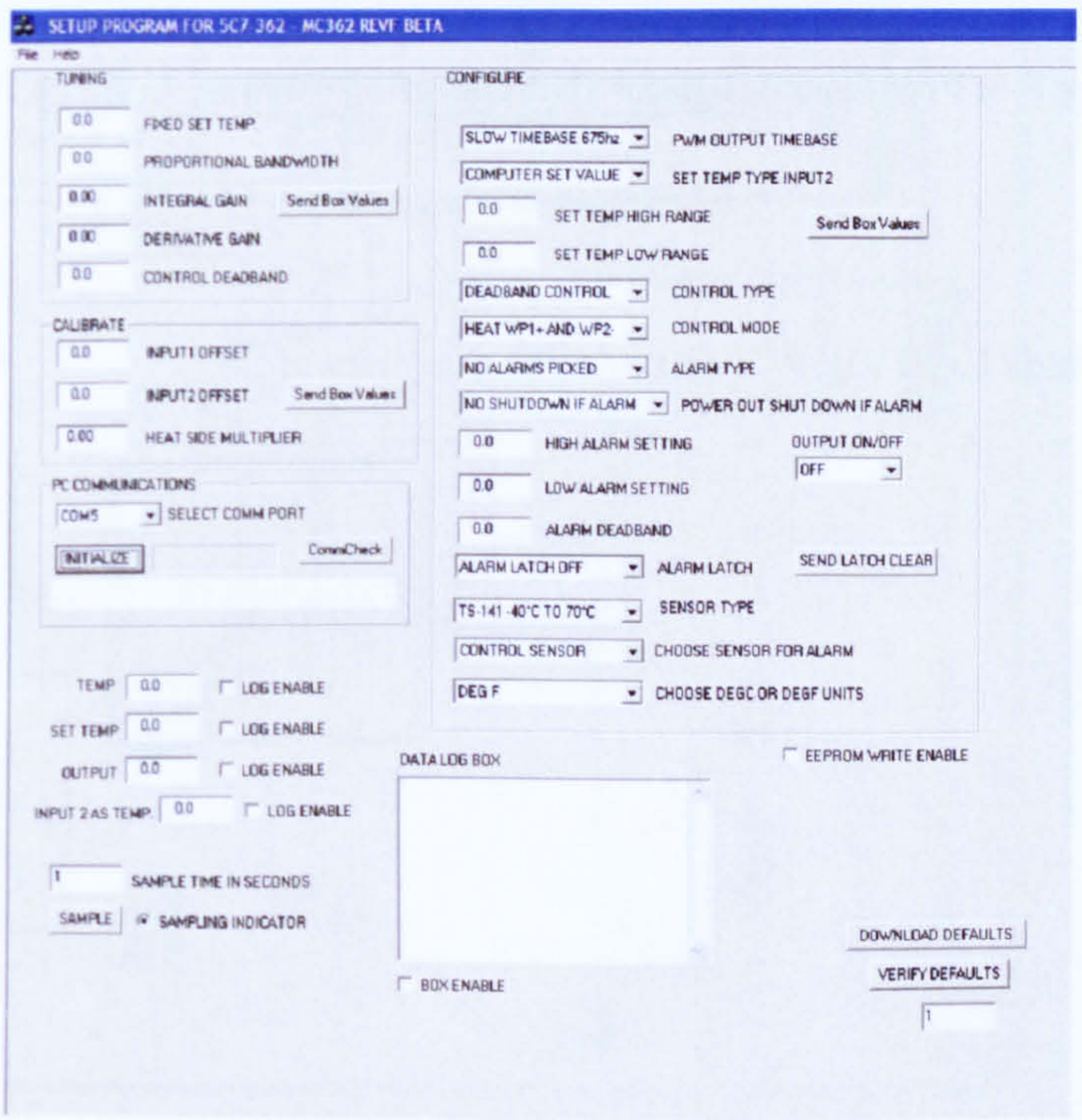


**Figure F-2: Typical parameters for the 5C7-362 temperature controller, programmable via RS-232 interface.**

The calibration software was realised in LABVIEW. Figures F-3 illustrates the user interface for in vivo calibration.

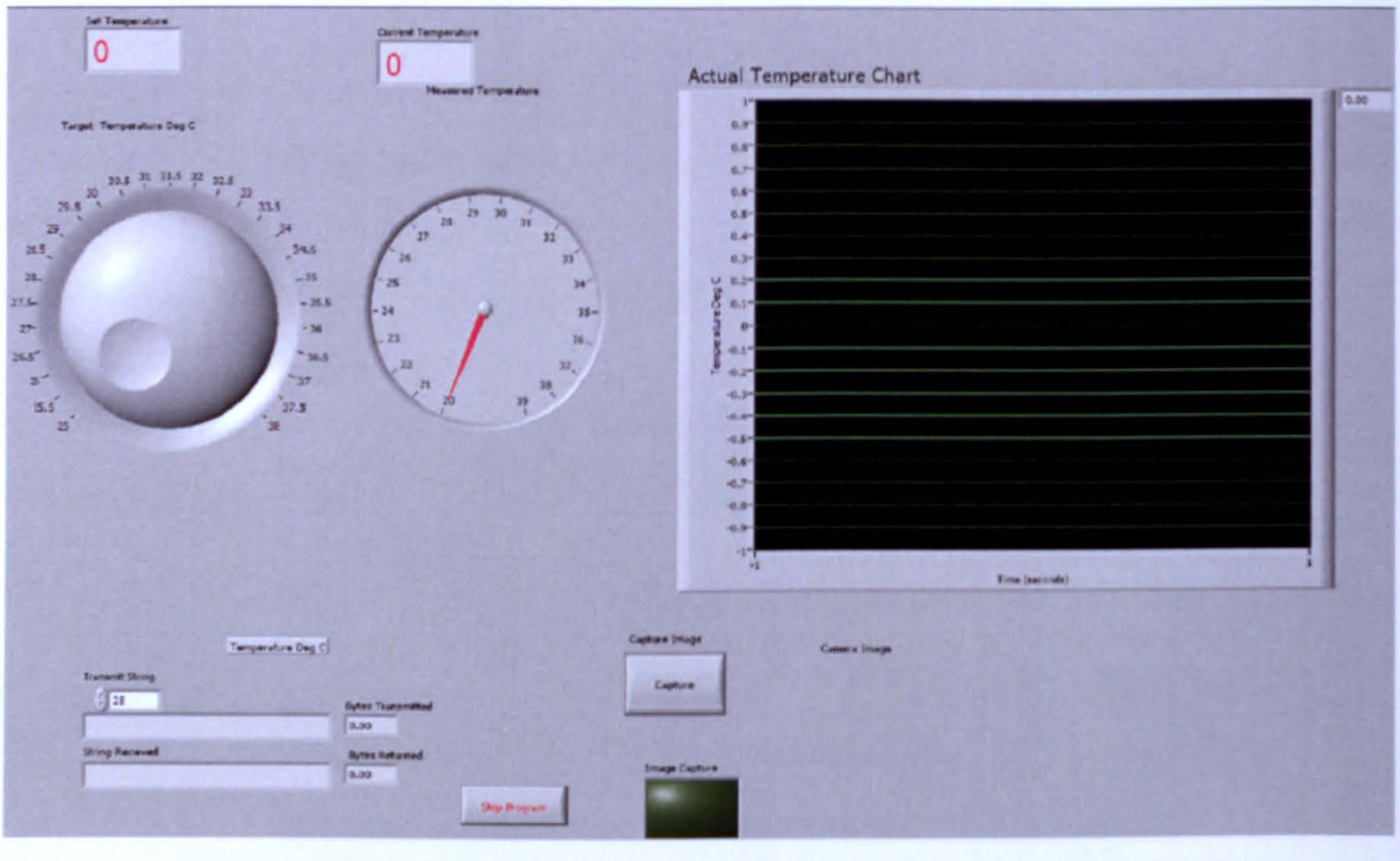


**Figure F-3: Front end design for the calibration software in LABVIEW.**

Figure F-4, illustrates LABVIEW's G-code for the software.

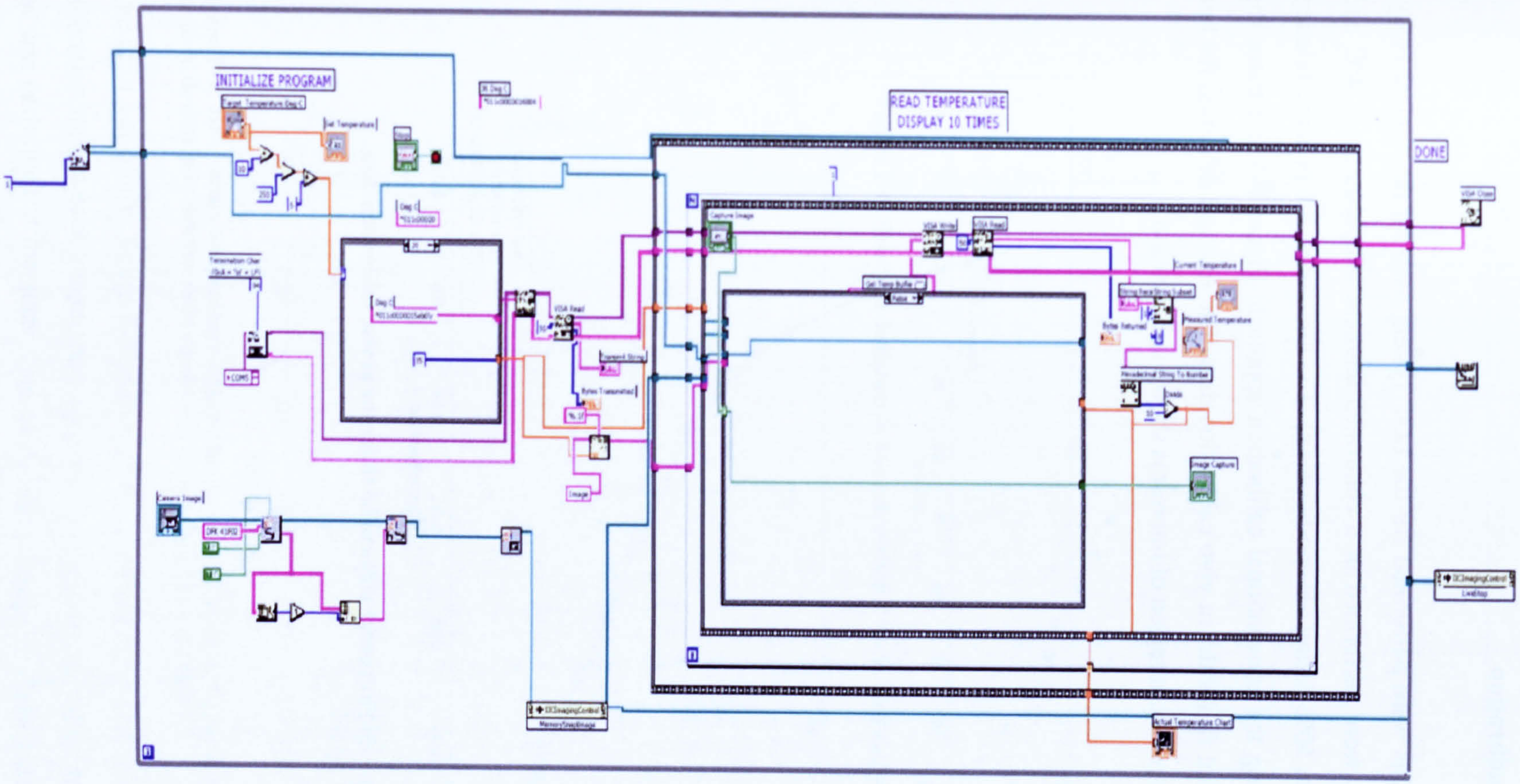


**Figure F-4: G-code for the in vivo calibration software.**

**Results of in vivo calibration**

Thirty calibration runs were performed for the LCT system used for the clinical study. All calibration runs were performed in a controlled ambient temperature of 24°C and humidity at less than 50% (using air conditioning). The hue versus temperature relation was determined using the conventional calibration approach. Figure F-5 illustrates the fifth order polynomial fit for the in vivo calibration data. The standard deviation for hue calculation from the pixels in region of interest is shown in figure F-6.

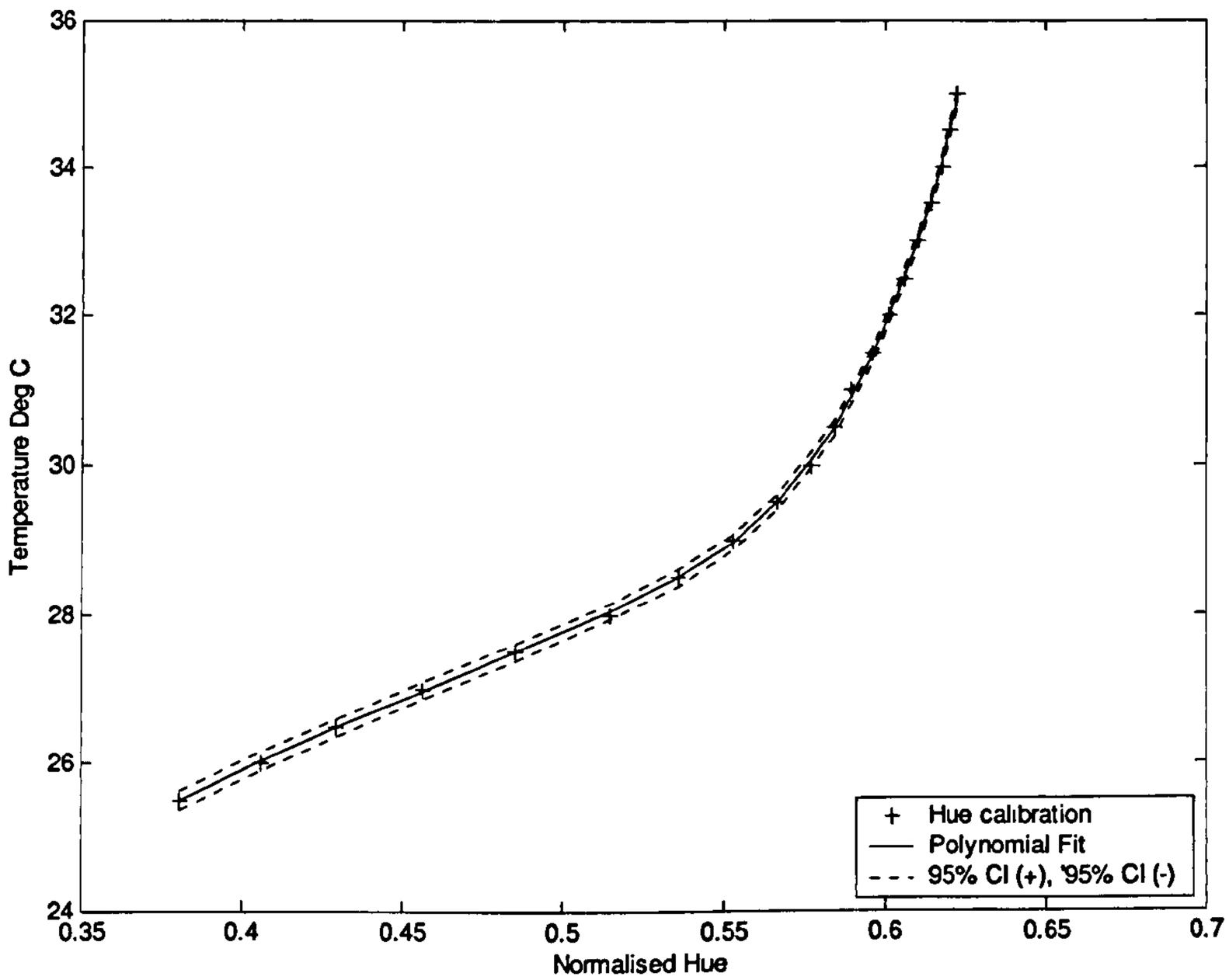


**Figure F-5: Fifth order polynomial fit for the in vivo calibration data.**

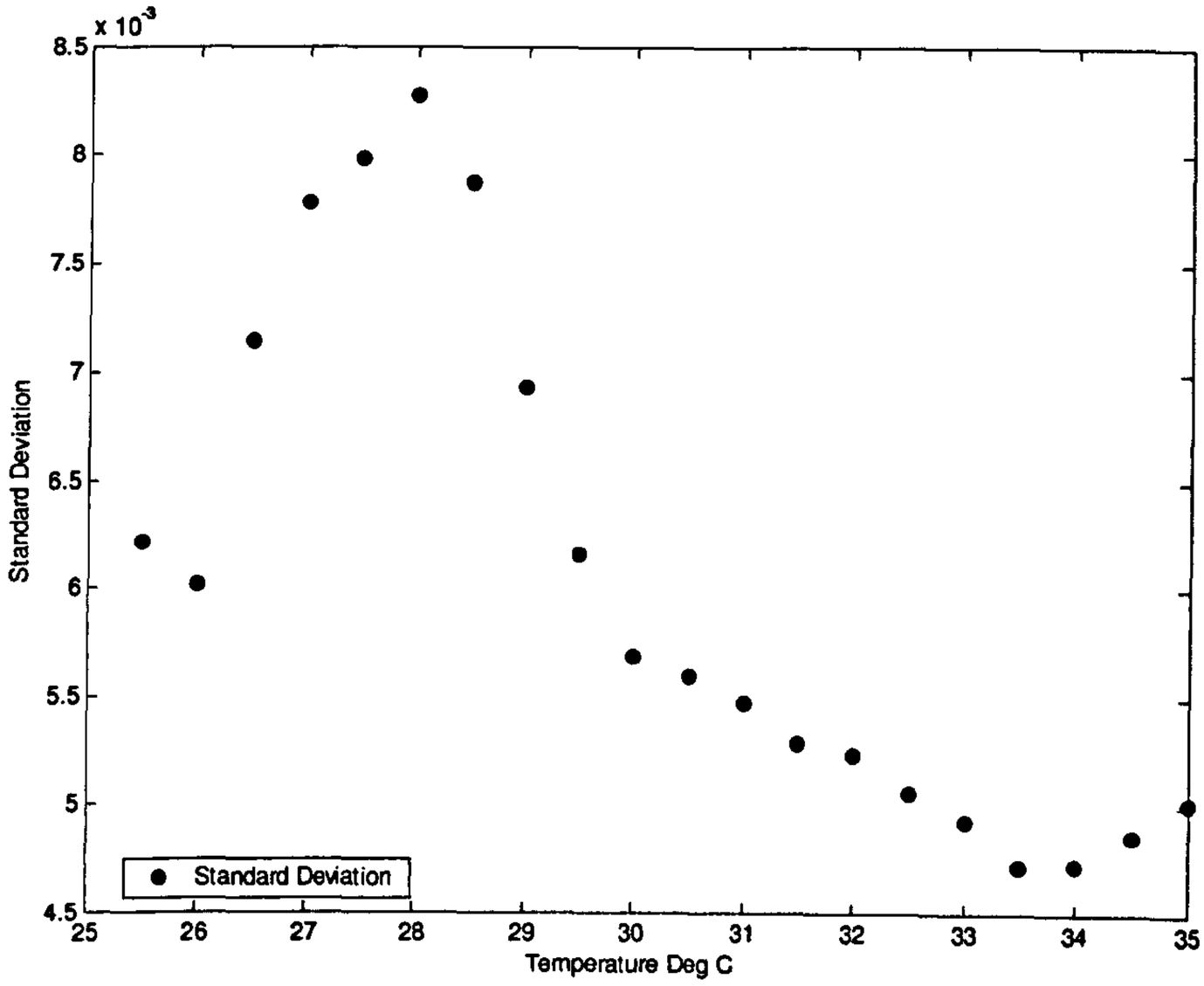


**Figure F-6: Standard deviation in hue calculation from in vivo calibration data.**

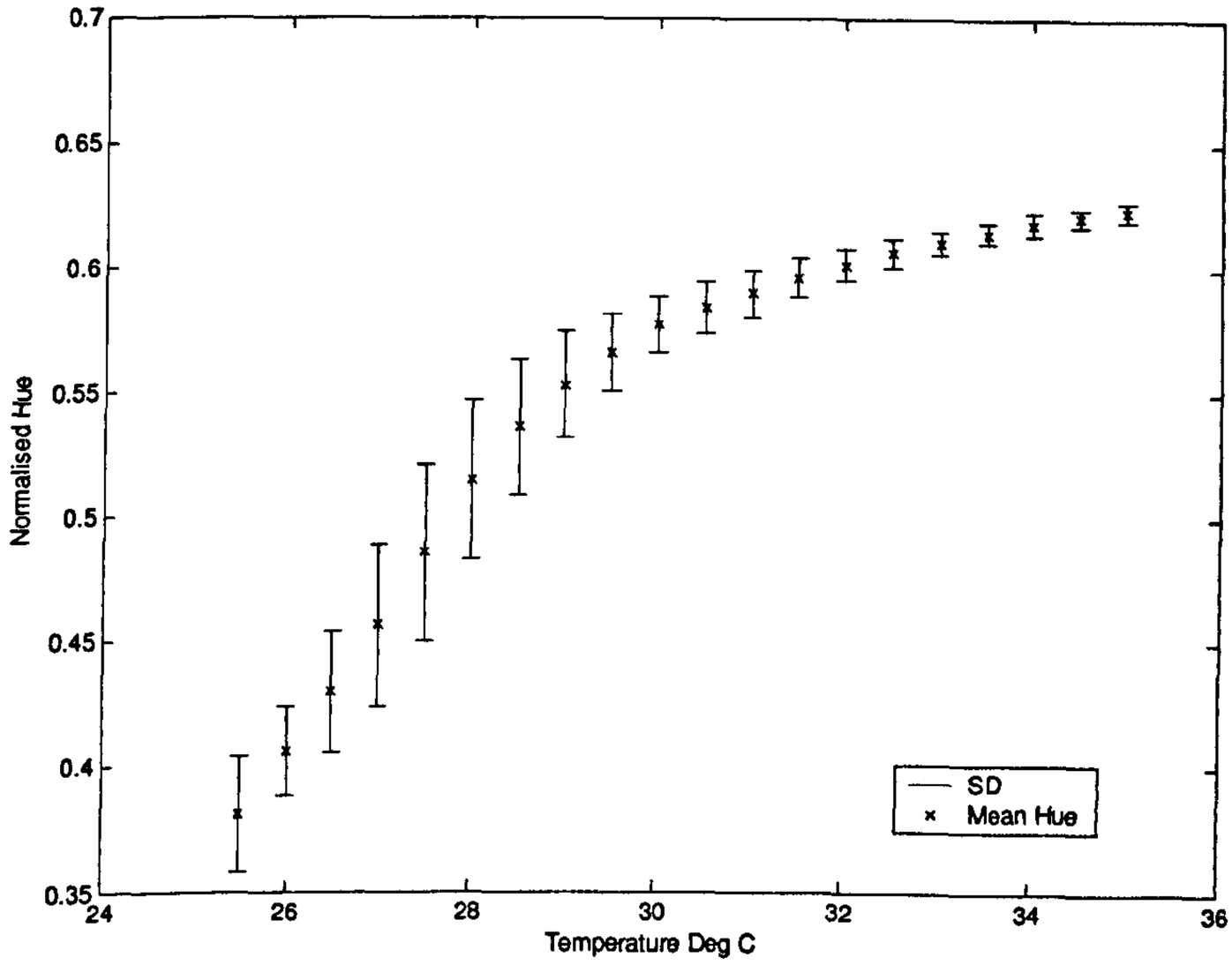


**Figure F-7: Hue versus temperature dataset for in vivo calibration. Error bars shown indicate the standard deviation in hue for n=30 samples at each temperature set point.**

The error bar plot in figure F-7 illustrates the standard deviation in hue from the n=30 calibration runs at each temperature set point. It is important to state that each calibration run was performed at the same time of the day, using consistent settings of the camera

and light source. However, the calibration response is significantly affected by the polycarbonate sheet in contact with the TLC sheet, ageing of the TLC sheet and the usage limitations on the TLC sheet. Polycarbonate was not present for the in vitro investigations of different TLC samples. These issues can be addressed by suitable modelling techniques and detailed in vivo studies on different samples of the TLC. A simple solution will be to change the TLC sheet at the end of certain number of loading (or usage) cycles during clinical investigations. Unfortunately, the manufacturer does not provide any objective data for these findings.

# Appendix G Pressure sensitivity results

## Wideband TLC sheet (R25C10W)

Non linear behaviour of hue against changing loads was observed for the R25C10W TLC polyester sheet at constant temperature of T=30°C. Figures G-1 and G-2 illustrate the hue and standard deviation plots for the R25C10W TLC sheet material using the improved setup.

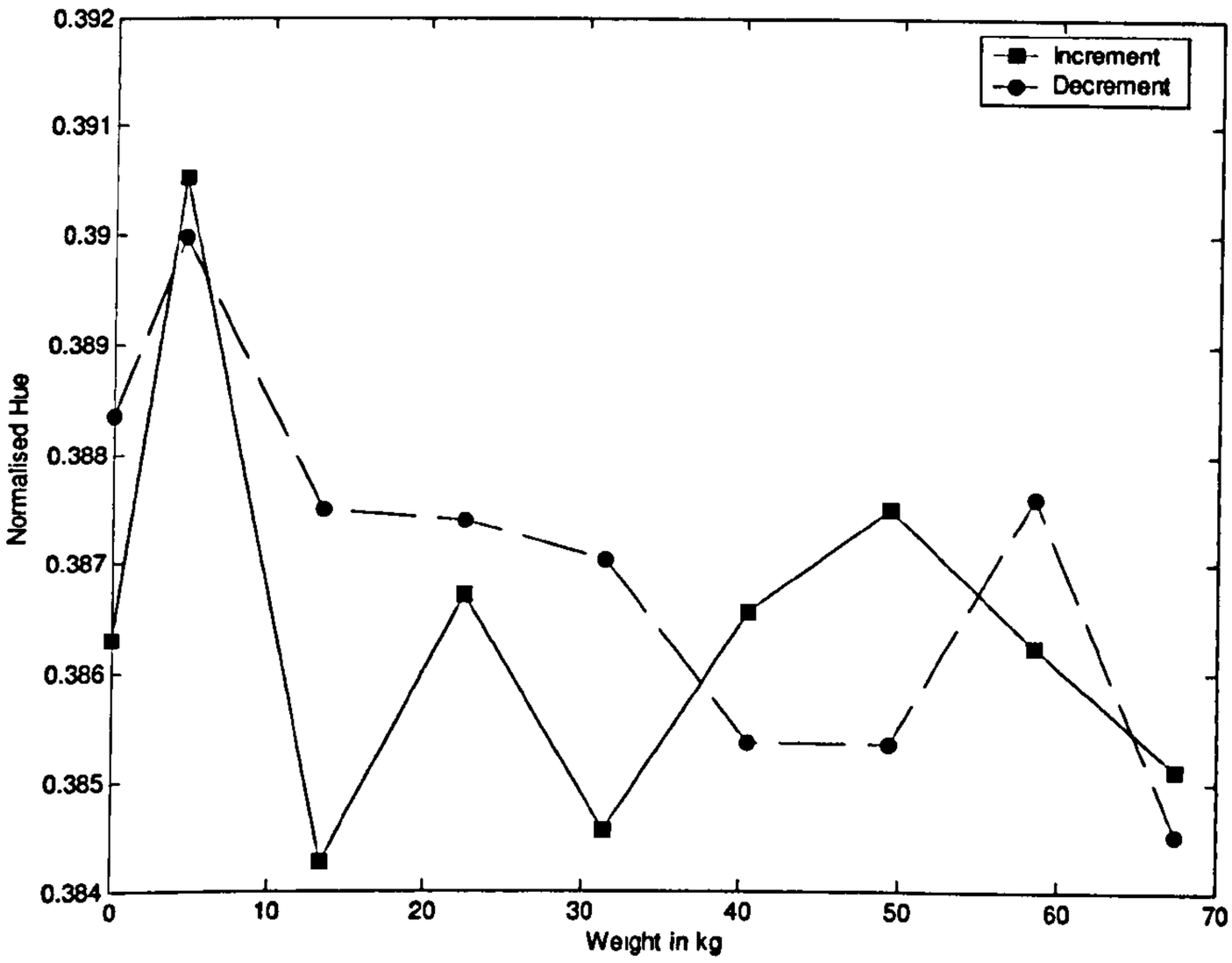


**Figure G-1: Hue versus load dataset for R25C10W TLC sheet. Data illustrated here is collected from improved pressure sensitivity setup.**

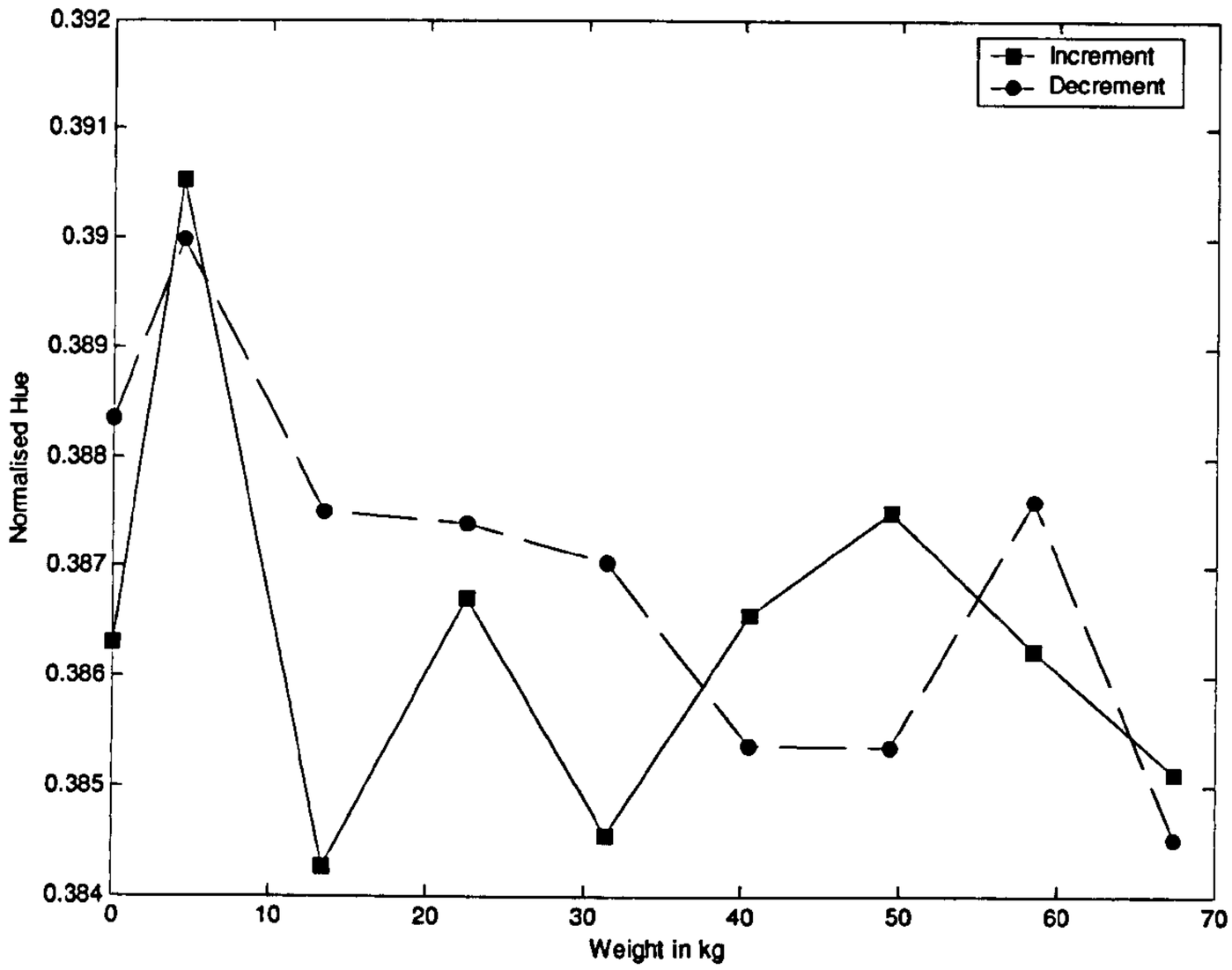


**Figure G-2: Standard deviation versus load dataset for R25C10W TLC sheet. Data illustrated here is collected from improved pressure sensitivity setup.**

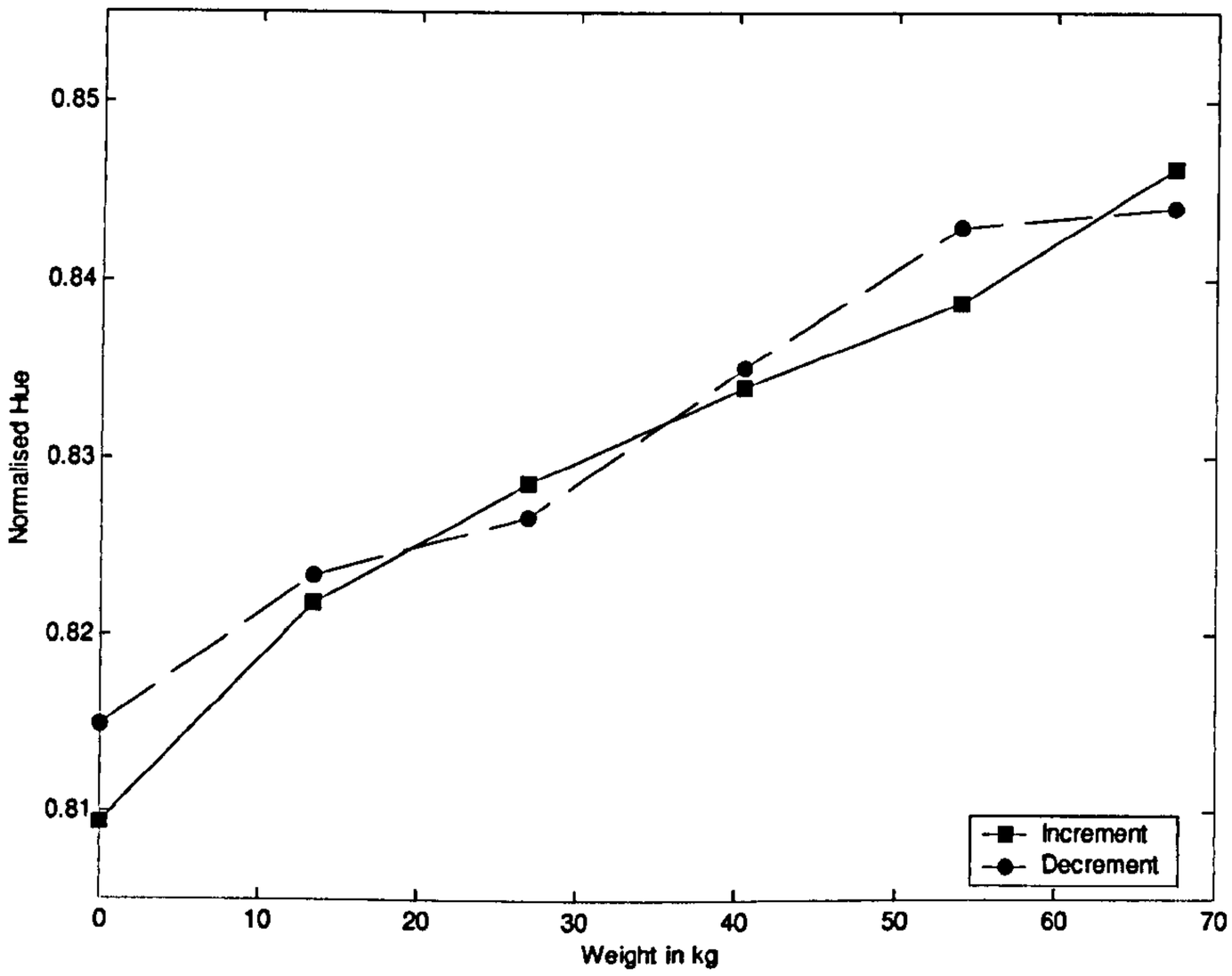


**Figure G-3: Hue versus load dataset for latex based TLC material. Data illustrated here is collected from improved pressure sensitivity setup.**

Figures G-3 illustrates the hue versus load plot for the latex based TLC material using the improved setup. Latex based TLC was not self adhesive like the TLC sheets. Thermal glue was used with the aluminium surface (good thermal contact). However, there was

significant movement in the latex material as it did not strongly bond to aluminium surface. This may be attributed to the material properties of latex. This is a design problem, as there will be some movement due to the elasticity of the latex, even if the latex is bonded to aluminium using better adhesive. The movement in the latex material changes the field of view and hence, the ROI for each image leading to abnormally high standard deviation.

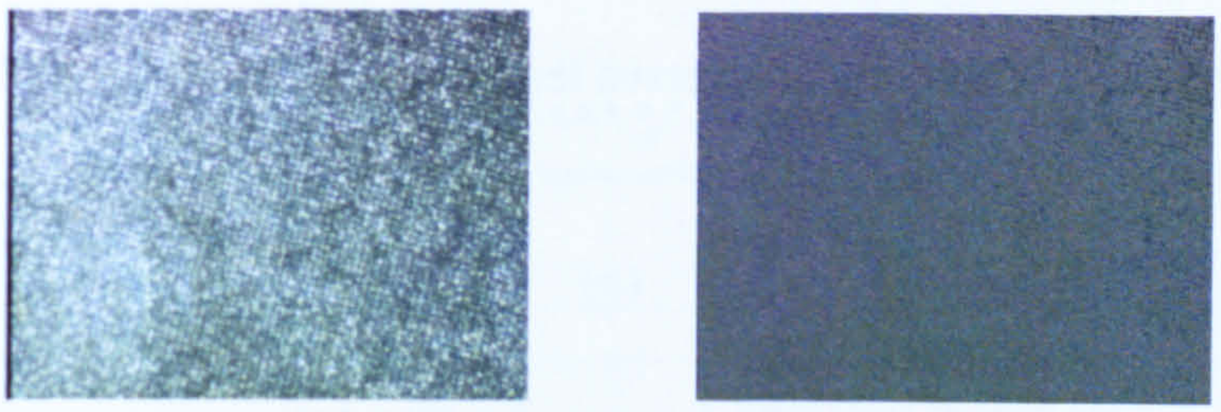

(a) (b)

**Figure G-4: Typical images of the latex based TLC, representing the green hue at 28°C temperature. The image (b) illustrates the effect of using the intensity threshold algorithm for image (a) in order to improve image quality.**

The white spots seen in the image for latex based TLC in figure G-4, may be direct reflections from the aluminium surface indicating poor spatial density of liquid crystals on the latex. Such an effect is also observed on the TLC polyester sheets upon ageing (Armstrong 2004). Contact with other surfaces and poor handling/storage may produce these effects on the TLC sheets. Due to the poor image quality obtained when using the latex material the standard deviation in hue calibration is abnormally high for 8 bit hue intensity. This can be solved by using hue and/or intensity threshold algorithms as shown in figure 4-62. However, these methods are highly subjective and still produce an unacceptable standard deviation in hue calculation (> five for 8 bit hue intensity). Such a large change in standard deviation indicates movement of liquid crystals on application of load. To establish if this movement in crystals produces a significant change in hue due to thermal or pressure effects would require further testing outside the scope of the current study.

# Appendix H Hysteresis results

In this section, hysteresis assessment of wideband TLC and emulsion based TLC is presented.

## R25C15W TLC sheet

The graph in figure H-1 illustrates hue versus temperature dataset for the R25C15W TLC sheet.

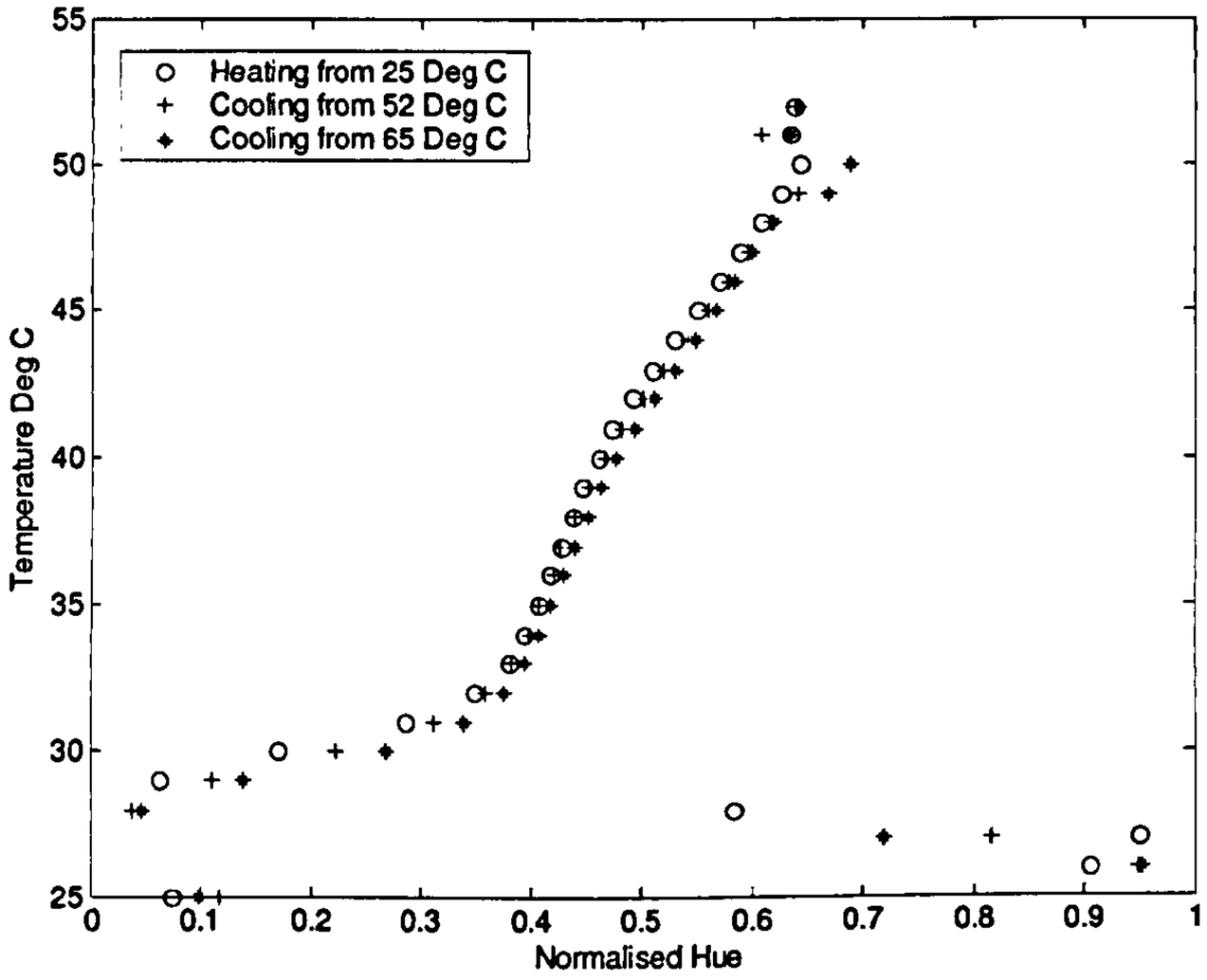


**Figure H-1: Results for hysteresis tests on R25C15W TLC sheet. The graphs show hue versus temperature curves for heating and cooling runs.**

Figure H-2 illustrates standard deviation in hue calculation at each temperature increment throughout the colour play interval and within the useful colour bandwidth (bottom) for the R25C15W TLC sheet. The standard deviation values are consistent with the calibration dataset. Wideband TLC material also show decrease in RGB intensities upon cooling as shown in figure H-3, similar to narrow band TLC material. A complete history of the testing order for R25C15W TLC sheet is presented in table H-1.

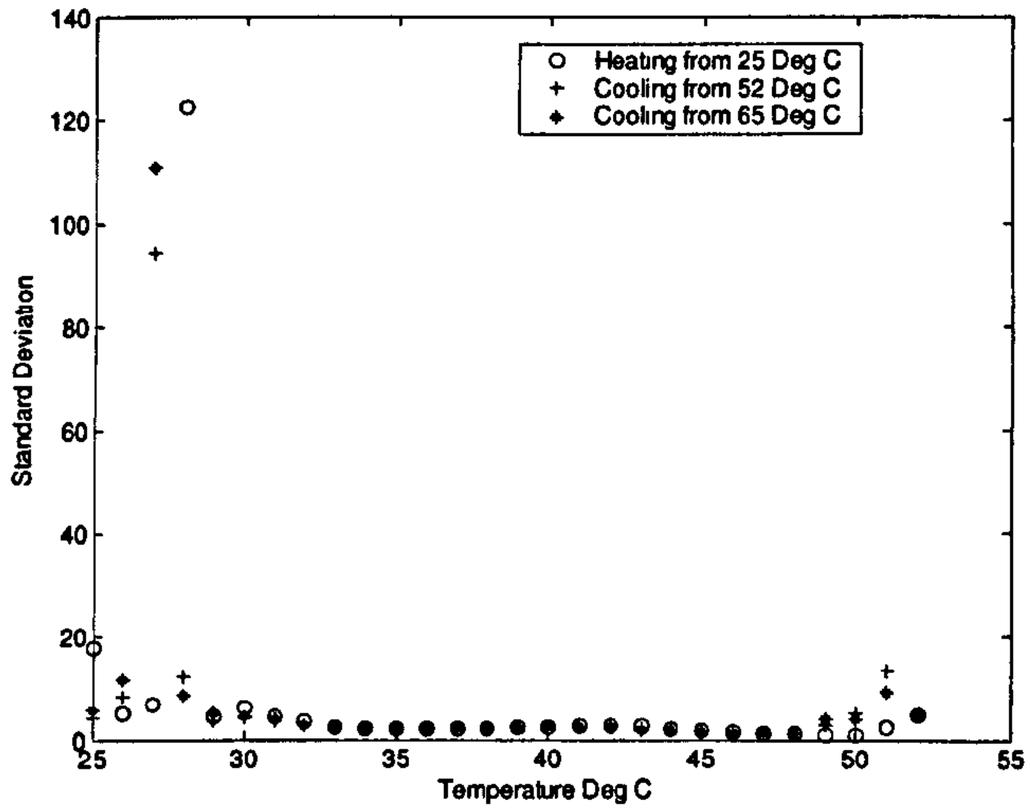


**(a)**

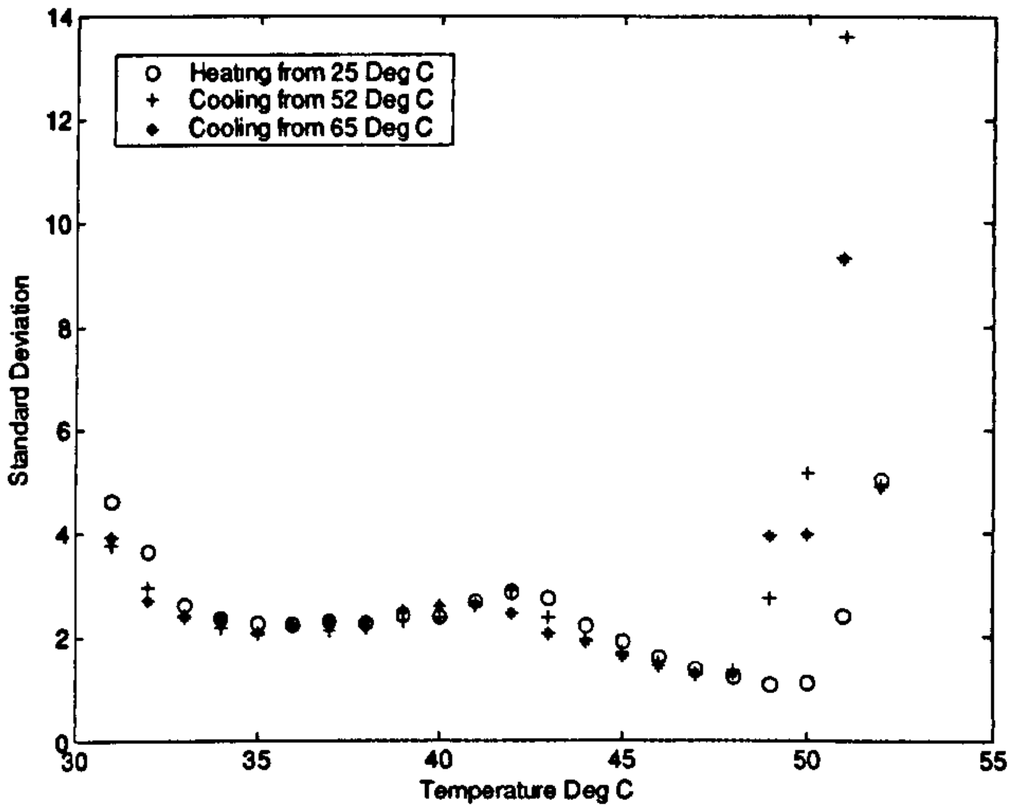


**(b)**

**Figure H-2: Standard deviation in hue calculation for the hysteresis tests on R25C15W TLC sheets. The graphs illustrate standard deviation in hue values for complete (top) and useful colour bandwidth (bottom).**

| Direction of calibration | Maximum or minimum temperature °C |
|---|---|
| Heating | 25 |
| Cooling | 52 (Clearing point temperature) |
| Cooling | 65 |

**Table H-1: Testing order for R25C15W TLC sheet.**

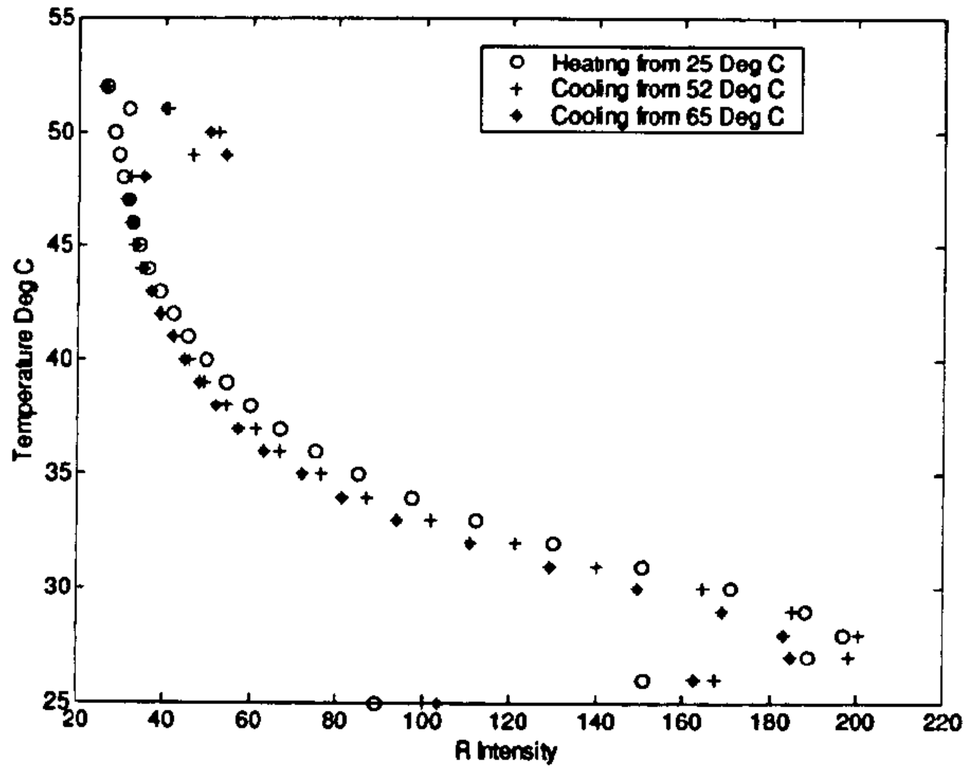


(a)

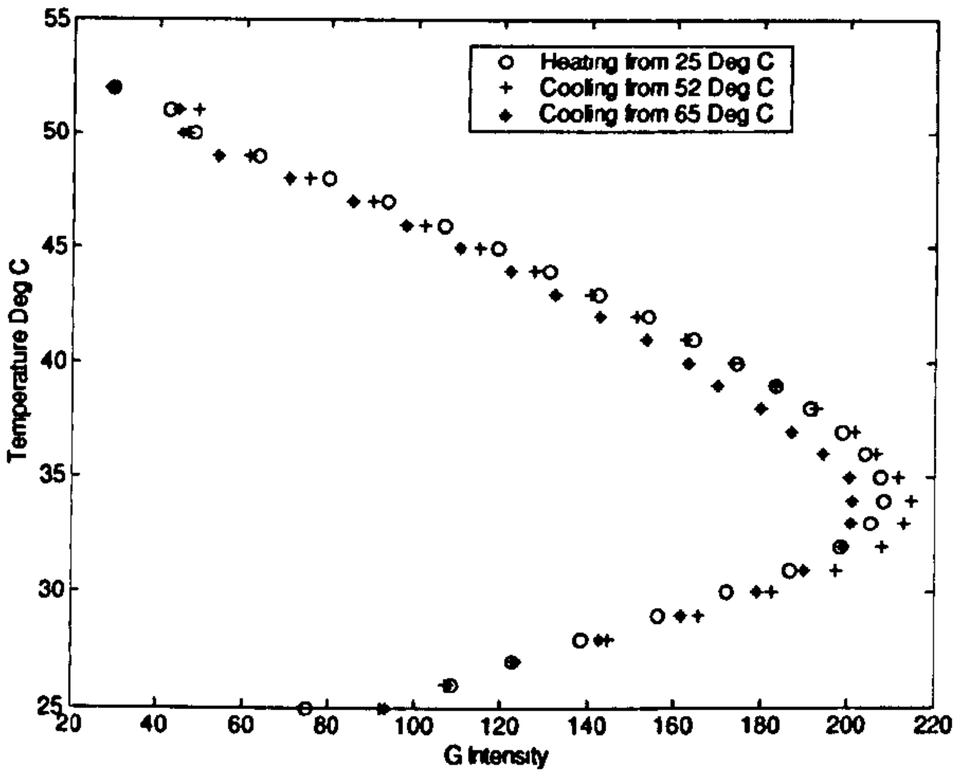


(b)

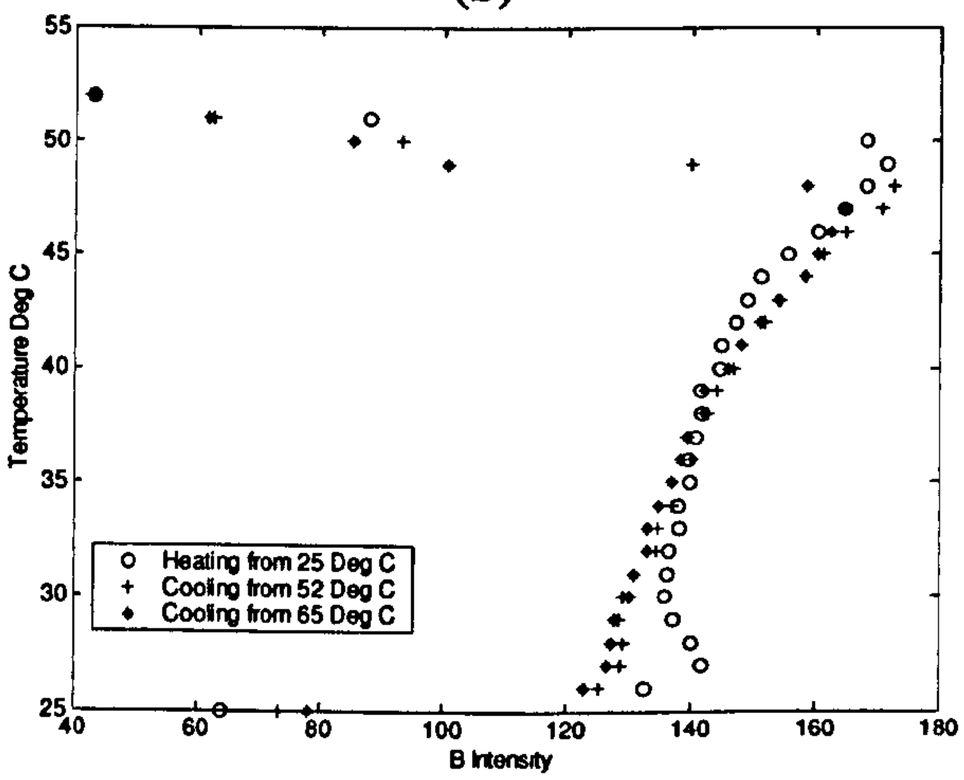


(c)

**Figure H-3: Results for hysteresis tests on R25C15W TLC sheet. The graphs show R, G and B intensities versus temperature curves for heating and cooling runs.**

**Emulsion based R25C10W TLC**

A representative of the image of R25C10W emulsion based TLC, taken from the heating and cooling runs is shown in figure H-4. Images are shown at 30°C and the image is at uniform temperature. Images confirm that the decrease in intensity during the cooling runs is highest amongst all the three datasets i.e. R25C5W, R25C15W TLC sheets and R25C10W emulsion based TLC.

**Figure H-4: Sample images at T=30°C for hysteresis tests. There is a decrease in intensity when cooling as against heating as observed in previous datasets. This decrease is the highest amongst 3 datasets.**

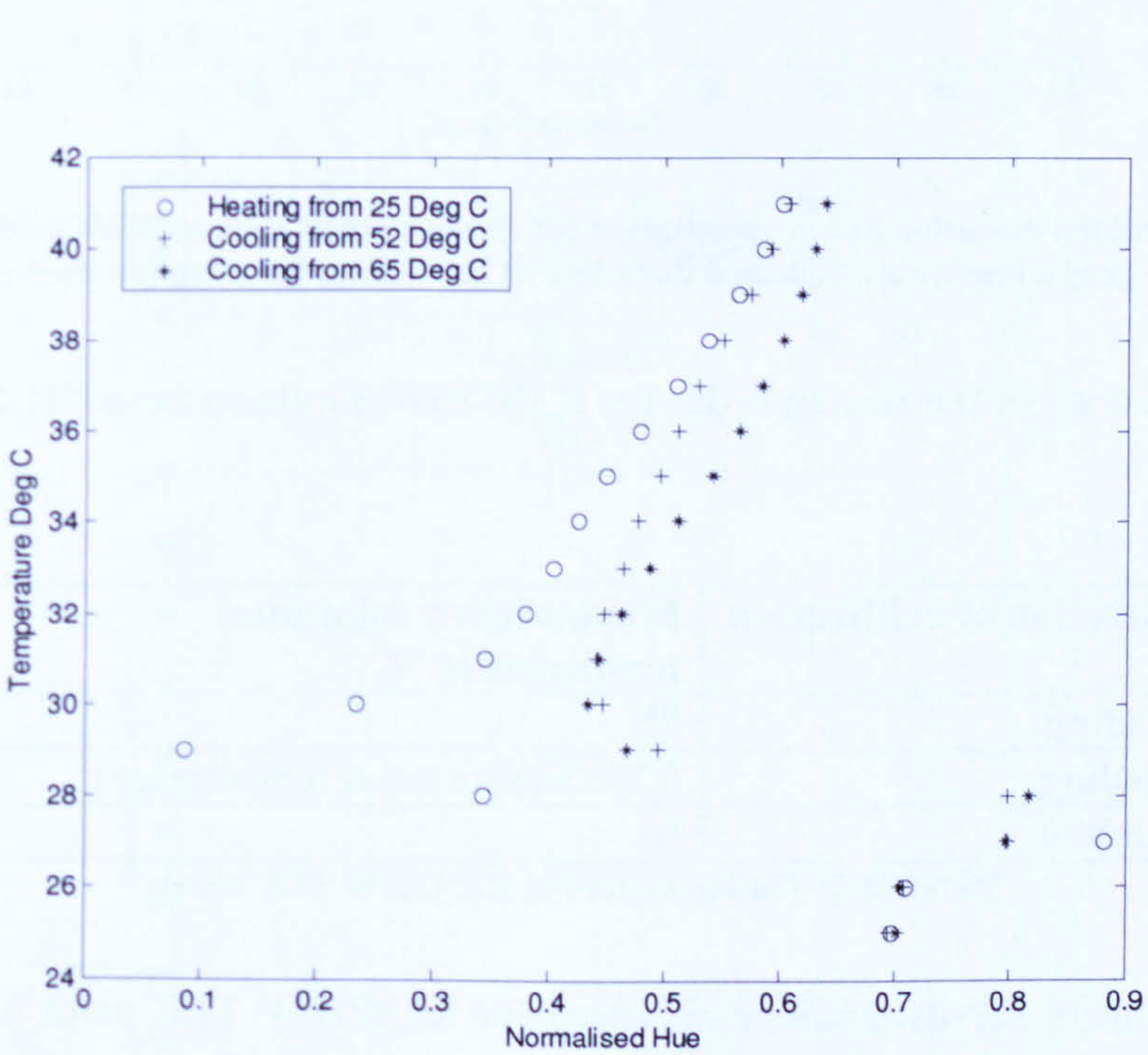


**Figure H-5: Results for hysteresis tests on R25C10W emulsion based TLC. The graphs show hue versus temperature curves for heating and cooling runs.**

The graph in figure H-5 illustrates hue versus temperature dataset for the R25C10W emulsion based TLC. Figure H-6 illustrates standard deviation in hue calculation at each temperature increment throughout the colour play interval for the R25C10W emulsion based TLC.

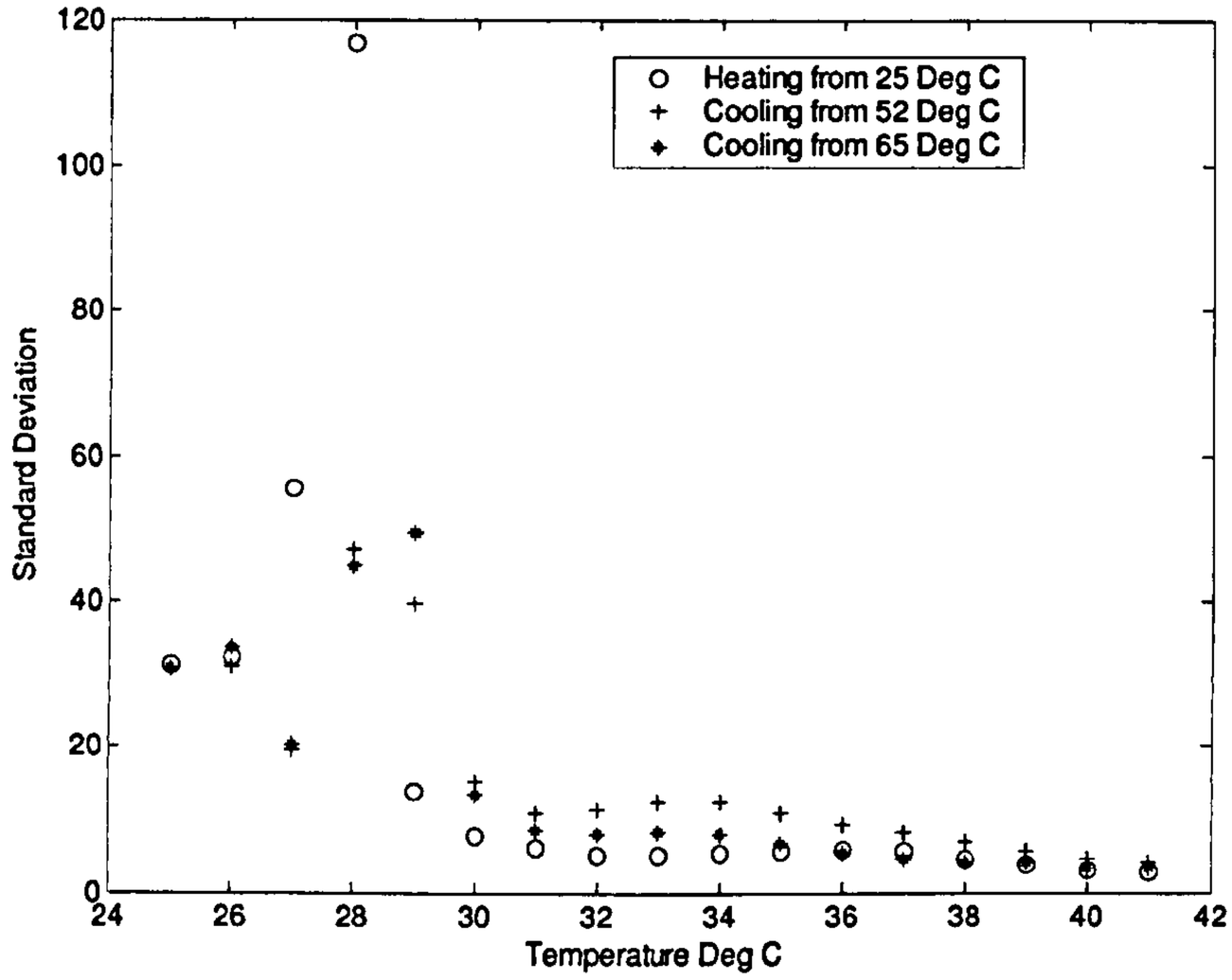


**Figure H-6: Standard deviation in hue calculation for the hysteresis tests on R25C10W emulsion based TLC. The graph illustrates standard deviation in hue values for complete colour bandwidth.**

A complete history of the testing order for R25C10W emulsion based TLC is presented in table H-2.

| Direction of calibration | Maximum or minimum temperature °C |
|---|---|
| Heating | 25 |
| Cooling | 52 (Clearing point temperature) |
| Cooling | 65 |

**Table H-2: Testing order for R25C15W TLC sheet.**

The RGB intensity versus temperature curve for R25C10W TLC paint is illustrated in figure H-7. The percentage decrease in RGB intensities for emulsion based TLC is listed in Table H-3.

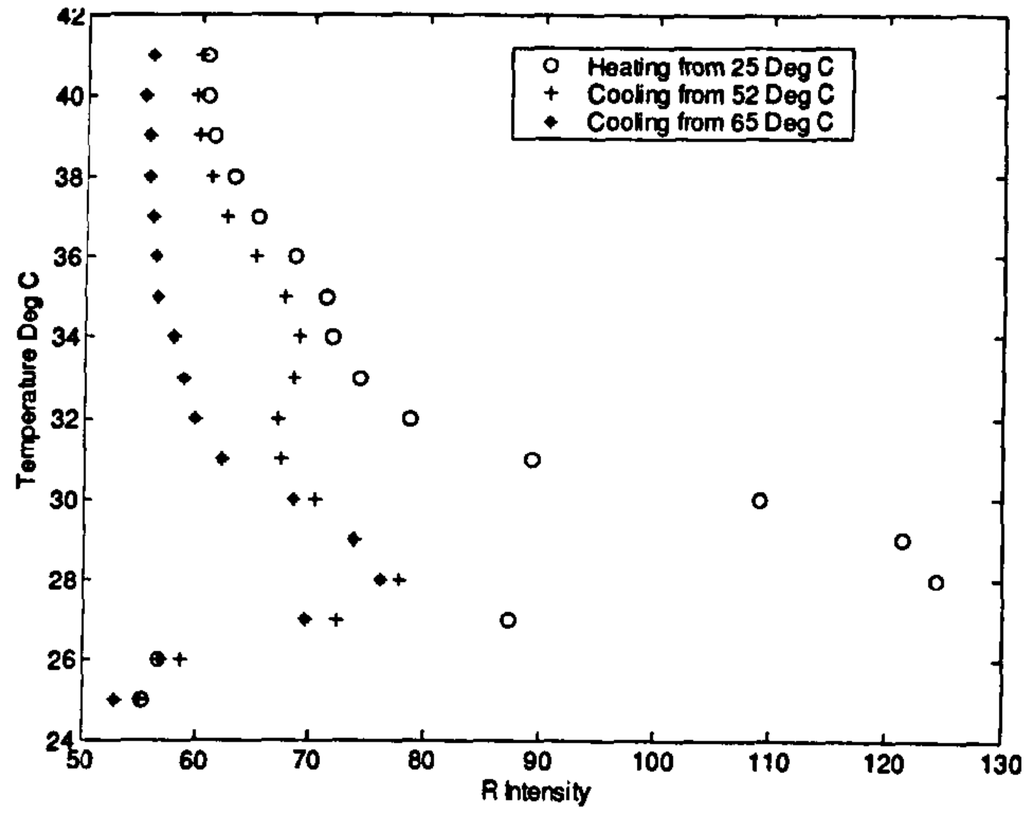


(a)

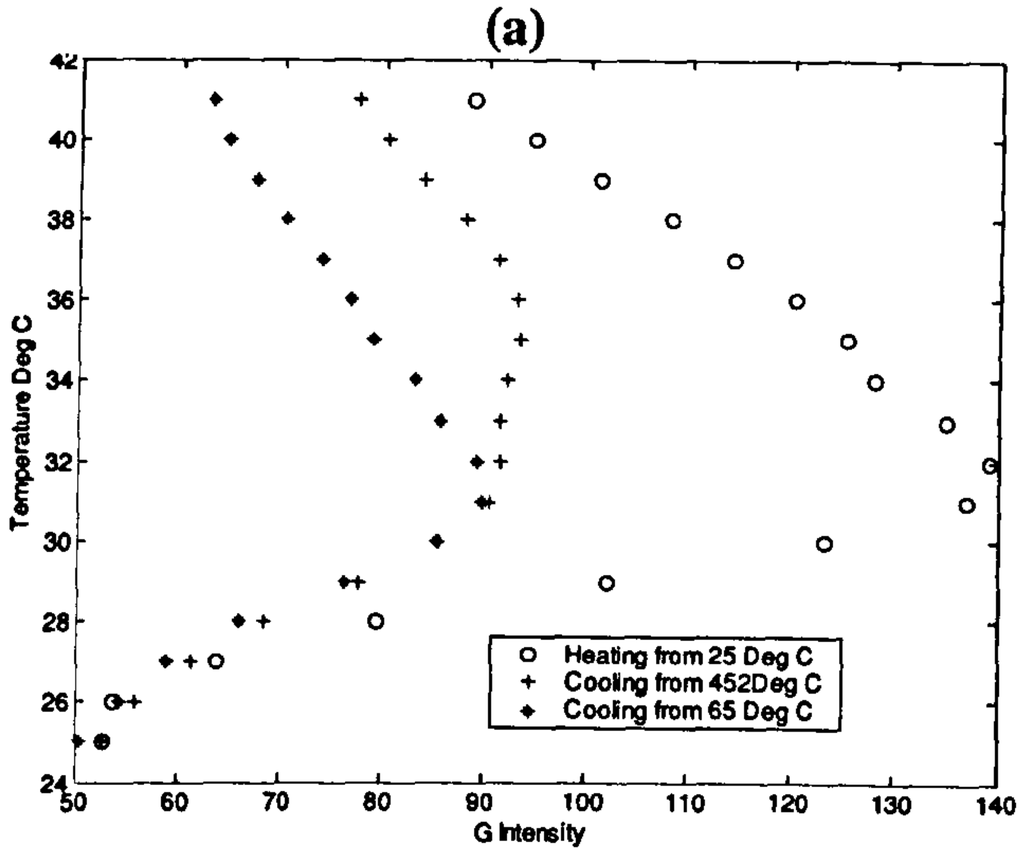


(b)

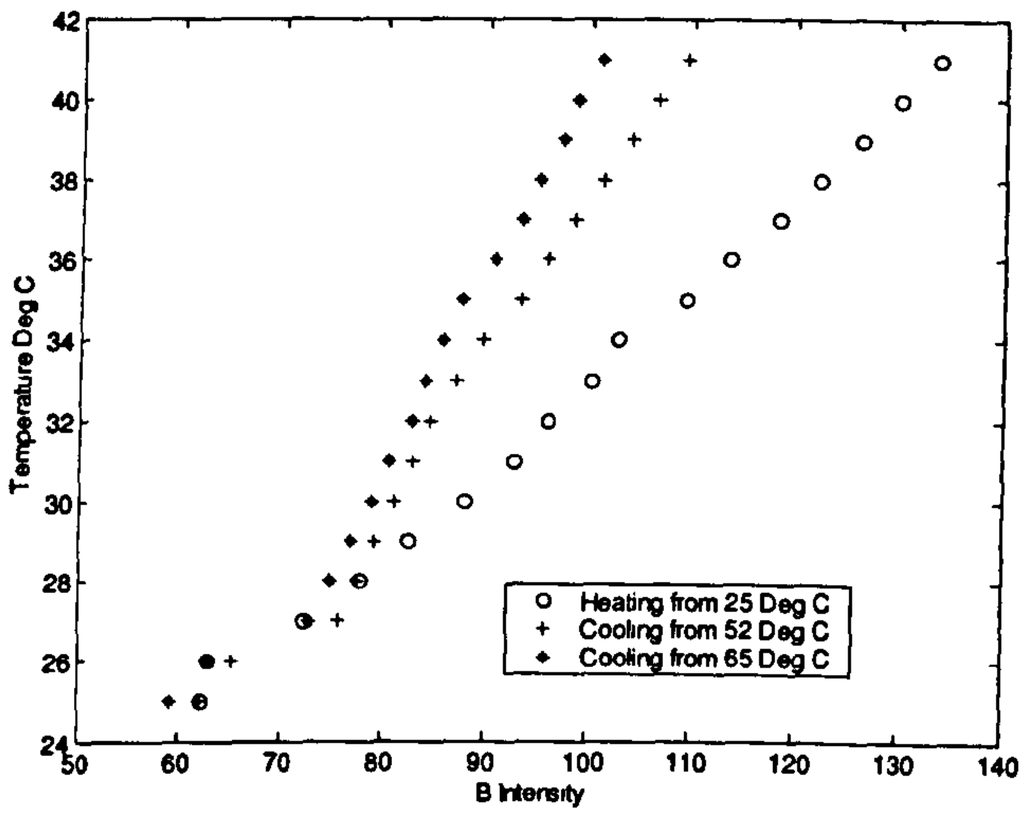


(c)

**Figure H-7: Results for hysteresis tests on R25C15W TLC sheet. The graphs show R, G and B intensities versus temperature curves for heating and cooling runs.**

# Appendix I Ansiscope - Autonomic neuropathy test

The Ansiscope (By Dyansys Inc. Chennai, India) is a medical instrument which works in real-time and measures the two components of the autonomic nervous system i.e. the sympathetic system and the parasympathetic system. It depends on a accurate three lead ECG and a high sampling rate, typically 1666 samples/sec. The instrument plots a sympathovagal balance trajectory in real-time and also updates it with every heartbeat in order to calculate the percentage autonomic dysfunction and classify the patient into one of the four groups i.e. healthy, early, late and advanced. Figures I-1 and I-2 illustrate typical result sheets for the subjects.

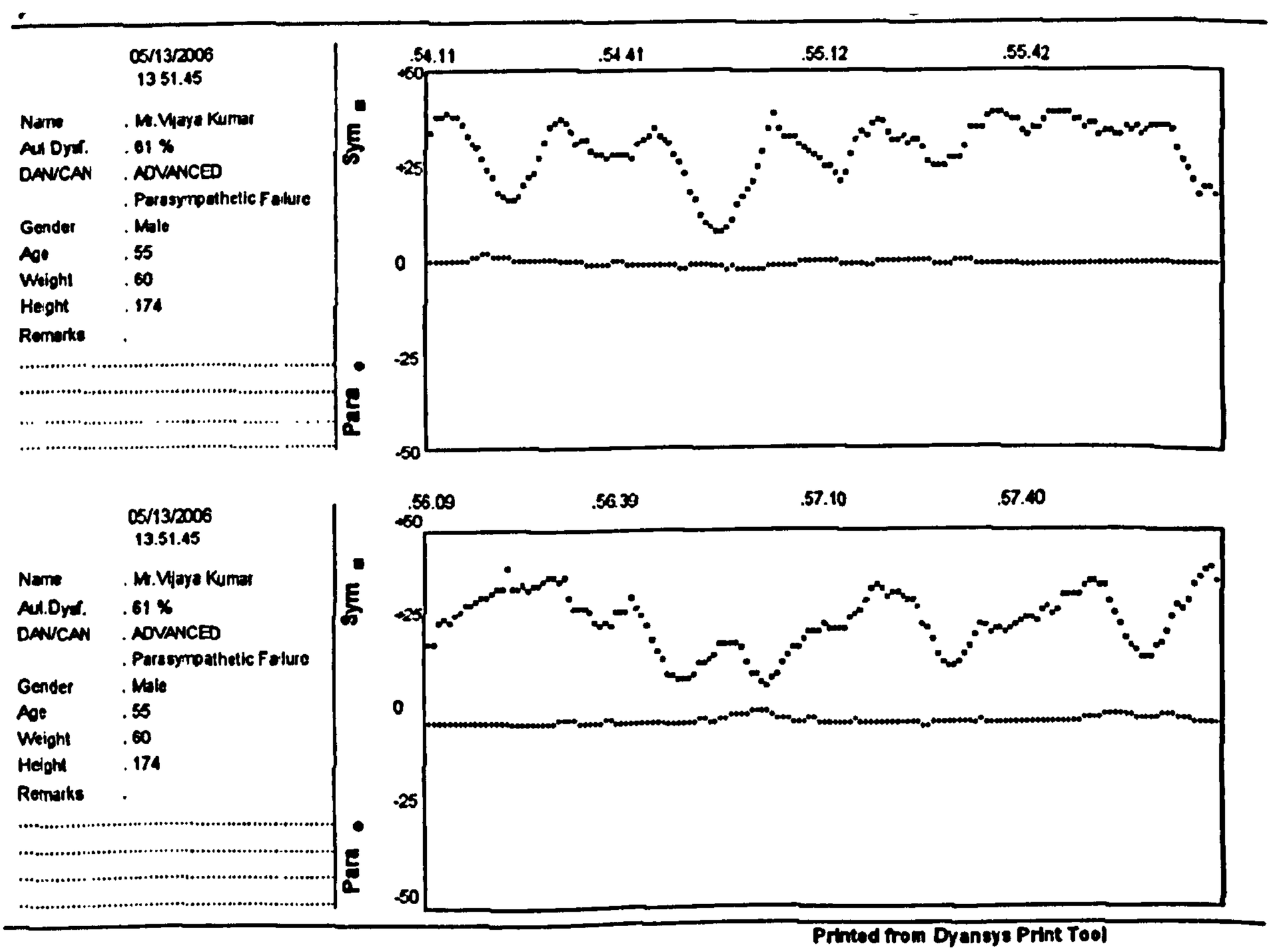


**Figure I-1: Typical result sheet from the Dyansys system for a neuropathic diabetic patient. This result is for a 55 yr Male patient with 61% autonomic dysfunction and is classified into advanced stage.**

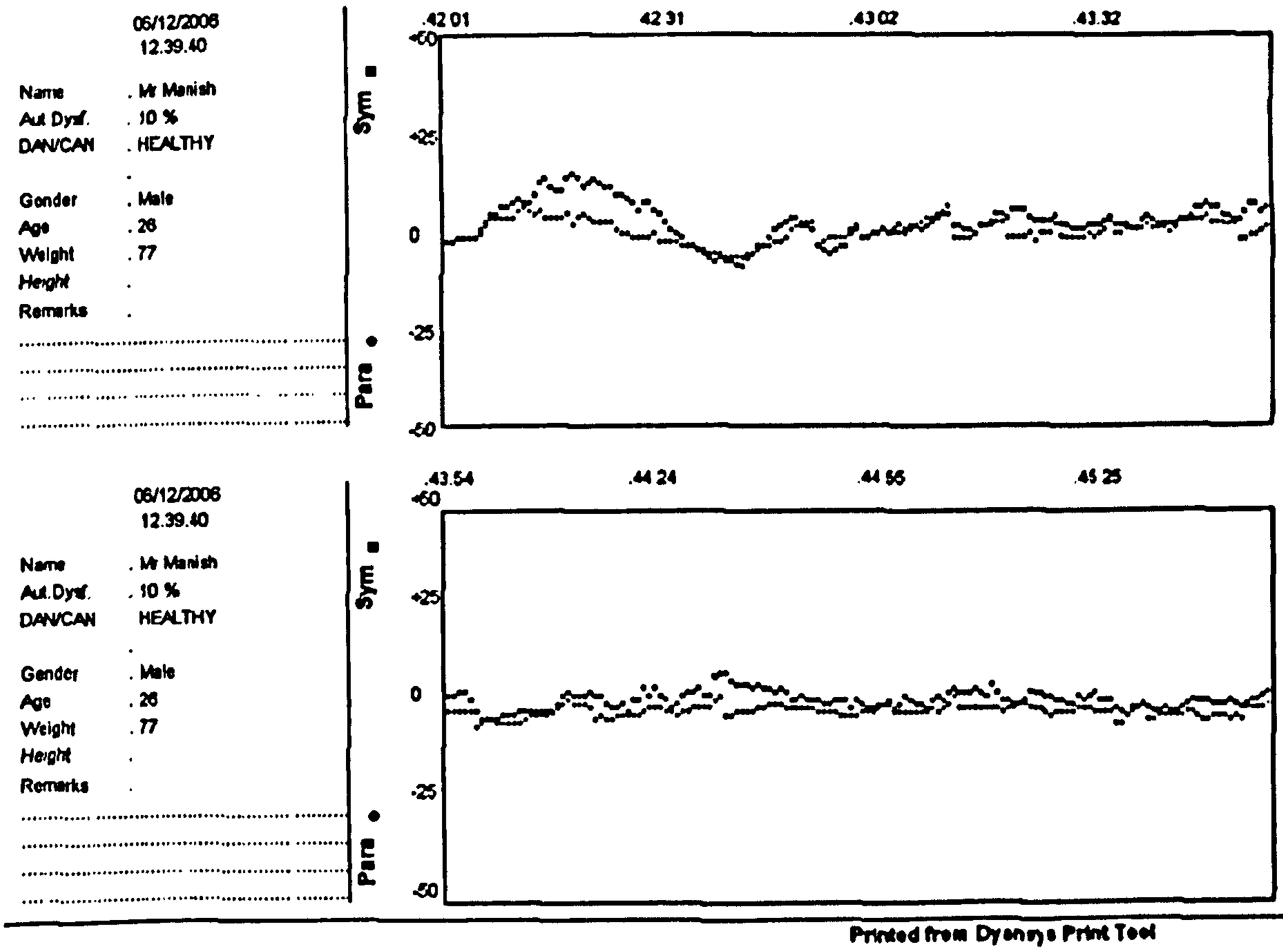


**Figure I-2: Typical result sheet from the Dyansys system for healthy subject. This result is for a 26 yr Male subject with 10% autonomic dysfunction and is classified into healthy stage.**

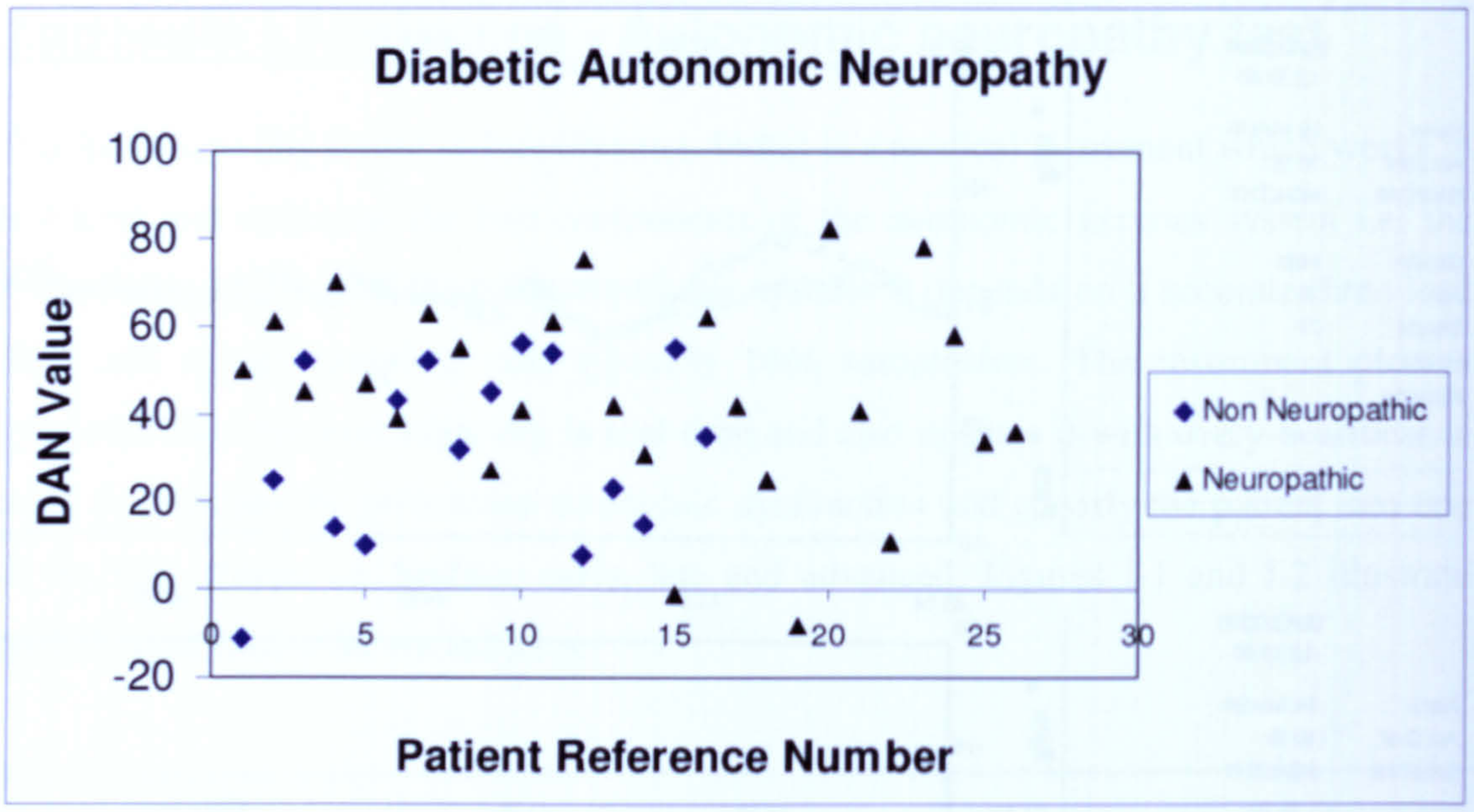


**Figure I-3: Graph representing the autonomic dysfunction value for the subjects the neuropathic and non neuropathic group.**

Diabetic autonomic neuropathy is a common condition, in which the autonomic nervous system that regulates the major physiologic processes such as sweating and blood pressure is affected. Dyansys Ansiscope has been validated in other studies (Lafitte, Fèvre-Genoulaz et al. 2005; Fèvre-Genoulaz, Lafitte et al. 2006; María, María et al. 2006). The Ansiscope computes a percentage of dysautonomia from a recording of 571 RR intervals recordings with the patient in supine position. This instrument was used to assess the autonomic neuropathy for the diabetic groups (neuropathic with n=26 and non neuropathic with n=17) in the clinical study. 65% subjects in non neuropathic diabetic group and 88.5% of the subjects in neuropathic diabetic group, show either late or advanced stage neuropathy. Figure I-3 represents the percentage autonomic dysfunction value for all subjects in the neuropathic and non neuropathic group.

# Appendix J Clinical case studies

**40 yrs old Female with pain and oedema on the medial heel surface**

The patient has a poor control of diabetes over the last three months (%HbA1C is 9), clinical obesity (BMI 31.18) and late stage diabetic autonomic neuropathy with parasympathetic failure (from Dyansys Ansiscope). There was however, no clinical neuropathy detected in the patient using the monofilament and biothesiometry technique.

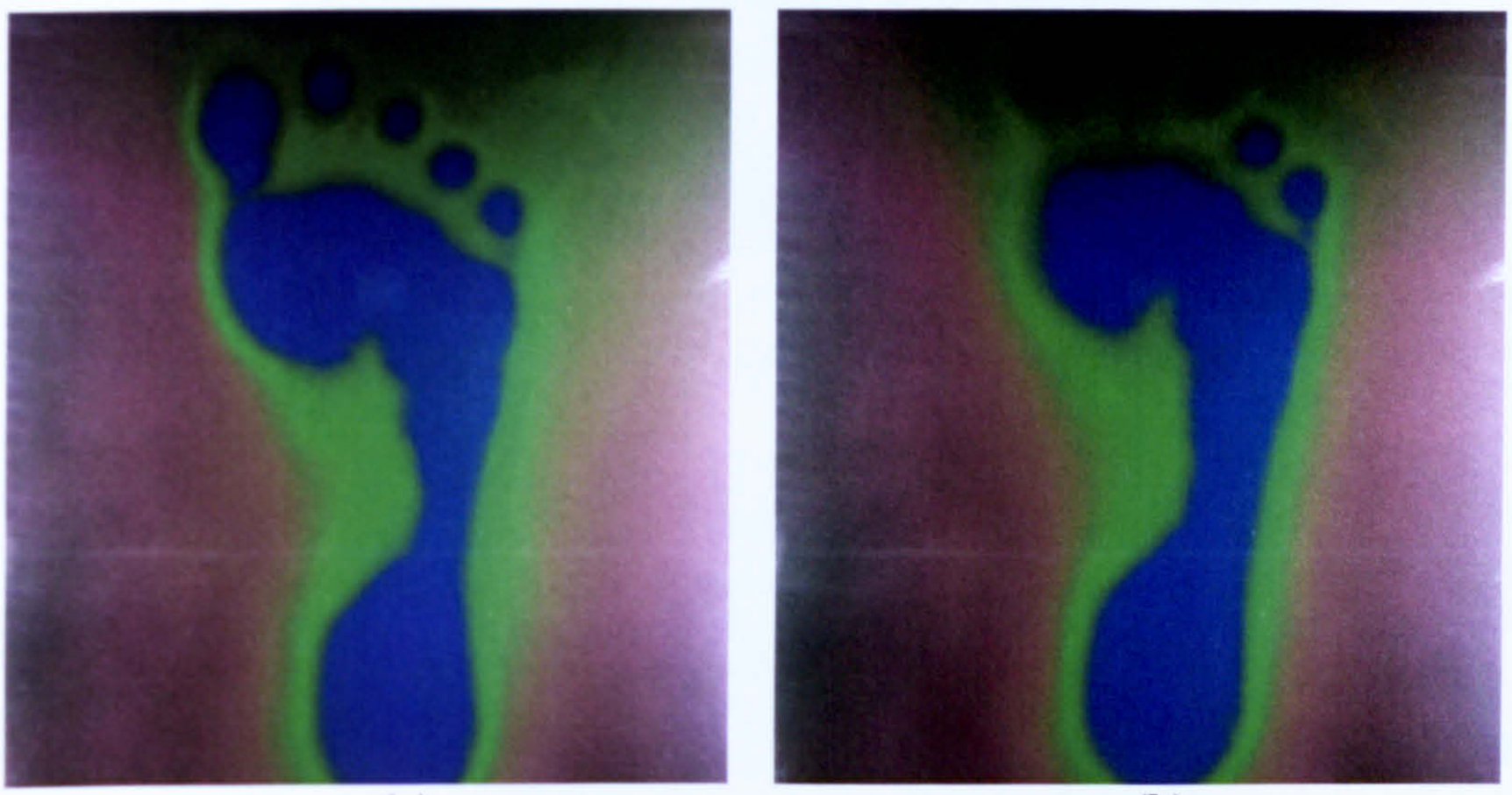

(a) (b)

**Figure J-1: Typical baseline (a) and repetitive stress (b) RGB images acquired from the LCT system.**

The foot temperature in both the tests is higher than the 30°C threshold (based on past studies) considered in the present study. Therefore, the task of identifying the inflammation areas in the images is complicated. The inflammation can however, be visualised better during the cold immersion test as shown in figures J-2 to J-3.

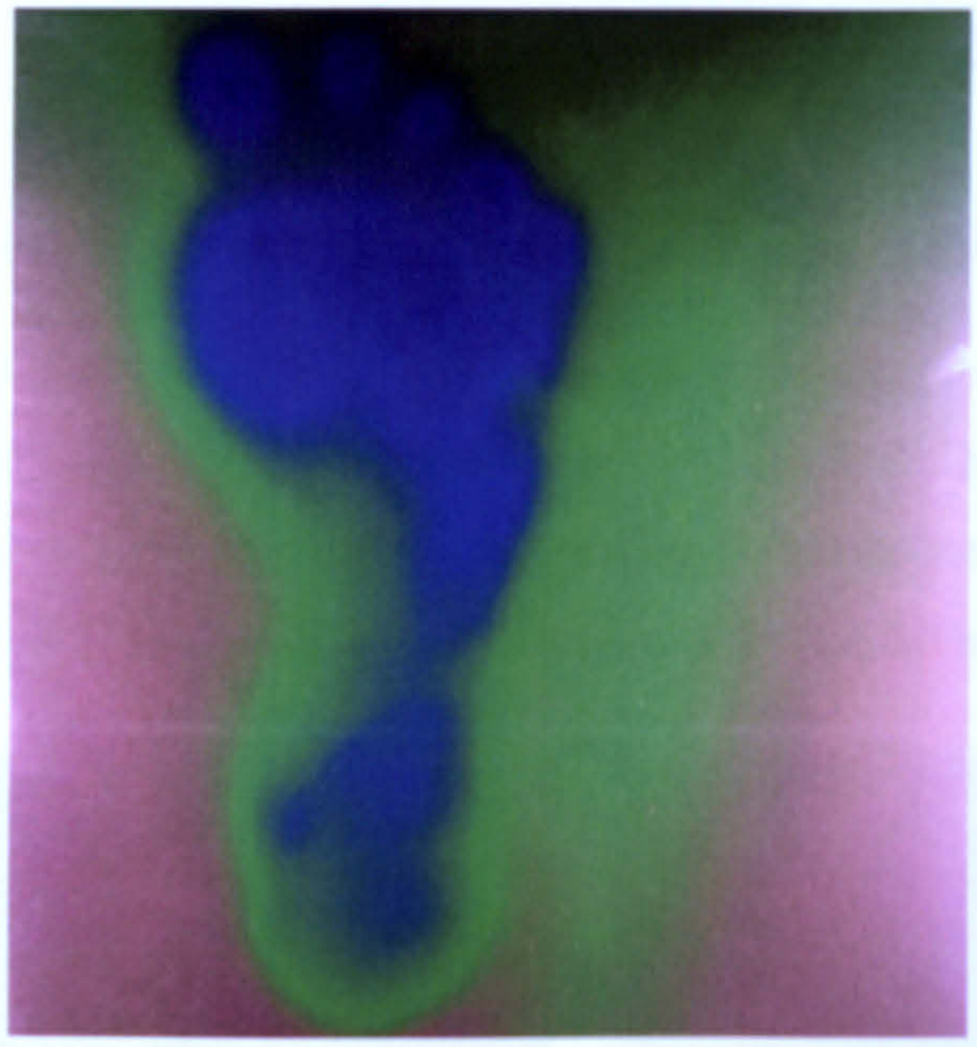

**Figure J-2: Typical cold immersion recovery acquired post five minutes during the test. The oedema is visible on the medial surface of the heel with 100% specificity.**




**Figure J-3: The pseudocolour image representing the hue plane of the HSV image illustrates the oedema during cold immersion recovery test.**

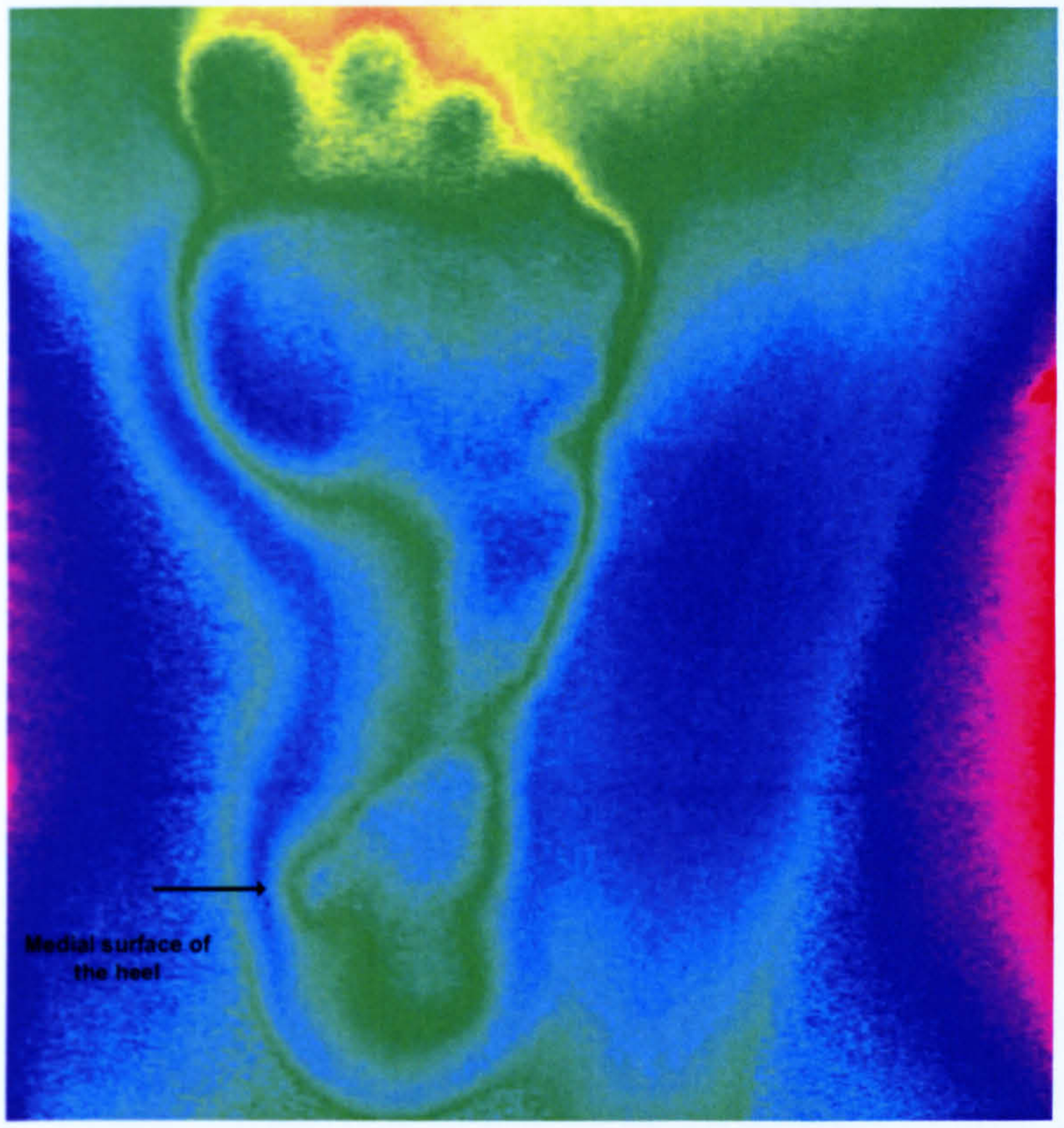


**Figure J-4: The intensity image representing the contours on the plantar surface highlights the raised temperature area during cold immersion recovery test.**

It must be stressed that only hue was used to relate the colour information with temperature. Intensity image is shown in pseudocolour format to highlight the capability of the system in detecting clinical presence of oedema. There were two patients with clinical oedema during the study. The other patient is now discussed.

**60 yrs old Female with pain and oedema on the medial heel surface**

The patient has a poor control of diabetes over the last three months (%HbA1C is 10.2), clinical obesity (BMI 30.45) and advanced stage diabetic autonomic neuropathy with parasympathetic failure (from Dyansys Ansiscope). Clinical neuropathy detected in the patient using the monofilament and biothesiometry technique.

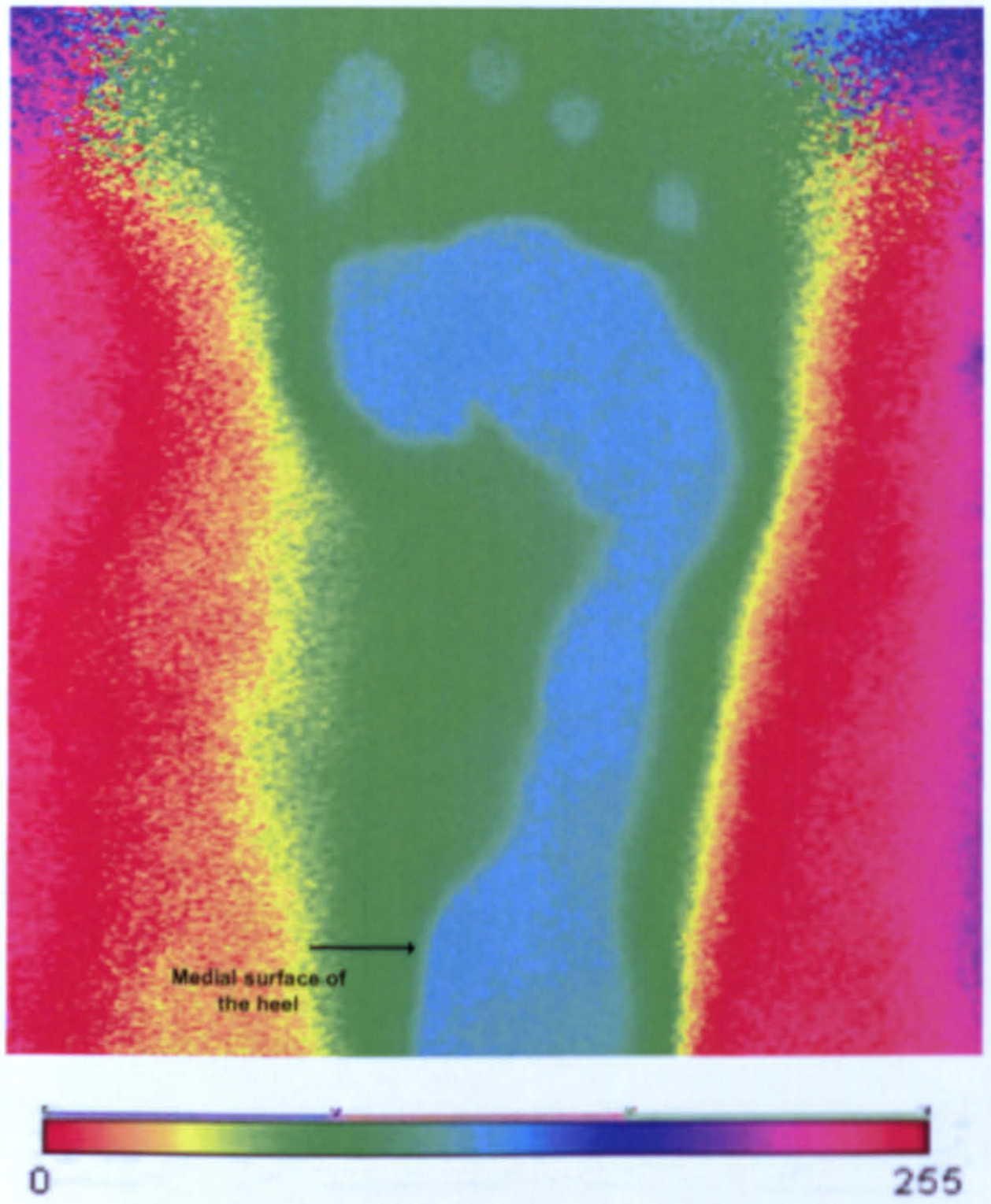


**Figure J-5: The pseudocolour image representing the hue plane of the HSV image illustrates the oedema during baseline test for 60 Yr/F patient.**

The presence of oedema can be visualised in both baseline and repetitive stress test for this patient as seen in figures J-5 and J-6. The reduced temperature in the repetitive stress test image on the medial surface is supported by the general discomfort for the patient during gait. Inflammation is not visualised in the cold immersion recovery test because of a mottled image.

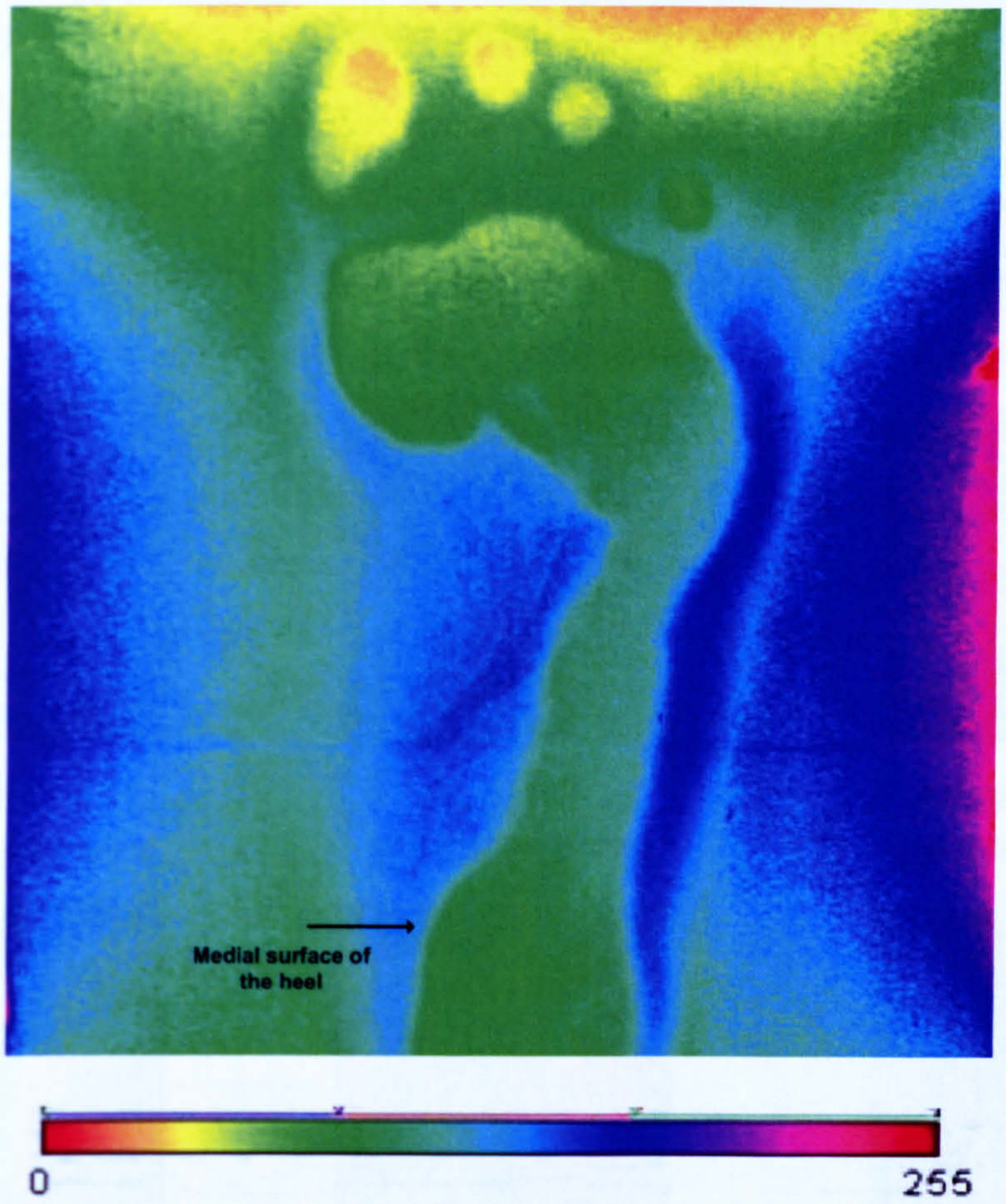


**Figure J-6: The pseudocolour image representing the hue plane of the HSV image illustrates the oedema during repetitive stress test for 60 Yr/F patient.**

**Comparison of response of thermoreceptors during cold immersion recovery test**

As discussed in the thesis, the response of thermoreceptors during the cold immersion recovery test suggests punctuate distribution of the receptors on the plantar surface of the foot. Figure J-7 illustrates the comparison for response of thermoreceptors for the three study groups.

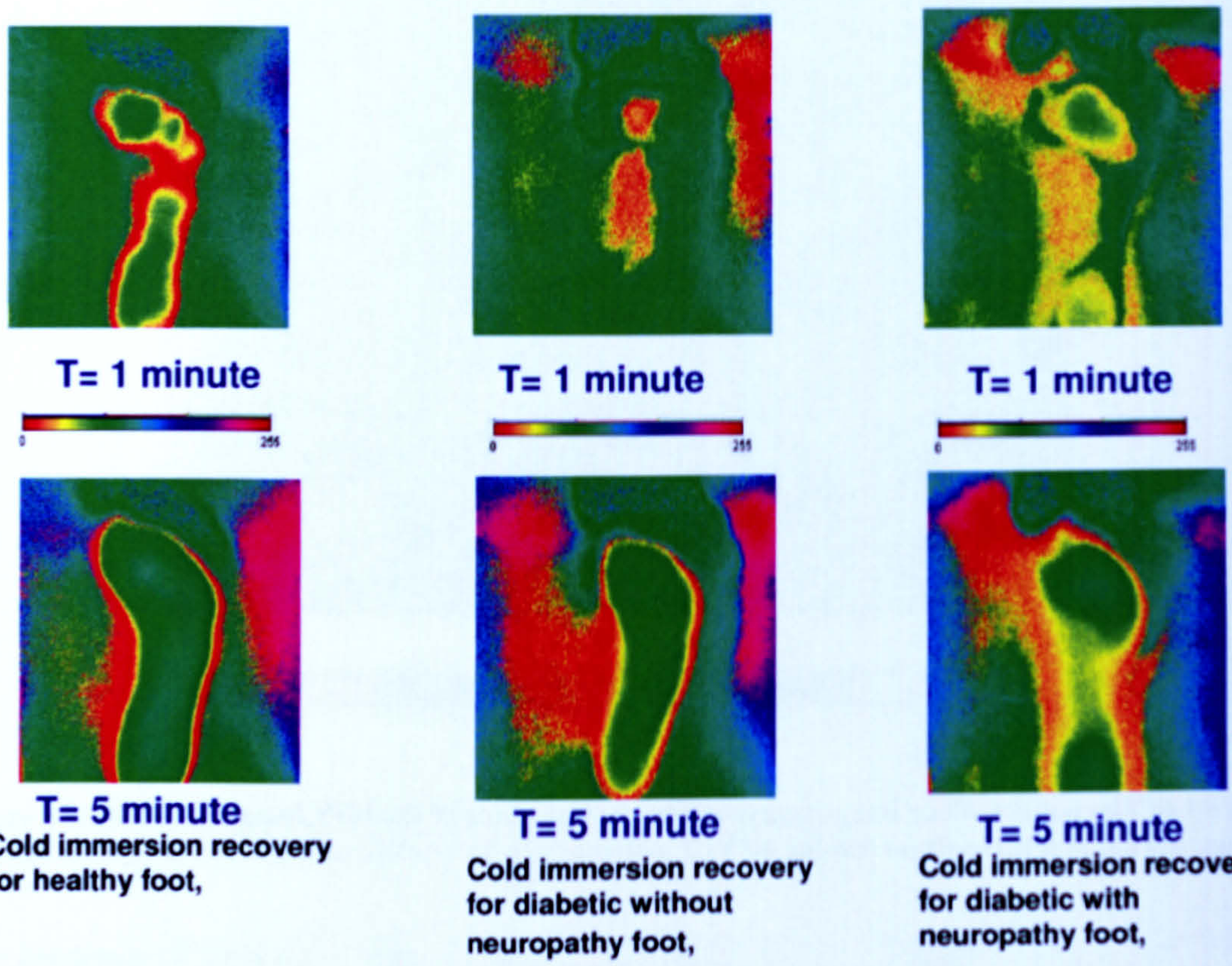


**Figure J-7: Comparison of response of thermoreceptors during cold immersion recovery test for the three study groups.**

These pseudocolour images suggest the delayed response for the diabetic groups, especially the neuropathic group as seen from the recovery images post five minutes. The recovery after cold immersion starts at the metatarsal head region and the heel suggesting higher density of thermoreceptors in these regions. The basis of this pattern can be confirmed in a larger clinical trial.

# Appendix K Proposed temperature and pressure evaluation system

It is envisaged that the LCT system investigated in the current study can be extended into combined temperature and pressure measurement system. A need for such a system has been identified in the current study. The proposed design is based on the grid type forceplate for pressure evaluation used by Manley et al. (1985). Figures K-1 and K-2 show the forceplate and the areas subject to high pressure during loading respectively. Each horizontal bar in the grid can be constructed using 15 mm thick polycarbonate lying in the direction of walking with cantilevered with strain gauge based pressure sensors on the sides.

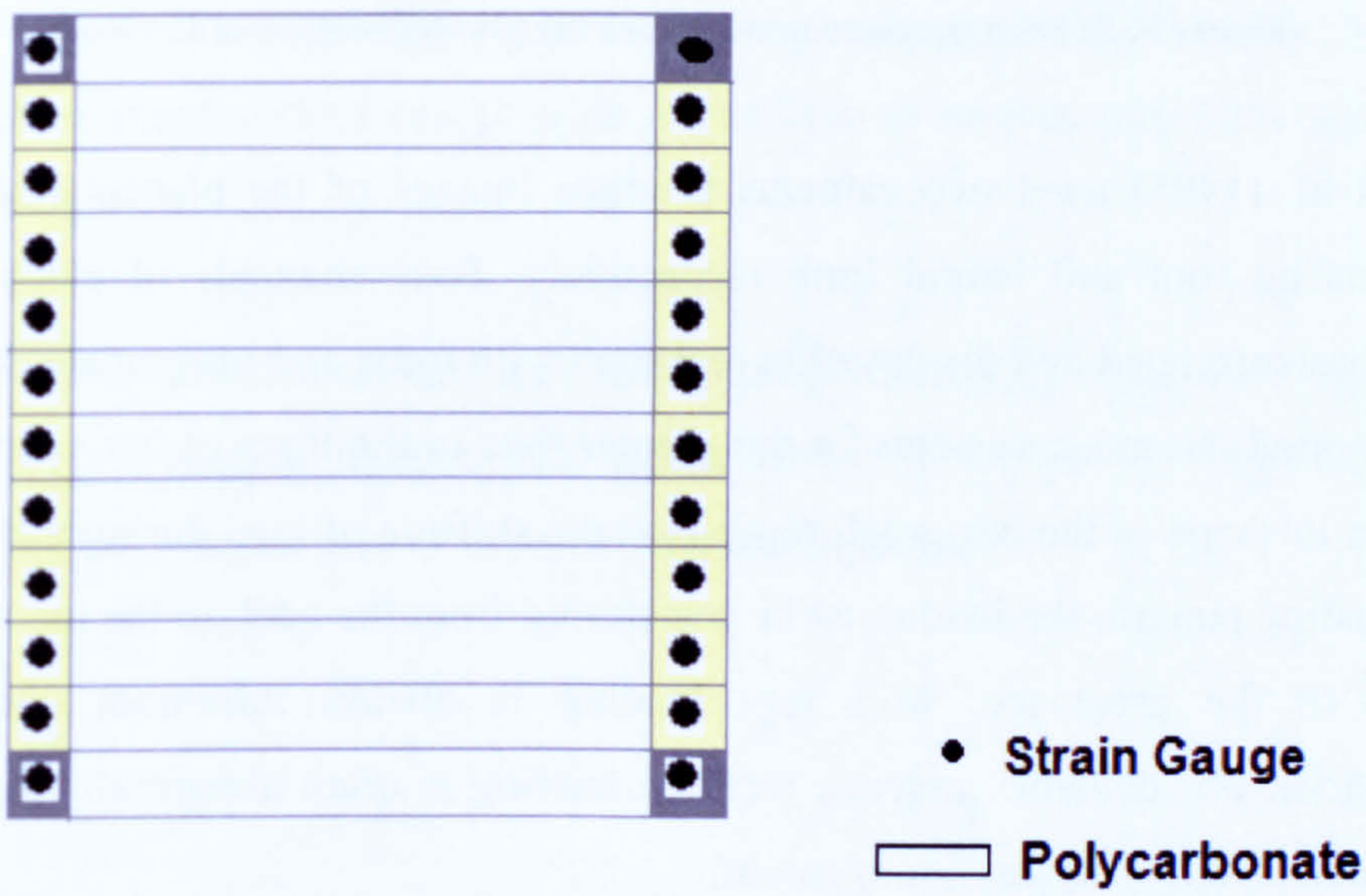


**Figure K-1: Force plate using polycarbonate beams and cantilevered strain gauge based load cells.**

Polycarbonate is used for optical access and mechanical support, with excellent transparency, weatherability, thermo-formability and high impact resistance. The specific design issues and selection of pressure sensors need to be investigated. Measurements can either be taken during normal gait by mounting the forceplate flush into the floor or in accordance with the current clinical protocol. This instrument may be useful in

evaluating temperature and pressure threshold values the weight bearing foot that lead to tissue breakdown in patients with impaired neurologic control.

**Figure K-2: High pressure areas under the plantar surface of the foot.**

Manley et al. (1985) used two cameras produce images of the plantar surface of the weight bearing foot and lateral limb respectively. Four channels of electromyogram (EMG) were correlated and displayed in real time with force and image data. Manley MT (1985) reported the measurements of the plantar foot in the form of bar charts, wherein the change in shape of the bar graph represents the shifting of load during walking. For a normal loading pattern, the load must be transferred from the heel, to the metatarsal head and then to the great toe. Mid foot loading is always minimum under normal circumstances. For diabetic subjects, forefoot loading is often abnormally high and can easily be detected by such an arrangement.

Advantages of a combined temperature and pressure measurement system are:

(a) Ability to monitor the effect of mechanical properties of the plantar skin in type 2 diabetes mellitus.

(b) EMG assessment gives the capability to monitor the specific muscles involved during walking. Although, occurrence of sensory neuropathy is higher than the motor neuropathy; motor neuropathy weakens the foot's intrinsic muscles causing foot

deformities (Birke James A et al. 1992). Therefore, the combined system provides possibility to assess specific patients with motor neuropathy. Abnormal gait can be visually identified and such a finding can be confirmed with force and time measurements obtained along with the thermal images. These results may give direct indications on abnormal weight bearing distribution due to distal motor neuropathy.

(c) Enhanced flexibility to assess repetitive stress injuries in neuropathic diabetic patients with better understanding of the association between vertical loading (magnitude and times) with thermal changes.

(d) There is a relatively better understanding about the biomechanics of the diabetic foot. Results of the current study and other thermal assessment devices reported in the thesis can further current understanding about the thermal changes under the foot. A low cost combined assessment system can provide a platform to answer questions raised in the current investigation.

(e) Capability to assess thermal and mechanical properties of the regenerated tissue at the ulcerated site (post surgical intervention) and suitability of specialised drugs that assist in wound healing (an integral part of diabetic foot management).

# Glossary

- **Ankle Brachial Index** – Ratio between the highest systolic pressure at the ankle and the systolic brachial pressure while a person is at rest.
- **Atherosclerosis** – Deposition of plaque and endothelial wall damage.
- **Basal Metabolism** - Energy used to maintain constant body temperature.
- **Birefringence** – Decomposition of a ray of light into two rays.
- **Colour Play** - Temperature range over which the TLC material actively reflects visible light and can be distinguished by the imaging equipment.
- **Contralateral** – On the unaffected foot.
- **Cooling Cycle** - Process in which TLC liquid crystal sheet is cooled down by heating it above the clearing point temperature.
- **Coverage Factor** - Ratio of TLC reflection to the background reflection.
- **Delta Temperature** - The temperature difference between the hot spot and cool area indicating the degree of inflammation and thus, danger of tissue breakdown.
- **Dichroism** - Phenomenon involving differential absorption of right hand and left hand circularly polarised light.
- **Homeostasis** - Temperature regulation along with psycho-physiological functions to keep body variables within normal range.
- **Hyperaemia** - Normal physiological response of the microcirculation to increased metabolic requirement following any incident of blood occlusion or ischeamia.
- **Hyperkeratosis** - Thickening of the outer layer of the skin.
- **Ipsilateral** - On the affected foot.
- **Ischaemic** – Inadequacy of blood supply.
- **Mechanoreceptors** - Body cells transducing mechanical stimuli to electrical impulses for the central nervous system.
- **Peripheral Neuropathy** - Refers to metabolic changes and poor blood supply in nerve cells as a result of altered blood glucose in diabetes.
- **Plantar Pressure** - Force measured over a small defined area, especially plantar prominences and the heel.

- **Somatosensory System** – Involves the receptors and pathways of cutaneous sensation.
- **Subclinical** - Symptomatic with absent clinical or neurophysiological signs.
- **Sudomotor** - Pertaining to nerves that stimulate sweating due to activity.
- **Thermoreceptors** – Body cells transducing thermal stimuli to electrical impulses for the central nervous system.
- **Thermoregulation** – Control of body core temperature by varying skin blood flow.
- **Warming Cycle** – Process in which TLC sheets are heated by cooling below the event temperature.

# References

Akhlagi, F. and Pepper, M. (1996). "In-shoe biaxial shear force measurement: The Kent shear system." Medical and Biological Engineering and Computing **34**: 315-317.

Anbar, M. (1998). "Clinical thermal imaging today." IEEE Engineering in Medicine and Biology **17**: 25-33.

Anbar, M. and Milescu, L. (1998). Prerequisites of dynamic area telethermometry (DAT). Proceedings of the 20th Annual International Conference of the IEEE Engineering in Medicine and Biology Society, IEEE.

Anderson, K. (2001). End of the year NSF scholarship student report, Colarado School of Mines. **2005**.

Anderson, M. (1999). Thermochromic liquid crystal thermography: Hysteresis, illumination and imaging system effects, image processing and applications. Mechanical and Aeronautical Engineering. California, University of California, Davis.

Anderson, M. and Baughn, J. (2004). "Hysteresis in Liquid Crystal Thermography." Journal of Heat Transfer **126**: 339-346.

Arcan, M. and Brull, A. (1976). "A fundamental characteristic of the human body and foot, the foot-ground pressure pattern." Journal of Biomechanics **9**: 453-457.

Archer, A. G., Roberts, V. C. and Watkins, P. J. (1984). "Blood flow patterns in painful diabetic neuropathy." Diabetologia **27**: 563-567.

Ariyaratnam, S. and Rood, J. (1990). "Measurement of facial skin temperature." Journal of Dentistry **18**: 250-253.

Armstrong, D. and Lavery, L. (1997). "Monitoring healing of acute Charcot's arthropathy with infrared dermal thermometry." Journal of Rehabilitation Research and Development **34**(3): 317-321.

Armstrong, D., Lavery, L., Liswood, P., Todd, W. and Tredwell, J. (1997). "Infrared dermal thermometry for the high-risk diabetic foot." Physical Therapy **77**(2): 169-175.

Armstrong, D., Lavery, L., Vela, S., Quebedeaux, T. and Fleischli, J. (1998). "Choosing a practical screening instrument to identify patients at risk for diabetic foot ulceration." Archives of Internal Medicine **158**(3): 289-293.

Armstrong, D., Lavery, L., Wunderlich, R. and Boulton, A. (2003). "Skin temperatures as a one-time screening tool do not predict future diabetic foot complications." Journal of American Podiatry Medical Association **93**(6): 443-447.

Armstrong, D., Sangalang, M., Jolley, D., Maben, F., Kimbriel, H., Nixon, B. and Cohen, I. (2005). "Cooling the foot to prevent diabetic foot wounds." Journal of American Podiatry Association **95**(2): 103-107.

Armstrong, D. G., Lipsky, B., Polis, A. and Abramson, M. (2006). "Does dermal thermometry predict clinical outcome in diabetic foot infection? Analysis of data from the SIDESTEP trial." International Wound Journal **3**(4): 302-207.

Armstrong, T. (2004). Personal Communication: Handling thermochromic liquid crystal polyester sheets. Bharara, M. Bournemouth.

Ashforth, F. S. (1996). "Quantitative thermal imaging using liquid crystals." Journal of Biomedical Optics **1**(1): 18-27.

Ashforth, F. S. and Rudel, U. (2003). "Thermal and hydrodynamic Visualisation of a water jet impinging on a flat surface using microencapsulated liquid crystals." International Journal of Fluid Dynamics.

Aspres, N., Egerton, I., Lim , A. and Shumack, S. (2003). "*Imaging the Skin.*" Australian Journal of Dermatology **44**: 19-27.

Azar, K., Benson, J. and Manno, V. (1991). Liquid crystal imaging for temperature measurement of electronic devices. IEEE Semicnductor Thermal Measurement and Management Symposium, Phoenix.

Baer, M., Hetherington, V., Lockyer, J. and Long, D. (1988). "Preliminary report on the use of liquid crystal thermography in podiatry." Journal of Foot Surgery **27**(5): 398-403.

Bahill, A. (1981). Bioengineering: Biomedical, Medical and Clinical Engineering. Englewood Cliffs, New Jersey, Prentice Hall.

Bakrania, S. and Anderson, A. (2002). A transient technique for calibrating thermochromic liquid crystals: The effects of surface preparation, lighting and overheat. ASME IMECE, New Orleans, Louisiana, ASME.

Barnett, S., Cunningham, J. L. and West, S. (2001). "A Comparison of vertical force and temporal parameters produced by an in-shoe pressure measuring system and a force platform." Clinical Biomechanics **16**(4): 353-357.

Bauman, J., Girling, E. and Brand, P. (1963). "Plantar pressures and trophic ulceration: An evaluaton of footwear." Journal of Bone Joint Surgery **45**(B): 652-673.

Behle, M., Schulz, K., Leiner, M. and Fiebig, M. (1996). "Color based image processing to measure local temperature distributions by wide band liquid crystal thermography." Applied Scientific Research **56**: 113-143.

Belcaro G, Vasdekis S, Rulo A and Nicolaides AN (1989). "Evaluation of skin blood flow and venoarteriolar response in patinets with diabetes and perpheral vascular disease by laser Doppler flowmetry." Angiology **40**(11): 953-957.

Benbow, S., Chan, A., Bowsher, D., Williams, G. and Macfarlane, I. (1994). "The prediction of diabetic neuropathic plantar foot ulceration by liquid-crystal contact thermography." Diabetes Care **17**(8): 835-839.

Benjamin, A. (1973). "Differential diagnosis with cholesteric liquid crystal thermography." Journal of the Biological Photographic Association **41**(1): 13-14.

Bergtholdt, H. (1979). "Temperature assessment of the insensitive foot." Physical Therapy **59**: 18-22.

Berne and Levy (1986). Cardiovascular Physiology, Mosby, Inc.

Bernstein, R. K. (2003). Dr. Bernsteins - The complete guide to achieving normal blood sugars., www.diabetes-book.com. **2003**.

Bertelsmann, F., JJ., H., Weber, E. and Veen, E. (1985). "Thermal discrimination thresholds in normal subjects and in patients with diabetic neuropathy." Journal of Neurology Neurosurgery & Psychiatry **48**: 686-690.

Bharara, M., Cobb, J. and Claremont, D. (2006). "Thermography and thermometry in the assessment of diabetic neuropathic foot: A case for furthering the role of thermal techniques." International Journal of Lower Extremity Wounds **5**(4): 250-260.

Bharara, M., Cobb, J., Claremont, D. and Anderson, A. (2005). "Liquid crystal thermography - Application in neuropathic assessment of diabetic foot." Thermology International **15**(4): 154-155.

Bharath, R. and Drosen, J. (1994). Neural networks and statistical analysis. Neural Network Computing, Windcrest: McGraw-Hill.

Bishop, C. (1995). Neural Networks for Pattern Recognition, Oxford University Press.

Bland, M. (2004). An Introduction to Medical Statistics. Norfolk, Oxforf University Press.

Boignard, A., Salvat-Melis, M., Carpentier, P., Minson, C., Grange, L., Duc, C., Sarrot-Reynauld, F. and Cracowski, J. (2005). "Local hyperemia to heating is imapaired in secondary Raynaud's phenomenon." Arthritis Research & Therapy 7(5): 1103-1112.

Boulton, A., Connor, H. and Cavanagh, P. R., Eds. (1998). The Foot in Diabetes, John Wiley & Sons.

Boulton, A., Hardisty, C., Betts, R., Franks, C., Worth, R., Ward, J. and Duckworth, T. (1983). "Dynamic foot pressure and other studies as diagnostic and management aids in diabetic neuropathy." Diabetes Care **6**(1): 26-33.

Boulton, A., Scarpello, J. and Ward , J. (1982). "Venous oxygenation in the diabetic neuropathic foot: Evidence of arteriovenous shunting." Diabetologia **22**: 6-8.

Boulton, A. J. M. (1998). Foot problems in patients with diabetes mellitus. Textbook of Diabetes. Pickup, J. and Williams, G. Italy, Blackwell Science. **2:** 58.1- 58.20.

Brand, P. (1981). Insensitive Feet. A Practical Handbook on Foot Problems in Leprosy. London, Leprosy Mission.

Brand, P. (1990). The diabetic foot. Ellenberg's and Rifkin's Diabetes Mellitus; Theory and Practice. Rifkin, H. and Ponte, D. New York, Elsevier**:** 829-849.

Brash, P. D., Foster, J., Vennart, W., Anthony, P. and Tooke, J. E. (1999). "Magnetic resonance imaging techniques demonstrate soft tissue damage in the diabetic foot." Diabetic Medicine **16**(1): 55-62.

Brown, A. and Saluja, C. (1978). "The use of cholesteric liquid crystals for surface temperature visualisation of film cooling process." Journal of Physics and Scientific Instrumentation **11**: 1068-1072.

Bus, S., Yang, Q., Wang, J., Smith, M., Wonderlich, R. and Cavanagh, P. R. (2002). "Intrinsic muscle atrophy and toe deformity in the diabetic neuropathic foot." Diabetes Care **25**: 1444-1450.

Camci, C., Kim, K. and Hippensteele, S. (1992). "A new hue capturing technique for quantitative interpretation of liquid crystal images used in convective heat transfer studies." ASME transaction: Journal of Turbomachinery **114**: 765-775.

Campbell, W. and Lebovitz, H. (1996). Diabetes Mellitus - Fast Facts. Oxford, Health Press.

Cavanagh, P. and Ulbrecht, J. (1995). Biomechanical aspects of foot problems in diabetes. The Foot in Diabetes. Cavanagh, P. Chichester, John Wiley & Sons: 25-36.

Cavanagh, P., Ulbrecht, J. and Caputo, G. (2001). The biomechanics of the foot in diabetes mellitus. Levin and O'Neal's - The Diabetic Foot. Pfeifer, M. St. Louis, Mosby: 125-196.

Cavanagh, P. R., Lipsky, B., Bradbury, A. and Botek, G. (2005). "Treatment for diabetic foot ulcers." The Lancet **366**(9498): 1725-1735.

Cavanagh, P. R., Simoneau, G. and Ulbrecht, J. (1993). "Ulceration, unsteadiness and uncertainty: The biomechanical consequences of diabetes mellitus." Journal of Biomechanics **26**(suppl): 23-40.

Chan, A., MacFarlane, I. and Bowsher, D. (1991). "Contact thermography of painful diabetic neuropathic foot." Diabetes Care **14**(10): 918-922.

Chan, T. L., Ashforth-Frost, S. and Jambunathan, K. (2001). "Calibrating for viewing angle effect during heat transfer measurements on a curved surface." International Journal of Heat and Mass Transfer **44**(12): 2209-2223.

Cherkas, L., Howell, K., Carter, L., Black, C. and MacGregor, A. (2001). "The use of portable radiometry to assess Raynaud's phenomenon: a practical alternative to thermal imaging." Rheumatology **40**: 1384-1387.

Chesnin, K. J., Selby, S. L. and Besser, M. P. (2000). "Comparison of an in-shoe pressure measurement device to a force plate: concurrent validity of center of pressure measurements." Gait & Posture **12**(2): 128-133.

Clark, R., Goff, M., Hughes, J. and Klenerman, L. (1988). "Thermography and Pedobarography in the assessment of tissue damage in neuropathic and atherosclerotic feet." Thermology **3**: 15-20.

Clark, S., Dunn, G., Moore, T., Jayson, M., King, T. and Herrick, A. (2003). "Comparison of thermography and laser Doppler imaging in the assessment of Raynaud's phenomenon." Microvascular Research **66**(1): 73-76.

Cobb, J. and Claremont, D. (1995). "Transducers for foot pressure measurement." Medicine Biology Engineering & Computing **33**: 525-532.

Cobb, J. and Claremont, D. (2002). "Noninvasive measurement techniques for monitoring of microvascular function in the diabetic foot." International Journal of Lower Extremity Wounds **1**(3): 161-169.

Cobb, J. E. (2000). An in-shoe laser Doppler sensor for assessing plantar blood flow in the diabetic foot. DEC. Bournemouth, Bournemouth University.

Commean, P., Mueller, M., Smith, K., Hastings, M., Klaesner, J., Pilgram, T. and Robertson, D. (2002). "Reliability and validity of combined imaging and pressures assessment methods for diabetic feet." Archives of Physical Medical Rehabilitation **83**: 497-505.

Currie, C., Morgan, C. and Peters, J. (1998). "The epidemiology and cost of inpatient care for peripheral vascular disease, infection, neuropathy and ulceration in diabetes." Diabetes Care **21**(1): 42-48.

Currie, C., Poole, C., Woehl, A., Morgan, C., Cawley, S., Rousculp, M., Covington, M. and Peters, J. (2007). "The financial costs of healthcare treatment for people with Type 1 or Type 2 diabetes in the UK with particular reference to differing severity of peripheral neuropathy." Diabetic Medicine **24**(2): 187-194.

Delpy, D., Cope, M. and Vanderzee, P. (1988). "Estimation of optical pathlength through tissue from direct time of flight measurement." Physics in Medicine & Biology **33**(12): 1433-1442.

Dribbon, B. (1983). "Application and value of Liquid Crystal Thermography." Journal of American Podiatry Association **73**(8): 400-404.

Edmonds, M., Foster, A. and Sanders, L. (2004). A Practical Manual of Diabetic Footcare. Denmark, Blackwell Publishing.

Elkeles, R. and Wolfe, J. (1991). "The Diabetic Foot." British Medical Journal **303**: 1053-1055.

Fagrell, B. (1984). Microcirculation of the skin. The Physiology and Pharmacology of the Microcirculation. Fagrell. London, Academic Press. **2**: 133-180.

Farina, D. (1995). "Making surface temperature measurements using liquid crystal thermography." Electronics Cooling **1**(2): 10-15.

Farina, D., Hacker, J., Moffat, R. and Eaton, J. (1994). "Illuminant invariant liquid crystal calibration of thermochromic liquid crystals'." Journal of Experimental Thermal Fluid Science **9**: 1-12.

Felder, D., Russ, E., Montgomery, H. and Horwitz, H. (1954). "Relationship in the toe of skin surface temperature to mean blood flow measured with a plethysmograph." Clinical Science **11**: 251-256.

Fisher, A., Gilula, L. and McEnery, K. (2001). Imaging of the diabetic foot. The Diabetic Foot. Bowker, J. and Pfeifer, M. St. Louis, Missouri, Mosby Inc.**:** 333-354.

Flesch, U. (1985). Techniques for Liquid Crystal Thermography in Medicine. Thermological Methods. J M Engel, U. F., G Stuttgen, VCH**:** 45-62.

Flynn, M., Edmonds, M., Tooke, J. and Watkins, P. (1988). "Direct measurement of capillary blood flow in the diabetic neuropathic foot." Diabetologia **31**: 652-656.

Flynn, M. and Tooke, J. (1995). "Diabetic neuropathy and the microcirculation." Diabetic Medicine **12**: 298-301.

Foerster, J., Kuerth, A., Niederstrasser, E., Krautwald, E., Pauli, R., Paulat, R., Eweleit, M., Riemekasten, G. and Worm, M. (2007). "A cold response index for the assessment of Raynaud's phenomenon." Journal of Dermatological Science **45**(2): 113-120.

Foerster, J., Wittstock, S., Fleischanderl, S., Storch, A., Riemekasten, G., Hochmuth, O., Meffert, B., Meffert, H. and M, W. (2006). "Infrared monitored cold response in the assessment of Raynaud's phenomenon." Clinical and Experimental Dermatology **31**(1): 6-12.

Foster, J., Damion, R., Vennart, W., Summers, I., Ellis, R., Brash, P. and Tooke, J. E. (1994). "Magnetic resonance imaging of peripheral vascular disease and muscle atrophy in diabetes." Magnetic Resonance Materials in Physics, Biology and Medicine **2**(3): 401-403.

Free, T. and Faerber, G. (1989). "Use of thermography in teh diagnosis of deep vein thrombosis." Journal of American Osteopathic Association **89**(6): 768-772.

Fridolin, I. and Lindberg, L. (2000). "Optical non invasive technique for vessel imaging: I - Experimental results." Physics in Medicine & Biology **45**: 3765-3778.

Gaylarde, P., Fonseca, V., llewellyn, G., Sarkany, I. and Thomas, P. (1988). "Transutaneous Oxygen Tension in Legs and Feet of Diabetic patients." Diabetes **37**: 714-716.

Giansanti, D. and Maccioni, G. (2007). "Development and testing of a wearable Integrated Thermometer sensor for skin contact thermography." Medical Engineering & Physics **29**(5): 556-565.

Giansanti, D., Maccioni, G. and Gigante, G. (2006). "A comparative study for the development of a thermal odoscope for the wearable dynamic thermography monitoring." Medical Engineering & Physics **28**(4): 363-371.

Gill, G. V. (1998). Diabetes Mellitus in developing countries. Textbook of Diabetes. Pickup, J. and Wlliams, G. Milan, Blackwell Science. **2:** 5.1-5.10.

Goblyos, P. and Szule, E. (1987). "Liquid crystal thermography in the localization of undescended testicles." European Journal of Radiology **7**: 266-267.

Goller, H., Lewis, D. and McLaghlin, R. (1971). "Thermographic studies of human skin subjected to localized pressure." American Journal of Roentgenology **113**(4): 749-754.

Gonzalez, R., Woods, R. and Eddins, S. (2004). Digital Image Processing Using MATLAB. Upper Saddle River, NJ, Pearson, Prentice Hall.

Gordois, A., Scuffham, P., Shearer, A. and Oglesby, A. (2003). "Cost-of-illness study: The healthcare costs of diabetic neuropathy in the UK." The Diabetic Foot **6**(2).

Got, I. (1998). "Transcutaneous oxygen pressure: advantages and limitations." Diabetes Metabolism . **24**(4): 379-384.

Grewal, G., Bharara, M., Cobb, J., Dubey, V. and Claremont, D. (2006). "A novel approach to thermochromic liquid crystal calibration using neural networks." Measurement Science &Technology **17**(7): 1918-1924.

Groop, L. (1998). Drug treatment of non-insulin dependent diabetes mellitus. Textbook of Diabetes. Pickup, J. and Williams, G. Milan, Blackwell Science. **2:** 38.1-38.18.

Grunfield, C. (1992). "Diabetic Foot Ulcers: Etiology, Treatment and Prevention." Advances in Internal Medicine **37**(19): 103-132.

Guy, R., Clark, C., Malcolm, P. and Watkins, P. (1985). "Evaluation of thermal and vibration sensation in diabetic neuropathy." Diabetologia **28**: 131-137.

Guyton (1992). Human Physiology and Mechanisms of the Disease. Philadelphia, W.B. Saunders Company.

Ha, T. and Lean, M. E. (1998). Diet and lifestyle modification in the management of non insulin dependent diabetes mellitus. Textbook of Diabetes. Pickup, J. and Williams, G. Italy, Blackwell Science. **1:** 37.1- 37.18.

Hales, J. (1983). "Thermoregulatory requirements for circulatory adjustments to promote heat loss in animals." Journal of Thermal Biology **8**(1-2): 219-224.

Hales, J., Iriki, M., Tsuchiya, K. and Kozawa, E. (1978). "Thermally induced cutaneous sympathetic activity related to blood flow through capillaries and arteriovenous anastomoses." Pflugers Arch **375**: 1724.

Hales, J., Jessen, C., Fawcett, A. and King, R. (1985). "Skin AVA and capillary dilation and constriction induced by local skin heating." Pflugers Arch **404**: 301-307.

Hallcrest (1991). Handbook of Thermochromic Liquid Crystals. Glenview, IL, Hallcrest.

Harding, J., Banerjee, D., Wertheim, D., Williams, R., Melhuish, J. and Harding, K. (1999). Infrared imaging in the long-term follow-up of osteomyelitis complicating diabetic foot ulceration. Proceedings of 21st Annual International Conference of the IEEE, Engineering in Medicine and Biology, IEEE.

Harding, J., Wertheim, D., Williams, R., Melhuish, J., Banerjee, D. and Harding, K. (1998). Infrared imaging in diabetic foot ulceration. Proceedings of Annual International Conference of the IEEE, Engineering in Medicine and Biology Society, Hong Kong, IEEE.

Hay, J. L. and Hollingsworth, D. K. (1996). "A comparison of trichromic systems for use in the calibration of polymer-dispersed thermochromic liquid crystals." Experimental Thermal and Fluid Science **12**(1): 1-12.

Hay, J. L. and Hollingsworth, D. K. (1998). "Calibration of micro-encapsulated liquid crystals using hue angle and a dimensionless temperature." Experimental Thermal and Fluid Science **18**(3): 251-257.

Hayes, A. and Seitz, P. (1997). "The average pressure distribution of the diabetic foot: can it be used as a clinical diagnostic aid?" Clinical Biomechanics **12**(3): S3-S4.

Hebden, J., Arridge, S. and Delpy, D. (1997). "Optical imaging in medicine: I - Experimental techniques." Physics, Medicine & Biology **42**: 825-840.

Herman, W. H. and Crofford, O. B. (1998). The relationship between diabetic control and complications. Textbook of Diabetes. Pickup, J. and Williams, G. Milan, Blackwell Science. **2**: 41.1-41.11.

Heuvel, C., Ferguson, S., Dawson, D. and Gilbert, S. (2003). "Comparison of digital infrared thermal imaging (DITI) with contact thermometry: pilot data from a sleep research laboratory." Physiological Measurement **24**(3): 717.

Hill, R. (1987). Diabetes health care: A guide to provision of health care services. London, Chapman and Hall: 177-190.

Howell, K., Kennedy, L., Smith, R. and Black, C. (1997). "Temperature of the toes in Raynaud's phenomenon measured using infra-red thermography." Thermology **7**: 132-137.

Huether, S. (1998). Structure, function and disorders of the integument. Pathophysiology and Biological Basis for Disease in Adults and Children. McCane, K. and Huether, S., Mosby, Inc: 1594-1654.

Hurkmans, H. L. P., Bussmann, J. B. J., Benda E, Verhaar J. A. N and Stam, H. J. (2003). "Techniques for measuring weight bearing during standing and walking." Clinical Biomechanics **18**(7): 576-589.

Hurley, J., Jung, M., Woods, J. and Hershey, F. (2001). Non invasive vascular testing: Basis, application and role in evaluating diabetic peripheral arterial disease. Levin and O' Neal's The Diabetic Foot. Bowker, J. and Pfeifer, M. St. Louis, Missouri, Mosby: 355-421.

Hutchinson, A., McIntosh, A. and Feder, G. (2000). Clinical guidelines and evidence review for type 2 diabetes: prevention and management of foot problems. London, Royal College of General Practioners.

Iiuch, A., Franzeck, U., Huch, R. and Bollinger, A. (1983). "A transparent transcutaneous oxygen electrode for simulataneous studies of skin capillary morphology, flow dynamics and oxygenation." International Journal of Microcirculaton: Clinical Experiments **2**: 103-108.

International Diabetes Federation (2003). Facts and Figures: International Diabetes Federation., IDF. **2004**.

Ireland, P. and Jones, R. (1987). "The response time of a surface thermometer employing encapsulated thermochromic liquid crystals." Journal of Physics and Scinetific Instrumentation **20**(10): 1195-1199.

Ireland, P., Neely, A., Gillispie, D. and Robertson, A. (1999). "Turbulent heat transfer measurement using liquid crystals." International Journal of Fluid Dynamics **20**: 355-367.

IWGDF (1999). International Consensus on the diabetic foot, International Working Group on the Diabetic Foot. **2003**.

Jaap, A. J. and E, T. J. (1995). "Pathophysiology of microvascular disease in non insulin dependent diabetes." Clinical Science **89**: 3-12.

Jambunathan, K., Hartle, S., Asforth- Frost, S. and Fontama, V. (1996). "Evaluation convective heat transfer coefficients using neural networks." International Journal of Heat & Mass Transfer **39**(11): 2329-2322.

Jones, B. and Plassmann, P. (2002). "Digital infrared thermal imaging of human skin." Engineering in Medicine and Biology Magazine, IEEE **21**(6): 41-48.

Jones, C., Ring, E., Plassmann, P., Ammer, K. and Wiecek, B. (2005). "Standardisation of infrared imaging: A reference atlas for clinical thermography - Initial results." Thermology International **15**(4): 157-158.

Jung, A. and Zuber, J. (1998). Thermographic Methods in Medical Diagnostics. Warsaw, MedPress.

Kabagambe, M., Swain, I. and Shakespeare, P. (1994). "An investigation of the effects of local pressure on the microcirculation of skin (reactive hyperaemia) in spinal cord injured patients." Journal of Tissue Viability **4**(4): 110-123.

Kalani, M., Brismar, K., Fagrell, B., Ostergren, J. and Jorneskog, G. (1999). "Transcutaneous oxygen tenstion and toe blood pressure as predictors for outcome of diabetic foot ulcers." Diabetes Care **22**(1): 147-151.

Kalodiki, E., Marston, R., Volteas, N., Leon, M., Labropoulos, N., Fisher, C., Christopoulos, D., Touquet, R. and Nicolaides, A. (1992). "The combination of liquid crystal thermography and duplex scanning in the diagnosis of deep vein thrombosis." European Journal of Vascular Surgery **6**(3): 311-316.

Kang, P., Hoffman, S., Krimitsos, E. and Rutkove, S. (2003). "Ambulatory foot temperature measurement: A new technique in polyneuropathy evaluation." Muscle & Nerve **27**(6): 737-742.

Kantro, S. (2006). Personal Communication: Preventive footcare and home monitoring of the diabetic foot using LCT technology. Bharara, M. Bournemouth, Visual Footcare.

Kao, P., Davis, B. and Hardy, P. (1999). "Characterisation of the calcaneal fat pad in diabetic and non diabetic patients using magnetic resonance imaging." Magnetic Resonance Imaging **17**(6): 851-857.

Katsilambros, N., Tentolouris, N. and Tsapogas, P. (2003). Atlas of Diabetic Foot. Chichester, Wiley.

Kelechi, T., Michel, Y. and Wiseman, J. (2006). "Are infrared and thermistor thermometers interchangeable for measuring localized skin temperature?" Journal of Nursing Measurement **14**(1): 19-30.

Kennedy, P. and Inglis, J. (2002). "Distribution and behaviour of glabrous cutaneous receptors in the human foot sole." The Journal of Physiology **538**(3): 995-1002.

Kimura, I., Uchide, K. and Ozawa, M. (1992). Temperature measurement using liquid crystals based on colour image processing (Improvement of color to temperature calibration line by neural networks). Japanese Visualisation Association.

Klosowicz, S., Jung, A. and Zuber, J. (2001). Liquid crystal thermography and thermovision in medical applications: Pulmonological diagnostics. Optical sensing for public safety, health and security, Proceedings of SPIE.

Knowles, E. and Boulton, A. (1996). "Do people with diabetes wear their prescrobed footwear?" Diabetic Medicine **13**(12): 1064-1068.

Lamah, L., Mortimer, P. and Dormandy, J. (1999). "Quantitative study of capillary density in the skin of the foot in peripheral vascular disease." British Journal of Surgery **86**: 342-348.

Langer, L., Fagerberg, S. and Johnsen, C. (1972). "Peripheral circulation in diabetes mellitus- a study with infrared thermography." Acta Med Scand **191**(1): 17-20.

Lavery, L., Higgins, K., Lactot, D., Constantinitides, G., Zamorano, R., Armstrong, D., Athanasiou, K. and Agrawal, C. (2004). "Home monitoring of foot skin temperatures to prrevent ulceration." Diabetes Care **27**(11): 2642-2647.

Lavery, L. A., Higgins, K. R., Lanctot, D. R., Constantinides, G. P., Zamorano, R. G., Armstrong, D. G., Athanasiou, K. A. and Agrawal, C. M. (2004). "Home monitoring of foot skin temperatures to prevent ulceration." Diabetes Care **27**(11): 2642-2647.

Leinidou, A. (2003). Contact Thermography (CD ROM), IPS, Italy. **2004**.

Levin, M. E. (2001). Pathogenesis and general management of foot lesions in the diabetic patient. Levin and O'Neal's The Diabetic Foot. Bowker, J. and Pfeifer, M. St. Louis, Missouri, Mosby: 219-260.

Liniger, C., Albeanu, A., Moody, J., Richez, J., Bloise, D. and Assal, J. P. (1991). "The Thermocross: A simple tool for rapid assessment of thermal sensation thresholds." Diabetes Research and Clinical Practice **12**: 25-34.

Little, R. C. and Little, W. C. (1989). Physiology of the heart and circulation. Chicago, Medical Publishers Inc.

Lord M, Hosein R and Williams RB (1992). "Method for in-shoe shear stress measurement." Journal of Biomedical Engineering **14**: 181-186.

Lord, M. and Hosein, R. (2000). "A study of in-shoe plantar shear in patients with diabetic neuropathy." Clinical Biomechanics **15**(4): 278-283.

Lord, M., Reynolds, D. and Hughes, J. (1986). "Foot pressure measurement: a review of clinical findings." Journal of Biomedical Engineering **8**: 283-294.

Manley, M. and Darby, T. (1980). "Repetitive mechanical stress and denervation in the plantar ulcer pathogenesis in rats." Archives of Physical Medical Rehabilitation **61**: 171.

Massi, N. (2004). Technological aspects of IPS plates with microencapsulated liquid crystals. Milan, IPS.

Mathworks (2002). Neural Network Toolbox in MATLAB (The language of technical computing), The Mathworks, Inc.

Matsuda, H., Ikeda, K., Nakata, Y., Otomo, F., Suga, T. and Fukuyama, Y. (2000). "A new thermochromic liquid crystal temperature identification technique using colour space interpolations and its applications to film cooling effectiveness measurements." Journal of Flow Visualisation and Image Processing **7**: 103-121.

McMillan, D. (2001). Hemorheology: Principles and concepts. Levin and O'Neal's The Diabetic Foot. Bowker, J. and Pfeifer, M. St. Louis, Missouri, Mosby, Inc.: 107-124.

McNeely, J. M., Boyko, J. E., Ahroni, H. J., Stensel, L. V., Reiber, E. G., Smith, G. D. and Pecoraro, E. R. (1995). "The independent contributions of diabetic neuropathy and vasculopathy in foot ulceration." Diabetes Care **18**(2): 216-219.

Meglinski, I. and Matcher, S. (2003). "Computer simulation of the skin reflectance spectra." Computer Methods and Programmes in Biomedicine . **70**: 179-186.

Meinders, M., Lange, A. d., Netten, P. and Wollesheim, H. (1996). "Microcirculation in the footsole as a function of mechanical pressure." Clinical Biomechanics **11**(7): 410-417.

Merla, A., Di Donato, L., Di Luzio, S., Farina, G., Pisarri, S., Proietti, M., Salsano, F. and Romani, G. (2002). "Infrared functional imaging applied to Raynaud's phenomenon." Engineering in Medicine and Biology Magazine, IEEE **21**(6): 73-79.

Meyers, S., Cros, D., Sherry, B. and Vermeire, P. (1989). "Liquid Crystal Thermography: Quantitative studies of abnormalities in carpal tunnel syndrome." Neurology **39**: 1465-1469.

Michel, C. C. and Gilliot, H. (1990). Microvascular mechanisms in stasis and ischaemia. Pressures sores clinical practice and scientific approach. Bader, D. L. London, Macmillan Press Ltd.: 153-163.

Middleton, J., Sinclair, P. and Patton, R. (1999). "Accuracy of centre of pressure measurement using a piezoelectric force platform." Clinical Biomechanics **14**(5): 357-360.

Millington, J. and Ellenzweig, J. (2003). "Management and Treatment of Diabetic Foot Wounds in the Elderly." Annals of Long-Term Care: Clinical Care and Aging **11**(1): 26-32.

Minamishima, C., Kuwaki, K., Shirota, E., Matsuzaki, M., Yamashita, K., Kamatani, M., Maeda, M. and Yano, F. (2005). "Thermal imaging properties of toes after walking stress test in diabetic patients." Japanese Journal of Clinical Pathology **53**(2): 118-122.

Miranda-Palma, B., Sosenko, J., Bowker, J., Mizel, M. and Boulton, A. (2005). "A comparison of the monofilament with other testing modalities for foot ulcer susceptibility." Diabetes Research and Clinical Practice **70**(1): 8-12.

Morbach, S., Lutale, J., Viswanathan, V., Mollenberg, J., Ochs, H., Rajashekar, S., Ramachandran, A. and Abbas, Z. (2004). "Regional differences in risk factors and clinical presentation of diabetic foot lesions." Diabetic Medicine **21**: 91-95.

Mork, C., Asker, C., Saleurd, E. and Kvernebo, K. (2000). "Microvascular arteriovenous shunting is a probable pathogenetic mechanism in erythromelalgia." Journal of Investigative Dermatology **114**: 643-646.

Nabarro, J. (1991). "Diabetes in the United Kingdom: a personal series." Diabetic Medicine **8**: 59-68.

Nakano, K. (1984). "Liquid crystal contact thermography (LCT) in the evaluation of patients with upper limb entrapment neuropathies." Neurol Orthop. Journal of Medical Surgery **5**: 97-102.

Nasseri, K., Strijers, R., Dekhuijzen, L., Buster, M. and Bertelsmann, F. (1998). "Reproducibility of different methods for diagnosing and monitoring diabetic neuropathy." Electromyography Clinical Neurophysiology **38**: 295-299.

National Institutes of Health (2004). Diabetic Neuropathies: The nerve damage of diabetes, National Diabetes Information Clearing House. **2004**.

Netten, P., Wollersheim, T. and Lutterman, J. (1996). "Skin microcirculation of the foot in diabetic neuropathy." Clinical Science **91**: 559-565.

Ng, E., Chen, Y. and Ung, I. (2001). "Computerised breast thermography: Study of image segmentation and temperature cyclic variations." Journal of Medical Engineering & Technology **25**(1): 12-16.

NHS (2004). Type 2 Diabetes - Prevention and management of foot problems, National Institutes of Health and Clinical Excellence. **2006**.

Nicolopoulos, C., Solomonidis, S., Anderson, E. and Black, J. (1995). In-shoe plantar pressure measurements for the diagnosis of different foot pathologies using FSR technology, Foot Pressure Interest Group. **2004**.

O'Brien, J., Patrick, A. and Caro, J. (2003). "Estimates of direct medical costs for microvascular and macrovascular complications resulting from type 2 diabetes mellitus in the United States in 2000." Clinical Therapeutics **25**(3): 1017-1038.

O'Reilly, D., Taylor, L., El-Hadidy, K. and Jayson, M. (1992). "Measurement of cold challenge responses in primary Raynaud's phenomenon and Raynaud's phenomenon associated with systemic sclerosis." Annals of the Rheumatic Diseases **51**: 1193-1196.

Otsuka, K., Okada, S., Hassan, M. and Togawa, T. (2002). "Imaging of skin thermal properties with estimation of ambient radiation temperature." Engineering in Medicine and Biology Magazine, IEEE **21**(6): 49-55.

Ouriel, K. (2001). "Peripheral Arterial Disease." Lancet **358**: 1257-1264.

Palastanga, N., Field, D. and Soames, R. (1994). Anatomy and Human Movement. Oxford, Butterworth Heinemann.

Palubo, P. and Melton, L. (1985). Peripheral vascular disease and diabetes. Diabetes in America. Harris, M. and Hamman, R. Washington DC, US Government Printing Office: 1-21.

Pecoraro, R., Ahroni, J., Boyko, E. and Stensel, V. (1991). "Chronology and detrminants of tissue repair in diabetic lower extremity ulcers." Diabetes **40**: 1305-1313.

Pendsey, S. (2003). Diabetic Foot: A clinical atlas. New Delhi, Jaypee Brothers - Medical Publishers (P) Ltd.

Perkins, B. and Bril, V. (2002). "Diagnosis and management of diabetic neuropathy." Current Diabetes Reports **2**(6): 495-500.

Perry, J. E., Hall, J. O. and Davis, B. L. (2002). "Simultaneous measurement of plantar pressure and shear forces in diabetic individuals." Gait & Posture **15**(1): 101-107.

Poirier, J., Garin, E., Derrien, C., A, D., Moisan, A., Bourguet, P. and Maugendre, D. (2002). "Diagnosis of osteomyelitis in the diabetic foot with a 99mTc-HMPAO leucocyte scintigraphy combined with a 99mTc-MDP bone scintigraphy." Diabetes Metabolism , **28**(6): 485-490.

Portnoy, W. M. (1970). "Tutorial: Liquid crystal thermography." Journal of the Associations for the Advancement of Medical Instrumentation **4**(5): 176-180.

Pospisil, E. and Pospisilov, J. (1990). "Application of liquid crystal thermoindicators and thermographic sheets for estimation of hygenic conditions of habitation." Acta Univ Patacki Olomuc Fac Med **125**: 277-282.

Quagliardi, M. (2005). Personal Communication: TLC applications and Cont-Flex system AGT 8 (I.P.S. s.r.l. - International Products & Services). Bharara, M. Bournemouth.

Rajapakse, C., Greennan, D., Jones, L. and Wilkinson, L. (1981). "Thermography in the assesssment of peripheral joint inflammation - A re-evaluation." Rheumatology **20**(2): 81-87.

Rajbhandari, S., Harris, N., M, S., Lockett, C., Eaton, S., Gadour, M., Tesfaye, S. and Ward, J. (1999). "Digital imaging: an accurate and easy method of measuring wound ulcers." Diabetic Medicine **16**: 339-342.

Randolph, A. L., Nelson, M., Akkapeddi, S., Levin, A. and Alexandrescu, R. (2000). "Reliability of measurements of pressures applied on the foot during walking by a computerized insole sensor system*1." Archives of Physical Medicine and Rehabilitation **81**(5): 573-578.

Raspovic, A., Newcombe, L., Lloyd, J. and Dalton, E. (2000). "Effect of customized insoles on vertical plantar pressures in sites of previous neuropathic ulceration in the diabetic foot." The Foot **10**(3): 133-138.

Rayman, G., Hassan, A. and Tooke, J. (1986a). "Blood flow in the skin of the foot related to the posture in diabetes mellitus." British Medical Journal **292**: 87-90.

Rayman, G., Williams , S., Spencer, P., Smaje, L., Wise, P. and Tooke, J. (1986b). "Impaired microvascular hyperaemic response to minor skin trauma in type 1 diabetes." British Medical Journal **292**: 1295-1298.

Reardon, J., Curwen, I., Jarman, P., Dewar, M. and Chodera, J. (1982). "Thermography and leg ulceration." Acta Thermographica **17**(1): 17-20.

Reiber, G. (1992). "Diabetic foot care: finanacial implications and practical guidelines." Diabetes Care **15**(Supplement 1): 29-31.

Rendell, M. and Bamisedun, O. (1992). "Diabetic cutaneous microangiopathy." The Americal Journal of Medicine **93**: 611-618.

Rhodes, A., Sherk, H., Black, J. and Margulies, C. (1988). "High resolution analysis of ground foot reaction forces." Foot Ankle **9**: 153-158.

Ring, E. (1987). "Thermographic and scintigraphic examination of the early phases of the inflammatory disease." Scandinavian Journal of Rheumatology(Supplement 65): 77-80.

Ring, E. (1988). "Raynaud's phenomenon: Assessment by thermography (consensus report, European Association of Thermology)." Thermology **3**: 69-73.

Ring, E. (1995). Cold stress testing of the hand. The thermal image in medicine and biology. Ammer, K. and Ring, E. Vienna., Uhlen Verlag**:** 237 - 240.

Ring, E., Aarts, N. and Black, C. (1998). "Raynaud's phenomenon: assessment by thermography." Thermology **3**: 69-73.

Ring, E. and Ammer, K. (2000). "The technique of infrared imaging in medicine." Thermology International **10**(1): 7-14.

Ring, E., Dieppe, P. and Bacon, P. (1981). "The thermographic assessment of inflammation and anti inflammatory drugs in osteoarthritis." British Journal of Clinical Practice: 263-264.

Ring, E. and Phillips, B. (1984). Recent advances in medical thermography. New York, Plenum Press.

Romanelli, M. and Falanga, V. (1999). Measurement of transcutaneous oxygen in chronic wounds. Chronic wound healing - Clinical measurement and basic science. Sandeman, D. London, WB Saunders Company Ltd.

Roth, T. and Anderson, A. (2005). Light transmission characteristics of thermochromic liquid crystals. Proceedings of IMECE, Orlando, IMECE.

Rubal, B., Traycoff, R. and Ewing, K. (1982). "Liquid crystal thermography - A new tool for evaluating low back pain." Physical Therapy **62**(11): 1593-1596.

Ryan, T. J. (1985). Dermal vasculature. Methods in skin research. Skerrow, C. J. London, Wiley. **527-558**.

Sandeman, D. and Shearman, C. (1999). Clinical aspects of lower limb ulceration. Chronic wound healing. Clinical Measurment and Basic Science. Sandeman, D. London, WB Saunders Company**:** 4-25.

Sandler, D. A. and Martin, J. F. (1985). "Liquid crystal thermography as a screening test for deep vein thrombosis." The Lancet **325**(8430): 665-668.

Schott (2005). Product Datasheet - DCR III Plus Light Source (Model A20800 Halogen Lamp), Schott North America Inc. **2005**.

Scott, E. (1986). Cardiovasuclar Physiology - An Integrative Approach. Manchester, Manchester University Press.

Seitz, L. (1901). "Die vordeven stutzpunkte des fusses under normalen and pathologische verhaltnissen." Z. Orthop. Chir **8**: 37-38.

Shaw, J. and Boulton, A. (1997). "The Pathogenesis of Diabetic Foot Problems: An Overview." Diabetes **46**(Supplement 2): S58-S61.

Shlens, M., Stoltz, M. and Benjamin, A. (1975). "Orthopedic applications of liquid crystal thermography." The Western Journal of Medicine **122**(5): 367-370.

Smith, K., Commean, P., Robertson, D., Pilgram, T. and Mueller, M. (2001). "Precision and accuracy of computed tomography foot measurements." Archives of Physical Medical Rehabilitation **82**: 925-929.

Stasiek, J. and Kowalewski, T. (2002). "Themochromic liquid crystals applied for heat transfer research." Opto Electronics Review **10**(1): 1-10.

Staub, D., Munger, B., Uno, H., Dent, C. and Davis, J. (1992). "Erythromelalgia as a form of neuropathy." Arch Dermatology **128**: 1654-1655.

Steele, J., Dillon, J., Plevris, J., Hauer, J., Bouchier, I. and Hayes, P. (1994). "Hand skin temperature changes in patients with chronic liver disease." Journal of Hepatology **21**(6): 927-933.

Stess RM, Sisney PC, Moss KM, Graf PM, Louie KS, Gooding GA and Grunfeld C (1986). "Use of liquid crystal thermography in the evaluation of the diabetic foot." Diabetes Care **9**(3): 267-272.

Stess, R. M., Sisney, P. C., Moss, K. M., Graf, P. M., Louie, K. S., Gooding, G. A. and Grunfeld, C. (1986). "Use of liquid crystal thermography in the evaluation of the diabetic foot." Diabetes Care **9**(3): 267-272.

Tanenberg, R., Schumer, M., Greene, D. and Pfeifer, M. (2001). Neuropathic problems of the lower extremities in diabetic patients. The Diabetic Foot. Pfeifer, M. St. Louis, Missouri, Mosby Inc.

Taylor, A. J., Menz, H. B. and Keenan, A. M. (2004). "The influence of walking speed on plantar pressure measurements using the two-step gait initiation protocol." The Foot **14**(1): 49-55.

The Diabetes Control & Complication Trial Research Group (1993). "The effect of intensive treatment of diabetes on the development and progression of long term complications in insulin dependent diabetes mellitus." N Engl J Med **329**: 977-986.

Tooke, J. (1996). "Review: Microvasculature in Diabetes." Cardiovascular Research **32**: 764-771.

Tsay, D. (1991). Pressure distribution in tissue. Prevention of Pressure Sores - Engineering and Clinical Aspects. Webster, J. Bristol, Adam Hilger**:** 19-33.

Uccioli, L., Mancini, L., Giordano, A., Solini, A., Magnani, P., Manto, A., Cotroneo, P., Greco, A. and Ghirlanda, G. (1992). "Lower limb arteriovenous shunts, autonomic neuropathy and diabetic foot." Diabetic Research Clinical Practice **162**(2): 123-130.

Uccioli, L., Monticone, G., Russo, F., Mormille, F., Durola, L., Mennuni, G., Bergamo, F. and Menzinger, G. (1994). "Autonomic neuropathy and transcutaneous oxymetery in diabetic lower extremities." Diabetologia **37**(1051-1055).

Uematsu, S. (1985). "Thermographic imaging of cutaneous sensory segments in patients with peripheral nerve injury. Skin temperature stability between sides of the body." Journal of Neurosurgery **62**: 716-720.

Urry, S. (1999). "Plantar pressure measurement sensors." Measurement Science & Technology **10**: R16-R32.

Van De Graff, K. M. and Fox, S. I. (1992). Concepts of Human Anatomy and Physiology. Dubuque, USA, WC Brown Publishers.

Van Someren, E. J. W., Raymann, R. J. E. M., Scherder, E. J. A., Daanen, H. A. M. and Swaab, D. F. (2002). "Circadian and age-related modulation of thermoreception and temperature regulation: mechanisms and functional implications." Ageing Research Reviews **1**(4): 721-778.

Vendrell, J., Nubioda, A., Goday, A., Bosch, X., Gomis, R., Esmatjes, E. and Vilardell, E. (1988). "Erythromelalgia associated with acute diabetic neuropathy: an unusual condition." Diabetes Research **7**: 149-151.

Viswanathan, V., Madhavan, S., Gnanasundaram, S., Gopalakrishna, G., Das, B. N., Rajasekar, S. and Ramachandran, A. (2004). "Effectiveness of Different Types of Footwear Insoles for the Diabetic Neuropathic Foot: A follow-up study " Diabetes Care **27**(2): 474-477.

Viswanathan, V., Madhavan, S., Rajasekar, S., Chamukttan, S. and Ambady, R. (2006). "Urban-rural differences in the prevalence of foot complications in South Indian diabetic patients." Diabetes Care **29**(3): 701-703.

Viswanathan, V., Madhavan, S., Rajashekar, S., Chamukuttan, S. and Ramachandran, A. (2005). "Amputation Prevention Initiative in South India." Diabetes Care **28**(5): 1019-1021.

Viswanathan, V., Sivagami, M., Seena, R., Snehalatha, C., Ramachandran, A. and Veves, A. (2004). "Increased forefoot to rearfoot plantar pressure ratio in South Indian patients with diabetic foot ulceration." Diabetic Medicine **21**(4): 396-397.

Viswanathan, V., Snehalatha, C., Seena, R. and Ramachandran, A. (2002). "Early recognition of diabetic neuropathy: evaluation of a simple outpatient procedure using thermal perception." Postgrad Medical Journal **78**(923): 541-542.

Viswanathan, V., Snehalatha, C., Sivagami, M., Seena, R. and Ramachandran, A. (2003). "Association of limited joint mobility and high plantar pressure in diabetic foot ulceration in Asian Indians." Diabetes Research and Clinical Practice **60**(1): 57-61.

Wang, H., Wade, D. and Kam, J. (2004). IR imaging of blood circulation of patients with vascular disease. Thermosense XXVI, Bellingham, WA, SPIE.

Ward, J. and Tesfaye, S. (1998). Pathogenesis of diabetic neuropathy. Textbook of Diabetes. Pickup, J. and Williams, G. Milan, Blackwell Science. **2:** 49.1-49.19.

Watkins, P. and Edmonds, M. (1998). Clinical features of diabetic neuropathy. Textbook of Diabetes. Pickup, J. and Williams, G. Milan, Blackwell Science. **2:** 50.1-50.20.

Williams , I., Picton, A. and McCollum, C. (1993). "The use of Doppler ultrasound: Arterial disease." Wound Management **4**(1): 1-4.

Wilmer, W., Voroshilova, O., Singh, I., Middendorf, D. and Cosio, F. (2001). "Transcutaneous oxygen tension in patients with calciphylaxis." American Journal of Kidney Diseases **37**(4): 797-806.

Wolinski, T., Nasilowski, T., Bajdecki, W., Domanski, A., Karpierz, M., Sierakowski, M., Szymanska, A. and Wojcik, J. (1998). "Fiber optic liquid crystal devices for pressure sensing." Proceedings of the SPIE - The International Society for Optical Engineering **3555**: 330-6.

World Health Organization (1999). Diagnosis and Classification of Diabetes Mellitus. Geneva, Department of Non Communicable Disease Surveillance: 1-66.

World Health Organization (2004). WHO: The Diabetes Programme, WHO. **2004**.

Wozniak, G., Wozniak, K. and Siekmann, J. (1996). "Non isothermal flow diagnostics using microencapsulated cholesteric particles." Applied Scientific Research **56**: 145-156.

Yong, K., Cobb, J. and Claremont, D. (2005). Near infrared spectroscopy of the diabetic foot. 5th Academic Biomedical Engineering Research Group Workshop. Bournemouth, Bournemouth University.

Zharkova, G., Khachaturyan, V., Vostokov, L. and Alekseev, M. (1980). Study of liquid thermoindicators. Advances in Liquid Crystal Research and Applications. Bata, L. Oxford, Pergammon Press. **2:** 1221-1239.

Ziegler, D., Mayer, P. and Wiefels, K. (1988). "Assessment of small and large fibre function in long term type 1 (insulin dependent) diabetic patients with and without painful neuropathy." Pain **34**: 1-10.